

UNIVERSITY OF OKLAHOMA

GRADUATE COLLEGE

MEASURING THE IMPACT OF MICROBIAL COMMUNITIES AND THEIR
PROLIFERATION IN ENGINEERED ECOSYSTEMS

A DISSERTATION

SUBMITTED TO THE GRADUATE FACULTY

in partial fulfillment of the requirements for the

Degree of

DOCTOR OF PHILOSOPHY

By

BLAKE WARREN STAMPS

Norman, Oklahoma

2016

MEASURING THE IMPACT OF MICROBIAL COMMUNITIES AND THEIR
PROLIFERATION IN ENGINEERED ECOSYSTEMS

A DISSERTATION APPROVED FOR THE
DEPARTMENT OF MICROBIOLOGY AND PLANT BIOLOGY

BY

Dr. Bradley Stevenson, Chair

Dr. Anne Dunn

Dr. Michael McInerney

Dr. Boris Wawrik

Dr. Ingo Schlupp

The path towards my Ph.D. has not been a linear one. For many years, my family was unsure if I would even make it past my B.Sc. To my parents, thank you for your patience and understanding. To my brother, you have always been there to make sure I didn't go too crazy. To my wife, your steadfast love and compassion has been a guiding light when the occasional darkness of graduate school closed in.

To Rosemary. Your life is just beginning but know that you are loved, and seeing you has given me the strength to finish what has been a very long road.

Acknowledgements

I must thank each member of my committee for their help during my general examination, and for the comments received that helped in the completion of my dissertation. To my advisor Dr. Bradley Stevenson, you have guided me since I was an undergraduate. Few would have taken me when I first started but you have given me the chance to soar.

This dissertation would not be complete without thanking each individual in the Stevenson lab that has helped immensely in its preparation. Brian, thank you for your numerous helpful comments and discussions over the past three years. James, thank you for your comments and for assisting in the fieldwork required to bring this research to light. Oderay, thank you for your assistance in isolating so many organisms from the samples I brought back from the field, and bringing together an amazing study of the chemical composition of biodiesel that is soon to become your thesis. Michael, you sent me on the path as a microbiologist when I first started as an undergraduate. Heather, no work in the lab is possible without your contribution. You have been in the lab since I began, and my development as a scientist would not have been the same without you.

Finally, I must thank all of our collaborators at the Air Force Research Laboratory. They provided essential site access and provided crucial data for my work in chapters 3, 4, and 5. Without your help the findings in each chapter would be less substantive. Thank you to everyone.

Table of Contents

Acknowledgements	iv
List of Tables	x
List of Figures.....	xii
Abstract.....	xviii
Chapter 1. Introduction.....	1
The Built Environment and Engineered Ecosystems	1
Biofouling Within Engineered Ecosystems.....	3
Biocorrosion in FAME Fuel Systems.....	7
Human Health and Engineered Ecosystems.....	9
Investigating Microbial Communities in Engineered Ecosystems.....	11
Scientific Contributions.....	15
References	17
Chapter 2. Municipal Solid Waste Landfills Harbor Distinct Microbiomes.....	28
Forward.....	28
Abstract.....	29
Introduction	30
Materials and Methods	33
Sample Collection	31
DNA Extraction and 16S rRNA Gene Library Preparation	34
Sequence Analysis.....	36
Meta-Analysis of Microbial Communities.....	37
Statistical Analyses.....	38

Data Availability	38
Results.	39
Discussion.....	48
Acknowledgments	56
References	56
List of supplementary files	66
Chapter 3: Fungal Contamination is the Root Cause of Fouling in USAF B20	
Biodiesel Storage Tanks	68
Foreward.....	68
Abstract.....	69
Introduction	70
Methods	74
Site Description	74
Measurement of ATP in SE Fuels	77
Fuel Acid Index	78
DNA Sampling, Preservation, and Extraction.....	78
PCR Amplification and DNA Sequencing.....	79
Quantitative PCR.....	80
Sequence Analysis.....	81
Genome Sequencing of Select Environmental Isolates.....	82
Expression of Key Genes Associated with B20 Degradation within <i>Byssochlamys</i> sp.....	83
Analysis of Putative Metabolites from RNA sequencing Cultures	84

Results.	85
Visual determination of fouling at SE and SW	86
Small Subunit rRNA Gene Community Analysis	89
Genome Sequencing of Select Isolates.....	101
RNA Sequencing Results	102
Fuel Acid Index of select samples from SE	104
GC/MS Identification of Putative Metabolites.....	104
Discussion.....	105
Conclusions	112
References	113
Chapter 4. Increased Risk of Microbially Influenced Corrosion from Fungal	
Proliferation and Contamination of B20 Biodiesel	123
Abstract.....	123
Foreward.....	124
Introduction	125
Methods	128
Site Descriptions and In Situ Corrosion Assessment	128
Coupon Surface Imaging and of Weight Loss Determination	131
DNA Sampling, Preservation, and Extraction.....	131
PCR Amplification and DNA Sequencing	132
Sequence Analysis.....	133
Growth of Consortia on a Defined B20 Fuel.....	134
Results.	136

Analysis of Bacterial and Fungal Communities Associated with Biofilms at SE and SW	136
Corrosion and Pitting Assessment <i>in situ</i> and in Laboratory Microcosms	151
Discussion.....	160
Conclusions	167
References	169
Chapter 5. Impact of Whole-Aircraft Sterilization on the Microbiome of a C-130	
Hercules	179
Foreward.....	179
Abstract.....	180
Introduction	181
Methods	183
Sampling.....	183
SSU rRNA gene library preparation.....	184
SSU rRNA gene library analysis	186
Viability of Microbial Communities by ATP Testing.....	187
Cultivation of Microorganisms.....	187
Identification of Cultivated Microorganisms	188
Results.	189
Discussion.....	217
References	222
Chapter 6. Conclusions.....	231
Landfills Represent an Untapped Source of Microbial Diversity	231

Microbial Communities in Biodiesel Tanks are Geographically Distinct.....	234
Hot, humid air is a viable method of decontamination	238
Final Thoughts.....	240
References	240

List of Tables

Chapter 2 Table 1. Summary of diversity indices ^a across all tested landfill leachates. .	44
Chapter 2 Table 2. PERMANOVA results of regional or operational parameters assumed to be significant <i>a priori</i>	47
Chapter 3 Table 1. Summary of PERMANOVA tests comparing bacterial community structure of the weighted UniFrac distance matrix to location (site), tank, position within tank (position), and the relative peak height of select fuel components.	93
Chapter 3 Table 2. Summary of PERMANOVA tests comparing eukaryotic community structure as a measure of the weighted UniFrac distance matrix to location (site), tank, position within tank (position), and the relative peak height of select fuel components. Comparisons with a $p < 0.05$ are denoted in bold.	95
Chapter 3 Table 3. ATP Values from bottom fuel samples at SE.	97
Chapter 3 Table 4. qPCR quantification of 18S rRNA gene copies in select fuel samples from April to August 2014. Standard deviation represents the average of triplicate biological replicates.	101
Chapter 3 Table 5. Acid index of select fuels from SE October of 2014, March and May of 2015. Values are expressed in mg KOH/g B20. Samples that exceed ASTM specification for B5 to B20 blends are denoted in bold.	104
Chapter 4 Table 1. Pairwise comparisons of bacterial diversity measured as the number of observed OTUs in biofilms across time and tank from the Southeast (SE) and Southwest (SW). Values are an average across all sampled time points.	138

Chapter 4 Table 2. Pairwise comparisons of eukaryal diversity measured as the number of observed OTUs in biofilms across time and tank position from the Southeast (SE) and Southwest (SW). Values are an average across all sampled time points.....	140
Chapter 4 Table 3. Summary of PERMANOVA results in both bacteria (16S) and eukaryotic (18S) datasets.....	150
Chapter 4 Table 4. Acid index of select fuels from SE October of 2014, March and May of 2015. Values are expressed in mg KOH/g B20.	155
Chapter 5 Table 1. ATP readings taken at select locations across the aircraft before and after decontamination.	195
Chapter 5 Table 2. List of cultivated organisms before before (Pre) and after (Post) decontamination. The number of cultures producing acid or degrading Impranil® are summarized as positive (+), negative (-), or no reaction is denoted as “NR” or no reaction.	197
Chapter 5 Table 3. List of bacterial taxonomic lineages significantly decreased after JBADS treatment. Significance was assessed using a non-parametric Kruskal Wallace test after false discovery rate (FDR) correction. Number of detected OTUs that were significantly decrease in relative abundance is also listed.	204
Chapter 5 Table 4. List of eukaryotic taxonomic lineages significantly decreased after JBADS treatment. Significance was assessed using a non-parametric Kruskal Wallace test after false discovery rate (FDR) correction. Number of detected OTUs that were significantly decrease in relative abundance is also listed.	211

List of Figures

Chapter 1 Figure 1. The base catalyzed reaction of a triglyceride and methanol to form a fatty acid methyl ester and glycerol. The R group is dependent upon source or feedstock and can vary commonly from 14 to 18 carbons in length and contain 0-2 points of unsaturation.	6
Chapter 2 Figure 1: Map of landfill sites sampled across regions of the United States. States containing sampled landfills are labeled in bold. One landfill was sampled per state, with the exception of OK (2) and ME (3). Adapted from (Masoner et al., 2014). 34	
Chapter 2 Figure 2. Taxonomic summary showing percent relative abundance of bacterial and archaeal phyla from sampled landfill leachates. Taxa representing less than an average of 1% relative abundance are grouped together as “Other Bacteria” or “Other candidate divisions” for clarity.	41
Chapter 2 Figure 3: Taxonomic summary showing percent relative abundance of classes within the most abundant phylum, Proteobacteria	42
Chapter 2 Figure 4: Cluster analysis of landfill leachates represented by a jackknifed UPGMA tree. Clade A (green) contained TX, OK1, and CO; clade B (red) contained ME1, ME3, VT and MN; clade C (purple) contained VA, WA, IA, ME2, OK2, and FL; and clade D (blue) contained AZ, AR, OR, and KY Two landfills, CA and WY (black) were outliers to the other four distinct clades.	45
Chapter 2 Figure 5. Principal component ordination analysis of microbial communities from diverse environments based on an unweighted UniFrac distance matrix, showing the distinct grouping of communities in landfill leachate sampled for this study from all others. Samples are colored by source.	46

Chapter 3 Figure 1. A diagram showing A) general locations of sampled USAF bases (left to right; NW, SW, TX, WE and MW), the number (n) of samples taken, and the type of fuels sampled at each location (B20 or USLD), and B) the general structure of a biodiesel storage tank. Fuel samples were taken either from each fuel tank from the main entry hatch (1) or the automated tank-gauging hatch (4). Other points of entry include the dispensing tubing (2) and a baffled filling tube (3).	76
Chapter 3 Figure 2. Fuel samples taken from B20 storage tanks at the SW AFB show (A) a range in water content, particulate matter, clarity, and color. The bottle third from the left is an example of the clarity and color of fuel upon delivery. A common feature of fouled biodiesel is a thick biofilm at the fuel-water interface (B).	87
Chapter 3 Figure 3. Scanning electron microscopy of a biofilm taken from SE E on October 2015. Biomass was almost entirely comprised of fungal hyphae (A). At higher magnification, branching conidiophores were also visible (B).	88
Chapter 3 Figure 4. Relative abundance of bacterial families detected in fuels at all sampled sites over time. Fuel samples from the bottom (or Bot), middle (Mid), and top (Top) of the fuel column, as well as the nozzle of a dispenser (Noz) at SE and SW. Individual tanks (3, 4, and E and SE; 2, 3, and 4 at SW) are also indicated. Taxonomic lineages that represented less than 1 percent on average of any sample were condensed into the “other” category.	90
Chapter 3 Figure 5. Relative abundance of eukaryotic families detected in fuels at all sampled sites over time. Fuel samples from the bottom (or Bot), middle (Mid), and top (Top) of the fuel column, as well as the nozzle of a dispenser (Noz) at SE and SW. Individual tanks (3, 4, and E and SE; 2, 3, and 4 at SW) are also indicated. Taxonomic	

lineages that represented less than 1 percent on average of any sample were condensed into the “other” category.	91
Chapter 3 Figure 6: The relative abundance of the Trichocomaceae in bottom fuel samples over time at SE 3. Elevated ATP readings (Table 3) are noted as an open circle with lines. Instances of both elevated ATP readings and visible flocculent material (reported by operator) are shown as a solid semi-circle and open semi-circle with lines	100
Chapter 3 Figure 7: Detected transcripts associated with the degradation of fatty acid methyl esters when the <i>Byssochlamys</i> sp. was grown on B20. Transcripts are noted as an average of the triplicate Transcripts Per Million (TPM) value. The mean TPM value for all detected transcripts in <i>Byssochlamys</i> sp. grown on B20 was 20.8.	103
Chapter 4 Figure 1. Overview of sampled locations including the number of samples (A). An overview of a biodiesel storage tank (B). Witness coupons and O-Rings were suspended from the main entry hatch (1). Witness coupons were placed in either the vapor filled space above the fuel layer (2) or near the bottom of the tank (3) at the predicted fuel-water interface.	130
Chapter 4 Figure 2. Taxonomy summary of the bacterial families detected in materials at SW. Position within the tank is denoted above each sample type. Bars are clustered by material and in order of increasing sampling date (left to right). Taxonomic lineages that represented less than 1 percent on average of any sample were condensed into the “other” category.	142
Chapter 4 Figure 3. Taxonomy summary of the bacterial families detected in materials at SE. Position within the tank is denoted above each sample type. Bars are clustered by	

material and in order of increasing sampling date (left to right). Taxonomic lineages that represented less than 1 percent on average of any sample were condensed into the “other” category.....	143
Chapter 4 Figure 4. Taxonomy summary of the eukaryotic families detected on different materials at SW. Position within the tank is denoted above each sample type. Bars are clustered by material and in order of increasing sampling date (left to right). Taxonomic lineages that represented less than 1 percent on average of any sample were condensed into the “other” category.	145
Chapter 4 Figure 5. Taxonomy summary of the eukaryotic families detected on materials at SE. Position within the tank is denoted above each sample type. Bars are clustered by material and in order of increasing sampling date (left to right). Taxonomic lineages that represented less than 1 percent on average of any sample were condensed into the “other” category.	146
Chapter 4 Figure 6. Principal Coordinates Analysis (PCoA) ordination of all bacterial and archaeal samples at SW (Blue) and SE (Red) at an even sampling depth of 1000 sequences per sample.	148
Chapter 4 Figure 7. Principal Coordinates Analysis (PCoA) ordination of all eukaryotic samples at SW (Blue) and SE (Red) at even sampling depth of 500 sequences per sample.....	149
Chapter 4 Figure 8. Images of uncoated steel witness coupons at each sampled time point at SE (top) and SW (bottom). Images are shown for SE 3 (left Top), SE 4 (middle top), and SE E (right top), SW 2 (bottom left), SW 3 (bottom middle), and SW 4 (bottom right) Twelve month samples at SE 4 and SE E are not shown.....	152

Chapter 4 Figure 9. After 7 months exposure in SE 3 near the bottom of the tank a thick biofilm formed (top). The dark green biofilm (B) was composed primarily of filamentous fungi (middle, bottom).....	153
Chapter 4 Figure 10. Biofilms at SE 3 were removed to identify pitting corrosion. After 3 months (A) and 7 months (B) exposure visible pits formed directly beneath biofilms.	154
Chapter 4 Figure 11. General corrosion rate (mm/yr) of uncoated steel witness coupons after 3, 7, 9, and 12 months exposure in all tanks at SE. Tank 3 was taken offline after 9 months. The dashed lines denote the median corrosion rate across fuel and vapor. Boxes indicate values within the first and third quartiles of data. Whiskers represent the 5 th and 9 th percentile of data while circles denote outlying points.	157
Chapter 4 Figure 12. Maximum pit depth of uncoated steel witness coupons 60 cm above the tank bottom at SE 3 and SE 4. Boxes indicate values within the first and third quartiles of data. Whiskers represent the 5 th and 9 th percentile of data while circles denote outlying points.	158
Chapter 4 Figure 13. Corrosion rate of laboratory co-cultures incubated for 9 weeks. Samples were taken at 24 hours, 1, 3, 5, 7, and 9 weeks, represented from right to left in each condition. Boxes indicate values within the first and third quartiles of data. Whiskers represent the 5 th and 9 th percentile of data.....	159
Chapter 5 Figure 1. Amount of DNA after PCR amplification before (blue) and after (red) decontamination across all sampled sites.	190

Chapter 5 Figure 2. Bacterial families that comprise on average more than 1% relative abundance of any sample. Samples are arranged in alternating order of pre/post decontamination.	192
Chapter 5 Figure 3. Fungal orders that comprise on average more than 1% relative abundance of any sample. Samples are arranged in alternating order of pre/post decontamination.	193
Chapter 5 Figure 4. Principal Coordinates Analysis (PCoA) ordination of all bacterial and archaeal samples pre (blue) and post (red) decontamination.....	201
Chapter 5 Figure 5. Principal Coordinates Analysis (PCoA) ordination of all eukaryotic samples pre (blue) and post (red) decontamination.....	202
Chapter 5 Figure 6 Overview of the number of cultivated microorganisms across the sampled C-130 prior to decontamination. Numbers in parentheses represent the lowest dilution in which an isolate was successfully recovered.	215
Chapter 5 Figure 7 Overview of the number of cultivated microorganisms across the sampled C-130 after decontamination. Numbers in parentheses represent the lowest dilution in which an isolate was successfully recovered. Locations marked with an asterisk denote locations where the only microorganisms recovered are from potential laboratory contaminants.	216

Abstract

The interactions between humans, the structures we build, and the microorganisms that inhabit these spaces are inescapable. Engineered ecosystems are classified broadly as any ecosystem built or managed by humans. Buildings and other infrastructure may corrode and fail as a result of microbial metabolism. Microbial fouling directly impacts fuel and water distribution systems. Microorganisms inhabiting surfaces in engineered ecosystems may also impact human health. Three engineered ecosystems; landfills, biodiesel storage tanks, and aircraft, were characterized as a part of this dissertation using a combination of small subunit ribosomal RNA sequencing, *in situ* measurements of microbial activity, cultivation, and laboratory experimentation. Landfills are one end point for the waste produced by humans and are of increasing concern due to the presence of chemicals of emerging concern. In order to better understand the role of microorganisms on the life cycle of landfills, it is important to characterize the microorganisms that inhabit landfill leachate and if the unique geochemical landscape of leachate impacts the microbial community composition. Landfill leachate microbiomes are distinct from many other engineered or natural ecosystems, possibly due to a combination of chemical and geographic parameters at each landfill.

One drawback of the landfill leachate study was a lack of sampling events over time and our ability to cultivate microorganisms that may directly impact the operation of an engineered ecosystem. In collaboration with the United States Air Force (USAF) and the Air Force Research Laboratory, we investigated the extent of fuel fouling and material corrosion within B20 biodiesel storage systems at multiple USAF facilities

over an eighteen-month survey. Bacterial and fungal communities were largely distinct at each sampled location although the abundant members of the fungal community were found at many sampled tanks. The risk to infrastructure through generalized corrosion was low; however, pitting corrosion was increased when associated with fungal biomass. The filamentous fungi found in underground storage tanks have the ability to degrade components of the fuel and increase the corrosion of metals, representing a risk to infrastructure. Information gathered in the *in situ* studies and laboratory experimentation described in this dissertation could help operators detect and assess the likelihood of biofouling and corrosion in B20 biodiesel blends.

In many engineered ecosystems, including B20 underground storage tanks, the removal or mitigation of microorganisms is desirable. An opportunity arose to test the impact on the microbiome of a C-130H aircraft using a novel means of whole-aircraft decontamination. After 72 hours of decontamination with hot, humid air, the bacterial, archaeal, and eukaryotic community structure was significantly altered. Fewer viable microorganisms were cultivable after decontamination. The use of hot, humid air decontamination appears to be a viable method of decontaminating an entire aircraft. The use of hot, humid air may also be useful in other engineered ecosystems such as the B20 biodiesel storage tanks that contain undesired microorganisms. By using a combination of techniques that compliment one another, we have identified and isolated abundant members of the bacterial and fungal community that contaminate USAF B20, the risk they pose to infrastructure, and a potential means to controlling microbial communities in engineered ecosystems.

Chapter 1. Introduction

Characterizing the Microbiology within Built Environments and Engineered Ecosystems and Determining their Impact

The interaction between humans, the structures we build or manage, and the impact of microorganisms that inhabit these spaces is of great interest. Byproducts of microbial metabolism can degrade materials used in the construction of buildings and biofilms may foul fuel or water distribution systems increasing the risk of failure. Pathogenic microorganisms may inhabit structures or surfaces posing a risk to human inhabitants. This dissertation focuses on the characterization of microbial communities within three engineered ecosystems, their impact, and the effectiveness of attempts to control the presence of microbial communities and their detrimental activities.

Humans have built structures for habitation and storage for millennia. The idea of these “built environments” becoming a field of study was first discussed within the context of urban design (Handy et al., 2002). More recently, microbiological studies have attempted to link building design, occupancy, and planning to the presence of microorganisms that may impact human health. A building can contain numerous environments, each with distinct microbial communities partitioning into multiple niches (Chase et al., 2016). The microbial communities found in office buildings varied by location (floor vs. ceiling) based on usage patterns rather than material. Other buildings, such as hospitals may be more likely to harbor microorganisms that could impact human health (Lax and Gilbert, 2015). The effectiveness of hospital surface disinfection protocols using adenosine triphosphate as a proxy for microbial activity

showed that current methods are not always effective in surface sterilization (Boyce et al., 2009). Other means of decontamination may be required to prevent the spread of pathogenic microorganisms.

There are numerous human built structures that should be placed within the context of the built environment, but are outside of the scope of its traditional definition. Studies of the built environment have traditionally focused on urban design or inhabited buildings. The built environment in the context of this dissertation can be thought of as any of a number of human-made environments, which we more widely classify as engineered ecosystems. Engineered ecosystems can include any structure or system that is managed by humans. Dwellings, office buildings (Kelley and Gilbert, 2013), water treatment facilities (Vuono et al., 2014), landfills (Stamps et al., 2016), fuel storage and production systems (Stevenson et. al 2011) are all examples of engineered ecosystems. Each of these is strongly influenced by the management practices and physical structure imposed by humans. Some engineered ecosystems rely on the microbial communities for their ultimate function, such as degradation in wastewater systems and landfills (Stamps et. al 2016).

This dissertation begins with a national survey of landfill leachate across the United States. Landfills are a repository for the solid waste produced by human activities potentially resulting in a distinct microbiome. Chapters 3 and 4 focus on a series of B20 biodiesel storage facilities in the United States reporting varying levels of fouling. The risk of corrosion due to microbial activity in the studied biodiesel storage tanks was unknown prior to the survey discussed in chapter 4. Fouling and corrosion cost an estimated 6 % of the United States gross domestic product, or almost 1 trillion dollars

(Koch et al., 2002), representing an enormous economic drain. Identifying the microbial community present over time at multiple facilities storing a 20 % blend of biodiesel may help in identifying the proper controls to put in place to correctly manage microbial contamination within these storage tanks. The final chapter of this dissertation investigates the ability of hot, humid air to decontaminate an entire C-130H aircraft. The relatively novel method of decontamination on a large scale was previously shown to be effective in significantly reducing the number of viable *Bacillus thuringiensis* spores inoculated onto aluminum witness coupons (Buhr et al., 2016) but no attempt was made to understand how this decontamination would impact the microbiome of the entire aircraft. In turn, hot, humid air decontamination could potentially be employed to control or mitigate the risk of microbial fouling and corrosion in biodiesel storage systems.

Biofouling Within Engineered Ecosystems

The accumulation of biofilms has a negative impact on the surfaces they colonize. Marine organisms such as coral and microorganisms can colonize the surfaces of ships and reduce fuel economy and maneuverability (Copisarow, 1945). In water distribution systems, reduced flow can be attributed to biofilms, which represent up to 95 % of the total biomass in the pipeline (Flemming et al., 1998). In the oil industry, biofilms may foul water injection systems or production systems, and potentially cause damaging corrosion (Sanders and Sturman, 2005).

The world relies on hydrocarbons as a source of building materials and energy. Different distillates of crude oil are used for different engine types. Kerosene (such as JetA), diesel, and gasoline fuels are the most common liquid transportation fuels. The United States (US) consumes over 19 million barrels of crude oil daily (Central Intelligence Agency, 2014). The US Department of Defense (DoD) is the single largest consumer of liquid transportation fuels (Dimotakis et al., 2006), representing a potential strategic and environmental concern. To reduce the dependence on foreign sources of oil, the DoD and United States Air Force (USAF) issued mandates that all branches of the armed services transition to renewable ground fleet fuels by 2025 (Air Force Energy Plan, 2009). Ultra low sulfur diesel (ULSD) was one fuel used across USAF ground vehicles that was easily replaced by a blend containing 20 % fatty acid methyl ester (FAME) biodiesel made from renewable resources and 80 % ULSD, commonly referred to as B20. This fuel was compatible with existing storage systems and vehicles, with essentially the same properties of the ULSD it replaced (Canakci, 2007; Chang et al., 1996). Biodiesel (FAME) is produced through a base catalyzed reaction of fatty acids with an alcohol (commonly methanol) to produce fatty acid methyl esters, or FAME and glycerol (Fig. 1). Biodiesel is commonly produced from soy, animal tallow, food-service grease, canola, and many other common vegetable oils (Moser 2010). The glycerol is removed from the final product, leaving a mostly pure FAME fuel that is ready for combustion. However, 100% biodiesel (also referred to as B100) cannot be used in unmodified diesel engines and may cause an undesired reduction in horsepower (Moshiri et al., 2006). Blends of biodiesel from B5 (5% v/v) to B20 (20% v/v), with ULSD are the most common and are used in existing engines and storage infrastructure

with little to no modification. Additionally, blends up to B20 have superior lubricating properties (Hazrat et al., 2015) over ULSD.

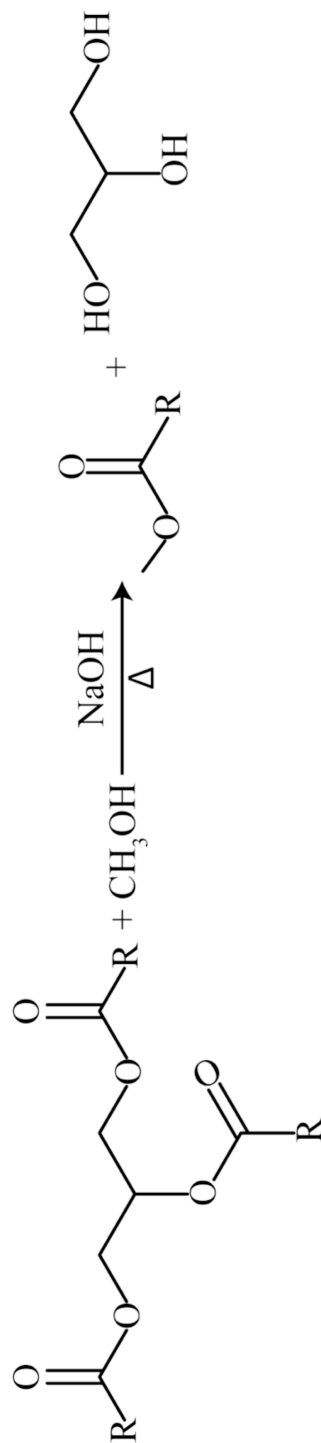


Figure 1. The base catalyzed reaction of a triglyceride and methanol to form a fatty acid methyl ester and glycerol. The R group is dependent upon source or feedstock and can vary commonly from 14 to 18 carbons in length and contain 0-2 points of unsaturation.

The use of biodiesel is not without potential risks. The chemical structure of FAME is readily activated and oxidized by many microorganisms that contain a lipase/carboxylesterase (Kumari and Gupta, 2014; Meyer et al., 2012). Biodiesel is rapidly degraded under aerobic conditions with a median half life in solution of 6.8 days (Prince et al., 2008). Although rapid biodegradation is an advantage in the event of an unintended spill, it can pose serious risks for extended storage. Biomass resulting from the growth of microorganisms can foul dispensing equipment and reduce the energy density of the fuel (Prince et al., 2008). Storage of biodiesel blends in marine systems can result in extensive fouling (often referred to by end users as “sludge”) and corrosion by anaerobic microorganisms (Lee et al., 2010; Lyles et al., 2013). Aerobic oxidation of diesel and biodiesel blends is also possible in marine environments and can result in engine fouling and filter clogging (Chao et al., 2010). Despite this potential risk, biodiesel blends including B20 have become commonplace within the DoD. Numerous reports of fouling across the USAF were noted soon after the introduction of B20 resulting in an increase in the annual tank maintenance costs (Dr. Wendy J. Crookes-Goodson, personal communication). The extent of biofouling or corrosion related to microbial growth is currently unknown, but is the subject of this dissertation.

Biocorrosion in FAME Fuel Systems

The metabolism of B20 by microbial communities could impact the life of a storage tank through microbially influenced corrosion. Biofilm accumulation in hydrocarbon bearing systems can result in corrosion. The corrosion of carbon steel through the

production of reactive sulfides in marine biofilms and oil production facilities is well known (Crolet, 1992; Enning and Garrelfs, 2014). Under aerobic conditions, microbial production of acetic acid can produce pitting corrosion in stainless steels (Little et al., 1988) although the specific mechanism of acid corrosion is poorly understood (Gu, 2014). By targeting engineered ecosystems where acid corrosion is likely occurring, we may increase our knowledge of the microorganisms capable of acid based corrosion.

Fatty acid methyl esters are highly susceptible to microbial attack (Aktas et al., 2013). The metabolism of FAME can produce small organic acids that are potentially corrosive (Aktas et al., 2010). Methylophilic fungi (Kumari and Gupta, 2014) and bacteria can oxidize methanol released during the initial activation of FAME to fatty acids and to CO_2 potentially increasing the risk of corrosion in environments with high concentrations of organic acids (Crolet et al., 1999). Fungi are capable of corroding iron and steel without direct contact with the metal surface through the production of both organic acids and other metabolites (Siegel et al., 1983). Volatile fatty and organic acids produced as a result of the degradation of FAME could induce corrosion in the vapor filled space above fuel within underground storage tanks (Williamson et al., 2015). Materials commonly used as fittings in fuel storage and distribution systems can also degrade as a result of biological contamination due to swelling and cracking caused by the increased acidity of fuels contaminated with fatty acids (Maru et al., 2009).

Corrosion represents a significant cost to the global economy. The actual cost of corrosion within the United States may represent up to 6 % of gross domestic product (GDP) or \approx 1 trillion US Dollars (Heitz and Sand, 1996). The USAF spends 5.87 billion USD yearly to mitigate corrosion damage (Herzberg et al., 2016). The amount of

corrosion related specifically to microbial processes is still unknown but estimated to be 20% (Herzberg et al., 2016, Dr. Wendy J. Crookes-Goodson, personal communication). Biodiesel, by way of its susceptibility to microbial degradation, may greatly increase the risk of corrosion to infrastructure and vehicles, further increasing the cost of corrosion to the USAF. In FY2015 fuel disposal and tank cleaning related to B20 fouling cost an estimated \$ 500,000 USD in the USAF (Dr. Wendy J. Crookes-Goodson, personal communication). The risk to vehicles is mostly unknown. A study of a small number of buses showed an increase in the number of fuel filter plugging events but no further issues (Proc et al., 2006). This could have been due to the small sample size ($n = 9$) or successful filtration of microorganisms in fuel systems prior to the fuel entering the tank. Without a study of fuel storage infrastructure we cannot conclusively determine the risk B20 may represent. The risk of failure to water handling systems, fuel transport and storage, as well as damage to vehicle fleets is potentially immense.

Human Health and Engineered Ecosystems

It is critical to decontaminate surfaces in engineered ecosystems such as hospitals or aircraft to prevent the spread of pathogens. Microorganisms can colonize surfaces presenting a risk to patients within hospitals (Lax and Gilbert, 2015). Biocides may control or eliminate microorganisms from surfaces, however resistant bacteria and fungi can recolonize surfaces and present a recurrent risk (Ma et al., 2015). Non chemical methods of surface sterilization using ultraviolet (UV) light is effective in reducing the viable microbial population present (Linnes et al., 2014) but the use of UV may not be

appropriate for other engineered ecosystems including aircraft. The spread of infectious microorganisms, either accidentally or through the release of a bioterror agent on an aircraft or other public place, is of great concern (National Research Council, 2006). The effectiveness of the global air transit system to rapidly spread infectious disease was illustrated during a coronavirus outbreak (Peiris et al., 2003). Tuberculosis can also spread rapidly through air travel (Abubakar, 2010; Kenyon et al., 1996). Therefore, the intentional release of pathogenic or weaponized microorganisms within aircraft is a significant concern. Aerosolized *Bacillus thuringiensis* spores, a proxy for pathogenic strains of *Bacillus anthracis*, were shown to spread rapidly in both transport and commercial aircraft (Clayton et al., 1976). In either the case of an infected individual or the dispersal of bacterial spores, decontamination of all surfaces on an aircraft is critical.

Once an infected passenger has been removed from an aircraft, decontamination is still required before an aircraft can be put back into service. Chlorine dioxide, vaporized hydrogen peroxide (VHP), and gaseous formaldehyde are all established methods of decontamination, but each poses potential risks to the structural integrity of the aircraft. Chlorine dioxide can readily corrode exposed metal surfaces (EPA, 2010), while VHP and formaldehyde carry restrictions to material compatibility and safety concerns (Wagner et al., 2007). Recently, a rapidly deployable decontamination method called the Joint Biological Agent Decontamination System (JBADS) was developed to decontaminate aircraft (Buhr et al., 2016). The JBADS uses hot, humid air within an enclosure designed to accommodate an entire aircraft, and avoids the use of potentially hazardous chemical agents. This treatment was able to effectively reduce the number of

viable *Bacillus thuringiensis* spores across an entire aircraft (Buhr et al., 2016).

Although JBADS was originally designed to decontaminate aircraft and other vehicles, it could also be used to reduce the overall microbial load in other engineered ecosystems such as B20 biodiesel storage tanks.

Investigating Microbial Communities in Engineered Ecosystems

A comprehensive approach to the characterization and investigation of microbial communities requires the combination of multiple techniques. Microbial ecology is based on determining abundance or density of the community, the microorganisms present and their abundance relative to one another, and their major metabolic activities. Cultivation-based techniques are important in addressing these questions but are often neglected, especially with the evolution of new and powerful molecular techniques. Cultivation provides the opportunity to quantify the population density of cultivable organisms by determining the number of colony forming units or most probable number of viable organisms. It also allows for the identification of populations detected with molecular approaches and the testing of their metabolic capabilities.

A major limitation to cultivation-based studies is that the vast majority of microorganisms are not amenable to isolation or cultivation, limiting the populations that are represented in a cultivation-based study of microbial communities (Staley and Konopka, 1985). A way to avoid this cultivation bias, while characterizing the entirety of a microbial community, is to detect a well-conserved gene that is shared across all three domains of life. The small subunit (SSU) ribosomal RNA (rRNA) gene is phylogenetically conserved, allowing it to be useful in the inference of community

composition and function (Olsen et al., 1986). Differences in community structure can be correlated to metadata collected during sampling and used to infer the effectiveness of management practices or decontamination in engineered ecosystems.

High throughput sequencing has made it possible to generate and analyze large ecological datasets that were previously unimaginable. Amplification of the 16S rRNA gene using short read high throughput sequencing technologies can be used to simultaneously analyze hundreds of samples inexpensively with millions of sequences assigned to each sample (Caporaso et al., 2011). The ability to generate large datasets at high resolution must also be treated with caution. Nucleic acid extraction and PCR amplification reagents can be contaminated with microbial DNA potentially confounding results (Salter et al., 2014). With proper experimental design, contaminants can be controlled for and removed from further analyses. More important than potential contaminants within reagents is the proper selection of primers to achieve an accurate representation of the sampled microbial community.

The choice of primers for 16S rRNA gene polymerase chain reaction (PCR) is essential in generating a dataset that is representative of the microbial community in an environment. Several recent publications have identified PCR primers generating an amplified DNA fragment suitable for high throughput sequencing (Hadziavdic et al., 2014; Klindworth et al., 2013). In the event that fungi, bacteria, and archaea are hypothesized to coexist in an environment being studied, a primer set that evenly and effectively amplifies the SSU rRNA genes from all three domains of life is also possible (Parada et al., 2015). There are also drawbacks to using the small subunit rRNA gene for characterizing microbial communities. Although sequence data from the full length

SSU rRNA gene can be used to accurately resolve most bacterial and archaeal genera (Janda and Abbott, 2007), the fragment size (150 - 450 bp) amplified using most primer sets used in high throughput sequencing analyses is more limited in resolving taxonomy (Soergel et al., 2012; Yarza et al., 2014). The taxonomic resolution possible with short sequences of eukaryotic SSU rRNA genes is even more limited because this gene has evolved at a more rapid rate than in the bacteria and archaea (Smit et al., 2007). The use of long-read sequencers can alleviate the loss in resolution found in short read sequencing studies (Singer et al., 2016), but with reduced sequencing depth and increased cost per sample.

In addition to determining the presence of key microbial taxa within a sample, it can be desirable to generate quantitative estimates of microbial density. Quantitative PCR (qPCR) amplification of the SSU rRNA gene is a useful tool for estimating the number of bacteria and archaea in a system; however, SSU rRNA gene copy number in fungi can vary greatly between genera from tens to hundreds of copies (Herrera et al., 2009). Data generated from qPCR can be combined with the results of a high throughput small subunit ribosomal RNA gene survey to produce an estimate of the absolute abundance of microorganisms present within a tested environment.

Prior to the reduction in sequencing cost, it was not financially feasible to generate large datasets encompassing latitudinal or longitudinal gradients. Long-term studies incorporating numerous replicates over time are crucial to accurately measuring population dynamics (Magurran et al., 2010). Long-term studies of megafauna are at a distinct disadvantage due to the long generation time of the organisms under study; however, microbial populations do not suffer from this limitation. Studies can cover

tens, if not hundreds of generations over the course of two to three years (Begon et al., 1996). Specifically within the context of the locations under study within this dissertation, the use of both long-term field studies and controlled laboratory studies was required to fully understand the impact of the increasing use of biofuels on existing infrastructure prior to the implementation of any mitigation techniques in the field. Incorporating both laboratory investigations and *in situ* studies over time could also produce a library of bacterial and fungal isolates representative of an engineered ecosystem useful for laboratory experimentation.

Microbial community studies can establish which organisms are present or the genomic potential and activity of an environment but they cannot identify what chemical end products are produced by their metabolic activities. Identification of metabolites could help in understanding the mechanism of hydrocarbon degradation present in an ecosystem (Callaghan, 2013; Haddock, 2010). Fuels can also be analyzed over time to observe the measure of fouling within fuel systems. The simplest method is a visual inspection of the fuel that is also combined with centrifugation to detect any dissolved water according to the ASTM D1796 standard. Fuels can also be measured by FT-IR according to ASTM D7371 or through gas chromatography/mass spectrometry to determine the relative concentration and identity of fuel constituents as well as any loss to the abiotic or biotic degradation (Aktas et al., 2013; Knothe, 2006). Chromatographic techniques are powerful for measuring the loss of fuel constituents when compared to a known reference or when sufficient volumes of material can be collected to identify putative metabolites of hydrocarbon degradation. In storage systems that maintain a large volume of fuel, metabolites may be dilute and difficult to identify if new fuel is

consistently delivered and consumed. Profiling metabolites by GC/MS is also possible as a part of laboratory experimentation with isolates obtained from the field grown in microcosms.

One method of assessing corrosion in pipeline systems is the use of witness coupons placed in-line with a fuel transmission system (pipelines), or within storage systems. The coupons are kept for a period of time, and a general corrosion rate (Mils per year or MPY) can be established through determining the amount of mass lost. The surfaces of witness coupons can also be imaged through SEM, white-light profilometry, or other means to identify pitting corrosion or observe microbial colonies (Chapter 4). Atomic absorption, IC-AES/MS, or ICP are also possible to investigate the elemental composition of fluids, as high concentrations of iron are indicative of corrosion or materials loss.

Scientific Contributions

This dissertation investigates the microbial communities of three distinct engineered ecosystems. Chapter 2 investigates landfills as one potential endpoint for materials used in engineered ecosystems. This study characterizes the bacterial and archaeal communities of landfills on a national scale and attempts to correlate these communities to a large number of environmental, geochemical, and management parameters. Chapters 3 and 4 investigate a storage infrastructure system containing a blend of biodiesel (B20) in the USAF in great detail over multiple years. Chapters 3 and 4 are part of a larger study that was carried out over the course of three years at multiple USAF facilities storing biodiesel (Fig. 2). The ecosystem of biodiesel storage tanks is

poorly understood and an attempt was made to not only characterize the microbial communities within each tank, but also correlate these community members to specific deleterious activities, such as fouling, fuel degradation, and microbially influenced corrosion (MIC) using multiple analytical techniques. Chapter 5 characterizes the microbial community of a C-130 transport aircraft across a large number of sample locations and assesses how the microbial community changes after an aggressive decontamination protocol using hot, humid forced air is employed. The ability to decontaminate an entire aircraft, in turn, has potential benefits for the biodiesel systems discussed in the previous chapters and presents a mechanism of decontamination that may be useful across engineered ecosystems.

References

- Abubakar, I. (2010). Tuberculosis and air travel: a systematic review and analysis of policy. *Lancet Infect Dis.* 10, 176–183. doi:10.1016/S1473-3099(10)70028-1.
- Air Force Energy Plan (2009). Air Force Energy Plan. 1–38.
- Aktas, D. F., Lee, J. S., Little, B. J., Duncan, K. E., Perez-Ibarra, B. M., and Suflita, J. M. (2013). Effects of oxygen on biodegradation of fuels in a corroding environment. *Int. Biodeter. Biodegradation* 81, 114–126. doi:10.1016/j.ibiod.2012.05.006.
- Aktas, D. F., Lee, J. S., Little, B. J., Ray, R. I., Davidova, I. A., Lyles, C. N., et al. (2010). Anaerobic Metabolism of Biodiesel and Its Impact on Metal Corrosion. *Energy Fuels* 24, 2924–2928. doi:10.1021/ef100084j.
- Begon, M., Harper, J. L., and Townsend, C. R. (1996). *Ecology*. Blackwell Publishing.
- Boyce, J. M., , MD, Havill, N. L., , MT, Dumigan, D. G., , RN, Golebiewski, M., Balogun, O., , BS, MBA, and Rizvani, R., , BS (2009). Monitoring the Effectiveness of Hospital Cleaning Practices by Use of an Adenosine Triphosphate Bioluminescence Assay. *Infect. Control Hosp. Epidemiol.* 30, 678–684. doi:10.1086/598243.
- Buhr, T. L., Young, A. A., Bensman, M., Minter, Z. A., Kennihan, N. L., Johnson, C. A., et al. (2016). Hot, humid air decontamination of a C-130 aircraft contaminated

- with spores of two acrySTALLiferous *Bacillus thuringiensis* strains, surrogates for *Bacillus anthracis*. *J. Appl. Microbiol.*, n/a–n/a. doi:10.1111/jam.13055.
- Callaghan, A. V. (2013). Metabolomic investigations of anaerobic hydrocarbon-impacted environments. *Curr. Opin. Biotechnol.*
- Canakci, M. (2007). Combustion characteristics of a turbocharged DI compression ignition engine fueled with petroleum diesel fuels and biodiesel. *Bioresour. Technol.* 98, 1167–1175. doi:10.1016/j.biortech.2006.05.024.
- Caporaso, J. G., Lauber, C. L., Walters, W. A., Berg-Lyons, D., Lozupone, C. A., Turnbaugh, P. J., et al. (2011). Global patterns of 16S rRNA diversity at a depth of millions of sequences per sample. *Proc. Natl. Acad. Sci. U.S.A.* 108 Suppl 1, 4516–4522. doi:10.1073/pnas.1000080107.
- Chang, D. Y. Z., Van Gerpen, J. H., Lee, I., Johnson, L. A., Hammond, E. G., and Marley, S. J. (1996). Fuel properties and emissions of soybean oil esters as diesel fuel. *J. Am. Oil Chem. Soc.* 73, 1549–1555. doi:10.1007/BF02523523.
- Chao, Y., Liu, N., Zhang, T., and Chen, S. (2010). Isolation and characterization of bacteria from engine sludge generated from biodiesel-diesel blends. *Fuel* 89, 3358–3364. doi:10.1016/j.fuel.2010.05.041.
- Chase, J. H., Fouquier, J., Zare, M., Sonderegger, D. L., Knight, R., Kelley, S., et al. (2016). Geography and location are the primary drivers of office microbiome composition. *PeerJ Preprints*. doi:10.7287/peerj.preprints.1797v1.

- Clayton, A. J., O'Connell, D. C., Gaunt, R. A., and Clarke, R. E. (1976). Study of the microbiological environment within long- and medium-range Canadian Forces aircraft. *Aviat. Space Environ. Med.* 47, 471–482.
- Copisarow, M. (1945). Marine Fouling and its Prevention. *Science* 101, 406–407.
doi:10.1126/science.101.2625.406.
- Crolet, J.-L. (1992). From Biology and Corrosion to Biocorrosion. *Oceanol. Acta* 15, 87–94.
- Crolet, J.-L., Thevenot, N., and Dugstad, A. (1999). Role of Free Acetic Acid on the CO₂ Corrosion of Steels. NACE International. ISBN 99024 1999 CP
- Dimotakis, P., Grober, R., and Lewis, N. (2006). Reducing DOD Fossil Fuel Dependence. McLean, Virginia 22102-7508.
- Enning, D., and Garrelfs, J. (2014). Corrosion of iron by sulfate-reducing bacteria: new views of an old problem. *Appl. Environ. Microbiol.* 80, 1226–1236.
doi:10.1128/AEM.02848-13.
- EPA, U. S. (2010). Compatibility of Material and Electronic Equipment With Hydrogen Peroxide and Chlorine Dioxide Fumigation. 1–106.
- Flemming, H. C., Tamachkiaorwa, A., and Klahre, J. (1998). Monitoring of fouling and biofouling in technical systems. *Water Sci. Technol.* doi:10.1016/S0273-1223(98)00704-5.
- Gu, T. (2014). Theoretical Modeling of the Possibility of Acid Producing Bacteria

- Causing Fast Pitting Biocorrosion. *J. Microb. Biochem Technol.* 06.
doi:10.4172/1948-5948.1000124.
- Haddock, J. D. (2010). Aerobic degradation of aromatic hydrocarbons: enzyme structures and catalytic mechanisms. *Handbook of Hydrocarbon and Lipid Microbiology*. doi:10.1007/978-3-540-77587-4_74.
- Hadziavdic, K., Lekang, K., Lanzen, A., Jonassen, I., Thompson, E. M., and Troedsson, C. (2014). Characterization of the 18S rRNA gene for designing universal eukaryote specific primers. *PLoS One* 9, e87624.
doi:10.1371/journal.pone.0087624.
- Handy, S. L., Boarnet, M. G., Ewing, R., and Killingsworth, R. E. (2002). How the built environment affects physical activity: views from urban planning. *Am. J. Prev. Med.* 23, 64–73.
- Hazrat, M. A., Rasul, M. G., and Khan, M. M. K. (2015). Lubricity Improvement of the Ultra-low Sulfur Diesel Fuel with the Biodiesel. *Energy Procedia* 75, 111–117.
doi:10.1016/j.egypro.2015.07.619.
- Heitz, E., and Sand, W. (1996). *Microbially influenced corrosion of materials*. Springer.
- Herrera, M. L., Vallor, A. C., Gelfond, J. A., Patterson, T. F., and Wickes, B. L. (2009). Strain-Dependent Variation in 18S Ribosomal DNA Copy Numbers in *Aspergillus fumigatus*. *J. Clin. Microbiol.* 47, 1325–1332. doi:10.1128/JCM.02073-08.
- Herzberg, E. F., Morris, A., Kelly, A. R., Stroh, R. F., Rutledge, L., and OMeara, N. T.

- (2016). Estimated Impact of Corrosion on Cost and Availability of DoD Weapon Systems. LMI Government Consulting.
- Janda, J. M., and Abbott, S. L. (2007). 16S rRNA gene sequencing for bacterial identification in the diagnostic laboratory: pluses, perils, and pitfalls. *J. Clin. Microbiol.* 45, 2761–2764. doi:10.1128/JCM.01228-07.
- Kelley, S. T., and Gilbert, J. A. (2013). Studying the microbiology of the indoor environment. *Genome Biol.* 14, 202. doi:10.1186/gb-2013-14-2-202.
- Kenyon, T. A., Valway, S. E., Ihle, W. W., Onorato, I. M., and Castro, K. G. (1996). Transmission of multidrug-resistant *Mycobacterium tuberculosis* during a long airplane flight. *N. Engl. J. Med.* 334, 933–938. doi:10.1056/NEJM199604113341501.
- Klindworth, A., Pruesse, E., Schweer, T., Peplies, J., Quast, C., Horn, M., et al. (2013). Evaluation of general 16S ribosomal RNA gene PCR primers for classical and next-generation sequencing-based diversity studies. *Nucleic Acids Res.* 41, e1. doi:10.1093/nar/gks808.
- Knothe, G. (2006). Analyzing biodiesel: standards and other methods. *J. Am. Oil. Chem Soc.* 83, 823–833. doi:10.1007/s11746-006-5033-y.
- Koch, G. H., Brongers, M., Thompson, N. G., Virmani, Y. P., and Payer, J. H. (2002). Corrosion Cost and Preventative Strategies in The United States.
- Kumari, A., and Gupta, R. (2014). Novel strategy of using methyl esters as slow release

- methanol source during lipase expression by mut⁺ *Pichia pastoris* X33. *PLoS One* 9, e104272. doi:10.1371/journal.pone.0104272.
- Lax, S., and Gilbert, J. A. (2015). Hospital-associated microbiota and implications for nosocomial infections. *Trends Mol. Med.* 21, 427–432. doi:10.1016/j.molmed.2015.03.005.
- Lee, J. S., Ray, R. I., and Little, B. J. (2010). An assessment of alternative diesel fuels: microbiological contamination and corrosion under storage conditions. *Biofouling* 26, 623–635. doi:10.1080/08927014.2010.504984.
- Linnes, J. C., Rudnick, S. N., Hunt, G. M., McDevitt, J. J., and Nardell, E. A. (2014). Eggcrate UV: a whole ceiling upper-room ultraviolet germicidal irradiation system for air disinfection in occupied rooms. *Indoor Air* 24, 116–124. doi:10.1111/ina.12063.
- Little, B., Wagner, P., and Duquette, D. (1988). Technical Note: Microbiologically Induced Increase in Corrosion Current Density of Stainless Steel under Cathodic Protection. *Corrosion* 44, 270–274. doi:10.5006/1.3583936.
- Lyles, C. N., Aktas, D. F., Duncan, K. E., Callaghan, A. V., Stevenson, B. S., and Suflita, J. M. (2013). Impact of organosulfur content on diesel fuel stability and implications for carbon steel corrosion. *Environ. Sci. Technol.* 47, 6052–6062. doi:10.1021/es4006702.
- Ma, X., Baron, J. L., Vikram, A., Stout, J. E., and Bibby, K. (2015). Fungal diversity and presence of potentially pathogenic fungi in a hospital hot water system treated

with on-site monochloramine. *Water Res.* 71, 197–206.

doi:10.1016/j.watres.2014.12.052.

Magurran, A. E. A., Baillie, S. R. S., Buckland, S. T. S., Dick, J. M. J., Elston, D. A. D., Scott, E. M. E., et al. (2010). Long-term datasets in biodiversity research and monitoring: assessing change in ecological communities through time. *Trends Ecol. Evol.* 25, 574–582. doi:10.1016/j.tree.2010.06.016.

Maru, M. M., Lucchese, M. M., Legnani, C., Quirino, W. G., Balbo, A., Aranha, I. B., et al. (2009). Biodiesel compatibility with carbon steel and HDPE parts. *Fuel Process. Technol.* 90, 1175–1182. doi:10.1016/j.fuproc.2009.05.014.

Meyer, D. D., Santestevan, N. A., Bucker, F., Salamoni, S. P., Andreazza, R., de Oliveira Camargo, F. A., et al. (2012). Capability of a selected bacterial consortium for degrading diesel/biodiesel blends (B20): enzyme and biosurfactant production. *J Environ. Sci. Health A Tox. Hazard Subst. Environ. Eng.* 47, 1776–1784. doi:10.1080/10934529.2012.689227.

Moser, B. R. (2010). "Biodiesel Production, Properties, and Feedstocks," in *Biofuels* (New York, NY: Springer New York), 285–347. doi:10.1007/978-1-4419-7145-6_15.

Moshiri, M. R., Payne, M. L., and Vasquez, M. (2006). Emission and Performance Effects of Biodiesel Blends of B5, B20 and B100 in a Single-Cylinder Medium-Speed Diesel Engine. *ASME 2006 Internal Combustion Engine Division Spring Technical Conference (ICES2006)* 2006, 383–392. doi:10.1115/ICES2006-1384.

- National Research Council (2006). *Defending the U.S. Air Transportation System Against Chemical and Biological Threats*. Washington, D.C.: National Academies Press doi:10.17226/11556.
- Olsen, G. J., Lane, D. J., Giovannoni, S. J., Pace, N. R., and Stahl, D. A. (1986). Microbial ecology and evolution: a ribosomal RNA approach. *Annu. Rev. Microbiol.* 40, 337–365. doi:10.1146/annurev.mi.40.100186.002005.
- Parada, A., Needham, D. M., and Fuhrman, J. A. (2015). Every base matters: assessing small subunit rRNA primers for marine microbiomes with mock communities, time-series and global field samples. *Environ Microbiol.* doi:10.1111/1462-2920.13023.
- Peiris, J. S. M., Lai, S. T., Poon, L. L. M., Guan, Y., Yam, L. Y. C., Lim, W., et al. (2003). Coronavirus as a possible cause of severe acute respiratory syndrome. *Lancet* 361, 1319–1325.
- Prince, R. C., Haitmanek, C., and Lee, C. C. (2008). The primary aerobic biodegradation of biodiesel B20. *Chemosphere* 71, 1446–1451. doi:10.1016/j.chemosphere.2007.12.010.
- Proc, K., Barnitt, R., Hayes, R. R., Ratcliff, M., McCormick, R. L., Ha, L., et al. (2006). 100,000-Mile Evaluation of Transit Buses Operated on Biodiesel Blends (B20). in (400 Commonwealth Drive, Warrendale, PA, United States: SAE International), 2006–01–3253. doi:10.4271/2006-01-3253.
- Salter, S., Cox, M. J., Turek, E. M., Calus, S. T., and Cookson, W. O. (2014). Reagent

- contamination can critically impact sequence-based microbiome analyses. *bioRxiv*.
- Sanders, P. F., and Sturman, P. J. (2005). “Biofouling in the Oil Industry,” in *Petroleum Microbiology* (American Society of Microbiology), 171–198.
doi:10.1128/9781555817589.ch9.
- Siegel, S. M., Siegel, B. Z., and Clark, K. E. (1983). Bio-corrosion: Solubilization and accumulation of metals by fungi. *Water Air Soil Poll.* 19, 229–236.
doi:10.1007/BF00599050.
- Singer, E., Bushnell, B., Coleman-Derr, D., Bowman, B., Bowers, R. M., Levy, A., et al. (2016). High-resolution phylogenetic microbial community profiling. *ISME J.*
doi:10.1038/ismej.2015.249.
- Smit, S., Widmann, J., and Knight, R. (2007). Evolutionary rates vary among rRNA structural elements. *Nucleic Acids Res.* 35, 3339–3354. doi:10.1093/nar/gkm101.
- Soergel, D. A. W., Dey, N., Knight, R., and Brenner, S. E. (2012). Selection of primers for optimal taxonomic classification of environmental 16S rRNA gene sequences. *ISME J.* 6, 1440–1444. doi:10.1038/ismej.2011.208.
- Staley, J. T., and Konopka, A. (1985). Measurement of in Situ Activities of Nonphotosynthetic Microorganisms in Aquatic and Terrestrial Habitats. *Annu. Rev. Microbiol.* 39, 321–346. doi:10.1146/annurev.mi.39.100185.001541.
- Stamps, B. W., Lyles, C. N., Suflita, J. M., Masoner, J. R., Cozzarelli, I. M., Kolpin, D. W., et al. (2016). Municipal Solid Waste Landfills Harbor Distinct Microbiomes.

Front. Microbiol. 7, 507. doi:10.3389/fmicb.2016.00534.

Stevenson, B. S., Drilling, H. S., Lawson, P. A., Duncan, K. E., Parisi, V. A., and Suflita, J. M. (2011). Microbial communities in bulk fluids and biofilms of an oil facility have similar composition but different structure. *Environ Microbiol* 13, 1078–1090. doi:10.1111/j.1462-2920.2010.02413.x.

The World Factbook 2013-14. Washington, DC: Central Intelligence Agency, 2013.

Vuono, D. C., Benecke, J., Henkel, J., Navidi, W. C., Cath, T. Y., Munakata-Marr, J., et al. (2015). Disturbance and temporal partitioning of the activated sludge metacommunity. *ISME J.* 9, 425–435. doi:10.1038/ismej.2014.139.

Wagner, G. W., Sorrick, D. C., Procell, L. R., Brickhouse, M. D., Mcvey, I. F., and Schwartz, L. I. (2007). Decontamination of VX, GD, and HD on a surface using modified vaporized hydrogen peroxide. *Langmuir* 23, 1178–1186. doi:10.1021/la062708i.

Williamson, C. H. D., Jain, L. A., Mishra, B., Olson, D. L., and Spear, J. R. (2015). Microbially influenced corrosion communities associated with fuel-grade ethanol environments. *Appl. Microbiol. Biotechnol.* 99, 6945–6957. doi:10.1007/s00253-015-6729-4.

Yarza, P., Yilmaz, P., Pruesse, E., Glöckner, F. O., Ludwig, W., Schleifer, K.-H., et al. (2014). Uniting the classification of cultured and uncultured bacteria and archaea using 16S rRNA gene sequences. *Nat. Rev. Microbiol.* 12, 635–645. doi:10.1038/nrmicro3330.

Chapter 2. Municipal Solid Waste Landfills Harbor Distinct

Microbiomes

Foreword

The microbial composition of landfills was investigated as a part of a greater nation-wide chemical survey of 19 landfills. I performed the initial quality control of returned sequence data, the analysis of all sequence data associated with the project, the statistical analyses, and wrote the manuscript. However, this work was conducted with a number of collaborators. Dr. Joseph Suflita edited the manuscript and aided in the experimental design. Dr. Chris Lyles assisted greatly in the preparation of the sampling kits sent across the nation, and performed all DNA extractions and PCR amplifications. Dr. Bradley Stevenson aided in the writing of the manuscript, as well as the experimental design. Our collaborators in the U.S. Geological Survey (USGS)- Dana Kolpin, Isabelle Cozzarelli, and Jason Masoner aided in the conception of the experiment, sample collection, and edited the manuscript. The manuscript was published in *Frontiers of Microbiology* and can be located at <http://dx.doi.org/10.3389/fmicb.2016.00534>.

Abstract

Landfills are the final repository for most of the discarded material from human society and its “built environments”. Microorganisms subsequently degrade this discarded material in the landfill, releasing gases (largely CH₄ and CO₂) and a complex mixture of soluble chemical compounds in leachate. Characterization of “landfill microbiomes” and their comparison across several landfills should allow the identification of environmental or operational properties that influence the composition of these microbiomes and potentially their biodegradation capabilities. To this end, the composition of landfill microbiomes was characterized as part of an ongoing USGS national survey studying the chemical composition of leachates from 19 non-hazardous landfills across 16 states in the continental U.S. The landfills varied in parameters such as size, waste composition, management strategy, geography, and climate zone. The diversity and composition of bacterial and archaeal populations in leachate samples were characterized by 16S rRNA gene sequence analysis, and compared against a variety of physical and chemical parameters in an attempt to identify their impact on selection. Members of the Epsilonproteobacteria, Gammaproteobacteria, Clostridia, and candidate division OP3 were the most abundant. The distribution of the observed phylogenetic diversity could best be explained by a combination of variables and was correlated most strongly with the concentrations of chloride and barium, rate of evapotranspiration, age of waste, and the number of detected household chemicals. This study illustrates how leachate microbiomes are distinct from those of other natural or

built environments, and sheds light on the major selective forces responsible for this microbial diversity.

Introduction

The global upsurge in urbanization of the human population is associated with even greater increases in the generation of municipal solid waste (MSW). By the year 2025, 4.3 billion urban residents are projected to generate approximately 1.42 kg of MSW per person, totaling 6.1 million metric tons per day, making the generation of MSW an even faster growing pollutant than greenhouse gases (Hoornweg et al., 2013). Advances in waste reduction, recycling, and composting have made an impact on the fate of MSW, but landfilling is still the most common waste disposal option and is likely to remain so for the foreseeable future. Despite the heavy reliance on this method of disposal, surprisingly little is known about the microbiology and its function in these engineered ecosystems.

The degradation of organic matter in landfills is broadly characterized by a succession of phases that ultimately result in the conversion of the waste materials to mineralized end products like water, CO₂, and CH₄ (Palmisano and Barlaz, 1996). Complex assemblages of bacteria and archaea carry out the majority of MSW degradation. These syntrophic consortia are far more capable of mineralizing the myriad of organic substances deposited in landfills than single microorganisms or populations. Both chemical profiles and microbial community composition change during the biodegradation of MSW, but the general patterns are consistent with the anaerobic cycling of organic matter (McInerney et al., 2009). In addition to the resident bacterial

and archaeal populations, landfill leachates are also home to populations of anaerobic fungi. Previously members of the order Neocallimastigales, known to degrade cellulose, were found in British landfill leachates (Lockhart et al., 2006). The accumulation of organic acids can decrease the pH of the landfill, occasionally inhibiting the overall degradation processes (Mormile et al., 1996). The accumulation of acid is transient and modulated by the subsequent metabolism of organic acid intermediates, which returns the pH of a landfill to near-neutral values that are conducive to methanogenesis (Barlaz et al., 1989). An additional factor related to microbial metabolic activity in landfills is the moisture content of the refuse material (Suflita et al., 1992; Gurijala and Suflita, 1993). The shifting, heterogeneous physical and chemical profiles of landfills are certainly a main reason why they are home to such a diverse assemblage of microorganisms exhibiting a broad range of metabolic activities (Mori et al., 2003; Gomez et al., 2011; Lu et al., 2012).

The materials deposited in landfills are the sum total of numerous human activities, chemically and physically diverse, and challenging to fully degrade. The incomplete degradation of MSW leads to the production of leachate that can solubilize many chemicals of emerging concern (CECs) (Eggen et al., 2010). These CECs include a complex range of chemicals found in household, commercial, and industrial products, whose impact on the environment and human health are not well understood (Palm et al., 2002; Pal et al., 2010; Andrews et al. 2012, Masoner et al., 2016). The interaction between the microbial community, leachate, and CECs in landfills is of great interest. Previous studies have suggested that a number of genes associated with the degradation of CECs are present within landfills (Lu et al., 2012). Specifically, it is of interest to

know if the complex chemistry of landfill leachate enriches or selects for particular types of microorganisms that might be capable of metabolizing such compounds. As an important step in exploring such potential interactions, we conducted *post hoc* tests for the potential correlation between leachate microbiota and the presence of numerous CECs.

The microbial assemblages associated with leachate samples from 19 landfills were characterized using high-throughput sequencing of 16S rRNA gene libraries. Species richness, evenness, and shared diversity were compared between each sample. We investigated the connection between microbial communities in landfill leachates and several operational and environmental variables, as part of a broader study (Masoner et al., 2014). The *a priori* predictions that geographic region, waste profiles, geology, or annual rainfall would impact the composition of the microbial community were tested. Correlations between the microbial communities and landfill management characteristics such as leachate produced per year, waste dissolution time, the amount of waste accepted per year, and the age of the landfills, also were tested *ad hoc*. While many previous studies have investigated the microbiology of landfills (McDonald et al., 2010; Mouser et al., 2010; Lu et al., 2012), this study surveyed a larger number of landfill leachate samples across the United States using a sequencing-based approach. Therefore, the present study represents a more comprehensive analysis of microbial diversity to characterize the “landfill microbiome” and the selective forces responsible for its formation.

Materials and Methods

Sample Collection

Fresh leachate samples were collected from 19 landfills from six different regions across the United States in triplicate (57 total samples) during the summer and fall of 2011 by on-site technicians (Fig. 1). The metadata used in this study were also used to determine the potential impact of environmental parameters on the distribution of CECs detected within landfills (Masoner et al., 2014). Any pipelines or tubing used to collect leachate were purged with at least three volumes or for five minutes to remove stagnant leachate or other contaminants. All equipment and tubing were field rinsed with at least one liter of leachate prior to sampling. Triplicate samples of biomass and particulate matter were collected through a sterile in-line polypropylene filter (Advantec; 47 mm diameter) pre-loaded with a nitrocellulose membrane filter (Whatman; 0.45 μm pore size, 47 mm diameter). Volumes of leachate filtered varied from 8 to 1500 mL at the discretion of the on-site technicians, based on restriction of flow due to filter obstruction (Table S1). After filtration, the nitrocellulose filter was removed from the holder using sterile forceps, transferred to 5 mL of DNAzol (Molecular Research Center, Inc., Cincinnati, OH, USA), shipped overnight to the University of Oklahoma, and stored at -80° C until DNA extraction.

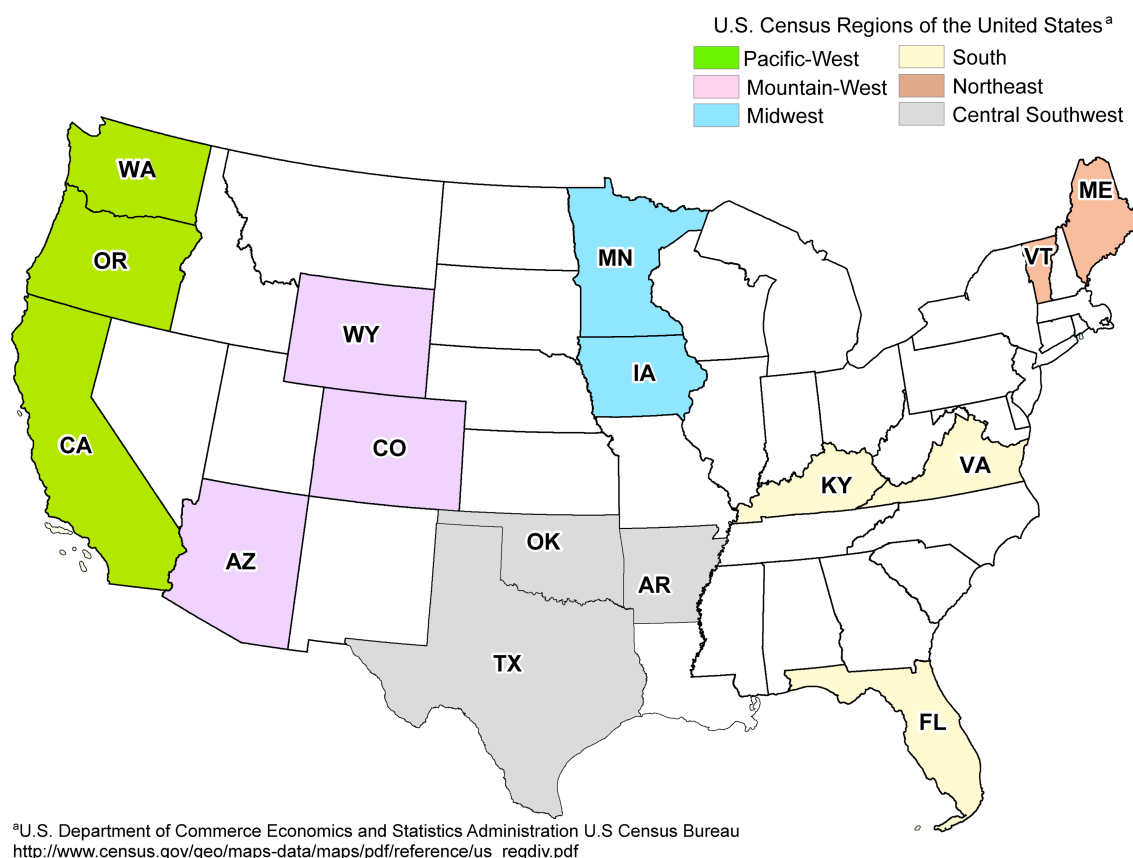


Figure 1: Map of landfill sites sampled across regions of the United States. States containing sampled landfills are labeled in bold. One landfill was sampled per state, with the exception of OK (2) and ME (3). Adapted from (Masoner et al., 2014).

DNA Extraction and 16S rRNA Gene Library Preparation

Each sample (filter and DNAzol) was vortexed for 30s at full speed upon thawing at room temperature. DNA was extracted from 1 mL of the DNAzol solution in each replicate sample using an automated Maxwell 16 Cell total RNA LEV Purification Kit (Promega, Madison, WI, USA), omitting the final DNase step as described in Oldham et al. (2012). Extracted DNA ranged in detected concentration from 1.04 to 12.3 ng/μL, with three samples that failed to quantify (Table S1). Libraries of bacterial and archaeal

16S rRNA gene fragments were amplified from each DNA extract using PCR with primers that spanned the V4 region between position 519 and 802 (*E. coli* numbering), producing a ~300 bp fragment. These primers evenly represent a broad distribution of both the Bacteria and Archaea (Klindworth et al., 2013). The forward primer (M13L-519F: 5'- **GTA AAA CGA CGG CCA G**CA CMG CCG CGG TAA -3') contains the M13 forward primer (in bold), followed by the 16S rRNA gene-specific sequence (underlined). The reverse primer (785R: 5'-TAC NVG GGT ATC TAA TCC-3') was taken directly from the reverse primer "S-D-Bact07850b-A-18" in Klindworth et al. (2013). Each 50 µL PCR consisted of 1× DreamTaq PCR master mix (ThermoFisher Scientific, Waltham, MA, USA), 0.1 µM of each primer, and 5-10 µL of 1:10 dilutions of DNA extracts. Additional details of the PCR are provided in the file Supplementary Information located at <http://dx.doi.org/10.3389/fmicb.2016.00534>. The amplified 16S rRNA gene fragments in each library were purified using the Wizard SV Gel and PCR Clean-Up System (Promega, Madison, WI, USA) according to manufacturer's protocols. A second, 6 cycle PCR was used to add a unique 12 bp barcode (Hamady et al., 2008) to each amplicon library using a forward primer containing the barcode+M13 forward sequence (5'-3') and the 785R primer (See the file Supplementary Information). The resulting barcoded PCR products were quantified using the QuBit HS assay (Life Technologies, Carlsbad, CA, USA), pooled in equimolar amounts, and concentrated to a final volume of 80 µL using two Amicon® Ultra-0.5 mL 30K Centrifugal Filters (Millipore). The final pooled library was then submitted for sequencing on the MiSeq platform using PE250 V2 chemistry (Illumina, San Diego, CA, USA).

Sequence Analysis

After sequencing, reads were merged using PEAR (Zhang et al., 2014), demultiplexed in QIIME (Caporaso et al., 2010b), filtered by quality, and clustered into operational taxonomic units (OTUs) using UPARSE (Edgar, 2013). Taxonomy of each OTU was assigned using UCLUST (Edgar, 2010) and the SILVA database (Release 119) (Pruesse et al., 2007). A representative sequence of each OTU was aligned with pyNAST (Caporaso et al., 2010a) against an aligned version of the SILVA r119 database, and filtered to remove uninformative bases. A phylogenetic tree was generated using the maximum likelihood method and a Jukes Cantor evolution model within FastTree (Price et al., 2010), and used for community composition analyses. Multiple diversity metrics including abundance-based coverage estimation (ACE; (Magurran, 2013)), the number of observed OTUs, and the Shannon equitability index, which is the inverse of the Shannon index H ($H = \sum_{i=1}^{Species} \frac{n_i}{N} \ln \frac{N}{n_i}$) (Shannon, 1948), were used at a normalized sequence depth ($n = 6000$). Differences in community composition were estimated using weighted and unweighted UniFrac indices (Lozupone and Knight, 2005). A tree comparing samples was generated with the Unweighted Pair Group Method with Arithmetic Mean (UPGMA) method based on a jackknifed distance matrix of the weighted UniFrac index. Each library was subsampled to 6000 reads to generate a weighted UniFrac distance matrix for comparison among landfill leachate samples, and 300 reads to generate an unweighted UniFrac distance matrix for the meta-analysis of multiple microbial communities. A core microbiome was computed for all samples within QIIME. A mapping file is included as Table S2, and the commands used to produce the final BIOM file are publicly available at

<http://dx.doi.org/10.5281/zenodo.15665>. Unclassified OTUs were identified during analysis in QIIME. Representative sequences aligned to the latest SILVA database, were added to the non-redundant tree (SILVA r123 NR99) within the phylogenetic software package ARB (Ludwig et. al 2004) in order to approximate taxonomy based on phylogeny. Closely related sequences were marked and retained with the unclassified OTU sequences to form the phylogenetic tree in Fig. S1.

Meta-Analysis of Microbial Communities

To compare the microbial assemblages in landfill leachate to those in other environments, datasets representing a broad diversity of environments were obtained from qiita.microbio.me. These studies represented diverse environments including sediments, soils (QIITA Study 619), saline and fresh waters (Caporaso et al., 2011), bog and permafrost soils (QIITA Study 1036), contaminated sediments and waters (QIITA Studies 1039 and 1197), sediments near the Deepwater Horizon Oil Spill (QIITA Study 1198), waste water treatment plant effluent, and human and canine associated microbiomes (Caporaso et al., 2012). A QIIME compatible mapping file of the samples used for the meta-analysis is included in Table S3. Closed reference OTU picking was required for the meta-analysis because different primers were used to generate the 16S rRNA gene fragments in each of these libraries. The OTUs were clustered using UCLUST (Edgar, 2010) and the SILVA database (release 119) as a reference, which itself was clustered at 97% sequence similarity. An even sampling depth of 300 sequences per sample was chosen for ordination of all samples using an unweighted UniFrac distance matrix.

Statistical Analyses

To assess the significance of *a priori* predictions, a non-parametric permutational multivariate analysis of variance (PERMANOVA) test was run within QIIME using the *adonis* method. All PERMANOVA analyses used the weighted UniFrac distance matrix as the community matrix input, which was then compared against categorical and continuous environmental variables. Multiple PERMANOVA analyses were run for *post hoc* testing of environmental variables (Table S4) and CECs (Tables S5). Given the large number of variables tested, p-values were adjusted with the false discovery rate (FDR) method (Benjamini and Yekutieli, 2001) using the command *p.adjust* in R. All other statistical analyses were performed within QIIME using the R package “*vegan*” (Dixon, 2003). As a final exploratory method for correlations not assumed *a priori*, the Bio-Env method (Clarke and Ainsworth, 1993) was used to identify combinations of continuous environmental parameters that were best correlated with community composition. Iterative comparisons between the weighted UniFrac distance matrix and the Euclidian distances generated by selected physiochemical categories listed in Table S6 were used to identify the subset of selected categories that best explains the variation in the distance matrix describing the microbial assemblages in landfill leachates.

Data Availability

After sequencing, raw reads were deposited in the NCBI sequence read archive (SRA) under the accession number SRX864556 (<http://www.ncbi.nlm.nih.gov/sra>). Raw sequencing reads generated in this study used for meta-analyses are deposited in the SRA under the accession number SRX1629938. The mapping file used to generate the BIOM file needed for figure generation is given in Table S2.

Results

Over 1 million high quality reads from triplicate leachate samples of 19 landfills were retained after processing for quality and removal of chimeric sequences. A total of 4987 OTUs were detected among all samples, representing a broad taxonomic diversity at 97% sequence similarity. More than 10% of all OTUs at CO, CA, OK1, TX, and WY were designated as “unclassified” (Fig. 2). The largest unclassified OTU, OTU2 was most closely related to mitochondrial 16S rRNA gene sequences from the eukaryotic fungal-like Oomycetes. All other “unclassified” OTUs represented a broad phylogenetic distribution (Fig. S1) and were present in low abundance in any leachate sample.

The most abundant taxa across all landfill leachates were numerous lineages of the Proteobacteria, including the Beta-, Delta-, Epsilon-, and Gammaproteobacteria. Alphaproteobacteria were detected in relative abundances below 5% in all tested landfills (Fig. 3). The abundance of the Proteobacteria differed between groups of landfills, with the Deltaproteobacteria being the most abundant at TX, OK1, CO, CA, and MN. The abundance of Deltaproteobacteria was distributed between numerous lineages, with the Syntrophobacterales, Desulfuromonadales, and Desulfovibrionales being the most abundant. The landfill leachates from ME1, ME2, ME3, MN, VT, and IA contained the highest relative abundance of Epsilonproteobacteria (> 15%), which were composed almost entirely of members of the order Campylobacterales (Fig. 3). The Betaproteobacteria were present across all landfills, yet they were the most abundant at KY, AR, and AZ (>10%), and primarily were composed of members of the order Burkholderiales. An exception was at AZ, where members of the order Hydrogenophilales were the most abundant Betaproteobacteria. The

Gammaproteobacteria were present in all landfills, with the highest abundance observed at AR, AZ, ME3, MN, and VT. The order Pseudomonadales was the most abundant across almost all landfills, although OK1 contained a population of Methylococcales and a correspondingly lower relative abundance of the Pseudomonadales. The Bacteroidetes and Firmicutes composed the next two most abundant phyla at almost all landfills, and were dominated by the Bacteroidales and Clostridiales. Relative abundances of detected OTUs can be found in Table S8, and the absolute abundances of each OTU can be found in Table S9.

Members of the Archaea were notably low in relative abundance, ranging from 0.8% to 4.35% across most landfills, with the exception of CA and VA, which contained between 6.28% and 9.33% Euryarchaeota (Fig. 2). No Crenarchaea were detected, and the Thaumarchaeota ranged from 0 to 0.03% in any landfill. The OTUs most closely related to methanogenic archaea were detected at the highest abundance in WA and VA. Each contained a different assemblage of methanogens, with WA primarily containing members of the order Methanobacteriales, with the most abundant OTU (1.62 to 2.16%) related to the genus *Methanothermobacter*. The landfill in VA, however, contained an OTU most closely related to the candidate genus "*Methanomethylophilus*", within the order Thermoplasmatales. Interestingly, this candidate genus was also recently detected in a directed search for archaea within a landfill in India (Yadav et al., 2015). These close relatives of the genus "*Methanomethylophilus*" were the most abundant methanogens detected across any sample, with a relative abundance of 4.58% to 5.58% within the VA landfill.

The species richness in each landfill leachate sample was expressed as the number of

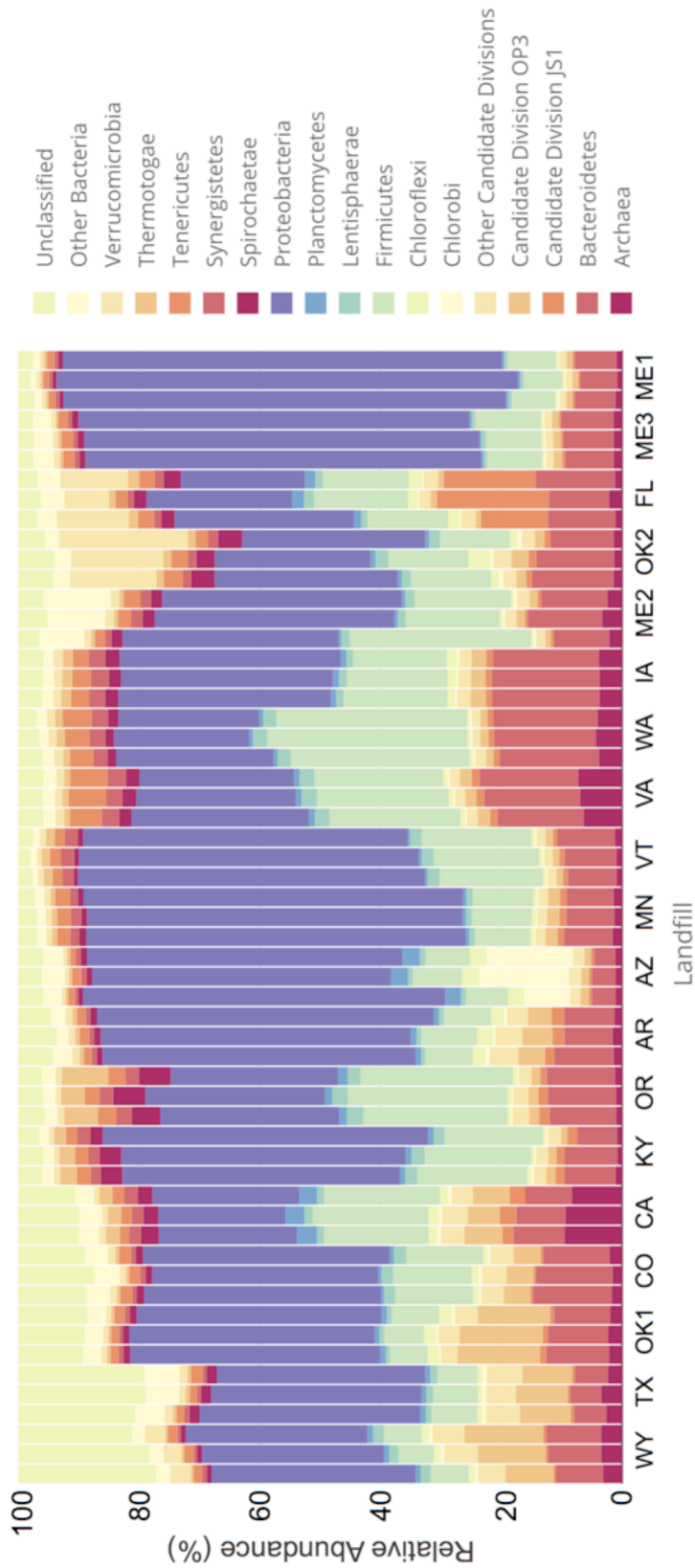


Figure 2. Taxonomic summary showing percent relative abundance of bacterial and archaeal phyla from sampled landfill leachates. Taxa representing less than an average of 1% relative abundance are grouped together as “Other Bacteria” or “Other candidate divisions” for clarity.

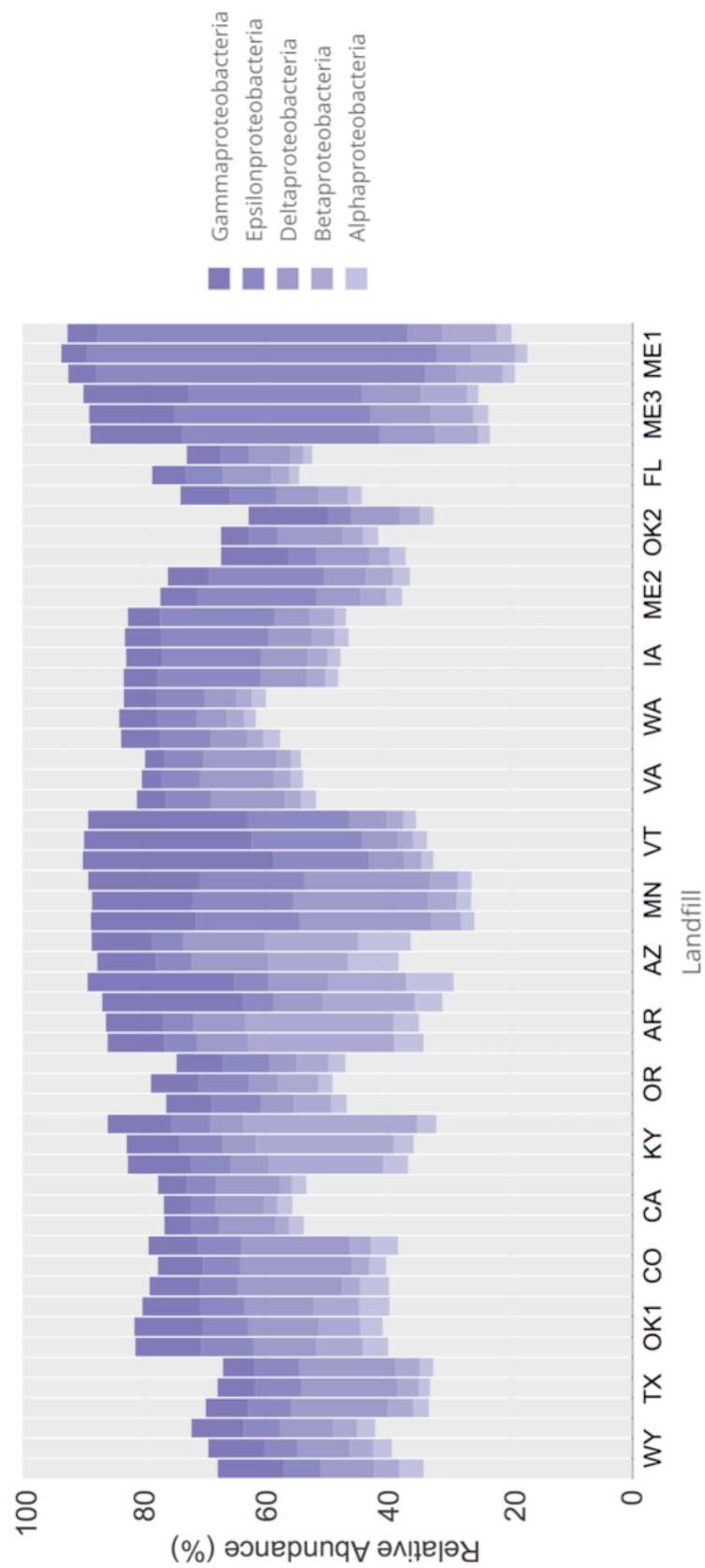


Figure 3: Taxonomic summary showing percent relative abundance of classes within the most abundant phylum, Proteobacteria

observed OTUs as a function of sample read depth in Table 1. Specific diversity values for each landfill are included in Table S7. In addition to high species richness, the relative abundance of OTUs present in each landfill leachate sample was distributed rather evenly, as indicated by Shannon's equitability values (E_H) above 0.700 for all samples with the exception of ME1. Samples from ME1 were the least even (median E_H of 0.643), which could be explained by the high relative abundance of Epsilonproteobacteria (Fig. 3). The abundant Epsilonproteobacterial OTUs in ME1 were members of the order Campylobacterales and closely related to the genus *Arcobacter* (Table S8). Because of the enrichment of the Campylobacterales, samples from ME1 were considered outliers and excluded from further ordination or analysis. Of the 4987 OTUs detected across all landfill leachates, only 147 OTUs (2.9% of all detected OTUs) were shared across all landfills. This core microbiome, however, represented 49% of all sequence reads in the study and represented the broad abundant taxonomic lineages detected in the landfill survey (Table S10).

Table 1. Summary of diversity indices^a across all tested landfill leachates.

Metric	Min	Max	Median
ACE	1776.077	2511.951	2172.765
PD	20.725	30.400	25.090
Observed OTUs	874.900	1396.500	1181.150
E_H	0.612	0.885	0.817

^a Values given represent minimum, maximum, and median values for abundance-based coverage estimation (ACE), Faith's Phylogenetic Diversity (PD), number of observed OTUs (Obs OTUs), and Shannon's equitability index values (E_H). A more detailed summary of diversity indices is available as Table S7.

The leachate microbial assemblages formed four significantly distinct clades ($p < 0.001$, $R^2 = 0.586$), with two outlying landfills (CA and WY) based on the phylogenetic similarity between samples (weighted and unweighted UniFrac) using the UPGMA method (Fig. 4). All landfill leachate microbial assemblages were unique among all other ecosystems included in the meta-analysis, based on a Principle Coordinate Analysis (Fig. 5). The results of the meta-analysis suggested that the selective forces within the landfill were unique.

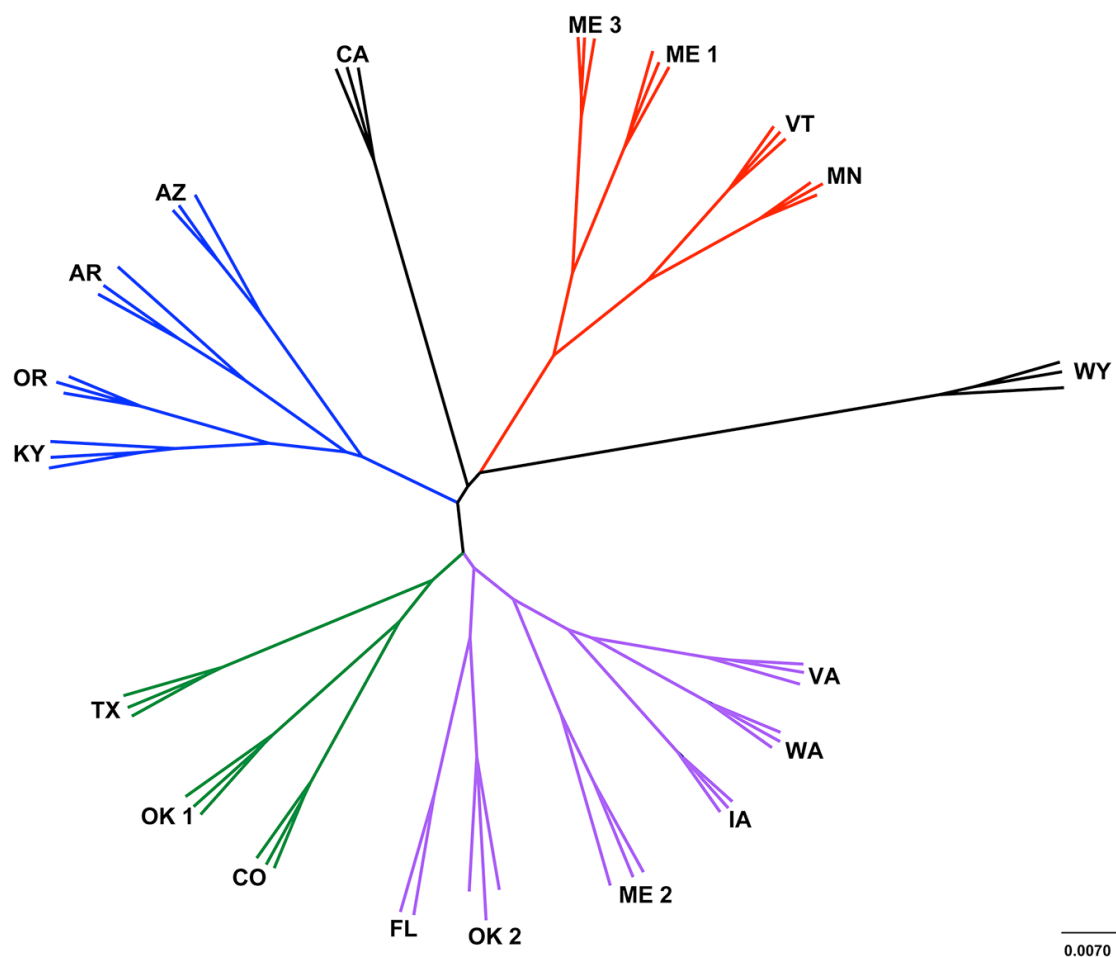


Figure 4: Cluster analysis of landfill leachates represented by a jackknifed UPGMA tree. Clade A (green) contained TX, OK1, and CO; clade B (red) contained ME1, ME3, VT and MN; clade C (purple) contained VA, WA, IA, ME2, OK2, and FL; and clade D (blue) contained AZ, AR, OR, and KY. Two landfills, CA and WY (black) were outliers to the other four distinct clades.

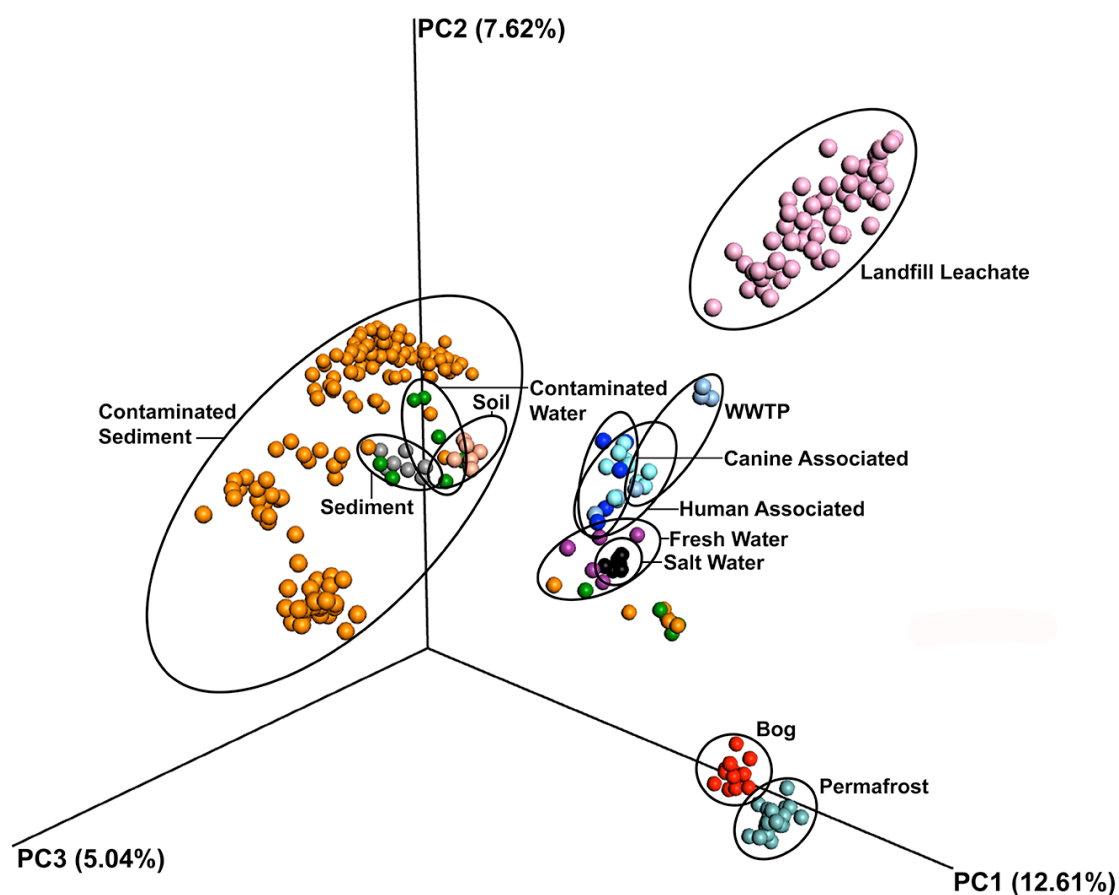


Figure 5. Principal component ordination analysis of microbial communities from diverse environments based on an unweighted UniFrac distance matrix, showing the distinct grouping of communities in landfill leachate sampled for this study from all others. Samples are colored by source.

Results of multiple PERMANOVA analyses suggested that while all parameters tested *a priori* were significant, the separation (indicated by the R^2 value) was poor (Table 2).

Testing the prediction that landfills would cluster by rainfall amounts produced a significant p-value ($p=0.001$), however the R^2 value was low (0.073) indicating poor separation of the communities by this variable alone. Instead, samples separated more clearly by geographic region ($p=0.01$, $R^2=0.357$). Of the other 159 geochemical and environmental parameters available, *post hoc* tests suggested that 125 were significant ($p\leq 0.05$), yet only sixteen R^2 values were above 0.10 (Table S6). The only CECs with an R^2 above 0.10 were camphor and chloroxylonol.

Table 2. PERMANOVA results of regional or operational parameters assumed to be significant *a priori*

Parameter	p-value	R^2 Value
Region	0.001	0.357
Rainfall	0.001	0.073
Age (Class)	0.001	0.117
Waste (Mton/Yr)	0.001	0.070
Leachate Produced (Mgal/Yr)	0.003	0.055
Waste Dissolution Time	0.006	0.052

The exploratory statistical method Bio-Env was used to identify combinations of variables that best explained the distribution of weighted UniFrac distances among the

landfill leachate microbial assemblages. The concentrations of barium and chloride, and the mean evapotranspiration time were identified as explanatory variables with the highest correlation ρ (rho) value of 0.568 (Table S11). A similar, but slightly lower ρ value of 0.533 was obtained that included the above variables, as well as age of waste and the number of detected household chemicals (Table S11; Masoner et al., 2014).

The microbial assemblages found in the landfill leachate samples were compared among each other and against the microbiomes of sediments, soils, fresh water, salt water, bogs, permafrost, humans, and canines. Ordination based on unweighted UniFrac distances from a total of 65697 OTUs revealed that microbial assemblages from landfill leachates formed a significantly ($p < 0.001$, $R^2 = 0.294$) distinct and distant clade (Fig. 5). Likewise, the microbial assemblages from soil, sediment, marine or freshwater, bogs and permafrost, and mammals largely clustered to the exclusion of one another.

Discussion

Much of what is produced and used by humans is eventually disposed of in a landfill along with its resident microorganisms. Landfills are, therefore, a potential final resting place for much of the human-derived (i.e. the built) environment and its biodegradation. The degradation of this waste releases greenhouse gases and solubilizes a vast array of chemicals including CECs (Masoner et al., 2014).

Landfills are home to diverse assemblages of bacteria and archaea capable of a broad range of biodegradation activities (Mori et al., 2003; Gomez et al., 2011; Lu et al., 2012). Consequently, microbial metabolism is a primary driver of the degradation of MSW in landfills, resulting in the release of Non-Volatile Dissolved Organic Carbon

(NVDOC), CECs, and landfill gases. These microbial communities are difficult to study, partly due to the high physical and chemical heterogeneity of a landfill. Previous studies have attempted to address this heterogeneity by collecting a large number of samples at a single landfill (Palmisano and Barlaz, 1996) or sampling a single location within a landfill to better understand the stratification and therefore the age of waste (Suflita et al., 1992). Both of these approaches can be costly, time-prohibitive, and still represent only a small cross section of the broad distribution of deposited waste. Other studies of landfills have investigated landfill cores or cover soils (Henneberger et al., 2014). These studies did not view landfills in a greater context, or as a single potentially novel biome. Unlike previous studies investigating the microbial communities of landfills (McDonald et al., 2010; Mouser et al., 2010; Lu et al., 2012), the study described here is the first to investigate a large number of landfills through sampling of leachate and high throughput sequencing of 16S rRNA gene libraries. Landfill leachate flows by the path of least resistance through the landfill and arguably is more representative of the broader microbiological communities in a large number of landfills.

The microbiomes characterized in the sampled landfill leachates grouped into four primary clades (Fig. 3). Leachate microbiomes in clade A were composed predominantly of members of the Clostridiales. Notably, no single family within the Clostridiales was dominant. Instead, a large number of different members of the Clostridiales appeared to inhabit the landfills within clade A. The Ruminococcaceae were the most abundant single family (3-6%), members of which are associated with the degradation of cellulose, a common carbon source within landfills and within

mammalian guts (Hungate 1966). In addition, members of the Peptococcaceae, Campylobacterales, and Bacteroidales have all been correlated with the degradation of hydrocarbons in multiple environments (Lyles et al., 2013), similar to the CECs detected within the landfills studied (Masoner et al., 2014).

The microbiomes in leachate samples within clade B were unique in the abundance of members of the order Campylobacterales. Almost half of the sequences in one landfills in clade B grouped within a single OTU within the Campylobacteraceae that was most closely related to the genus *Arcobacter*. Members of the genus *Arcobacter* have been discovered previously in MSW leachate plumes (Huang et al., 2005; Tian et al., 2005), wastewater effluent streams (Santos et al., 2009; Merga et al., 2014), and are commonly associated with pathogenesis (Vandenberg et al., 2004). To the exclusion of the Campylobacteraceae, the abundance of members of the order Pseudomonadales was also a notable trait of leachate microbiomes in this clade. Detected members of the Pseudomonadales were most closely related to the genera *Pseudomonas* and *Acinetobacter*, both of which are capable of mineralizing many of the recalcitrant aromatic compounds present in MSW (Beal and Betts, 2000). In addition, landfills within this clade were less diverse than any other grouping of landfills. This was due to the abundance of the Campylobacteraceae, possibly due to the intrusion of dissolved oxygen in the leachates of this clade, although this prediction was not tested during the chemical study of the landfills.

Landfill leachate microbiomes within clade C were unique in their relative dissimilarity to all other landfills (Fig. 3). Their microbiomes were phylogenetically diverse, and included members of the Chlorobi and within one landfill (FL), OP9. Detected members

of the Chlorobi were closely related to uncultured lineages of the class Ignavibacteriales, which contains organisms capable of fermentation under slightly thermophilic conditions (Iino et al., 2010; Podosokorskaya et al., 2013). Single-cell genomic and metagenomic approaches have identified members of candidate division OP9 as being capable of anaerobic, fermentative metabolism of sugars resulting in the production of hydrogen, acetate, and ethanol (Dodsworth et al., 2013). The OP9 genomes also contained genes for putative glucohydrolase and endonuclease enzymes that could be used for the catabolism of (hemi)celluloses. While (hemi)cellulose was not specifically assayed for, FL was depleted in low molecular weight carbon sources such as acetate, yet high in NVDOC relative to the other sampled landfills.

Landfills grouping within clade D contained a larger population of the candidate division OP3, Methylococcales, and the Desulfobacterales. Except for AR, these landfills displayed a high concentration of barium (AZ, KY, and OR) and a correspondingly low concentration of sulfate (Table S4). Members of the candidate division OP3 belong to the PVC superphylum. Metagenomic and single-cell genome studies have revealed that members of OP3 share characteristics with the Deltaproteobacteria, including the ability to reduce sulfate (Glöckner et al., 2010). Sulfate reduction of barite, which is found in clays, drilling muds, paint, paper, cloth, and rubber, could produce the high concentration of barium observed (Ulrich et al., 2003).

Outlying landfills (WY and CA) were also notable in the abundance of the Euryarchaeota and unclassified OTUs. For instance, a single unclassified OTU represented between 6% and 13% of detected taxa at the WY landfill that was most

closely related to mitochondrial sequence from Oomycetes. These organisms are similar in morphology to fungi and capable of degrading a broad diversity of carbohydrates (Horner et al., 2012), but the specific role they may play in landfills is unknown (Lockhart et al., 2006). Other unclassified members of the community were related to clones found in subsurface waters, or oxygen minimum zones (Divya et al., 2011), which along with the abundance of Deltaproteobacteria and OP3 suggest that the landfills of clade D are oxygen depleted. The landfill CA contained the highest percentage of methanogenic archaea of any landfill leachate sampled, along with the high relative abundance (5.7-6.9%) of Thermoplasmatales (composite relative abundance for all Thermoplasmatales OTUs in Table S8). Members of the Thermoplasmatales are commonly acidophilic thermophiles that are not known to be methanogenic, although recent research has shown that a candidate genus "*Methanomethylophilus*", within the order Thermoplasmatales is capable of methanogenesis (Paul et al., 2012; Yadav et al., 2015). Based on their abundance in landfills in this study and others (Yadav et al., 2015), landfills appear to be an ecosystem that favors these novel methanogens.

The findings described in this study suggest that landfills are a source of considerable bacterial and archaeal diversity. A functional gene array-based survey of groundwater impacted by landfill leachate however, suggested that diversity decreases with proximity to landfill sites (Lu et al., 2012). One explanation for the findings of Lu et al. would be that genes from the abundant, deeply branching bacterial lineages detected in this study may have little homology to the probes on their gene array. Alternatively, the microorganisms found in landfill leachates may not be capable of surviving in the more

dilute groundwater environment, and the diversity of microorganisms in the impacted groundwater may be negatively impacted by the leachate chemistry, thus explaining the reduction in organismal diversity. Metagenomic characterization of landfills could provide some insight towards the functional genes of the unclassified, but abundant populations across many landfill leachate systems.

More than 100 geochemical and environmental parameters were tested *post hoc* in this study. Such a large number of tested parameters caused difficulty by likely resulting in spurious correlations. To reduce the effect of such a large number of pairwise comparisons, we employed FDR correction of p-values. A complex set of CECs were present in the leachate from most of the 19 landfills in this study, with rainfall previously implicated as a predictor of CEC abundance (Masoner et al., 2014). The majority of CECs and rainfall also had an effect on microbial community structure and composition ($p < 0.05$), but the low R^2 values suggested that their influence on the distribution and relative abundance of the microbial population was minimal. This finding would reject the prediction that rainfall strongly influences the overall distribution and relative abundance of microbial communities in landfill leachate. Instead, the single most powerful influence on landfill community distribution and composition appeared to be geographic region, suggesting that numerous regional factors play a role in establishing the members of the landfill leachate microbial community. Examples of contributing regional factors might include climate conditions, the composition of deposited wastes, and the geochemistry of soils used for entombment.

Much like the varied input to the landfills, a combination of parameters instead of any

single input may have the greatest impact on the overall observed diversity of landfills. In combination, the concentration of barium and chloride, the rate of evapotranspiration, and the age of waste were variables that best explained the distribution of microbial composition across all landfill leachates sampled. Only a small number of CECs detected could be considered as producing a significant effect and more than a minimal correlation. It is possible that this is due to the reduced statistical power of running such a large number of tests. An alternative explanation for this would be that the resident microbial community at each site is either unaffected by many of the CECs, does not interact with them in any meaningful way, or both.

This study affirms that landfills and their leachates foster a unique microbiome, essentially distinct from any ecosystem previously investigated (Fig. 4). When using a conservative OTU picking method, such as UPARSE, over 4000 OTUs were detected across the characterized microbiomes. The large number and phylogenetic diversity of OTUs is likely due to the large number of available niches linked, in part, to the diversity of possible soluble electron acceptors and oxidizable substrates present within the leachate of each landfill (Masoner et al., 2014). These compounds are dispersed throughout the depositional structure of a landfill. Over time, however, endogenous water production, water infiltration, and rainfall allow the chemistry and biology to potentially come together, and produce the unique geochemical composition of landfill leachate. While not all deposited materials in a landfill will solubilize, landfill leachate still contains a large quantity of dissolved organic components (Nanny and Ratasuk, 2002). Over time scales spanning hours (initially) to seasons and decades, there is significant variation in the availability of electron acceptors and carbon sources

(Cozzarelli et al., 2011). The result of this variability is an environment under constantly changing selective pressures, which could also account for the high evenness and species (OTU) richness seen across the leachate microbial assemblages. The landfill leachate, therefore, represents a rich, diverse “seed bank” (Konopka et al., 2014) potentially able to respond to the extensive and varying chemical inputs a landfill receives. This study did not attempt to study landfill leachates over time, and therefore cannot specifically address the temporal influence potentially driving the microbial community of this unique biome.

The daily deposition of heterogeneous materials into landfills and their progressive biodegradation create a unique selective landscape responsible for the novel biodiversity found in their leachates. This biodiversity is an untapped source of genomic, metabolic, and biochemical innovation with great potential benefit to bioremediation efforts, bioindustrial processes, and the discovery of new natural products. The work presented here provides the foundation for subsequent efforts that should focus on establishing direct links between observed unclassified taxa and their metabolic capabilities. Directed and novel cultivation-based approaches could lead to the enrichment of consortia or isolation of individual microorganisms capable of degrading targeted compounds (Nichols et al., 2010; Stevenson et al., 2004).

Additionally, metagenomics and single-cell genomics approaches have proven invaluable in characterizing the putative metabolic capacity of yet uncultured organisms (Dodsworth et al., 2013; McLean et al., 2013; Stamps et al., 2014; Nobu et al., 2015).

Landfills and their leachates are an essential component in modeling the interaction between humanity and the biosphere, and therefore should be included in the ongoing,

coordinated efforts to understand and harness the capabilities of Earth's microbial ecosystems (Alivisatos et al., 2015).

Acknowledgments

The authors would like to acknowledge the efforts of those personnel at each landfill who assisted in collecting leachate samples. Access to landfill sites and sampling was gained through a collaborative effort that included private solid-waste companies, State environmental agencies, and County and municipal governments. This project was supported by the USGS Toxics Substances Hydrology Program under grant #G12AC20148. Any use of trade, firm, or product names is for descriptive purposes only and does not imply endorsement by the U.S. Government.

References

- Alivisatos, A. P., Blaser, M. J., Brodie, E. L., Chun, M., Dangl, J. L., Donohue, T. J., et al. (2015). MICROBIOME. A unified initiative to harness Earth's microbiomes. *Science* 350, 507–508. doi:10.1126/science.aac8480.
- Barlaz, M. A., Schaefer, D. M., and Ham, R. K. (1989). Bacterial population development and chemical characteristics of refuse decomposition in a simulated sanitary landfill. *Appl. Environ. Microbiol.* 55, 55–65.
- Beal, R., and Betts, W. B. (2000). Role of rhamnolipid biosurfactants in the uptake and mineralization of hexadecane in *Pseudomonas aeruginosa*. *J. Appl. Microbiol.* 89, 158–

168. doi:10.1046/j.1365-2672.2000.01104.x.

Benjamini, Y., and Yekutieli, D. (2001). The control of the false discovery rate in multiple testing under dependency. *Ann. Stat.* doi:10.2307/2674075.

Caporaso, J. G., Bittinger, K., Bushman, F. D., DeSantis, T. Z., Andersen, G. L., and Knight, R. (2010a). PyNAST: a flexible tool for aligning sequences to a template alignment. *Bioinformatics* 26, 266–267. doi:10.1093/bioinformatics/btp636.

Caporaso, J. G., Kuczynski, J., Stombaugh, J., Bittinger, K., Bushman, F. D., Costello, E. K., et al. (2010b). QIIME allows analysis of high-throughput community sequencing data. *Nat. Meth.* 7, 335–336. doi:10.1038/nmeth.f.303.

Caporaso, J. G., Lauber, C. L., Walters, W. A., Berg-Lyons, D., Huntley, J., Fierer, N., et al. (2012). Ultra-high-throughput microbial community analysis on the Illumina HiSeq and MiSeq platforms. *ISME J.* 6, 1621–1624. doi:10.1038/ismej.2012.8.

Caporaso, J. G., Lauber, C. L., Walters, W. A., Berg-Lyons, D., Lozupone, C. A., Turnbaugh, P. J., et al. (2011). Global patterns of 16S rRNA diversity at a depth of millions of sequences per sample. *Proc. Natl. Acad. Sci. U.S.A.* 108 Suppl 1, 4516–4522. doi:10.1073/pnas.1000080107.

Clarke, K. R., and Ainsworth, M. (1993). A method of linking multivariate community structure to environmental variables. *Mar. Ecol. Prog. Ser.* 92, 205–219. doi:10.3354/meps092205.

Cozzarelli, I. M., Böhlke, J. K., Masoner, J., Breit, G. N., Lorah, M. M., Tuttle, M. L.

W., et al. (2011). Biogeochemical evolution of a landfill leachate plume, Norman, Oklahoma. *Ground Water* 49, 663–687. doi:10.1111/j.1745-6584.2010.00792.x.

Divya, B., Parvathi, A., Loka Bharathi, P. A., and Nair, S. (2011). 16S rRNA-based bacterial diversity in the organic-rich sediments underlying oxygen-deficient waters of the eastern Arabian Sea. *World J. Microb. Biot.* 27, 2821–2833. doi:10.1007/s11274-011-0760-0.

Dixon, P. (2003). VEGAN, a package of R functions for community ecology. *J Veg. Sci.* 14, 927–930. doi:10.1111/j.1654-1103.2003.tb02228.x.

Dodsworth, J. A., Blainey, P. C., Murugapiran, S. K., Swingley, W. D., Ross, C. A., Tringe, S. G., et al. (2013). Single-cell and metagenomic analyses indicate a fermentative and saccharolytic lifestyle for members of the OP9 lineage. *Nat. Commun.* 4, 1854. doi:10.1038/ncomms2884.

Edgar, R. C. (2010). Search and clustering orders of magnitude faster than BLAST. *Bioinformatics* 26, 2460–2461. doi:10.1093/bioinformatics/btq461.

Edgar, R. C. (2013). UPARSE: highly accurate OTU sequences from microbial amplicon reads. *Nat. Meth.* 10, 996–998. doi:10.1038/nmeth.2604.

Eggen, T., Moeder, M., and Arukwe, A. (2010). Municipal landfill leachates: a significant source for new and emerging pollutants. *Sci. Total Environ.* 408, 5147–5157. doi:10.1016/j.scitotenv.2010.07.049.

Glöckner, J., Kube, M., Shrestha, P. M., Weber, M., Glöckner, F. O., Reinhardt, R., et

- al. (2010). Phylogenetic diversity and metagenomics of candidate division OP3. *Environ Microbiol* 12, 1218–1229. doi:10.1111/j.1462-2920.2010.02164.x.
- Gomez, A. M., Yannarell, A. C., Sims, G. K., Cadavid-Restrepo, G., and Moreno Herrera, C. X. (2011). Characterization of bacterial diversity at different depths in the Moravia Hill landfill site at Medellín, Colombia. *Soil Biol. Biochem.* 43, 1275–1284. doi:10.1016/j.soilbio.2011.02.018.
- Gurijala, K. R., and Suflita, J. M. (1993). Environmental factors influencing methanogenesis from refuse in landfill samples. *Environ. Sci. Technol.* 27, 1176–1181. doi:10.1021/es00043a018.
- Hamady, M., Walker, J. J., Harris, J. K., Gold, N. J., and Knight, R. (2008). Error-correcting barcoded primers for pyrosequencing hundreds of samples in multiplex. *Nat. Meth.* 5, 235–237. doi:10.1038/nmeth.1184.
- Henneberger, R., Chiri, E., Bodelier, P. E. L., Frenzel, P., Lüke, C., and Schroth, M. H. (2014). Field-scale tracking of active methane-oxidizing communities in a landfill cover soil reveals spatial and seasonal variability. *Environ. Microbiol.* doi:10.1111/1462-2920.12617.
- Hoornweg, D., Bhada-Tata, P., and Kennedy, C. (2013). Environment: Waste production must peak this century. *Nature* 502, 615–617. doi:10.1038/502615a.
- Horner, N. R., Grenville-Briggs, L. J. & van West, P. (2012). The oomycete *Pythium oligandrum* expresses putative effectors during mycoparasitism of *Phytophthora infestans* and is amenable to transformation. *Fungal Biol.* **116**, 24–41.

- Huang, L. N., Zhu, S., Zhou, H., and Qu, L. H. (2005). Molecular phylogenetic diversity of bacteria associated with the leachate of a closed municipal solid waste landfill. *FEMS Microbiol. Lett.* 242, 297–303. doi:10.1016/j.femsle.2004.11.021.
- Hungate, R.E. (1966) *The rumen and its microbes*. 1966. Academic Press, Inc.
- Iino, T., Mori, K., Uchino, Y., Nakagawa, T., Harayama, S., and Suzuki, K.-I. (2010). *Ignavibacterium album* gen. nov., sp. nov., a moderately thermophilic anaerobic bacterium isolated from microbial mats at a terrestrial hot spring and proposal of *Ignavibacteria* classis nov., for a novel lineage at the periphery of green sulfur bacteria. *Int. J. Syst. Evol. Microbiol.* 60, 1376–1382. doi:10.1099/ij.s.0.012484-0.
- Klindworth, A., Pruesse, E., Schweer, T., Peplies, J., Quast, C., Horn, M., et al. (2013). Evaluation of general 16S ribosomal RNA gene PCR primers for classical and next-generation sequencing-based diversity studies. *Nucleic Acids Res.* 41, e1. doi:10.1093/nar/gks808.
- Konopka, A., Lindemann, S., and Fredrickson, J. (2014). Dynamics in microbial communities: unraveling mechanisms to identify principles. *ISME J.* doi:10.1038/ismej.2014.251.
- Lockhart, R. J., Van Dyke, M. I., Beadle, I. R., Humphreys, P. & McCarthy, A. J. (2006). Molecular biological detection of anaerobic gut fungi (Neocallimastigales) from landfill sites. *Appl. Environ. Microbiol.* 72, 5659–5661.
- Lozupone, C., and Knight, R. (2005). UniFrac: a new phylogenetic method for comparing microbial communities. *Appl. Environ. Microbiol.* 71, 8228–8235.

doi:10.1128/AEM.71.12.8228-8235.2005.

Lu, Z., He, Z., Parisi, V. A., Kang, S., Deng, Y., Van Nostrand, J. D., et al. (2012). GeoChip-based analysis of microbial functional gene diversity in a landfill leachate-contaminated aquifer. *Environ. Sci. Technol.* 46, 5824–5833. doi:10.1021/es300478j.

Ludwig, W., Strunk, O., Westram, R., Richter, L., Meier, H., Yadhukumar, et al. (2004). ARB: a software environment for sequence data. *Nucleic Acids Res.* 32, 1363–1371. doi:10.1093/nar/gkh293.

Lyles, C. N., Aktas, D. F., Duncan, K. E., Callaghan, A. V., Stevenson, B. S., and Sufliata, J. M. (2013). Impact of organosulfur content on diesel fuel stability and implications for carbon steel corrosion. *Environ. Sci. Technol.* 47, 6052–6062. doi:10.1021/es4006702.

Magurran, A. E. (2013). *Measuring Biological Diversity*. John Wiley & Sons.

Masoner, J. R., Kolpin, D. W., Furlong, E. T., Cozzarelli, I. M., Gray, J. L., and Schwab, E. A. (2014). Contaminants of emerging concern in fresh leachate from landfills in the conterminous United States. *Env. Sci. Process. Impact* 16, 2335–2354. doi:10.1039/c4em00124a.

Masoner, J. R., Kolpin, D. W., Furlong, E. T., Cozzarelli, I. M., and Gray, J. L. (2015). Landfill leachate as a mirror of today's disposable society: Pharmaceuticals and other contaminants of emerging concern in final leachate from landfills in the conterminous United States. *Environmental Toxicology and Chemistry* 35, 906–918. doi:10.1002/etc.3219.

- McDonald, J. E., Allison, H. E., and McCarth, A. J. (2010). Composition of the landfill microbial community as determined by application of domain- and group-specific 16S and 18S rRNA-targeted oligonucleotide probes. *Appl. Environ. Microbiol.* 76, 1301–1306. doi:10.1128/AEM.01783-09.
- McInerney, M. J., Sieber, J. R., and Gunsalus, R. P. (2009). Syntrophy in anaerobic global carbon cycles. *Curr. Opin. Biotechnol.* 20, 623–632.
doi:10.1016/j.copbio.2009.10.001.
- McLean, J. S., Lombardo, M.-J., Badger, J. H., Edlund, A., Novotny, M., Yee-Greenbaum, J., et al. (2013). Candidate phylum TM6 genome recovered from a hospital sink biofilm provides genomic insights into this uncultivated phylum. *Proc. Natl. Acad. Sci. U.S.A.* 110, E2390–9. doi:10.1073/pnas.1219809110.
- Merga, J. Y., Royden, A., Pandey, A. K., and Williams, N. J. (2014). *Arcobacter* spp. isolated from untreated domestic effluent. *Lett. Appl. Microbiol.* 59, 122–126.
doi:10.1111/lam.12256.
- Mori, K., Sparling, R., Hatsu, M., and Takamizawa, K. (2003). Quantification and diversity of the archaeal community in a landfill site. *Can. J. Microbiol.* 49, 28–36.
doi:10.1139/w03-006.
- Mormile, M. R., Gurijala, K. R., Robinson, J. A., McInerney, M. J., and Suflita, J. M. (1996). The importance of hydrogen in landfill fermentations. *Appl. Environ. Microbiol.* 62, 1583–1588.
- Mouser, P. J., Rizzo, D. M., Druschel, G. K., Morales, S. E., Hayden, N., O'Grady, P.,

et al. (2010). Enhanced detection of groundwater contamination from a leaking waste disposal site by microbial community profiles. *Water Resour. Res.* 46, n/a–n/a. doi:10.1029/2010WR009459.

Nanny, M. A., and Ratasuk, N. (2002). Characterization and comparison of hydrophobic neutral and hydrophobic acid dissolved organic carbon isolated from three municipal landfill leachates. *Water Res.* 36, 1572–1584.

Nichols, D., Cahoon, N., Trakhtenberg, E. M., Pham, L., Mehta, A., Belanger, A., et al. (2010). Use of iChip for high-throughput in situ cultivation of “uncultivable” microbial species. *Appl. Environ. Microbiol.* 76, 2445–2450. doi:10.1128/AEM.01754-09.

Nobu, M. K., Narihiro, T., Rinke, C., Kamagata, Y., Tringe, S. G., Woyke, T., et al. (2015). Microbial dark matter ecogenomics reveals complex synergistic networks in a methanogenic bioreactor. *ISME J.* 9, 1710–1722. doi:10.1038/ismej.2014.256.

Oldham, A. L., Drilling, H. S., Stamps, B. W., Stevenson, B. S., and Duncan, K. E. (2012). Automated DNA extraction platforms offer solutions to challenges of assessing microbial biofouling in oil production facilities. *AMB Express* 2, 60.

Pal, A., Gin, K. Y.-H., Lin, A. Y.-C., and Reinhard, M. (2010). Impacts of emerging organic contaminants on freshwater resources: review of recent occurrences, sources, fate and effects. *Sci. Total Environ.* 408, 6062–6069. doi:10.1016/j.scitotenv.2010.09.026.

Palm, A., Cousins, I. T., Mackay, D., Tysklind, M., Metcalfe, C., and Alaei, M. (2002). Assessing the environmental fate of chemicals of emerging concern: a case study of the

polybrominated diphenyl ethers. *Environ. Pollut.* 117, 195–213. doi:10.1016/S0269-7491(01)00276-7.

Palmisano, A. C., and Barlaz, M. A. (1996). *Microbiology of Solid Waste*. CRC Press.

Paul, K., Nonoh, J. O., Mikulski, L., and Brune, A. (2012). “Methanoplasmatales,” Thermoplasmatales-related archaea in termite guts and other environments, are the seventh order of methanogens. *Appl. Environ. Microbiol.* 78, 8245–8253. doi:10.1128/AEM.02193-12.

Podosokorskaya, O. A., Kadnikov, V. V., Gavrilov, S. N., Mardanov, A. V., Merkel, A. Y., Karnachuk, O. V., et al. (2013). Characterization of *Melioribacter roseus* gen. nov., sp. nov., a novel facultatively anaerobic thermophilic cellulolytic bacterium from the class Ignavibacteria, and a proposal of a novel bacterial phylum Ignavibacteriae. *Environ. Microbiol.* 15, 1759–1771. doi:10.1111/1462-2920.12067.

Price, M. N., Dehal, P. S., and Arkin, A. P. (2010). FastTree 2 – Approximately maximum-likelihood trees for large alignments. *PLoS One* 5, e9490. doi:10.1371/journal.pone.0009490.

Pruesse, E., Quast, C., Knittel, K., Fuchs, B. M., Ludwig, W., Peplies, J., et al. (2007). SILVA: a comprehensive online resource for quality checked and aligned ribosomal RNA sequence data compatible with ARB. *Nucleic Acids Res.* 35, 7188–7196. doi:10.1093/nar/gkm864.

Santos, A. L., Peixoto, R., and Rosado, A. S. (2009). New approaches to understanding microbial diversity in wastewater, landfills and leachate treatment. *Oecologia Australis*

13, 631-648.

Shannon, C. E. (1948). A mathematical theory of communication. *The Bell System Technical Journal* 27, 379–423.

Stamps, B. W., Corsetti, F. A., Spear, J. R., and Stevenson, B. S. (2014). Draft genome of a novel chlorobi member assembled by tetranucleotide binning of a hot spring metagenome. *Genome Announc.* 2, e00897–14–e00897–14.
doi:10.1128/genomeA.00897-14.

Stevenson, B. S., Eichorst, S. A., Wertz, J. T., Schmidt, T. M., and Breznak, J. A. (2004). New strategies for cultivation and detection of previously uncultured microbes. *Appl. Environ. Microbiol.* 70, 4748–4755. doi:10.1128/AEM.70.8.4748-4755.2004.

Suflita, J. M., Gerba, C. P., Ham, R. K., Palmisano, A. C., Rathje, W. L., and Robinson, J. A. (1992). The world's largest landfill. *Environ. Sci. Technol.* 26, 1486–1495.
doi:10.1021/es00032a002.

Tian, Y. J., Yang, H., Li, D. T., and Lin, Z. X. (2005). Evaluation of the potential for using molecular approaches to deduce redox conditions in groundwater contaminant plumes. *Ann. Microbiol.* 55, 9-16.

Ulrich, G. A., Breit, G. N., and Cozzarelli, I. M. (2003). Sources of sulfate supporting anaerobic metabolism in a contaminated aquifer. *Environ. Sci. Technol.*.
doi:10.1021/es011288a.

Vandenberg, O., Dediste, A., Houf, K., Ibekwem, S., Souayah, H., Cadranet, S., et al.

(2004). *Arcobacter* Species in Humans. *Emerging Infect. Dis.* 10, 1863–1867.

doi:10.3201/eid1010.040241.

Yadav, S., Kundu, S., Ghosh, S. K., and Maitra, S. S. (2015). Molecular analysis of methanogen richness in landfill and marshland targeting 16S rDNA sequences. *Archaea* 2015, 563414–9. doi:10.1155/2015/563414.

Zhang, J., Kobert, K., Flouri, T., Stamatakis, A. (2014). PEAR: a fast and accurate Illumina Paired-End reAd mergeR. *Bioinformatics* 30, 614–620.

doi:10.1093/bioinformatics/btt593.

List of supplementary files

All supplementary files are available online at

<http://journal.frontiersin.org/article/10.3389/fmicb.2016.00534/full>

Supplementary Information: Details of PCR and Barcoding PCR conditions.

Figure S1: Phylogenetic tree based on the non-redundant tree (SILVA r123 NR99) within the phylogenetic software package ARB, which is composed of all unclassified OTUs from landfill leachates and closely related sequences. Taxonomic groupings are

labeled and delineated with brackets. Scale bar represents a nucleotide dissimilarity of 0.10.

Table S1: Volume (mL) filtered and concentration (ng/mL) of DNA recovered from each leachate sample.

Table S2: QIIME-compatible mapping file used for comparison of landfill leachates.

Table S3: QIIME-compatible mapping file used for meta-analyses of microbial communities.

Table S4: Environmental variables for leachates used in PERMANOVA analyses.

Table S5: Concentrations of CECs (ng/mL) for leachates used in PERMANOVA analyses.

Table S6: Results from PERMANOVA analyses of all^a *post hoc* tests of environmental variables and CEC concentrations.

Table S7: Diversity indices for sampled leachate microbiomes.

Table S8: Relative abundance of OTUs detected in each landfill leachate sample.

Table S9: Absolute abundance of OTUs detected in each landfill leachate sample.

Table S10: Taxonomy of OTUs found in the landfill leachate core microbiome.

Table S11: Results of BIOENV analysis.

Chapter 3: Fungal Contamination is the Root Cause of Fouling in USAF B20 Biodiesel Storage Tanks

Foreword

The research discussed within chapter three was a collaborative effort between the University of Oklahoma and the Air Force Research Laboratory (AFRL). My direct contribution was through the collection of samples, DNA extraction, and PCR amplification of samples collected from April 2014 to May of 2015. In addition I conducted all data analyses, participated in experimental design, carried out all aspects of the transcriptomic experiment and assisted in cultivation and characterization of isolated microorganisms. My advisor Dr. Bradley Stevenson conceived of the experiment, assisted in sampling, data interpretation, and advised me on the creation and execution of laboratory experiments. Dr. Heather Nunn assisted in the collection of samples, DNA extraction, and PCR amplification of samples collected from May 2015 to January 2016. James Floyd assisted in the collection of fuels and in the imaging of biofilms. Oderay Andrade cultivated numerous microorganisms from fuels and biofilms collected at each location and assessed their ability to degrade biodiesel. Dr. Wendy J. Crookes-Goodson (AFRL) assisted in site access, collection of samples, and experimental design. Caitlin Bojanowski, Angela Campo, Carrie Drake, Dr. Chia Hung, Pamela Lloyd, and Lloyd Nadeau at AFRL all assisted in the collection of samples.

Abstract

Biodiesel blends have become a common liquid transportation fuel within the United States. One blend (B20 or BDI) is a mixture including 80 % (v/v) Ultra Low Sulfur Diesel (ULSD) and 20 % (v/v) biodiesel. Biodiesel is composed of fatty acid methyl esters (FAME) derived from plant and animal triglycerides. Many fungi and bacteria can readily degrade the FAME and some of the alkanes in B20, suggesting a significant risk to infrastructure may exist. Despite this potential risk, no longitudinal investigations had been conducted previously to study the impact of microbial contamination on fuel storage infrastructure. Biodiesel storage tanks at two locations in the southeastern (SE) and southwestern (SW) US were investigated over the course of eighteen months using a combination of small subunit rRNA gene sequencing, ATP quantification as a proxy for microbial activity, and fuel acidity measurements. Three other locations were sampled at various single time points to determine if bacterial and fungal community members were shared at sites across the US. The bacterial and fungal community structure was significantly different between all tested locations. A small number of bacterial and fungal OTUs were shared between all locations. Isolated fungi were shown to have the genomic capacity to degrade FAME, resulting in acidified fuel. A large number of transcripts were expressed in *Byssoschlamys* sp. for a gene associated with the degradation of FAME, a complete beta-oxidation cycle, and methanol oxidation. The acidification and degradation of B20 could present a risk to storage infrastructure and vehicles. Information from this survey will allow operators to assess the likelihood of biofouling in B20 blends and modify standard operating procedures for the cleaning and storage of B20.

Introduction

In fiscal year 2014, the United States (US) consumed over 19 million barrels of oil per day (Central Intelligence Agency, 2014), making the US the largest consumer of all petroleum products in the world. The US government consumed 1.9 % of this fuel, with the US Air Force (USAF) consuming 58 % of this fuel (Dimotakis et al., 2006). As the world's largest single consumer of liquid transportation fuels, energy independence is a strategic concern to the US and the DoD (Dimotakis et al., 2006, Air Force Energy Plan, 2009). A mandate for the DoD to reduce the need for foreign energy sources and increase the use of renewable fuels was issued in 2007. As a result, branches of the DoD, including the USAF, began to increase their use of alternative, renewable liquid transportation fuels in ground vehicles.

Ultra low sulfur diesel (ULSD) is a common fuel for ground vehicles within the USAF that was replaced by a blend containing 20 % biodiesel (fatty acid methyl esters, FAME) made from renewable resources and 80 % ULSD. This blend is commonly referred to as B20 or BDI and helps to meet the goals of the mandate. Moreover, B20 is compatible with existing storage systems and vehicle fleets with similar storage and combustion properties to ULSD (Canakci, 2007; Chang et al., 1996). Biodiesel blends are advantageous to use because of enhanced lubricity (Van Gerpen et al., 1998), and biodegradability in the event of a spill (Lisiecki et al., 2014).

Many storage tanks within the USAF previously containing ULSD were converted to B20 beginning in 2005. Soon after converting tanks to B20 storage, more frequent fuel issues were reported due to particulates and fouling. Operators frequently observed

thick mats of unknown origin although no attempt to identify the biogenicity of the material was made (Dr. Wendy J. Crookes-Goodson, personal communication). Furthermore, several USAF B20 tanks experienced repeated fouling resulting in the loss of large quantities of fuel and the need for expensive and time-consuming tank cleanings (Dr. Wendy J. Crookes-Goodson, personal communication). Many USAF and commercial operators of underground B20 storage tanks assume that the films and “waxes” observed when a B20 tank fouds are due to the abiotic oxidation of FAME (Dr. Wendy J. Crookes-Goodson, personal communication). Within the USAF no test protocol currently exists to confirm or reject the level of microbial activity within a B20 storage tank (Dr. Wendy J. Crookes-Goodson, personal communication) even though the ability of microorganisms to degrade FAME is known.

A wide range of bacteria and fungi are capable of degrading FAME both aerobically (Bücker et al., 2011; Owsianiak et al., 2009; Prince et al., 2008) and anaerobically (Aktas et al., 2010). Microorganisms metabolize the fatty acid methyl esters in biodiesel by first cleaving the ester with a lipase or carboxylesterase, resulting in methanol. The fatty acid is further metabolized through the beta-oxidation pathway (Kumari and Gupta, 2014). Using fatty acids as a sole carbon and energy source is a widespread trait (Hiltunen et al., 2003; Kazakov et al., 2008). Methanol released from the initial activation of FAME can also be consumed (Kumari and Gupta, 2014), although the phylogenetic distribution of microorganisms capable of methylotrophy is more restricted (Kist and Tate, 2013; Kondo et al., 2008).

Biodiesel storage tanks are a highly structured environment, containing a gradient of carbon (the biodiesel), nitrogen, phosphorus, sulfur, oxygen, as well as habitat based on

the availability of surfaces and patches of water pooled at the bottom of the tank. Small quantities of sulfur (as S^0 or SO^4) and phosphorus may also be present in biodiesel (ASTM D6751-03). No nitrogenous compounds are present in unadulterated B20 however the cetane improver Ethyl Hexyl Nitrate can be degraded through a carboxylesterase yielding a source of nitrate (Solano-Serena et al., 2008). Sources of fixed nitrogen from sediment or soil from around the exterior of the tank might also enter the tank during periods of significant rainfall or flooding into the tank. Alternatively, microorganisms capable of nitrogen fixation present within the tank may provide the community with a source of fixed nitrogen.

The availability of oxygen and physical space at the fuel-water interface may limit the growth of the resident microbial community in biodiesel storage tanks. Rapid consumption of dissolved oxygen at this interface could allow strictly anaerobic, or facultatively anaerobic microorganisms to grow near the bottom of a tank (Aktas et al., 2010). This also suggests that aerobic and facultatively anaerobic microorganisms may live and compete at the fuel-water interface where oxygen is present. Biodiesel also contains a higher percentage of oxygen by weight than ULSD and is prone to abiotic oxidation of FAME that may produce insoluble free fatty acids (often reported as “waxes”) and a loss of combustion (NREL-P-540-43672). Habitat space is also a likely constraint on growth within a B20 storage tank, which is dictated by the presence of a water layer. Most microorganisms will grow within a defined water layer that can be transient and dependent upon rainfall or flooding events that allow intrusion of water into the tank. Even in the absence of rainfall, biodiesel is capable of retaining significantly more water than ULSD (Fregolente et al., 2012). Water that enters the tank

either from humid air or during a rain event may emulsify in the fuel which would allow for microorganisms to grow within the fuel layer of a tank, oil pipeline, or other hydrocarbon bearing layer (Meckenstock et al., 2014). The likelihood of water accumulation within underground storage tanks coupled to the inherent ability of B20 to retain greater concentrations of water could increase the risk of microbial fouling and degradation.

Understanding if microorganisms contribute to recurrent fouling issues observed in biodiesel blends represents a critical need to both industry and governments across the world, as the use of such fuels becomes more commonplace. Because of the known risk of microbial contamination in B20, we hypothesized that *microorganisms are the root cause of fouling in USAF B20 fuel tanks*. We predicted that this fouling was due to large accumulations of biomass, through the metabolism of the FAME present in B20.

Furthermore we predicted that the microbial degradation of FAME would produce increased concentrations of fatty acids that would acidify the fuel and further fouling.

Longitudinal studies of microbial communities have the ability to provide information on the stability and composition of microbiomes that cannot be understood in a single time-point analysis (Gerber, 2014). Correlation between operational activities, regional effects, and microbial communities can be understood in surveys that extend into multiple sampling events. The USAF provided unprecedented access to two primary active biodiesel storage and dispensing systems over the course of 18 months allowing for an in-depth investigation of the microbiology in biodiesel storage tanks. While the in-service nature of the dispensing systems was an advantage, it also presented challenges as an uncontrolled experiment. To further confirm findings from our large-

scale molecular study, fungal and bacterial isolates were identified from both sites and tested for their ability and/or genetic potential to degrade FAME. A transcriptome from a single isolate grown on B20 as the sole carbon substrate was generated to identify which genes were associated with the degradation of FAME in an abundant member of the fungal community. The transcriptome provided further evidence towards the primary mechanism of degradation and fouling with the tanks.

Methods

Site Description

Two USAF bases located in southeastern (SE) and southwestern (SW) United States were chosen for the longitudinal study because they were experiencing recurring fuel quality issues, offered easy access to the affected fuel systems, warmer year-round temperatures, but differed considerable in the amount of precipitation annually. Samples were also taken from fuel storage and distribution systems for ULSD and B20 at USAF bases in the Northwest (NW) and Midwest (MW) US, and Texas (TX)(Fig. 1a). The fuel storage tanks were below ground and composed of carbon steel at all tested locations with the exception of two of the three tanks sampled at SE, which were fiberglass. The tanks at NW and TX were above ground storage systems, and MW had a one below ground tank, and one above ground.

The SW Air Force Base (AFB) is located in an arid environment and receives an average ≈ 30 cm of rainfall per year. The average annual temperature is 28.7 °C. The

tanks reside roughly 1 m below grade, and were secured by a large steel cover preventing intrusion of rainwater to a large entry point. This access point allowed for cleaning and sampling at each time point. Small gauging and fuel ingress hatches were also present in each tank (Fig. 1b).

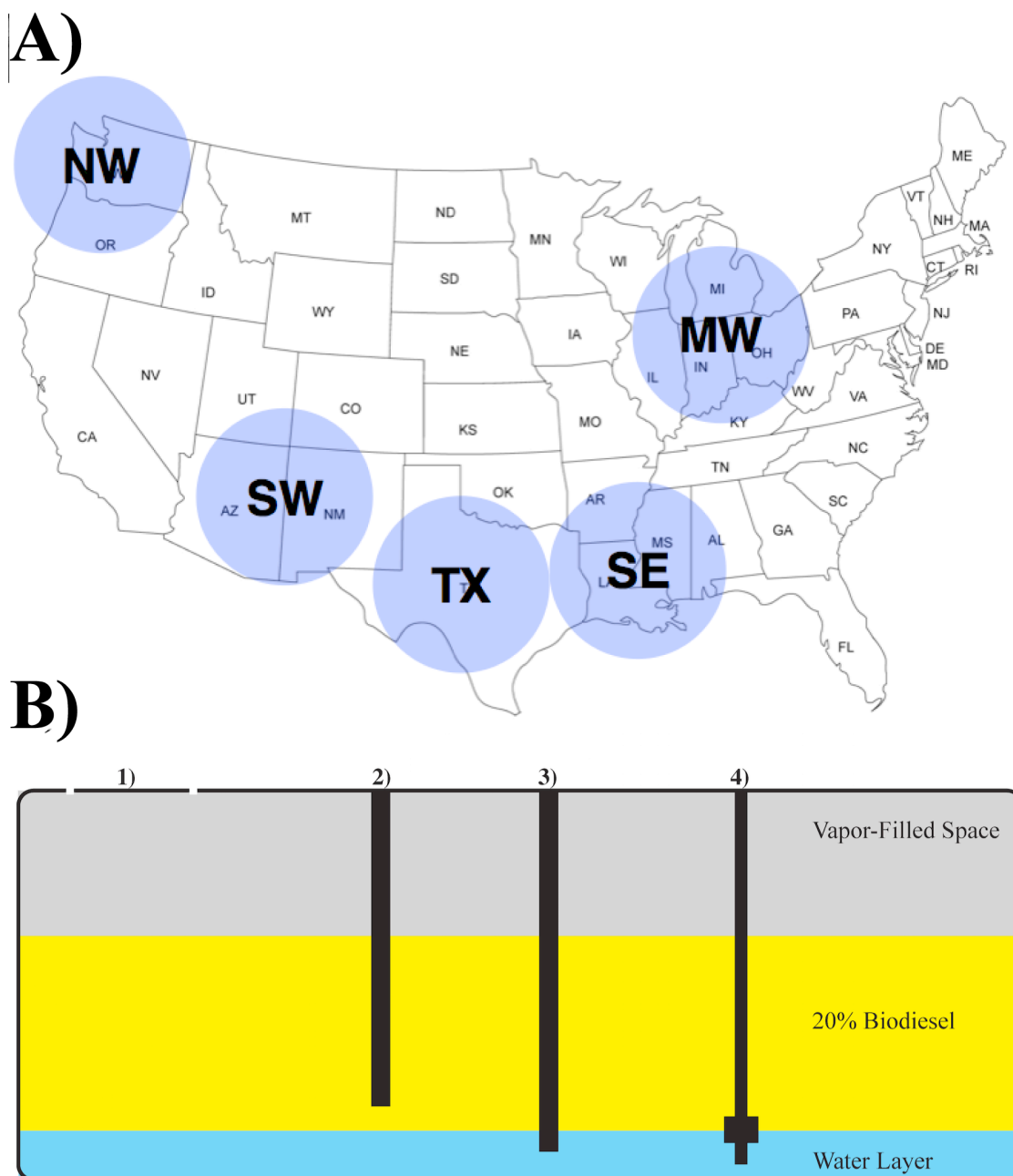


Figure 1. A diagram showing A) general locations of sampled USAF bases (left to right; NW, SW, TX, WE and MW), and B) the general structure of a biodiesel storage tank. Fuel samples were taken either from each fuel tank from the main entry hatch (1) or the automated tank-gauging hatch (4). Other points of entry include the dispensing tubing (2) and a baffled filling tube (3).

The SE AFB is located in a semitropical environment, with a much higher average annual rainfall of ≈ 130 cm. This area experiences a higher average humidity than SW, and has a lower average annual temperature of 24.7 °C. At SE, the two fiberglass tanks are physically connected by a T-junction to allow for the transfer of fuels between each tank (SE 3 and SE 4), while the third tank (SE E) is composed of carbon steel-lined fiberglass and is located in a separate area of the facility. Each tank had access similar to SW, with a large steel cover protecting the bolted down steel access hatch.

Images were taken during each sampling event at SE and SW using a Pentax K-30 digital single lens reflex camera (Ricoh Imaging Americas Corp., Denver, CO) using a 50 mm fixed focal length lens. Particulate filtered at SE E in October 2015 was imaged using a Zeiss NEON 40 EsB scanning electron microscope (Carl Zeiss Microscopy GmbH, Jena).

Measurement of ATP in SE Fuels

As a proxy for microbial activity, the concentration of adenosine triphosphate (ATP) was determined for fuels at SE between April 2014 and October 2015 following the ASTM D7463 standard using the Hy-LiTE[®] assay system (Fuel Quality Services, Inc., Flowery Branch, GA) in duplicate. Approximately 1 L of fuel was collected using a Bacon Bomb fuel sampler (Koehler Instrument Company, Inc., Holtsville, New York) and transferred to a sterile HDPE bottle and used for the ATP assay according to manufacturer's protocol and ASTM D7463.

Fuel Acid Index

The acid index of fuel samples from SE was measured by acid titration using the ASTM standard D974 (D27 Committee, 2008) method in October 2014, March 2015, and May of 2015 to quantify the acidification of fuels due to the biological and/or abiotic oxidation of FAME. Briefly, ≈ 20 g of B20 was suspended in 100 mL of titration solvent (Toluene/Water/Isopropyl alcohol) and 0.5 mL of an p-Naphtholbenzein Indicator (Sigma-Aldrich) indicator solution at a final concentration of 10 g/L, and titrated using a 0.1 N solution of KOH dissolved in isopropyl alcohol (Sigma-Aldrich, St. Louis, MO).

DNA Sampling, Preservation, and Extraction

Fuel was sampled at all sites using a Bacon Bomb fuel sampler (Koehler Instrument Company) and transferred to a sterile HDPE bottle. Biomass and other particulate matter were collected via filtration using a Steritop[®] filter unit containing a 120 mm dia PES filter with a 0.22 μm pore size (EMD Millipore, Billerica, MA) attached to a sterile 1 L glass bottle. After filtration, each filter was cut into quarters using sterile disposable scalpels. The DNA from each filter quarter was preserved in a 2.0 mL bead tube with 750 μL DNA Lysis/Preservation solution (Zymo Research Corp., Irvine, CA) and homogenized for 30-45s on site. Homogenization was carried out on-site using a battery-powered reciprocating saw (One World Technologies, Inc., Anderson, SC) fitted with a custom head to accommodate a number of bead tubes at once. Preserved samples were then transported at room temperature and stored at -20°C until DNA was extracted. Prior to DNA extraction, each sample was homogenized for an additional 30

s using a Mini-BeadBeater-8 (BioSpec Products Inc., Bartlesville, OK) and DNA was extracted according to the manufacturer's protocol using the Zymo Xpedition Soil/Fecal kit (Zymo Research Corp.).

PCR Amplification and DNA Sequencing

Libraries of bacterial, archaeal, and eukaryotic SSU rRNA gene fragments were amplified from each DNA extraction using PCR with primers that spanned the SSU rRNA gene V4 hypervariable region between position 515 and 926 (*E. coli* numbering) that produced a ~400 bp fragment for bacteria and archaea, and a 600 bp fragment for the eukaryotes. These primers evenly represent a broad distribution of all three domains of life (Parada et al., 2015). The forward primer 515F-Y (**GTA AAA CGA CGG CCA G CCG TGY CAG CMG CCG CGG TAA-3'**) contains the M13 forward primer (in bold) fused to the SSU rRNA gene specific forward primer (underlined) while the reverse primer 926R (5'-CCG YCA ATT YMT TTR AGT TT-3') was unmodified from Parada et. al 2015. A PCR master mix (5 PRIME HOT master mix; 5 PRIME Inc., Gaithersburg, MD) was used for all reactions at a final volume of 50 μ L. Following amplification, reactions were purified using Agencourt AMPure XP paramagnetic beads (Beckman Coulter Inc., Indianapolis, IN) at a final concentration of 0.8 x v/v. After purification, 4 μ L of PCR product was used in a barcoding reaction to attach a unique 12 bp barcode to each library in duplicate 50 μ L reactions (Appendix 1), which were pooled after amplification. The resulting amplified products were purified using Agencourt AMPure XP paramagnetic beads to a final volume of 40 μ L, quantified using the QuBit HS DS DNA assay kit (Thermo Fisher Scientific Inc., Waltham, MA), and pooled in equimolar amounts before concentration using an Amicon Ultra-0.5

Centrifugal Filter Unit with Ultracel-30 membrane (EMD Millipore) to a final volume of 80 μ L. Multiple extraction blanks and negative controls were sequenced from each batch of extractions in order to detect and characterize any contamination from reagents (Salter et al., 2014).

SSU rRNA gene libraries were sequenced using Illumina MiSeq V2 PE250 chemistry. Libraries were prepared with the TruSeq DNA LT Sample Prep kit (Illumina, San Diego, CA). The sequencing libraries were loaded at a final concentration of 10 pM for libraries sequenced with additional genomic samples, or 6 pM for amplicon libraries prepared and sequenced individually. Sequence diversity for the sequencing run was increased by the addition of 10-40 % phiX DNA.

Quantitative PCR

Quantitative PCR (qPCR) was used to quantify the abundance of the 18S rRNA gene (Liu et al., 2012) as a proxy for biomass in fuels taken during an initial sampling period at SE in both biological (n=3) and technical replicates (n=3) from April 2014 to August 2014 to assess the success of tank cleaning. Due to the apparent abundance of fungi rather than bacteria or archaea present in SEM images taken at SE, 16S rRNA gene qPCR was not attempted. Briefly, 1 μ L of template was added to a master mix containing 1.8 μ M of the primers FungiQuantF (5'-GGR AAA CTC ACC AGG TCC AG-3') and FungiQuantR (5'-GSW CTA TCC CCA KCA CGA-3'), 225 nM of the TaqMan[®] probe (6FAM 5'-TGGTGCATGGCCGTT-3' MGBNFQ), and 1 X using Platinum Quantitative PCR SuperMix-UDG with ROX (Thermo Fisher Scientific Inc). The reaction was carried out under the following conditions: 3 min at 50 °C for UNG

treatment, 10 min at 95 °C for Taq activation, 50 cycles of 15 s at 95 °C for denaturation and 1 min at 65 °C for annealing. The Ct-value for each reaction was determined using a manual Ct threshold of 0.10 and automatic baseline detection. Linear 18S rRNA gene standards were prepared by amplifying a known isolate using the primers (*T. Inflatum*) in seven 50 µL reactions, and purifying and pooling the final product using an 0.9 X concentration of Agencourt AMPure XP paramagnetic beads (Beckman Coulter, Inc.), and two successive 75 % EtOH washes. Standards were quantified using the QuBit BR assay (Thermo Fisher Scientific Inc.). Standard concentrations were 20 ng/µL, 2 ng/µL, 0.2 ng/µL, 20 pg/µL, 2 pg/µL, 0.2 pg/µL, and 20 fg/µL. Each standard was frozen once, and never refrozen. The number of copies was estimated using the approximate length of the amplified 18S fragment of ≈750 bp.

Sequence Analysis

The sequence reads from SSU rRNA libraries were merged using PEAR (Zhang et al., 2014), demultiplexed in QIIME version 1.9.1 (Caporaso et al., 2010b), and filtered by quality and clustered into OTUs using UPARSE (Edgar, 2013). Experimental samples were compared to controls using DESeq2 (Love et al., 2014) to identify OTUs that originated from potentially contaminated DNA extraction or PCR reagents (Salter et al., 2014). Any OTUs not significantly differentially abundant from extraction blanks or negative controls were then filtered from downstream analyses.

Taxonomy was assigned using mothur (Schloss et al., 2009) and the r123 SILVA database (Pruesse et al., 2007). A representative sequence of each OTU was aligned with pyNAST (Caporaso et al., 2010a) against an aligned version of the SILVA r123

database, and filtered to remove uninformative bases. A phylogenetic tree for both the Bacteria and Archaea, and the Eukarya was produced using the maximum likelihood method and the Jukes Cantor evolutionary model within FastTree (Price et al., 2010).

A core microbiome was computed for both 16S and 18S rRNA gene libraries within QIIME. An OTU was included in the core microbiome if it was present in at least 50 % of all tested samples.

Differences in community composition were estimated using the weighted UniFrac index (Lozupone and Knight, 2005). The effect of site, tank, and the location of fuels within each tank were tested using a PERMANOVA using the R package vegan (Dixon, 2003) within QIIME. Additionally, fuel composition data for fuels sampled at SE and SW (unpublished research, Oderay Andrade) was correlated to community composition using a PERMANOVA.

Genome Sequencing of Select Environmental Isolates

Several fungi and bacteria isolated from SE and SW (unpublished research, Oderay Andrade) were representative of dominant OTUs from the genera *Pseudomonas*, *Burkholderia*, *Roseomonas*, *Gluconacetobacter*, and the fungal genera *Byssoschlamys* and *Wickerhamomyces* at each site and were selected for whole genome sequencing. Genomic DNA was extracted from 50 mL cultures grown to stationary phase (48-72h) in Hestrin-Schramm broth (Hestrin and Schramm, 1954) and extracted using the Zymo Xpedition Soil/Fecal DNA kit as above. Genomic sequencing libraries were sequenced using Illumina MiSeq V2 PE250 chemistry. Libraries were prepared with the TruSeq DNA LT Sample Prep kit (Illumina). Sequencing libraries were loaded at a final

concentration of 10 pM. Illumina sequence adapters were trimmed using PEAT (Li et al., 2015) prior to assembly using SPAdes (Bankevich et al., 2012) with kmer values of 21, 33, 55, 77, 99, and 127 in paired-end mode with the “--careful” option selected.

The genome of a *Byssochlamys* sp. isolate was improved using the MinION single molecule sequencer following the manufacturer’s protocol (Oxford Nanopore Technologies, Oxford UK). Raw sequence data was converted to the FASTA format using NanoOK (Leggett et al., 2016) and combined with the Illumina trimmed sequencing library to produce a final assembly within SPAdes.

Expression of Key Genes Associated with B20 Degradation within Byssochlamys sp.

Preparations of *Byssochlamys* spores were prepared fresh by first heating 50 mL of a stationary phase culture to 70 °C, and then passing this mixture through a 10 µm filter (EMD Millipore). The filtrate was centrifuged at 8000 xRCF for 20 min, and the pelleted spores were resuspended in 1 mL of artificial sump water (ASW)(McNamara et al., 2005) to a concentration of 10^7 spores/mL, standardized using a hemocytometer. To inoculate each culture, 10^5 spores were added to 50 mL of ASW amended with 10 mL of sterile ultra low sulfur diesel (ULSD), B20 biodiesel, ULSD amended with 20 % methyl palmitate (v/v), or ULSD amended with 20 % v/v of palmitic acid. The cultures were incubated for 3 weeks at 25 °C shaking at 100 RPM. After three weeks, cultures were filtered onto 0.22 µm PES filters (EMD Millipore). The filters were then placed in lysing matrix F tubes (MP Biomedicals LLC, Santa Ana, CA) containing 1 mL of TRIzol (Thermo Fisher Scientific, Inc.) and flash frozen using liquid nitrogen. Prior to RNA extraction, the samples were thawed on ice and homogenized for 30s using a Bead

Beater 8 (BioSpec Products, Inc.), rested for 10 s on ice, and then homogenized for an additional 30 s prior to being cooled again. After lysis, RNA was extracted using the PureLink RNA mini kit (Thermo Fisher Scientific, Inc.) and quantified using the QuBit high sensitivity RNA assay (Thermo Fisher Scientific, Inc.). RNA sequencing libraries were prepared using the NEBnext Ultra Directional RNA library preparation kit (New England Biolabs, Inc.), and barcoded using the NEBnext Illumina Index 1 kit (New England Biolabs, Inc.) following the manufacturer's protocol.

Prepared cDNA libraries were sequenced on the Illumina NextSeq platform using PE75bp chemistry (Illumina). Sequence reads were trimmed for adapters and quality using Trimmomatic (Bolger et al., 2014) prior to transcript assembly. The reads from all growth conditions were pooled and assembled *de novo* using Trinity (Grabherr et al., 2011). Reads were not trimmed prior to mapping to reduce the potential impact on transcript abundance estimates (Williams et al., 2016). Due to the low number of reads across some replicates in the ULSD, PAME, and palmitic acid growth conditions, only untrimmed libraries from *Byssochlamys* grown on B20 were quantified against the *de novo* assembled transcripts using Salmon (Patro et al., 2015) and normalized by transcripts per million (TPM).

Analysis of Putative Metabolites from RNA sequencing Cultures

After filtration and removal of biomass, aqueous supernatant and fuel from *Byssochlamys* cultures grown in ASW amended with B20 were separated and analyzed. The fuel fraction was derivatized by incubating 10 μ L of fuel with 10 μ L of BSTFA/TMS mixture (MilliporeSigma, St. Louis, MO) for 20 min at 75 °C. Derivatized

samples were diluted 1:50 in hexane. The aqueous fraction was first extracted with 50 mL of ethyl acetate, dried using sodium sulfate (MilliporeSigma, St. Louis, MO), and concentrated to ≈ 500 μL using a rotary evaporator (IKA Works, Inc., Wilmington, NC). Samples were further concentrated to 100 μL under a stream of nitrogen. Aqueous extracts were derivatized using 20 μL of a BSTFA/TMS mixture (MilliporeSigma) as above. The extract was diluted with 500 μL of hexane after derivatization due to minimum sample volume limits on our auto-injector. Both fuel and aqueous extracts were analyzed on a Shimadzu QP2010-SE GCMS (Shimadzu Scientific Instruments, Inc., Columbia, MD) using a 30 m RTX-5MS 0.25 mm diameter capillary column (Shimadzu Scientific Instruments, Inc.). A volume of 1 μL of each sample was injected at 300 $^{\circ}\text{C}$, and the column began at 40 $^{\circ}\text{C}$, holding for 30 s, before ramping to 300 $^{\circ}\text{C}$ at 4 $^{\circ}\text{C}/\text{min}$. The column was then held at 300 $^{\circ}\text{C}$ for 2.75 min. Helium was used as the carrier gas at a flow rate of 1.04 mL/min and a linear velocity of 36.8 cm/s. The mass spectrometer was held at 200 $^{\circ}\text{C}$, with an interface temperature of 300 $^{\circ}\text{C}$. Spectra were obtained after a 2.25 min solvent cut, with masses between 35.00 and 500.0 m/z scanned every 0.25 s. Gravimetric reference standards for B20, FAME, and alkanes were used to positively identify major peaks within each sample (Restek Corp., Bellefonte, PA). Fatty acids potentially produced during the initial activation of FAME were identified using a quantitative reference standard (Restek Corp.). Any other compounds were putatively identified using the NIST release 14 reference library.

Results

Visual determination of fouling at SE and SW

Bottom fuel samples at SW varied in clarity and apparent biofilm contamination at SW (Fig. 2a). A thick microbial biofilm with a filamentous morphology and trapped sediment was visible in a SW 2 sample at the fuel-water interface (Fig. 2b). At SE E in October of 2015 particulate captured on a 0.22 μm filter was primarily filamentous (Fig. 3a) in morphology. At higher magnification branching conidiophores were also visible (Fig. 3b).

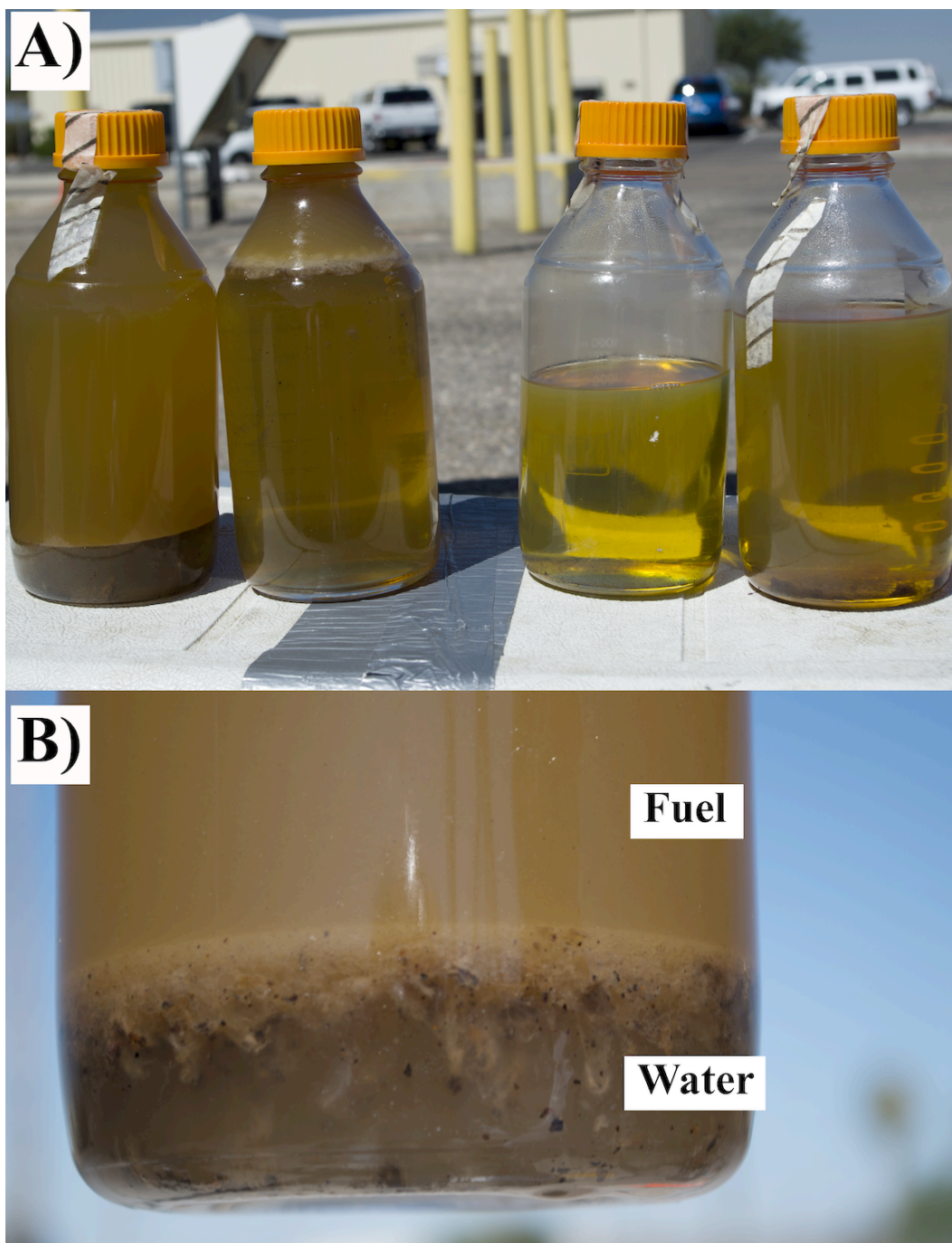


Figure 2. Fuel samples taken from B20 storage tanks at the SW AFB show (A) a range in water content, particulate matter, clarity, and color. The bottle third from the left is an example of the clarity and color of fuel upon delivery. A common feature of fouled biodiesel is a thick biofilm at the fuel-water interface (B).

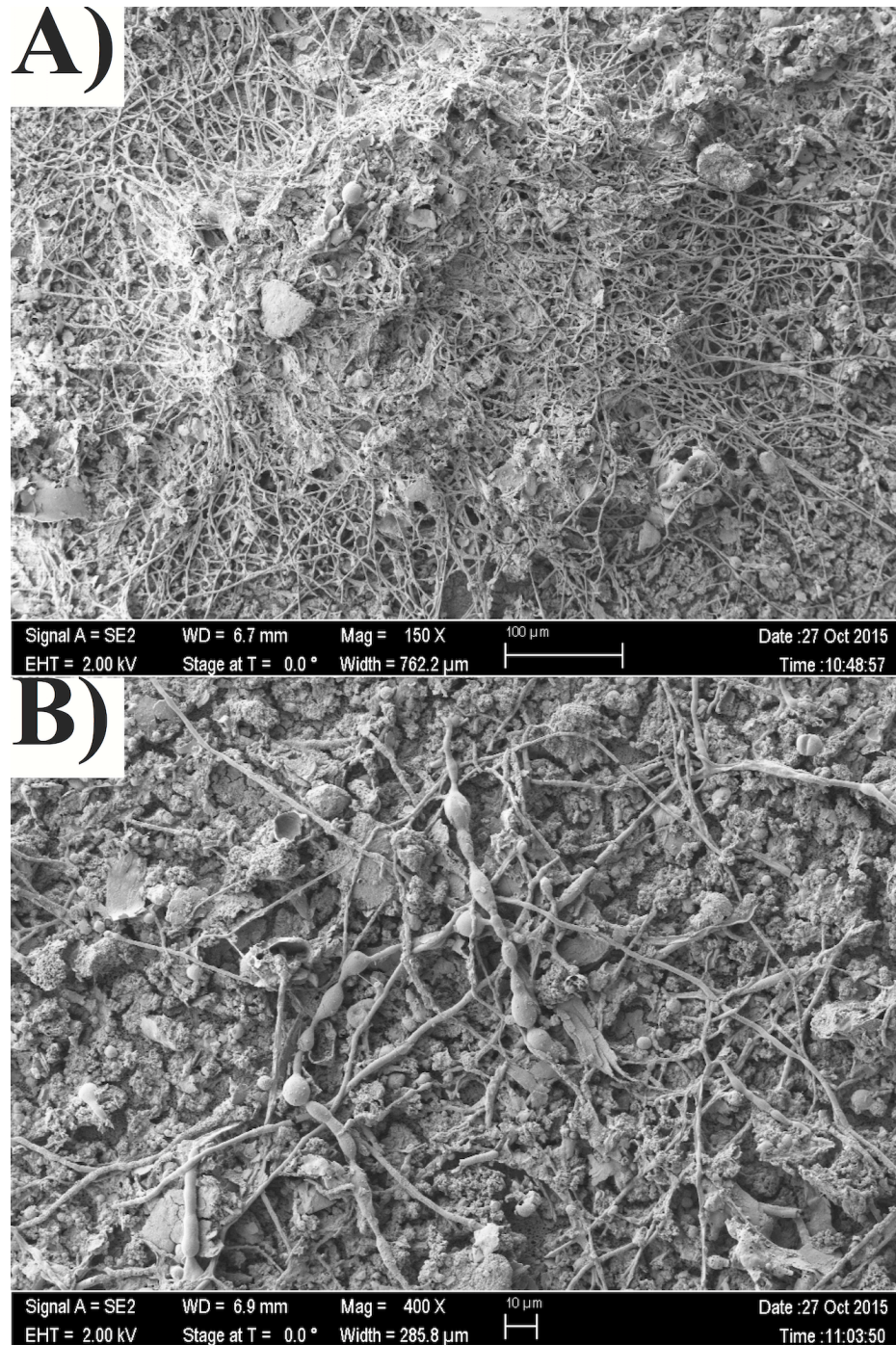


Figure 3. Scanning electron microscopy of a biofilm taken from SE E on October 2015. Biomass was almost entirely comprised of fungal hyphae (A). At higher magnification branching conidiophores were also visible (B).

Small Subunit rRNA Gene Community Analysis

In total, 348 samples with a total of 2.48 million bacterial and archaeal sequences, and 346 samples with 488.7 thousand sequences passed quality control and filtering.

Bacterial and eukaryotic libraries clustered into 2589 and 591 OTUs respectively.

The Ruminococcaceae and Clostridiaceae 1 were the most abundant bacterial families across all sampled time points at SW. Both families represented 36 to 54 % of the total relative bacterial abundance detected in bottom fuels at SW (Fig. 4). At SE, members of the Burkholderiales, Ruminococcaceae, Acetobacteraceae and other proteobacteria were most abundant (Fig. 4). At SE 3 and SE 4, the Acetobacteraceae ranged in average relative abundance from 28 to 42 % in bottom and mid-tank fuel samples and up to 67 % in nozzle samples at SE 4. Tanks at TX, MW, and NW contained a greater abundance of Betaproteobacteria including the Oxalobacteraceae and Comamonadaceae.

In all tanks at SE and SW, members of the fungal families Trichocomaceae and Saccharomycetaceae were present in the greatest relative abundance within 18S rRNA sequencing libraries. The Trichocomaceae varied in average relative abundance across bottom fuel samples at SE from 47 to 60 %. At SW the Trichocomaceae represented greater than 95 % relative abundance in all bottom fuel samples (Fig. 5). The At certain time points, the Saccharomycetaceae were detected in higher relative abundance in bottom fuel samples at SE 3 and 4, but averaged 16 and 12 % of the fungal community, respectively. At TX, MW, and NW both the Trichocomaceae and Saccharomycetaceae were less abundant (Fig. 5).

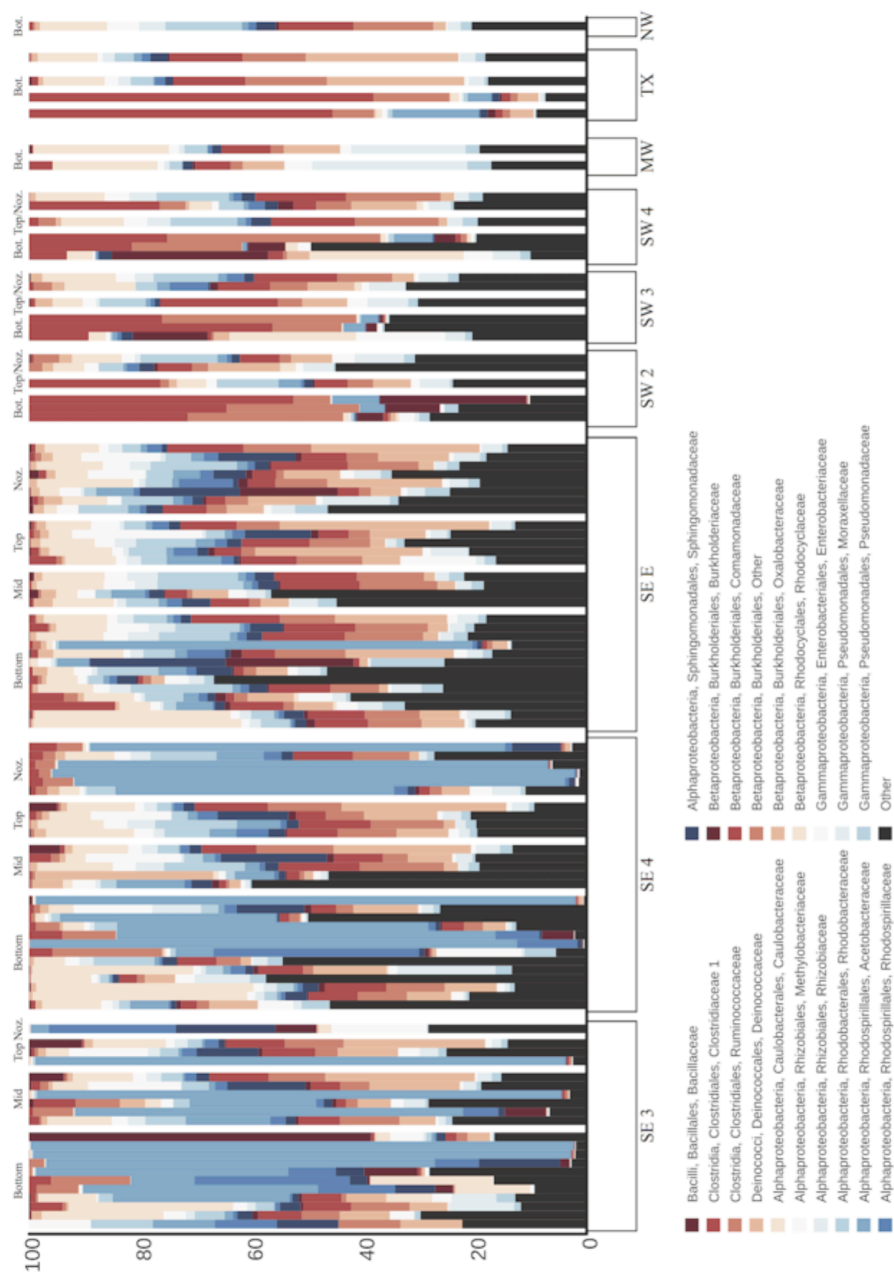


Figure 4. Relative abundance of bacterial families detected in fuels at all sampled sites over time. Fuel samples from the bottom (or Bot), middle (Mid), and top (Top) of the fuel column, as well as the nozzle of a dispenser (Noz) at SE and SW. Individual tanks (3, 4, and E and SE; 2, 3, and 4 at SW) are also indicated. Taxonomic lineages that represented less than 1 percent on average of any sample were condensed into the “other” category.

Both bacterial and fungal communities were significantly distinct between sites ($p = 0.001$), although a stronger predictor of community membership was the tank at each site ($p = 0.001$, $R^2 = 0.22$ and 0.20 for bacteria and fungi respectively), and finally what date each tank was sampled ($p = 0.001$, $R^2 = 0.67$). Samples from the bottom, middle, top of the fuel column within each tank or nozzle at SE and SW were also significantly different from another ($p = 0.001$, Table 1 and 2). A subset of samples with corresponding GCMS fuel profiles (Oderay Andrade, unpublished data) at SE was analyzed separately. The bacterial (Table 1) and eukaryotic (Table 2) community structure of samples grouped by FAME concentration was significantly different. A core microbiome analysis was performed to determine what, if any OTUs were shared between all samples. No OTU was shared across all samples, however 64 bacterial and 6 fungal OTUs were shared across 50 percent of all samples, including the most dominant OTUs of the Trichocomaceae and Saccharomycetaceae

Table 1. Summary of PERMANOVA tests comparing bacterial community structure of the weighted UniFrac distance matrix to location (site), tank, position within tank (position), and the relative peak height of select fuel components.

Factor	Sum of Squares	Mean Squares	F	R ²	p
Site	0.504	0.126	13.971	0.152	0.001
Tank	0.742	0.074	8.807	0.223	0.001
Position	0.216	0.054	5.933	0.088	0.001
Methyl	0.161	0.161	15.307	0.209	0.001
Palmitate					
Methyl Stearate	0.137	0.137	12.562	0.178	0.001
Methyl Oleate	0.098	0.098	8.389	0.126	0.001
Methyl	0.184	0.184	18.205	0.239	0.001
Linoleate					
C10	0.026	0.026	2.044	0.034	0.108
C11	0.019	0.019	1.447	0.024	0.189
C12	0.025	0.025	1.957	0.033	0.111

C13	0.098	0.098	8.45	0.127	0.001
C14	0.119	0.119	10.554	0.154	0.001
C15	0.021	0.021	1.643	0.027	0.148
C16	0.022	0.022	1.738	0.029	0.128
C17	0.02	0.02	1.52	0.025	0.174
C18	0.015	0.015	1.133	0.019	0.309
C19	0.15	0.15	14.027	0.195	0.001
C20	0.123	0.123	11.047	0.16	0.001

Table 2. Summary of PERMANOVA tests comparing eukaryotic community structure as a measure of the weighted UniFrac distance matrix to location (site), tank, position within tank (position), and the relative peak height of select fuel components. Comparisons with a $p < 0.05$ are denoted in bold.

Factor	Sum of Squares	Mean Squares	F	R ²	p
Site	0.438	0.11	7.129	0.137	0.001
Tank	0.648	0.072	4.925	0.202	0.001
Position	1.004	0.046	3.356	0.313	0.001
Methyl	0.96	0.192	27.09	0.344	0.001
Palmitate					
Methyl Stearate	0.059	0.029	2.994	0.02	0.001
Methyl Oleate	0.41	0.205	22.483	0.147	0.001
Methyl	1.255	0.031	4.671	0.436	0.001
Linoleate					

C10	0.165	0.165	5.644	0.101	0.012
C11	0.148	0.148	5	0.091	0.013
C12	0.178	0.178	6.138	0.004	0.109
C13	0.173	0.173	5.948	0.007	0.106
C14	0.089	0.089	2.887	0.054	0.061
C15	0.323	0.323	12.333	0.198	0.001
C16	0.152	0.152	5.131	0.093	0.01
C17	0.041	0.041	1.275	0.025	0.291
C18	0.018	0.018	0.553	0.011	0.584
C19	0.047	0.047	1.501	0.029	0.229
C20	0.054	0.054	1.727	0.0334	0.172

Table 3. ATP Values from bottom fuel samples at SE.

Date	SE 3			SE 4			SE E		
	Sample	Sample	Average	Sample	Average	Sample	Sample	Average	Sample
	1	2		1	2		1	2	
4/1/14	2.9x10 ⁴	ADL ^a	ADL ^a	ADL ^a	ADL ^a	ADL ^a	280	330	305
5/1/14	ADL ^a	ADL ^a	ADL ^a	6.0x10 ²	3.0x10 ²	4.5x10 ²	1.6x10 ⁴	NA	1.6x10 ⁴
7/25/14	1.4x10 ⁴	14	1.4x10 ⁴	7	20	13.5	NA ^b	NA ^b	NA ^b
8/20/14	4.7x10 ⁴	2.7x10 ⁴	3.7x10 ⁴	10	13	11.5	NA ^b	NA ^b	NA ^b
9/26/1	7.5x10 ³	NA ^b	7.5x10 ³	41	NA ^b	41	81	NA ^b	81
10/28/14	3.2x10 ²	NA ^b	3.2x10 ²	1.7x10 ³	17	8.6x10 ²	11	NA ^b	11
3/12/15	6.1x10 ⁴	ADL ^a	ADL ^a	1.3x10 ⁴	1.2x10 ⁴	1.2x10 ⁴	NA ^b	NA ^b	NA ^b
4/29/15	3.3x10 ³	1.2x10 ³	2.2x10 ³	19	22	20.5	87	7.4x10 ³	3.7x10 ³
5/7/15	ADL ^a	NA ^b	ADL ^a	ADL ^a	NA ^b	ADL ^a	2500	NA ^b	2.5x10 ³

6/5/15	NA ^b	NA ^b	NA ^b	6.6x10 ⁴	NA ^b	6.6x10 ⁴	3.2x10 ²	NA ^b	3.2x10 ²
7/10/15	NA ^b	NA ^b	NA ^b	16	NA ^b	16	2.8x10 ²	NA ^b	2.8x10 ²
8/13/15	NA ^b	NA ^b	NA ^b	830	NA ^b	830	78	NA ^b	78
9/1/15	5.0x10 ³	5.6x10 ³	5.3x10 ³	1.4x10 ⁴	1.5x10 ⁴	1.4x10 ⁴	NA ^b	NA ^b	NA ^b
10/28/15	NA ^b	NA ^b	NA ^b	1.7x10 ³	NA ^b	1.7x10 ³	NA ^b	NA ^b	NA ^b

^a Above detection limit.

^b ATP Reading not taken due to a lack of available testing pens, or significant accumulation of water or solids that caused the test to fail.

The tank SE 4 saw a reduction in ATP from above detection limits to 1×10^2 Relative Light Units (RLU) after cleaning and lower for the following 4 months. In October of 2014 ATP levels rose to 10^4 RLU, and ranged from above to below detection limits during the remainder of the sampling period. The tank SE 3 varied from 1×10^2 RLU to above detection limits throughout the sampling period. The eastside tank produced highly variable results, likely due to the high levels of dark particulate that obscured the ability of the instrument to make accurate measures of ATP (Table 3). Elevated ATP readings and visible flocculent material in fuel correlated to an increased relative abundance of the Trichocomaceae in SE 3 (Fig. 6). A decrease in the relative abundance of the Trichocomaceae corresponded to cleaning events in August of 2014 and May of 2015, as well as a series of three fuel receipts into the tank from April to May 2015. Interestingly the relative abundance of the Trichocomaceae increased soon after both tank cleaning events and fuel receipts. There was a large reduction in the overall number of 18S rRNA gene copies per L of fuel from a peak of 9.61×10^5 to 4.12×10^3 copies/L B20 in SE tank 4 after the cleaning in April of 2014 (Table 4). During May 2014 to July 2014 there was no visible biomass or flocculent material observed in bottom fuel samples in SE tank 4. The mean number of 18S rRNA gene copies was variable at SE tank 3 during this time, with an average of 1×10^5 copies over the four sampled months. The tank SE E also showed a higher mean number of 18S rRNA gene copies than that of SE 4 over this time period, with an average of 1×10^4 copies/L B20.

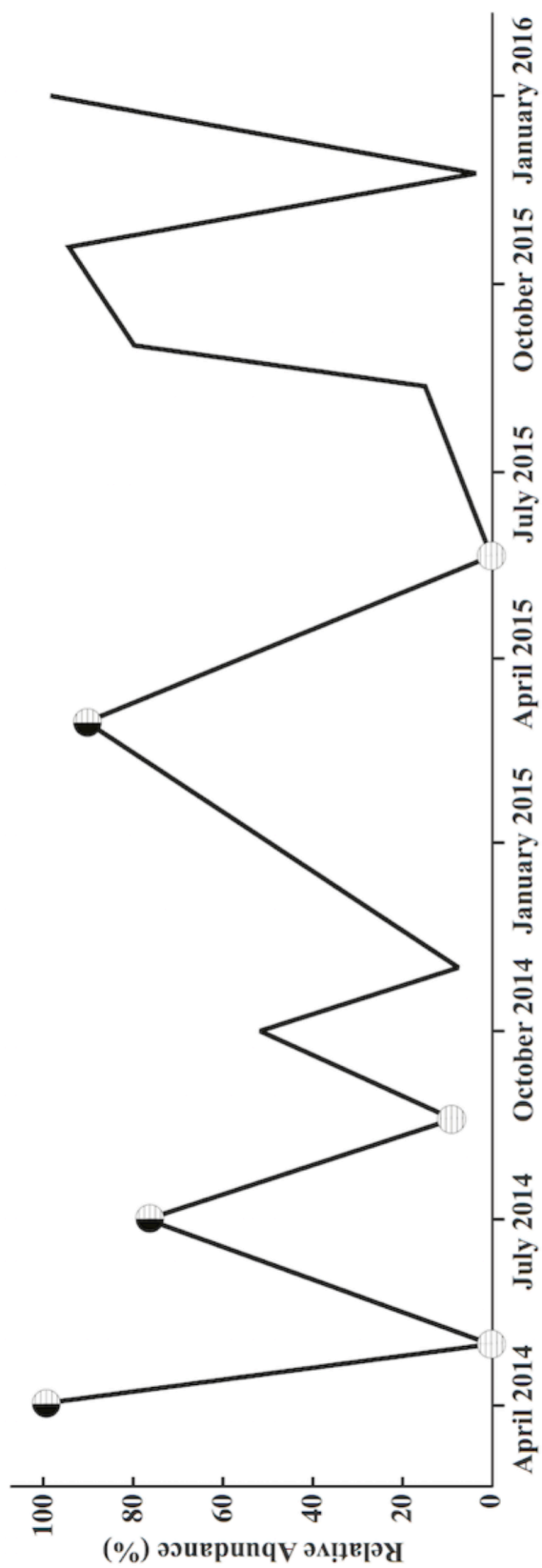


Figure 6. The relative abundance of the Trichocomaceae in bottom fuel samples over time at SE 3. Elevated ATP readings (Table 3) are noted as an open circle with lines. Instances of both elevated ATP readings and visible flocculent material (reported by operator) are shown as a solid semi-circle and open semi-circle with lines.

Table 4. qPCR quantification of 18S rRNA gene copies in select fuel samples from April to August 2014. Standard deviation represents the average of triplicate biological replicates.

Sample/Date	Copies 18S/L B20	Standard Deviation
SE 3 April 2014	3.75x10 ⁵	4.90x10 ⁵
SE 3 May 2014	4.12x10 ³	3.54x10 ³
SE 3 July 2014	9.54x10 ¹	5.91x10 ¹
SE 3 August 2014	2.39x10 ⁵	4.12x10 ⁵
SE 4 April 2014	9.61x10 ⁵	1.62x10 ⁶
SE 4 May 2014	4.74x10 ¹	4.39x10 ¹
SE 4 July 2014	1.01x10 ¹	6.02
SE 4 August 2014	6.13x10 ¹	7.89x10 ¹
SE E April 2014	1.47x10 ³	1.65x10 ³
SE E May 2014	3.35x10 ³	3.43x10 ³
SE E July 2014	1.27x10 ⁵	1.11x10 ⁵
SE E August 2014	9.98x10 ³	8.31x10 ³
SE Receipt July 2014	BDL	BDL

Genome Sequencing of Select Isolates

Bacteria and fungi were isolated from fuels at SE and SW belonging to the bacterial genera *Pseudomonas*, *Burkholderia*, *Roseomonas*, *Gluconacetobacter*, and the fungal genera *Byssoschlamys* and *Wickerhamomyces* (Oderay Andrade, unpublished research). A genome was sequenced for an isolate of each genus. After genome sequencing and

annotation, each genome contained putative esterase/lipase clusters and complete beta-oxidation pathways. Each sequenced bacterial isolate also contained putative mono- and di-oxygenases, suggesting a potential ability to degrade the hydrocarbons present in B20. Both the *Wickerhamomyces* sp. and *Byssochlamys* sp. isolates that were sequenced also had gene clusters with similarity to known di-oxygenases. A single metagenome sequenced from SE 3 contained a number of esterase/lipases, mono- and di-oxygenases, and putative benzylsuccinate synthases. Nitrogenase gene clusters were also found in metagenomic sequence, but not in isolated genomes. The *Byssochlamys* sp. isolate contained sixty-three putative biosynthetic gene clusters identified by antiSMASH, including clusters predicted to produce a beta-lactam similar to penicillin, mycotoxins with similarity to Roquefortine C, Fujikurin (Bargen et al., 2015), and yanuthone (Petersen et al., 2014).

RNA Sequencing of Byssochlamys sp. Grown on B20

Approximately 438 million paired reads for all treatments were obtained from the RNA sequencing experiment samples. After mapping the reads to the genome sequence, transcripts were recovered associated with the degradation of FAME in high abundance relative to other transcripts (Fig. 7) in the B20 growth condition. All genes associated with FAME oxidation were greater than one standard deviation above the average of all other transcripts, which was on average 20.8 transcripts per million (TPM_{avg}). The genome of the *Byssochlamys* sp. would predict the capability of oxidizing methanol to CO₂ in addition to the activation of FAME and the beta-oxidation of the corresponding fatty acids (Fig. 7).

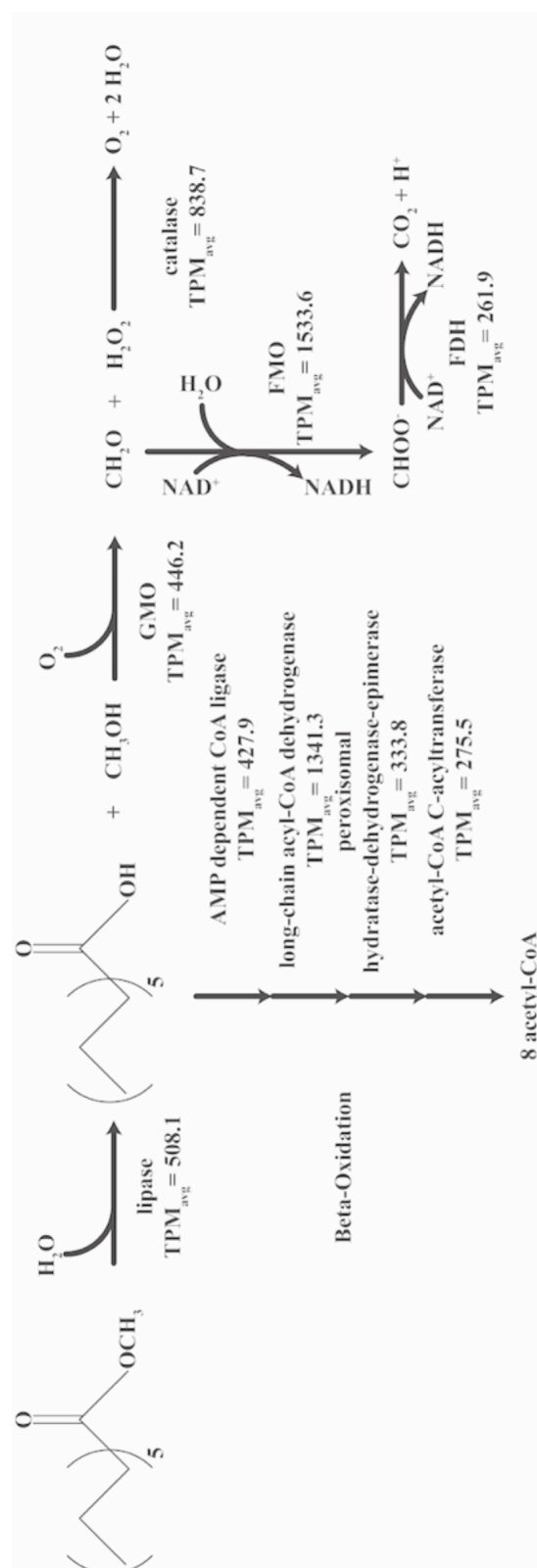


Figure 7: Detected transcripts associated with the degradation of fatty acid methyl esters when the *Byssoschlamys* sp. was grown on B20. Transcripts are noted as an average of the triplicate Transcripts Per Million (TPM) value. The mean TPM value for all detected transcripts in *Byssoschlamys* sp. grown on B20 was 20.8.

Fuel Acid Index of select samples from SE

Fuels at SE E and SE 4 were within specification between August 2014 and March 2015. In May of 2015 SE 3 exceeded the maximum allowable fuel acid index according to ASTM specification D973 (Table 5).

Table 5. Acid index of select fuels from SE October of 2014, March and May of 2015. Values are expressed in mg KOH/g B20. Samples that exceed ASTM specification for B5 to B20 blends are denoted in bold.

	October 2014	March 2015	May 2015
SE 3	0.17	0.30	1.51
SE 4	0.08	0.16	0.28
SE E	0.22	0.09	0.24
Receipt ^a			0.06

^aReceipt fuel taken only in May of 2015 due to availability

GC/MS Identification of Putative Metabolites in Byssochlamys sp. Grown in B20

Detectable amounts of the trimethylsilyl (TMS) derivative of palmitic acid were detected after 3 weeks of incubation in aqueous extracts of *Byssochlamys* sp. grown on B20. Only two of the three replicates had detectable oleic or linoleic acid TMS derivatives. Acetic acid and ethanol TMS derivatives were also putatively identified using the NIST library in all cultures, however the identified peak was near the trailing edge of the solvent peak, and near the BSTFA and TMS peaks, making them difficult to distinguish.

Discussion

The use of biodiesel as a liquid transportation fuel has many advantages, including increased energy independence and reduced carbon emissions. The use of a twenty percent blend of biodiesel with ULSD met the goals of the DoD mandate to decrease carbon emissions and reduce dependence on foreign oil sources (Air Force Energy Plan, 2009). In addition to the desired reduction in petroleum oil usage, B20 was compatible with existing storage and dispensing hardware within the USAF and shares combustion characteristics with ULSD (Canakci, 2007; Chang et al., 1996), making biodiesel a desirable alternative fuel.

Reduced fuel stability is one of the potential trade-offs for using biodiesel.

Contamination and fouling were noted by operators within one year of its' deployment to facilities throughout the USAF, (Dr. Wendy J. Crookes-Goodson, personal communication). Despite the potential for microbial growth in the fuel, operators assumed that the "waxes" or solids observed in bottom fuel samples were due to the abiotic oxidation and instability of FAME biodiesel compared to ULSD (Dr. Wendy J. Crookes-Goodson, personal communication). Biodiesel was susceptible to microbial contamination and proliferation by a diverse bacterial and fungal community, resulting in recurrent fouling. The structure of these communities varied with time, and isolated bacteria and fungi found in fuels at both SE and SW had the genetic capability to degrade FAME. Viscous biofilms were apparent (Fig. 1b) in fuels at SW, and biofilms at SE imaged using SEM were largely made of filamentous fungal cells (Fig. 2a). No bacteria were visible in SEM of biofilms taken from SE or SW suggesting that fungi are the primary component of observed biofilms. Eighty-seven percent of the 18S rRNA

gene library at SE E in October of 2015 was composed of members of the Trichocomaceae (Fig. 5). This supports the hypothesis that microorganisms are responsible for fouling in biodiesel tanks. More specifically, the biofilms are primarily hyphal fungi, suggesting that fungi compose the bulk of the observable biomass in biodiesel tanks.

Both the bacteria and fungi from the microbial communities were distinct between all sampled locations using an adonis test ($p = 0.001$, $R^2 = 0.152$ and 0.137 for bacteria and fungi respectively), although a stronger predictor of community membership was the tank at each location ($p = 0.001$, $R^2 = 0.22$ and 0.20 for bacteria and fungi respectively), and finally the date on which each tank was sampled ($p = 0.001$, $R^2 = 0.67$ and 0.662 for bacteria and fungi respectively). This appears to be primarily correlated to the relative abundance of the Acetobacteraceae at SE (Fig. 4) and the Trichocomaceae at SW (Fig. 5). No attempts were made to disrupt the microbial community present at SW during the sampling period (i.e. tank cleaning). It is therefore possible that the high relative abundance of the Trichocomaceae represents a stable biofilm community at the bottom of the three SW tanks. In all tanks where fuel was sampled at multiple positions, the Trichocomaceae were more abundant at the bottom of the tank and less abundant at the top of the fuel column (Fig. 5). Filamentous fungi may be better suited to the fuel water interface near the bottom of the tank representing a form of structure and a specific niche that the Trichocomaceae could occupy.

The abundance of FAME may be another potential explanation for the distribution of bacterial and fungal communities throughout the fuel column. Both fungal and bacterial communities separated significantly at SE by the relative abundance of FAME (Table 1

and 2) detected by GC/MS in fuels (Oderay Andrade, unpublished data). Palmitic acid methyl ester and linoleic acid methyl ester produced the strongest correlation to community structure. It is possible that this is driven by the ability of organisms to selectively consume these FAMES though this must be confirmed in isolate growth studies. It is possibly even more likely that this pattern is simply from the correlation between fungal biomass and their impact on the fuel. Filamentous fungi are abundant in the bottom of the tank/fuel column, they are metabolizing the FAME in the fuels and; therefore, the FAME content in the fuels at these locations in the fuel column is decreased.

Attempting to determine which OTUs were shared between all samples showed that only 64 bacterial and 6 fungal OTUs were shared across 50 percent of all samples, including many of the most dominant OTUs. The diverse community of microorganisms in low abundance in B20 storage tank may impart some randomness to community distribution that is reflected in the small number of shared OTUs between locations, although these OTUs may have little impact on the metabolic activity of the community. Only a few abundant bacterial and fungal OTUs that may have a greater impact on the metabolism of B20 were shared between locations, notably the Trichocomaceae. Any organism that can first establish itself at the fuel-water interface or grow anaerobically at the bottom of a tank may be able to propagate.

Events related to the management of the fuel storage systems seemed to influence the distribution of the microbial community and detectable microbial activity. Numerous management events such as fuel deliveries, tank cleanings, and water infiltration occurred just prior to or after sampling events. Correspondingly, shifts in community

structure and quantities of ATP appeared after these events. At the SE AFB after an extended survey beginning in April 2014, and ending in January of 2016 multiple cleaning events occurred during or after sampling. Cleaning events ranged from water removal to a complete removal of fuel and pressure washing of the tanks. Despite attempts to control the resident microbial community, the system rebounded within 3-6 months, signaled by the return of flocculent material in the fuel. Observable fouling events correlated to a bloom of the Trichocomaceae, and elevated levels of detectable ATP in fuels (Fig. 6). Conversely, samples taken soon after fuel receipts, after a heavy rain, or soon after a cleaning event (Fig. 6) typically showed a reduction in the relative abundance of OTUs related to the Trichocomaceae (Fig. 2). In its place were Saccharomycetaceae and other fungi. The Trichocomaceae may grow at a slower rate than the Saccharomycetaceae, allowing a short-lived high abundance of yeast during periods of low biomass before a bloom of the filamentous Trichocomaceae can establish itself at the fuel-water interface near the bottom of a tank.

While not visible in the imaging of biofilms, the bacteria may still play a role in the metabolism and acidification of B20. Members of the Acetobacteraceae were numerically abundant in our samples from SE (Fig. 2) and are likely capable of degrading trace amounts of glycerol remaining in biodiesel, which could produce ethanol, acetic acid, and 2,3-Dihydroxypropanoic acid (Almeida et al., 2012; Habe et al., 2009). A single isolate was recovered most closely related to the genus *Gluconacetobacter* that is a member of the family Acetobacteraceae. A putative lipase/esterase was annotated in the *Gluconacetobacter* sp. genome along with a complete beta-oxidation pathway required to degrade FAME. The Clostridiaceae 1 and

Ruminococcaceae were also present at both SE and SW in bottom tank samples (Fig. 4). The Ruminococcaceae are capable of fermentative growth and the production of acetic acid and ethanol (Robinson and Ritchie, 1981). In addition to trace amounts of glycerol (Biebl et al., 1999), the Clostridiaceae 1 could ferment any number of metabolic products found in B20 undergoing biodegradation, although no attempt was made to cultivate these organisms. Both obligately aerobic and anaerobic bacteria were found in fuels taken at all sites, suggesting that the gradient of oxygen throughout the within each tank and fuel column may play a significant selective role. Biodiesel and biodiesel blends can retain a higher concentration of dissolved oxygen compared to ULSD (NREL-P-540-43672) potentially allowing aerobic microorganisms to proliferate at the fuel water interface near the bottom of each tank. The proliferation of biofilms could create locally anoxic conditions at the bottom of the tank.

The number of potentially acetogenic bacteria including the Acetobacteraceae, Ruminococcaceae, and the Clostridiaceae 1 discovered at both locations is particularly worrisome for tank and fuel health. In SE tank 3, the acid index of the fuel increased beyond acceptable levels (Table 5) possibly from the conversion of FAME to fatty acids and further organic acid production from fermentative bacteria.

At the SE AFB, members of the Burkholderiales and other proteobacteria were relatively abundant. Members of the genus *Burkholderia* are known to be able to fix nitrogen (Estrada-De Los Santos et al., 2001), which may represent an essential ecological role for these organisms in the fuel tank. Genes for the molybdenum/iron (MoFE) nitrogenase were identified in the metagenome sequenced from SE tank 3. The genome from the single *Burkholderia* (most closely related to *Burkholderia tropica*)

isolated from this tank did not contain nitrogen fixation genes. Like all other bacterial isolates sequenced, it had the genomic capability to oxidize FAME.

The fungal families Trichocomaceae and Saccharomycetaceae were most abundant in all tanks at SE and SW (Fig. 5). The eukarya appeared less diverse than the bacteria across all tanks, although the 18S rRNA gene lacks the ability to resolve eukaryotic phylogeny as easily as bacteria or archaea (Philippe et al., 2000; Stiller and Hall, 1999). Members of the Saccharomycetaceae, including the genus *Pichia*, are known to use FAME as a carbon and energy source (Kumari and Gupta, 2014) by first producing a large standing pool of free fatty acids and consuming the available methanol prior to oxidizing the fatty acids. This would increase the acidity of fuel or lower the pH of any water bottom that is present. One isolate from the genus *Wickerhamomyces* (family Saccharomycetaceae) recovered from contaminated B20 at SW was capable of growth on FAME as a sole carbon and energy source (unpublished research, Oderay Andrade). Other members of the Saccharomycetaceae are known to degrade alkanes and fatty acids (Liu et al., 2015), so it is not surprising that a yeast is capable of growth in a B20 tank. Genomic sequence from *Wickerhamomyces* sp. also suggested that it could degrade FAME, and potentially grow on the alkanes in petroleum diesel through the use of monooxygenases. Despite the ability of the Saccharomycetaceae to rapidly degrade FAME, it appears unable to remain numerically dominant in any tank. The majority of visible biomass at SE E was filamentous fungi (Fig. 2a), with the Trichocomaceae being the most numerically abundant. A single abundant OTU within the Trichocomaceae was shared between all locations sampled.

A member of the genus *Byssochlamys* was isolated from a tank in the SW where thick filamentous biofilm was observed. This sequenced 18S rRNA gene of the organism shares significant homology with a dominant OTU present at both SE and SW (Oderay Andrade, unpublished data). Transcripts recovered from the *Byssochlamys* sp. isolate grown on B20 as the sole carbon substrate suggested the ability to grow on the fatty acid methyl esters present in the fuel through the use of lipase/esterases to convert the FAME to free fatty acids, and the oxidation of methanol to CO₂ (Fig. 7). In a separate experiment, the *Byssochlamys* sp. isolate was shown to degrade all major FAMES present within B20 over 80 days (Oderay Andrade, unpublished data). No metabolites associated with the aerobic or anaerobic activation of alkanes present in B20 were detected suggesting that FAME was the primary carbon substrate for the *Byssochlamys* sp. isolate. A corresponding increase in fatty acids was also detected in derivatized fuels, although methanol or acetic were not detected (Oderay Andrade, unpublished data). The detected lipase transcript was greater than two standard deviations more abundant than the mean TPM value of all recovered transcripts. Transcription of the genes involved in the pathway to degrade methanol was similarly up regulated (Fig. 7). Other Trichocomaceae are capable of growth on C₁ compounds (Meyers, 1982); however, the transcriptome data appears to be the first evidence of a member of the *Byssochlamys* growing on methanol. Further characterization of *Byssochlamys* sp. growing on methanol as the sole carbon substrate is required before this can be confirmed. Beta-oxidation associated genes were also highly transcribed suggesting that *Byssochlamys* sp. is capable of the oxidation of FAME to acetyl-CoA.

Another key trait of the isolate was the potential ability to produce numerous antimicrobial secondary metabolites. Sixty-three biosynthetic gene clusters were identified in the completed genome, including a cluster predicted to produce a beta-lactam similar to penicillin. Numerous mycotoxins production pathways with similarity to Roquefortine C, Fujikurin (Bargen et al., 2015), and yanuthone (Petersen et al., 2014) were found in the *Byssochlamys* sp. genome. This potential capacity to produce antibacterial and antifungal compounds may be linked to the apparent ability of the *Byssochlamys* sp. to competitively exclude other fungi and bacteria from surfaces or the fuel-water interface, which would confer a significant advantage over time. The *Byssochlamys* sp. isolate was characterized by the ability to degrade FAME aerobically, the production of thick, viscous biofilms, and the potential to produce a number of antimicrobial compounds. This combination could allow it to occupy much of the available physical space at the fuel-water-oxygen interface, competitively excluding other organisms from the primary carbon source present in the system.

Conclusions

Repeated fouling of biodiesel was observed across storage tanks at USAF bases in the southeastern and southwestern United States. The presence of biofilms was correlated to filamentous fungi and a representative of an abundant OTU was isolated. The isolate, *Byssochlamys* sp., was capable of growing on B20 through the use of a lipase to initially convert the FAME to fatty acids and methanol, which were then most likely oxidized to acetic acid and CO₂. Increased microbial contamination of fuel in a tank at SE showed an increase in the relative abundance of the Trichocomaceae and a concomitant increase in acidity. Here, we used SSU rRNA gene sequencing, microscopy, cultivation, genome

sequencing, metabolomics, and transcriptomics to create a high-resolution description of the role of microorganisms in the fouling and fuel degradation of B20 at multiple locations across the United States.

While fouling was noted at the bottom of tanks, the fuel at the dispensing point was consistently acceptable and little to no impact was noted to the vehicle fleet (Personal communication). A much larger survey would be required to assess the impact of fouled/acidified fuel to ground fleet vehicles, however the acid index of the fuel suggests that the fuel could pose a risk over an extended time. A previous study found no significant risk to vehicles, but the sample size was far too small (Proc et al., 2006). The relative abundance of acetogenic bacteria and fungi is potentially concerning. Localized production of acetic acid could increase corrosion under biofilms (Crolet et al., 1999; Little et al., 1992). How the resident bacterial and fungal community impacts the corrosion of materials within each tank remains to be discovered. The research also suggests that during periods of high usage the community is disturbed, and the major fungal community members fail to establish numerical dominance. Maintaining a smaller standing pool of fuel that is used more rapidly could ensure that costly cleaning and disposal of fuel is kept to a minimum. Understanding the microbial community dynamics within biodiesel storage tanks is essential prior to the development of mitigation strategies.

References

Air Force Energy Plan (2009). Air Force Energy Plan. 1–38.

Aktas, D. F., Lee, J. S., Little, B. J., Ray, R. I., Davidova, I. A., Lyles, C. N., et al.

- (2010). Anaerobic Metabolism of Biodiesel and Its Impact on Metal Corrosion. *Energy Fuels* 24, 2924–2928. doi:10.1021/ef100084j.
- Almeida, J. R. M., Fávaro, L. C. L., and Quirino, B. F. (2012). Biodiesel biorefinery: opportunities and challenges for microbial production of fuels and chemicals from glycerol waste. *Biotechnol. Biofuels* 5, 48. doi:10.1186/1754-6834-5-48.
- ASTM D7463-15, Standard Test Method for Adenosine Triphosphate (ATP) Content of Microorganisms in Fuel, Fuel/Water Mixtures, and Fuel Associated Water, ASTM International, West Conshohocken, PA, 2015, www.astm.org
- Bankevich, A., Nurk, S., Antipov, D., Gurevich, A. A., Dvorkin, M., Kulikov, A. S., et al. (2012). SPAdes: a new genome assembly algorithm and its applications to single-cell sequencing. *J. Comput. Biol.* 19, 455–477. doi:10.1089/cmb.2012.0021.
- Bargen, von, K. W., Niehaus, E.-M., Krug, I., Bergander, K., Würthwein, E.-U., Tudzynski, B., et al. (2015). Isolation and Structure Elucidation of Fujikurins A–D: Products of the PKS19 Gene Cluster in *Fusarium fujikuroi*. *J. Nat. Prod.* 78, 1809–1815. doi:10.1021/np5008137.
- Biebl, H., Menzel, K., Zeng, A. P., and Deckwer, W. D. (1999). Microbial production of 1,3-propanediol. *Appl. Microbiol. Biotechnol.* 52, 289–297. doi:10.1007/s002530051523.
- Bolger, A. M., Lohse, M., and Usadel, B. (2014). Trimmomatic: a flexible trimmer for Illumina sequence data. *Bioinformatics* 30, 2114–2120. doi:10.1093/bioinformatics/btu170.

- Bücker, F., Santestevan, N. A., Roesch, L. F., Jacques, R. J. S., do Carmo Ruaro Peralba, M., de Oliveira Camargo, F. A., et al. (2011). Impact of biodiesel on biodeterioration of stored Brazilian diesel oil. *Int. Biodeterior. Biodegradation* 65, 172–178. doi:10.1016/j.ibiod.2010.09.008.
- Canakci, M. (2007). Combustion characteristics of a turbocharged DI compression ignition engine fueled with petroleum diesel fuels and biodiesel. *Bioresour. Technol.* 98, 1167–1175. doi:10.1016/j.biortech.2006.05.024.
- Caporaso, J. G., Bittinger, K., Bushman, F. D., DeSantis, T. Z., Andersen, G. L., and Knight, R. (2010a). PyNAST: a flexible tool for aligning sequences to a template alignment. *Bioinformatics* 26, 266–267. doi:10.1093/bioinformatics/btp636.
- Caporaso, J. G., Kuczynski, J., Stombaugh, J., Bittinger, K., Bushman, F. D., Costello, E. K., et al. (2010b). QIIME allows analysis of high-throughput community sequencing data. *Nat. Meth.* 7, 335–336. doi:10.1038/nmeth.f.303.
- Chang, D. Y. Z., Van Gerpen, J. H., Lee, I., Johnson, L. A., Hammond, E. G., and Marley, S. J. (1996). Fuel properties and emissions of soybean oil esters as diesel fuel. *J. Am. Oil Chem. Soc.* 73, 1549–1555. doi:10.1007/BF02523523.
- Crolet, J.-L., Thevenot, N., and Dugstad, A. (1999). Role of Free Acetic Acid on the CO₂ Corrosion of Steels. NACE International ISBN: 99024 1999 CP
- D27 Committee (2008). Guide for Sampling, Test Methods, and Specifications for Electrical Insulating Oils of Petroleum Origin. 2008 ed. West Conshohocken, PA: ASTM International doi:10.1520/D0117.

- DeMello, J. A., Carmichael, C. A., Peacock, E. E., Nelson, R. K., Samuel Arey, J., and Reddy, C. M. (2007). Biodegradation and environmental behavior of biodiesel mixtures in the sea: An initial study. *Marine. Poll. Bull.* 54, 894–904. doi:10.1016/j.marpolbul.2007.02.016.
- Dimotakis, P., Grober, R., and Lewis, N. (2006). Reducing DOD Fossil Fuel Dependence. McLean, Virginia 22102-7508.
- Dixon, P. (2003). VEGAN, a package of R functions for community ecology. *J. Veg. Sci.* 14, 927–930. doi:10.1111/j.1654-1103.2003.tb02228.x.
- Edgar, R. C. (2013). UPARSE: highly accurate OTU sequences from microbial amplicon reads. *Nat. Meth.* 10, 996–998. doi:10.1038/nmeth.2604.
- Estrada-De Los Santos, P., Bustillos-Cristales, R., and Caballero-Mellado, J. (2001). Burkholderia, a genus rich in plant-associated nitrogen fixers with wide environmental and geographic distribution. *Appl. Environ. Microbiol.* 67, 2790–2798. doi:10.1128/AEM.67.6.2790-2798.2001.
- Fregolente, P. B. L., Fregolente, L. V., and Maciel, M. R. W. (2012). Water content in biodiesel, diesel, and biodiesel–diesel blends. *J. Chem. Eng. Data* doi:10.1021/je300279c.
- Gerber, G. K. (2014). The dynamic microbiome. *FEBS Lett.* 588, 4131–4139. doi:10.1016/j.febslet.2014.02.037.
- Grabherr, M. G., Haas, B. J., Yassour, M., Levin, J. Z., Thompson, D. A., Amit, I., et al.

- (2011). Full-length transcriptome assembly from RNA-Seq data without a reference genome. *Nat. Biotechnol.* 29, 644–652. doi:10.1038/nbt.1883.
- Habe, H., Shimada, Y., Yakushi, T., Hattori, H., Ano, Y., Fukuoka, T., et al. (2009). Microbial production of glyceric acid, an organic acid that can be mass produced from glycerol. *Appl. Environ. Microbiol.* 75, 7760–7766. doi:10.1128/AEM.01535-09.
- Hestrin, S., and Schramm, M. (1954). Synthesis of cellulose by *Acetobacter xylinum*. II. Preparation of freeze-dried cells capable of polymerizing glucose to cellulose. *Biochem. J.* 58, 345–352.
- Hiltunen, J. K., Mursula, A. M., Rottensteiner, H., Wierenga, R. K., Kastaniotis, A. J., and Gurvitz, A. (2003). The biochemistry of peroxisomal beta-oxidation in the yeast *Saccharomyces cerevisiae*. *FEMS Microbiol. Rev.* 27, 35–64. doi:10.1016/S0168-6445(03)00017-2.
- Kazakov, A. E., Rodionov, D. A., Alm, E., Arkin, A. P., Dubchak, I., and Gelfand, M. S. (2008). Comparative Genomics of Regulation of Fatty Acid and Branched-Chain Amino Acid Utilization in Proteobacteria. *J. Bacteriol.* 191, 52–64. doi:10.1128/JB.01175-08.
- Kist, J., and Tate, R. L., III (2013). Phylogeny of bacterial methylotrophy genes reveals robustness in *Methylobacterium mx*A sequences and *mx*A operon construction. *Soil Biol. Biochem.* 59, 49–57. doi:10.1016/j.soilbio.2012.12.010.
- Kondo, T., Morikawa, Y., and Hayashi, N. (2008). Purification and characterization of

- alcohol oxidase from *Paecilomyces variotii* isolated as a formaldehyde-resistant fungus. *Appl. Microbiol. Biotechnol.* 77, 995–1002. doi:10.1007/s00253-007-1237-9.
- Kumari, A., and Gupta, R. (2014). Novel strategy of using methyl esters as slow release methanol source during lipase expression by mut⁺ *Pichia pastoris* X33. *PLoS One* 9, e104272. doi:10.1371/journal.pone.0104272.
- Leggett, R. M., Heavens, D., Caccamo, M., Clark, M. D., and Davey, R. P. (2016). NanoOK: multi-reference alignment analysis of nanopore sequencing data, quality and error profiles. *Bioinformatics* 32, 142–144. doi:10.1093/bioinformatics/btv540.
- Li, Y.-L., Weng, J.-C., Hsiao, C.-C., Chou, M.-T., Tseng, C.-W., and Hung, J.-H. (2015). PEAT: an intelligent and efficient paired-end sequencing adapter trimming algorithm. *BMC Bioinformatics* 16 Suppl 1, S2. doi:10.1186/1471-2105-16-S1-S2.
- Lisiecki, P., Chrzanowski, Ł., Szulc, A., and Ławniczak, Ł. (2014). Biodegradation of diesel/biodiesel blends in saturated sand microcosms. *Fuel*. doi:10.1016/j.fuel.2013.08.009.
- Little, B., Wagner, P., and Mansfeld, F. (1992). An overview of microbiologically influenced corrosion. *Electrochim. Acta* 37, 2185–2194. doi:10.1016/0013-4686(92)85110-7.
- Liu, C. M., Kachur, S., Dwan, M. G., Abraham, A. G., Aziz, M., Hsueh, P.-R., et al. (2012). FungiQuant: a broad-coverage fungal quantitative real-time PCR assay. *BMC Microbiol.* 12, 255. doi:10.1186/1471-2180-12-255.

- Liu, H.-H., Ji, X.-J., and Huang, H. (2015). Biotechnological applications of *Yarrowia lipolytica*: Past, present and future. *Biotechnol. Adv.* 33, 1522–1546.
doi:10.1016/j.biotechadv.2015.07.010.
- Love, M. I., Huber, W., and Anders, S. (2014). Moderated estimation of fold change and dispersion for RNA-seq data with DESeq2. *Genome Biol.* 15, 1–21.
doi:10.1186/s13059-014-0550-8.
- Lozupone, C., and Knight, R. (2005). UniFrac: a New Phylogenetic Method for Comparing Microbial Communities. *Appl. Environ. Microbiol.* 71, 8228–8235.
doi:10.1128/AEM.71.12.8228-8235.2005.
- McNamara, C. J., Perry, T. D., IV, Leard, R., Bearce, K., Dante, J., and Mitchell, R. (2005). Corrosion of aluminum alloy 2024 by microorganisms isolated from aircraft fuel tanks. *Biofouling* 21, 257–265. doi:10.1080/08927010500389921.
- Meckenstock, R. U., Netzer, von, F., Stumpp, C., Lueders, T., Himmelberg, A. M., Hertkorn, N., et al. (2014). Water droplets in oil are microhabitats for microbial life. *Science* 345, 673–676. doi:10.1126/science.1252215.
- Meyers, A. J., Jr (1982). Obligate methylotrophy: evaluation of methyl formate as a C₁ compound. *Can. J. Microbiol.* 28, 1401–1404. doi:10.1139/m82-209.
- Nichols, D., Cahoon, N., Trakhtenberg, E. M., Pham, L., Mehta, A., Belanger, A., et al. (2010). Use of ichip for high-throughput in situ cultivation of “uncultivable” microbial species. *Appl. Environ. Microbiol.* 76, 2445–2450.
doi:10.1128/AEM.01754-09.

- National Renewable Energy Laboratory staff (January 2009). Biodiesel Handling and Use Guide (PDF) (Report) (Fourth ed.). National Renewable Energy Laboratory. p. 23. NREL/TP-540-43672.
- Owsianiak, M., Chrzanowski, Ł., Szulc, A., Staniewski, J., Olszanowski, A., Olejnik-Schmidt, A. K., et al. (2009). Biodegradation of diesel/biodiesel blends by a consortium of hydrocarbon degraders: Effect of the type of blend and the addition of biosurfactants. *Bioresour Technol* 100, 1497–1500. doi:10.1016/j.biortech.2008.08.028.
- Parada, A., Needham, D. M., and Fuhrman, J. A. (2015). Every base matters: assessing small subunit rRNA primers for marine microbiomes with mock communities, time-series and global field samples. *Environ Microbiol.* doi:10.1111/1462-2920.13023.
- Patro, R., Duggal, G., and Kingsford, C. (2015). Accurate, fast, and model-aware transcript expression quantification with Salmon. Cold Spring Harbor Labs Journals doi:10.1101/021592.
- Petersen, L. M., Holm, D. K., Knudsen, P. B., Nielsen, K. F., Gotfredsen, C. H., Mortensen, U. H., et al. (2014). Characterization of four new antifungal yanuthones from *Aspergillus niger*. *J. Antibiot.* 68, 201–205. doi:10.1038/ja.2014.130.
- Philippe, H., Lopez, P., Brinkmann, H., Budin, K., Germot, A., Laurent, J., et al. (2000). Early-branching or fast-evolving eukaryotes? An answer based on slowly evolving positions. *Proc. R. Soc. Lond. [Biol.]* 267, 1213–1221. doi:10.1098/rspb.2000.1130.

- Price, M. N., Dehal, P. S., and Arkin, A. P. (2010). FastTree 2 – Approximately Maximum-Likelihood Trees for Large Alignments. *PLoS One* 5, e9490. doi:10.1371/journal.pone.0009490.
- Prince, R. C., Haitmanek, C., and Lee, C. C. (2008). The primary aerobic biodegradation of biodiesel B20. *Chemosphere* 71, 1446–1451. doi:10.1016/j.chemosphere.2007.12.010.
- Proc, K., Barnitt, R., Hayes, R. R., Ratcliff, M., McCormick, R. L., Ha, L., et al. (2006). 100,000-Mile Evaluation of Transit Buses Operated on Biodiesel Blends (B20). in (400 Commonwealth Drive, Warrendale, PA, United States: SAE International), 2006–01–3253. doi:10.4271/2006-01-3253.
- Pruesse, E., Quast, C., Knittel, K., Fuchs, B. M., Ludwig, W., Peplies, J., et al. (2007). SILVA: a comprehensive online resource for quality checked and aligned ribosomal RNA sequence data compatible with ARB. *Nucleic Acids Res.* 35, 7188–7196. doi:10.1093/nar/gkm864.
- Robinson, I. M., and Ritchie, A. E. (1981). Emendation of *Acetivibrio* and Description of *Acetivibrio ethanoligignens*, a New Species from the Colons of Pigs with Dysentery. *Int. J. Syst. Bacteriol.* 31, 333–338. doi:10.1099/00207713-31-3-333.
- Salter, S., Cox, M. J., Turek, E. M., Calus, S. T., and Cookson, W. O. (2014). Reagent contamination can critically impact sequence-based microbiome analyses. *bioRxiv*.
- Schloss, P. D., Westcott, S. L., Ryabin, T., Hall, J. R., Hartmann, M., Hollister, E. B., et al. (2009). Introducing mothur: open-source, platform-independent, community-

- supported software for describing and comparing microbial communities. *Appl. Environ. Microbiol.* 75, 7537–7541. doi:10.1128/AEM.01541-09.
- Solano-Serena, F., Nicolau, E., Favreau, G., Jouanneau, Y., and Marchal, R. (2008). Biodegradability of 2-ethylhexyl nitrate (2-EHN), a cetane improver of diesel oil. *Biodegradation* 20, 85–94. doi:10.1007/s10532-008-9202-6.
- Stiller, J. W., and Hall, B. D. (1999). Long-branch attraction and the rDNA model of early eukaryotic evolution. *Mol. Biol. Evol.* 16, 1270–1279.
- The World Factbook 2013-14. Washington, DC: Central Intelligence Agency, 2013 .
- Van Gerpen, J. H., Soylu, S., and Chang, D. (1998). *Evaluation of the lubricity of soybean oil-based additives in diesel fuel. Prepared for The United Soybean Board.* Mechanical Engineering Department.
- Williams, C. R., Baccarella, A., Parrish, J. Z., and Kim, C. C. (2016). Trimming of sequence reads alters RNA-Seq gene expression estimates. *BMC Bioinformatics* 17, 103. doi:10.1186/s12859-016-0956-2.
- Zhang, J., Kobert, K., Flouri, T., and Stamatakis, A. (2014). PEAR: a fast and accurate Illumina Paired-End reAd mergeR. *Bioinformatics* 30, 614–620.

Chapter 4. Increased Risk of Microbially Influenced Corrosion in B20 Biodiesel Storage Systems due to Fungal Contamination and Proliferation

Foreword

The research discussed in this chapter was a collaborative effort between the University of Oklahoma and the Air Force Research Laboratory (AFRL). My direct contribution was through the collection of samples, DNA extraction, and PCR amplification of samples collected during the initial placement of materials within each tank, and at all time points with the exception of the 12 month sampling at each location. I also performed the statistical analyses of corrosion rates and pitting data generated by our collaborators at AFRL. My advisor Dr. Bradley Stevenson conceived the experiment, assisted in sampling, data interpretation, and advised me on the creation and execution of laboratory experiments. Dr. Heather Nunn assisted in the collection of samples, DNA extraction, and PCR amplification of samples collected at the 12 month time point at both sampling locations. James Floyd assisted in the collection of samples. Dr. Wendy J. Crookes-Goodson (AFRL) assisted in site access, collection of samples, and experimental design. Caitlin Bojanowski, Angela Campo, Carrie Drake, and Dr. Chia Hung at AFRL all assisted in the collection of samples. Caitlin Bojanowski and Carrie Drake also contributed by cleaning and weighing uncoated steel witness coupons to determine corrosion rates and in the white light interferometry used to determine pit depth on select witness coupons.

Abstract

Microorganisms have the ability to degrade components of biodiesel. The degradation of biodiesel and the presence of microbial biofilms have the potential to accelerate the corrosion of storage systems. The extent of microbially influenced corrosion (MIC) in an operational B20 storage system is unknown. To assess the community composition of biofilms and measure their corrosive capacity, uncoated and polyurethane coated steel witness coupons, and nitrile and fluorocarbon O-rings were incubated *in situ* for up to 18 months in B20 storage tanks at an Air Force Base (AFB) in the Southeastern (SE) and Southwestern (SW) United States. Biofilms observed on all materials were composed almost exclusively of a single operational taxonomic unit (OTU) representing a family of filamentous fungi, the Trichocomaceae. Members of the bacterial families Acetobacteraceae, Ruminococcaceae, and the Clostridiaceae group 1 were the most numerically abundant in biofilms at the SW AFB. Biofilms at the SE AFB however, were composed of largely members of the Burkholderiaceae, Sphingomonadaceae, and Rhodobacteraceae. The bacterial and fungal communities in biofilms at one AFB were both significantly distinct from those at the other AFB, just as they were in the fuels. Overall, the microbial communities (bacteria and fungi) were significantly less diverse at the SE AFB compared to the SW AFB. At the SE AFB, witness coupons were removed in three-month intervals and assessed for corrosion and pitting. At 9 months there was a significant difference in the corrosion rate of uncoated steel coupons located near the bottom of SE tank 3, which experienced recurring fungal contamination and proliferation. Significant differences in maximum pit depth, a measure of pitting corrosion, was observed after 3 months on uncoated steel coupons

mounted approximately 0.5 m from the bottom of the same tank. Visible pits were observed under these biofilms, which were composed primarily the Trichocomaceae. Localized production of organic acids by fungi in these biofilms could lead to increased pitting corrosion when significant biomass is present. Consequently, no significant corrosion was measured above background in all other sampled tanks, which did not contain large amounts of biomass, suggesting a direct link between fungal biofilm proliferation and an increased risk of microbially influenced corrosion.

Introduction

One of the single largest expenses to the United States (US) economy is the cost of corrosion, which is estimated at 6 % of gross domestic product per year (Koch et al., 2002). Within the United States, 14.6 % of corrosion costs are attributed to the U.S. Air Force (USAF) and Department of Defense (DoD) infrastructure. Maintenance records in the USAF that mention “corrosion” in FY’08-09 represented direct costs of over \$5.87 Billion (Herzberg et. al 2016). Corrosion accounts for 23.4 % of Air Force aviation and missile maintenance costs and 17.8 % of system non-availability hours. Since the introduction of biodiesel, costs related to the maintenance of storage tanks and fuel dispensing systems have risen considerably each year by FY 2014 (Dr. Wendy J. Crookes-Goodson, personal communication). Estimates of corrosion vary considerably between sources due to issues relating to non-disclosure or fear of reporting an issue (Mansfield et al., 2015).

Corrosion of steel surfaces can occur through several abiotic processes. Unprotected mild steel surfaces can oxidize and form a layer of protective iron oxide. If the layer is disturbed, further oxidation can occur. Under anaerobic conditions protons are reduced through a reaction with Fe^0 generating hydrogen and Fe^{2+} . The Fe^{2+} can then react with sulfide or carbonate present within the environment and form an iron sulfide or iron carbonate mineral (Enning and Garrelfs, 2014).

Microbially influenced corrosion (MIC) can occur through numerous processes by a wide taxonomic distribution of microorganisms through several proposed mechanisms (NACE TM02012-2012) including the localized production of acids, reactive sulfides, enzymes or the direct shuttling of electrons (Enning and Garrelfs, 2014). Under anaerobic conditions, acetic acid can increase the rate of steel corrosion by the direct reduction of acetic acid to acetate at the metal surface (Tran et al., 2013). Production of CO_2 can also increase the rate of acetic acid corrosion (Gu, 2014). Anaerobic sulfate reducers can directly withdraw electrons from an iron surface and produce thick iron carbonate corrosion products (Enning and Garrelfs, 2014). The reduction of sulfate to produce sulfide can also interact with the abiotic oxidation of Fe^0 to generate iron sulfide (Beech and Sunner, 2004).

Microbial biofilms can accelerate corrosion due to the localized production of pits caused by reactive sulfides or acids (Lee et al., 2009) that create an environment that is drastically different from the surrounding fluid (Little et al., 1992). This can create an environment conducive to the dissolution of iron oxides in aerobic systems increasing the rate of corrosion relative to abiotic systems or the formation of iron sulfides in anaerobic sulfidic environments.

Bacteria and fungi, which formed biofilms and were capable of producing organic acids under aerobic and anaerobic conditions, were found in tanks storing a biodiesel blend at multiple USAF facilities in the United States (Chapter 3). Biodiesel is a “drop in” fuel replacement for ultra low sulfur diesel (ULSD) used in a 20 % blend (B20) within the DoD. It was relatively easy for the USAF to transition their non-emergency, non-combat vehicles to B20 fuel in order to reduce both carbon emissions and dependence on foreign oil sources.

As discussed and shown in Chapter 3, microorganisms are capable of growing in B20 biodiesel, using the FAME component as a source of carbon and energy. Microbial metabolism of the FAME results in fouling due to increased microbial biomass and the production of organic acids. A member of the filamentous fungal family Trichocomaceae was largely responsible for significant fouling observed in fuels at USAF bases in the Southeastern (SE) and Southwestern (SW) United States. Fuels exposed to prolonged microbial degradation, especially those stored in steel tanks, are often heavily discolored and contain thick biofilms at the fuel-water interface (Chapter 3). Fungi are known to solubilize metals through the production of organic acids and other metabolites that may enhance corrosion (Clark et al., 1984). Filamentous fungi are also known to degrade biodiesel (Bücker et al., 2011) although the link between biodegradation and biocorrosion has not been made *in situ*. Specifically, the fungi found in USAF biodiesel tanks (Chapter 3) including the Trichocomaceae are known to produce organic acids that can enhance pitting corrosion (De Leo et al., 2013). In the research described in this chapter, we tested the hypothesis that *fungal contamination is the cause of biocorrosion in biodiesel storage tanks*.

The percentage of corrosion costs within the USAF attributable directly to microorganisms was not explored and remains unknown. Because of the lack of reporting, the ability to investigate biocorrosion and fouling within an active system is of significant interest. This study aims to better understand how fungi not only corrode or weaken materials, but potentially how multiple members within a microbial community can interact to enhance, or reduce corrosive processes using a combination of *in situ* surveys and laboratory microcosm experiments. To adequately understand the risk to USAF biodiesel storage tanks, it was necessary to monitor biofilms and corrosion *in situ* over a period of eighteen months. Biofilms were sampled from a large number of witness coupons and O-rings at three or six month intervals in six B20 storage tanks at two USAF facilities in collaboration with the Air Force Research Laboratories. Mass loss and pitting depth was measured simultaneously in an attempt to link key fungal or bacterial taxa to increased rates of corrosion.

Methods

Site Descriptions and In Situ Corrosion Assessment

Six B20 tanks at two United States Air Force bases (AFBs) were chosen for a one-year survey of materials in the southeast (SE) and southwest (SW) United States (Fig. 1a). The sites were chosen based on availability and reported contamination issues. The three tanks at the SW AFB were constructed of carbon steel, and installed in the early 1950s. At the SE AFB, two tanks were constructed of fiberglass and a third tank was made of carbon steel lined with fiberglass. All six tanks were below ground and had a large maintenance hatch. A PVC rack roughly 51 cm wide, 51 cm long, and 61 cm high (Fig. 1b) was placed in each tank through the maintenance hatch. Polymer coated and

uncoated 1010 carbon steel witness coupons approximately 2.54 cm wide by 7.62 cm tall (ACT Test Panel LLC., Hillsdale, MI) were suspended 61 cm and 2.5 cm from the bottom of the tank on a PVC rack (Fig. 1b). Witness coupons were removed at ≈ 3 month intervals at SE, and ≈ 6 month intervals at SW. These locations were chosen because each set of coupons was likely to be exposed to potential fouling and corrosion at the fuel-water interface, and within the fuel layer of each tank. Nitrile and fluorocarbon O-Rings, which are common materials used for fittings within tanks, were suspended at the lower level on each rack. The O-rings were removed at ≈ 6 month intervals at all sites. Coated and uncoated carbon steel witness coupons were suspended within the vapor space in each tank. Vapor phase coupons were taken at 6 months and 1 year. The survey of SE tank 3 concluded at 9 months due to heavy fouling and water influx. A total of 264 uncoated and 175 coated steel coupons, and 72 of each type of O-ring (Nitrile and fluorocarbon) were placed in the tanks at SE. At SW a total of 132 uncoated and 108 coated steel coupons, and 36 of each type of O-ring (nitrile and fluorocarbon) were placed in the three B20 storage tanks. As a control, coated and uncoated control witness coupons were incubated in filter sterilized B20 taken from fuel samples received at each site prior to exposure to any potentially contaminated storage tank ($n = 9$ for each treatment). Coated and uncoated control witness coupons were also suspended over filter sterilized B20 as a control for vapor space coupons.

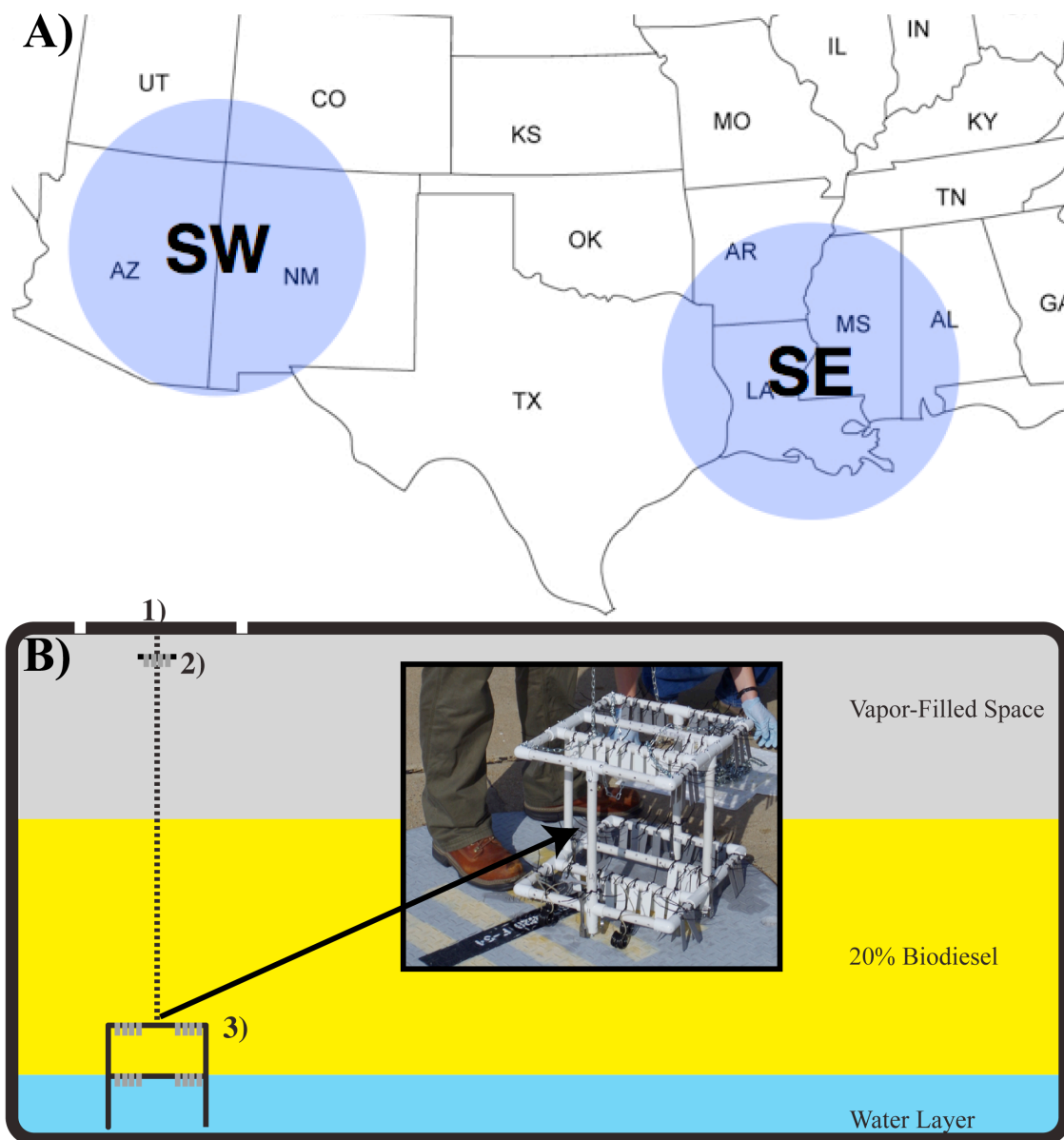


Figure 1. Overview of sampled locations including the number of samples (A). An overview of a biodiesel storage tank (B). Witness coupons and O-Rings were suspended from the main entry hatch (1). Witness coupons were placed in either the vapor filled space above the fuel layer (2) or near the bottom of the tank (3) at the predicted fuel-water interface.

Coupon Surface Imaging and of Weight Loss Determination

Replicate witness coupons ($n = 5$) removed from tanks were photographed on-site and shipped overnight. Biofilm and corrosion products were removed following ASTM standard G1-03 using the hydrochloric acid method (ASTM G1-03). Briefly, coupons were sonicated for 10 min in soapy water, rinsed in deionized water, dried, and incubated in 3 M hydrochloric acid with 3.5 g/L hexamethylene tetramine solution for 10 min. Acid cleaned coupons were washed in deionized water, acetone, and methanol, dried under a stream of nitrogen, and weighed. Cleaned coupons ($n = 1$) from the top position in SE tanks 3, 4, and control coupons were imaged using a Keyence VK-X200 3D Laser Scanning Confocal Microscope (Keyence Corp., Itasca, IL). Maximum and average pit depth was measured using three points at 14 positions for each uncoated coupon. Mass loss and pit depth data failed the Shapiro-Wilk (Shapiro and Wilk, 1965) test of normalcy ($p > 0.05$), so a nonparametric Van der Waerden test (Van Der Waerden, 1953) was used to compare field coupons to sterile controls. Multiple pairwise tests comparing *in situ* incubations to controls were carried out *post hoc* using a Conover test (Gellings and Gudger, 1998) within the package PMCMR (Pohlert 2014), and p values were corrected using the false discovery rate (FDR) method (Benjamini and Yekutieli, 2001) within PMCMR.

DNA Sampling, Preservation, and Extraction

Biofilms on coupon surfaces were sampled using nylon flocked swabs (Therapak Corp, Los Angeles, CA), and placed into a 2.0 mL ZR BashingBead™ Lysis Tube (Zymo Research Corp., Irvine, CA) containing 0.7 mL (dry volume) of 0.5 mm ZR BashingBead™ lysis matrix (Zymo Research Corp.) and 750 μ L DNA

Lysis/Preservation solution (Zymo Research Corp.). Homogenization was carried out on-site using a battery-powered reciprocating saw (One World Technologies, Inc., Anderson, SC) fitted with a custom head to accommodate a number of bead tubes at once. Samples were shipped at room temperature and stored at -20 °C. Prior to DNA extraction samples were homogenized for an additional 30 s using a BioSpec Mini-BeadBeater-8 (Biospec Products Inc., Bartlesville, OK). DNA extractions were performed according to manufacturer specifications using the Zymo Xpedition Soil/Fecal kit (Zymo Research Corp.).

PCR Amplification and DNA Sequencing

Libraries of bacterial, archaeal, and eukaryotic SSU rRNA gene fragments were amplified from each DNA extraction using PCR with primers that spanned the ribosomal RNA gene V4 hypervariable region between position 515 and 926 (*E. coli* numbering) that produced a ~400 bp fragment for bacteria and archaea, and a 600 bp fragment for the eukaryotes. These primers evenly represent a broad distribution of all three domains of life (Parada et al., 2015). The forward primer 515F-Y (**GTA AAA CGA CGG CCA G** CCG TGY CAG CMG CCG CGG TAA-3') contains the M13 forward primer (in bold) fused to the SSU rRNA gene specific forward primer (underlined) while the reverse primer 926R (5'-CCG YCA ATT YMT TTR AGT TT-3') was unmodified from Parada et. al 2015. 5 PRIME HOT master mix (5 PRIME Inc., Gaithersburg, MD) was used for all reactions at a final volume of 50 µL. Reactions were purified using Agencourt AMPure XP paramagnetic beads (Beckman Coulter Inc., Indianapolis, IN) at a final concentration of 0.8 x v/v. After purification, 4 µL of PCR product was used in a barcoding reaction to attach a unique 12 bp barcode to each

library in duplicate 50 μ L reactions (Appendix 1). Duplicate reactions were pooled, purified using Agencourt AMPure XP paramagnetic beads (Beckman Coulter Inc.) to a final volume of 40 μ L, quantified using the QuBit HS DS DNA assay kit (Thermo Fisher Scientific Inc., Waltham, MA), and pooled in equimolar amounts before concentration using an Amicon 30 K centrifugation column (EMD Millipore, Billerica, MA) to a final volume of 80 μ L. To mitigate the effects of reagent contamination (Salter et al., 2014) multiple extraction blanks and negative controls were sequenced from each batch of extractions.

SSU rRNA gene libraries were sequenced using Illumina MiSeq V2 PE250 chemistry. Libraries were prepared with the TruSeq DNA LT Sample Prep kit (Illumina). Sequencing libraries were loaded at a final concentration of 10 pM for libraries sequenced with additional genomic samples, or 6 pM for amplicon libraries prepared and sequenced individually. A spike-in of 10-40 percent phiX DNA was used to increase the sequence diversity.

Sequence Analysis

Sequence reads were merged using PEAR (Zhang et al., 2014), demultiplexed in QIIME version 1.9.1 (Caporaso et al., 2010b), and filtered by quality and clustered into OTUs using UPARSE (Edgar, 2013). Experimental samples were compared to controls using DEseq2 (Love et al., 2014) to identify OTUs that originated from potentially contaminated DNA extraction or PCR reagents (Salter et al., 2014). Any OTUs not significantly differentially abundant from controls were then filtered from downstream analyses.

Taxonomy was assigned using mothur (Schloss et al., 2009) and the r123 SILVA database (Pruesse et al., 2007). A representative sequence of each OTU was aligned with pyNAST (Caporaso et al., 2010a) against an aligned version of the SILVA r123 database, and filtered to remove uninformative bases. Phylogenetic trees for both the Bacteria and Archaea, and the Eukarya were produced using the maximum likelihood method and the Jukes Cantor evolutionary model within FastTree (Price et al., 2010).

Differences in community composition were estimated using the weighted UniFrac index (Lozupone and Knight, 2005). The effect of site, tank, material, and the location of materials within each tank were tested using a PERMANOVA using the R package Vegan (Dixon, 2003) within QIIME.

Growth of Consortia on a Defined B20 Fuel

The *Byssochlamys* sp. isolate and either the *Burkholderia* sp. or *Gluconacetobacter* sp. isolate obtained from tanks in the SE and SW (Oderay Andrade, unpublished data) were co-cultured in 1 mL of artificial sump water (ASW) medium (McNamara et al., 2005) with 1 mL ultra low sulfur diesel (ULSD) amended with 20 % v/v methyl palmitate (Sigma-Aldrich, St. Louis, MO) and a single carbon steel wire nail with a total surface area of 0.94 cm² to assess how species interactions impact corrosion rates. Uninoculated controls containing 1mL of the ULSD/methyl palmitate mixture and 1mL of ASW with a carbon steel nail were also prepared.

Byssochlamys spores were prepared by heating 50 mL of culture medium to 70 °C, before passing through a 10 µm filter (EMD Millipore, Billerica, MA). The filtrate was centrifuged at 8000 xRCF for 20 min, and the pelleted spores were resuspended in 1 mL

of ASW. Spore suspensions were prepared fresh and used immediately. Bacterial cultures were first inoculated from a single colony into 50 mL of Hestrin-Schramm broth (Hestrin and Schramm, 1954). After 72 hours, 5 mL of culture was pelleted at 5,000 xRCF for 10 min and the broth removed. Each culture was counted by hemocytometry and inoculated at a total density of 1×10^5 cells or spores per mL.

Cultures were destructively sampled at 1-week intervals for 9 weeks. Each culture was vortexed for 10 s prior to filtration in order to remove any biofilm attached to the wire nail. At each time point, the aqueous layer was filtered onto a pre-weighed 0.22 μm PES filter, and dried at 60 °C for 72 h. Dried filters were then weighed to assess the total dry-weight biomass of each culture.

The wire nails were removed from cultures at each time interval and cleaned using a modified version of the hydrochloric acid method (ASTM G1-03). Each nail was also photographed for a qualitative assessment of biomass and corrosion prior to biofilm removal. Nails were vortexed in each culture tube to remove loosely attached corrosion product and biofilm. Any remaining corrosion products or biofilms were removed in 800 μL of a 3 M solution of hydrochloric acid and 3.5 g/L hexamethylene tetramine. Acid cleaned nails were washed in sterile distilled water, acetone, and finally methanol, and dried under a stream of nitrogen. After cleaning, the nails were weighed on an analytical balance. Mass loss data failed the Shapiro-Wilk test of normalcy ($p > 0.05$), so a nonparametric Van der Waerden test was used, as described above.

Results

Analysis of Bacterial and Fungal Communities Associated with Biofilms at SE and SW

A total of 250 samples contained a total of 2.24 million bacterial and archaeal sequences after quality control, which clustered into 2589 OTUs. The number of observed bacterial and archaeal OTUs was significantly lower ($p = 0.001$) at SW than those detected at SE. Significant differences ($p < 0.05$) were also found in all pairwise comparisons of the microbial biofilm communities in tanks at SE and SW with the exception of comparisons between SW 3 and 4, SE 3 and SW 3, and SE 3 and SW 4 (Table 1). No significant difference ($p > 0.050$) in the number of observed OTUs was observed between materials. A total of 347 samples with 0.92 million eukaryotic sequences and 591 OTUs passed quality control and filtering. As with the bacterial and archaeal OTUs, the number of observed eukaryotic OTUs was significantly lower ($p = 0.001$) at SW than SE. Significant differences ($p < 0.05$) were also found in all pairwise comparisons of tanks at SE and SW with the exception of comparisons between SW 2 and 4, SW 3 and 4, SE 3 and SW 3, and SE 3 and SW 4 (Table 2). No significant difference ($p > 0.050$) in the number of observed OTUs was observed between materials.

Members of the bacterial family Acetobacteraceae were abundant in the majority of biofilm samples taken at SW across all time points while the family was less abundant compared to other families at SE (Fig. 2). A single abundant OTU within the Acetobacteraceae was unique to the SE and SW. Members of the Clostridiaceae group 1 were present in greater abundance at SW as well as the Moraxellaceae and the

Rhodobacteraceae. At the SE AFB, the Burkholderiaceae were found in greater abundance than at SW (Fig. 3).

Table 1. Pairwise comparisons of bacterial diversity measured as the number of observed OTUs in biofilms across time and the Southeast (SE) and Southwest (SW). Values are an average across all sampled time points.

	Group 1	Group 2	Group 1		Group 2		t stat	p-value
			mean	SD	mean	SD		
SE 3	SE 4		58.5	35.5	116.5	27.2	-9.339	0.008
SE 3	SW 2		58.5	35.5	32.3	11.7	4.666	0.002
SE 3	SW 3		58.5	35.5	71.7	47.8	-1.454	0.164
SE 3	SW 4		58.5	35.5	69.6	43.7	-1.315	0.226
SE E	SE 3		135.8	46.9	58.5	35.5	9.297	0.004
SE E	SE 4		135.8	46.9	116.5	27.2	2.678	0.006
SE E	SW 2		135.8	46.9	32.3	11.7	14.319	0.002
SE E	SW 3		135.8	46.9	71.7	47.8	6.523	0.015
SE E	SW 4		135.8	46.9	69.6	43.7	7.129	0.003
SW 2	SE 4		32.3	11.7	116.5	27.2	-19.186	0.002

SW 2	SW 3	32.3	11.7	71.7	47.8	-5.29	0.002
SW 2	SW 4	32.3	11.7	69.6	43.7	-5.461	0.003
SW 3	SE 4	71.7	47.8	116.5	27.2	-5.766	0.005
SW 3	SW 4	71.7	47.8	69.6	43.7	0.199	0.852
SW 4	SE 4	69.6	43.7	116.5	27.2	-6.477	0.001

Table 2. Pairwise comparisons of eukaryal diversity measured as the number of observed OTUs in biofilms across time and t position from the Southeast (SE) and Southwest (SW). Values are an average across all sampled time points.

Group 1	Group 2	Group 1		Group 2		t stat	p-value
		mean	SD	mean	SD		
SE 3	SE 4	9.1	3.1	15.1	7.3	-5.394	0.008
SE 3	SW 2	9.1	3.1	6.8	2.7	3.878	0.002
SE 3	SW 3	9.1	3.1	9.7	6.1	-0.699	0.511
SE 3	SW 4	9.1	3.1	8.0	4.1	1.505	0.151
SE E	SE 3	21.3	6.3	9.1	3.1	11.612	0.004
SE E	SE 4	21.3	6.3	15.1	7.3	3.610	0.005
SE E	SW 2	21.3	6.3	6.8	2.7	13.803	0.002
SE E	SW 3	21.3	6.3	9.7	6.1	7.795	0.015
SE E	SW 4	21.3	6.3	8.0	4.1	10.844	0.003
SW 2	SE 4	6.8	2.7	15.1	7.3	-7.291	0.003

SW 2	SW 3	6.8	2.7	9.7	6.1	-3.031	0.007
SW 2	SW 4	6.8	2.7	8.0	4.1	-1.621	0.128
SW 3	SE 4	9.7	6.1	15.1	7.3	-3.701	0.005
SW 3	SW 4	9.7	6.1	8.0	4.1	1.610	0.140
SW 4	SE 4	8	4.1	15.1	7.3	-5.584	0.002

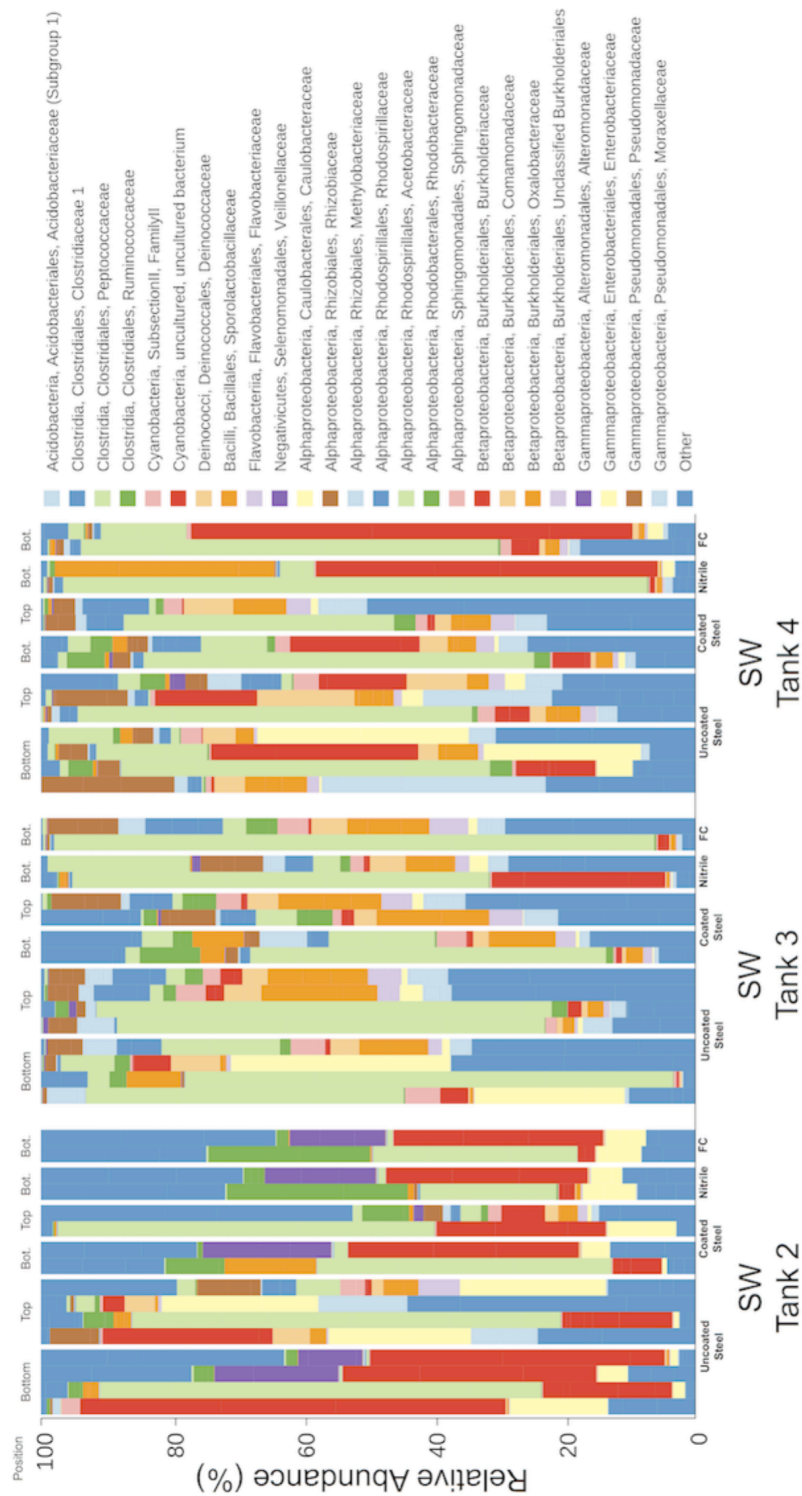


Figure 2. Taxonomy summary of the bacterial families detected in materials at SW. Position within the tank is denoted above each sample type. Bars are clustered by material and in order of increasing sampling date (left to right). Taxonomic lineages that represented less than 1 percent on average of any sample were condensed into the “other” category.

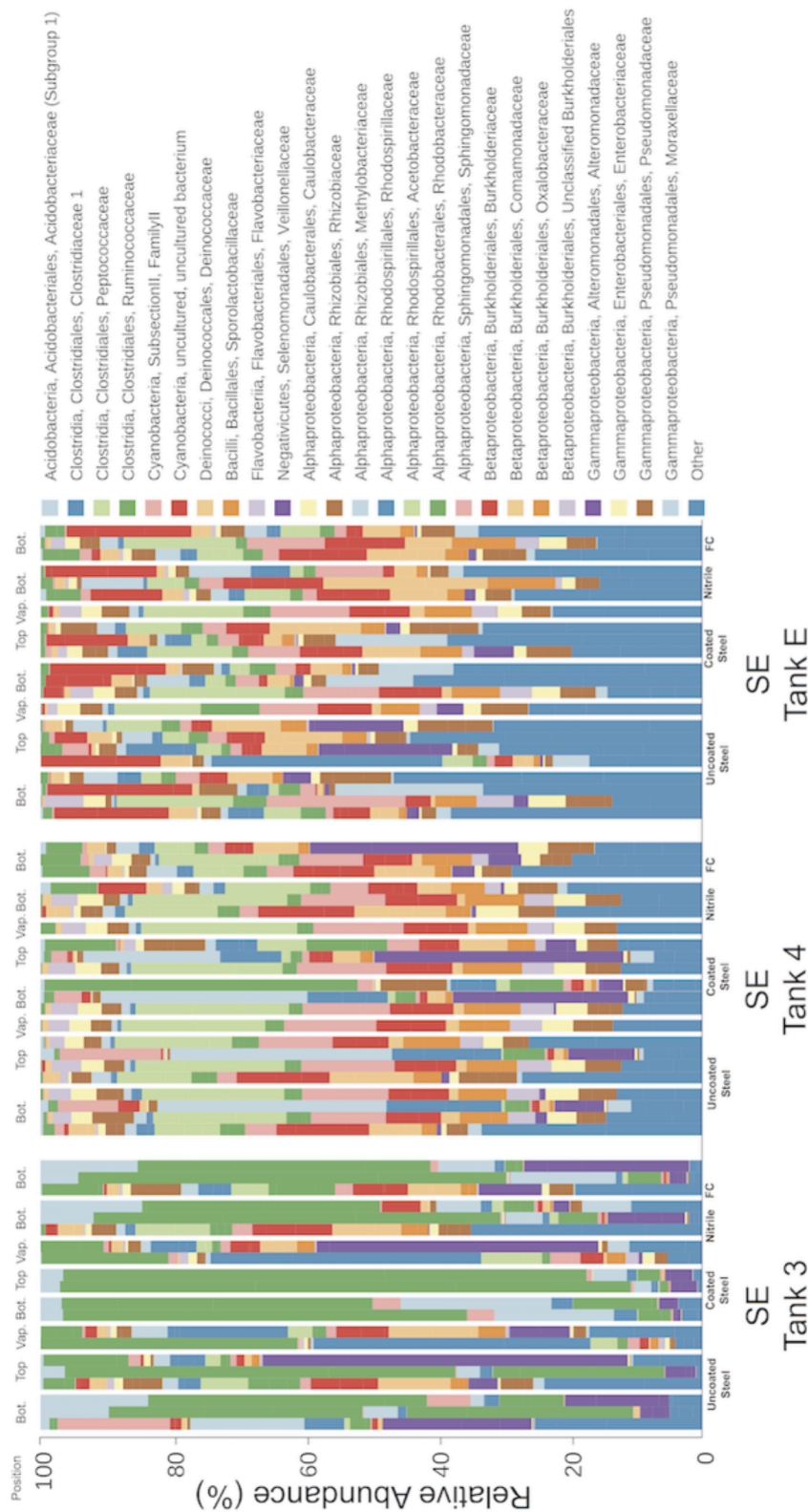


Figure 3. Taxonomy summary of the bacterial families detected in materials at SE. Position within the tank is denoted above each sample type. Bars are clustered by material and in order of increasing sampling date (left to right). Taxonomic lineages that represented less than 1 percent on average of any sample were condensed into the “other” category.

The filamentous fungal family Trichocomaceae was the most abundant at SW across all time points and on all tested materials (Fig. 4). The Trichocomaceae were also abundant in biofilms at the bottom of SE 3 (Fig. 5). Otherwise, the Uncultivated Pleosporales and the Saccharomycetaceae were relatively abundant in biofilms from SE 4 and E. Other members of the Pezizomycotina including the Mycosphaerellaceae and uncultivated members of the Pleosporales were relatively abundant in biofilms taken from witness coupons suspended 61 cm above the bottom of the tank in SW 3 and 4.

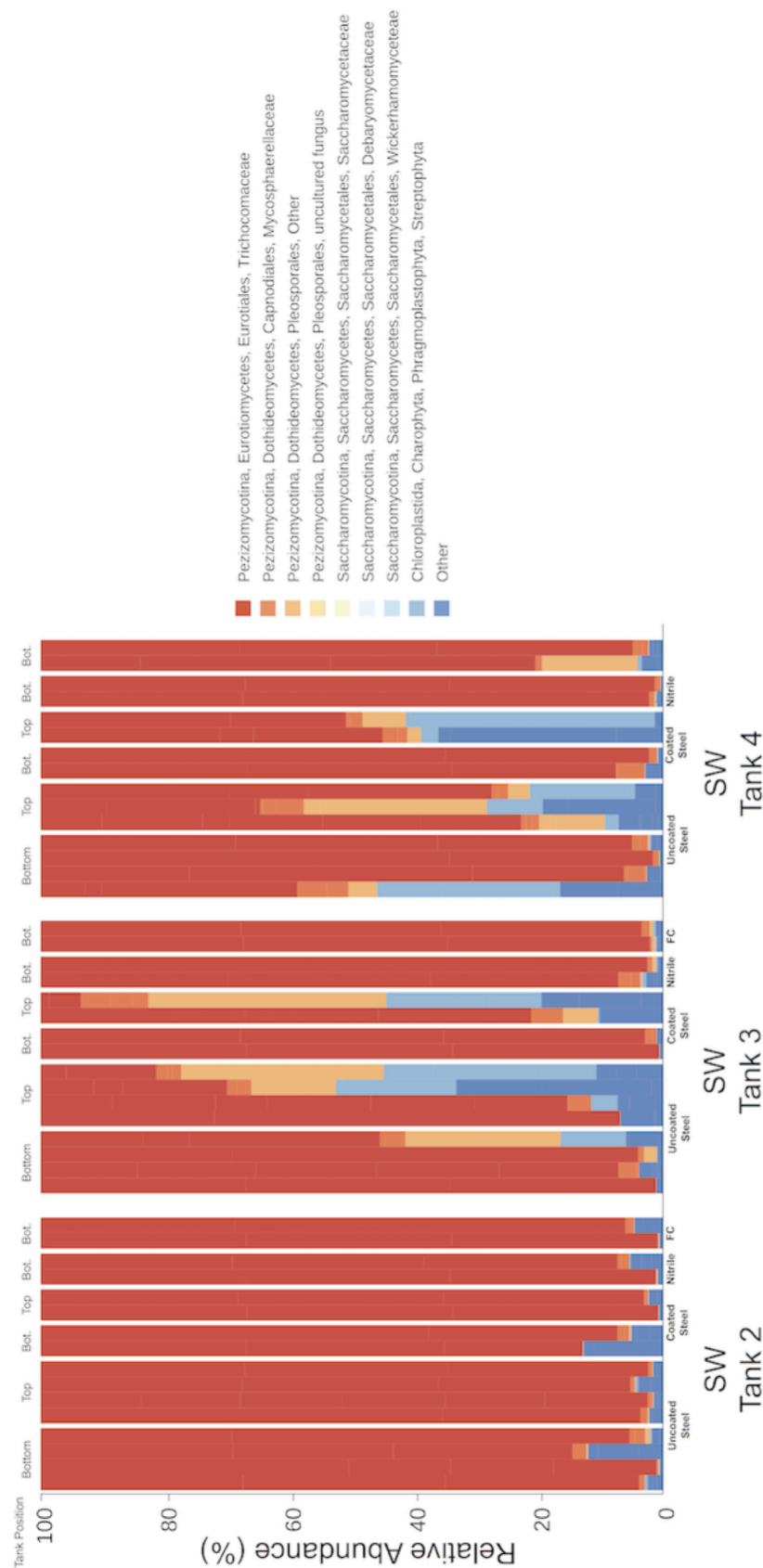


Figure 4. Taxonomy summary of the eukaryotic families detected on different materials at SW. Position within the tank is denoted above each sample type. Bars are clustered by material and in order of increasing sampling date (left to right). Taxonomic lineages that represented less than 1 percent on average of any sample were condensed into the “other” category.

Community structure was significantly different by site ($p < 0.001$, $R^2 = 0.118$) in bacterial and archaeal samples (Fig. 6), and for eukarya ($p = 0.001$, $R^2 = 0.251$, Fig. 7). No significant differences in community structure were observed on different materials across both sites ($p > 0.050$). Community structure was more strongly correlated by tank ($p < 0.001$, $R^2 = 0.297$ for bacteria and 0.344 for eukarya) and the position of materials within each tank ($p = 0.001$, $R^2 = 0.436$ for bacteria and archaea, $p = 0.001$, $R^2 = 0.568$ for eukarya, Table 3).

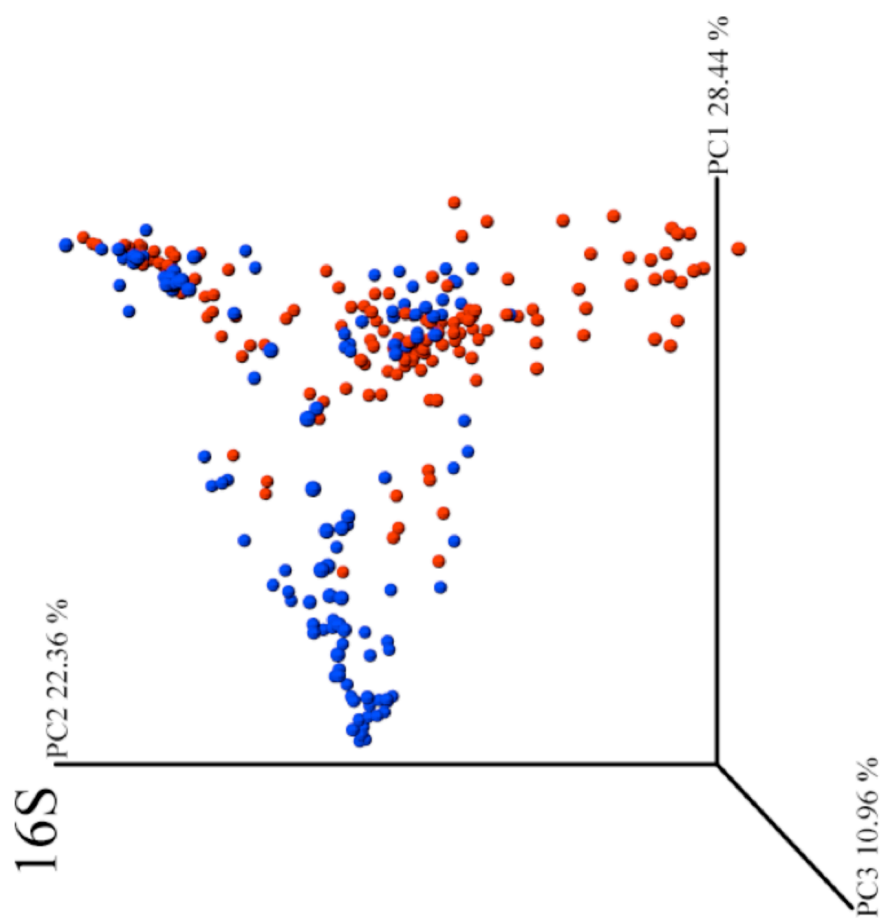


Figure 6. Principal Coordinates Analysis (PCoA) ordination of all bacterial and archaeal samples at SW (Blue) and SE (Red) at an even sampling depth of 1000 sequences per sample.

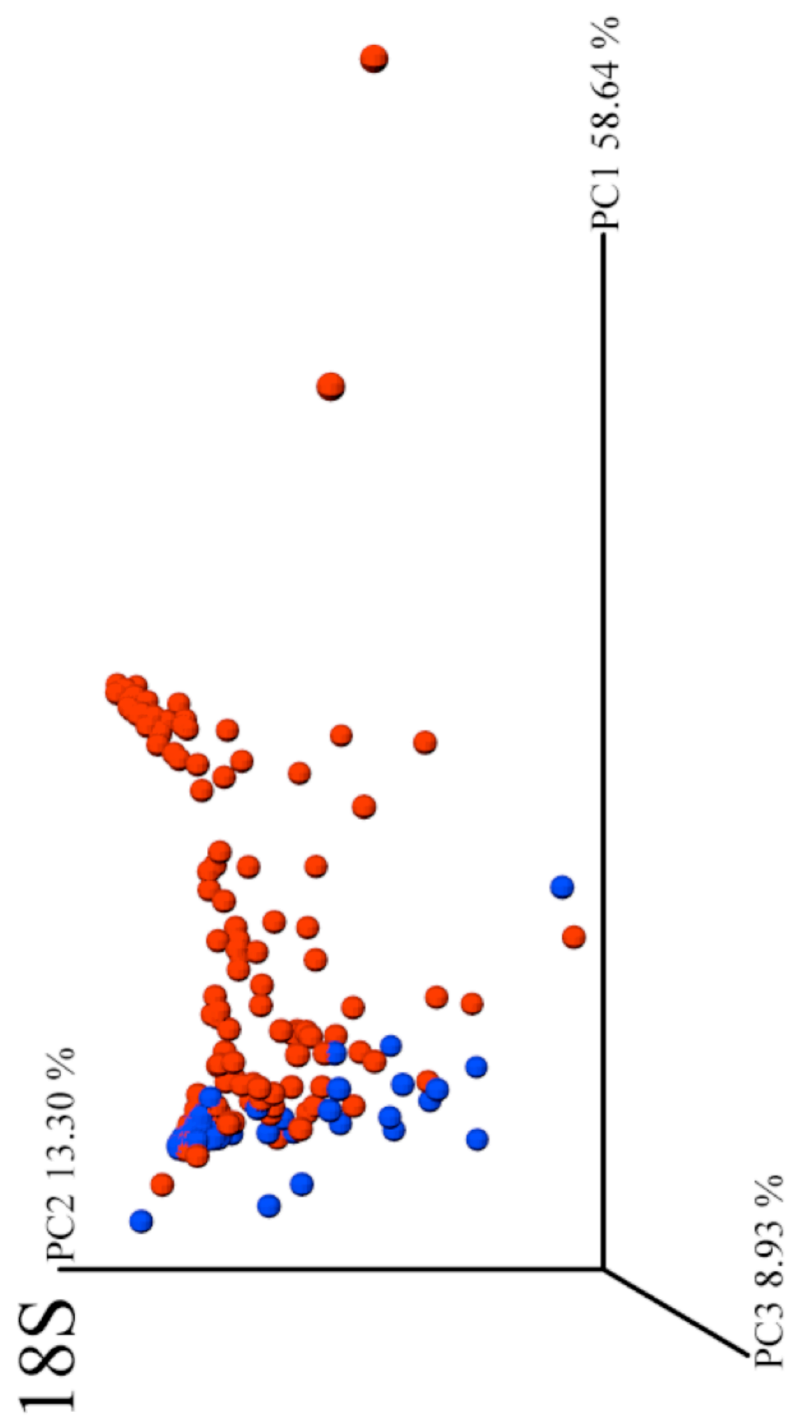


Figure 7. Principal Coordinates Analysis (PCoA) ordination of all eukaryotic samples at SW (Blue) and SE (Red) at even sampling depth of 500 sequences per sample.

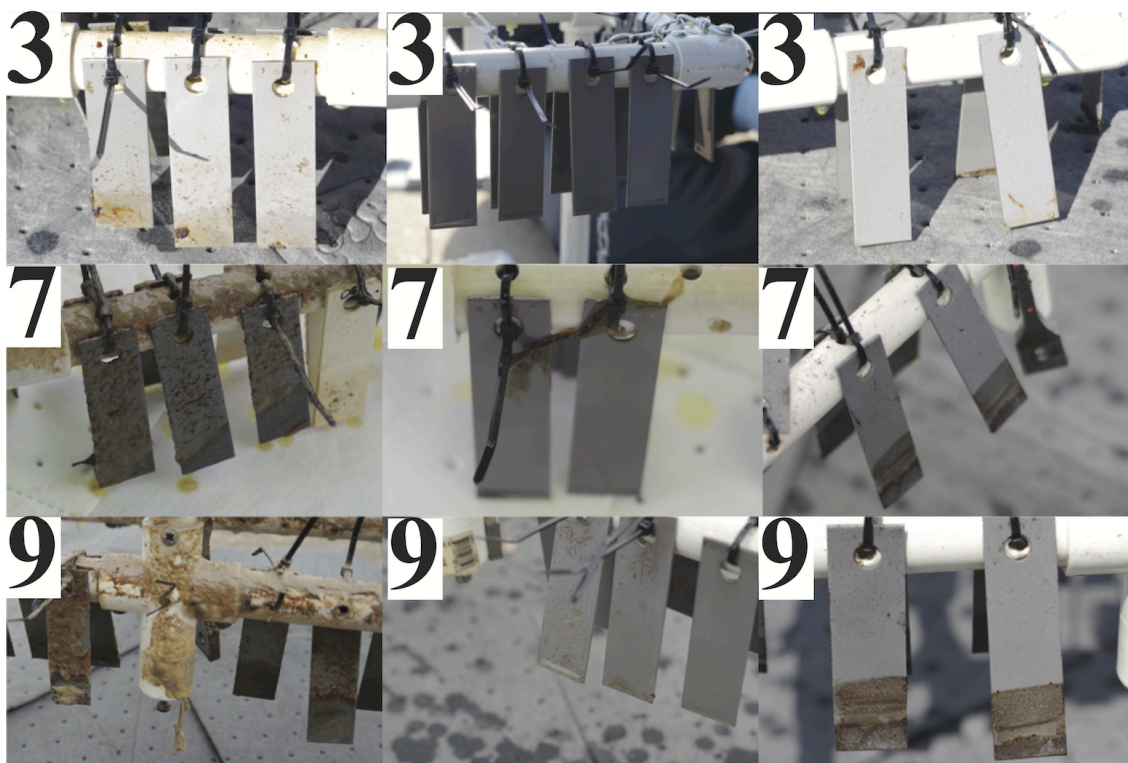
Table 3. Summary of PERMANOVA results in both bacteria (16S) and eukaryotic (18S) datasets.

Factor	Library	Sum of Squares	Mean Squares	F	p	R²
Site	16S	0.339	0.339	38.408	0.001	0.118
Site	18S	0.701	0.701	87.919	0.001	0.251
Tank	16S	0.855	0.171	23.989	0.001	0.297
Tank	18S	0.96	0.192	27.09	0.001	0.344
Material	16S	0.047	0.016	1.58	0.072	0.016
Material	18S	0.042	0.014	1.316	0.263	0.014
Position	16S	0.059	0.029	2.994	0.001	0.02
Position	18S	0.41	0.205	22.483	0.001	0.147
Tank+Material+Position	16S	1.255	0.031	4.671	0.001	0.436
Tank+Material+Position	18S	1.584	0.043	8.037	0.001	0.568

Corrosion and Pitting Assessment in situ and in Laboratory Microcosms

Biofilm was visible on uncoated steel witness coupons after 3 months in SE 3 and 6 months at SW 2 and 3 (Fig. 8), and took longer to become visible at SE 4 and E, and SW 4. Scanning electron microscopy of the biofilm producing pits at SE 3 at 7 months were composed almost entirely of hyphal filaments (Fig. 9). Imaging of coupons placed within the tanks revealed pitting correlated to the position of dark biofilms on the surfaces of witness coupons (Fig 10). Biofilms were observed on some, but not all surfaces, and draped across the horizontal surfaces of each coupon rig. The acid index at SE 3 was 1.51 by 9 months (Table 4) exceeding the limit noted in ASTM standard D7467.

SE



SW

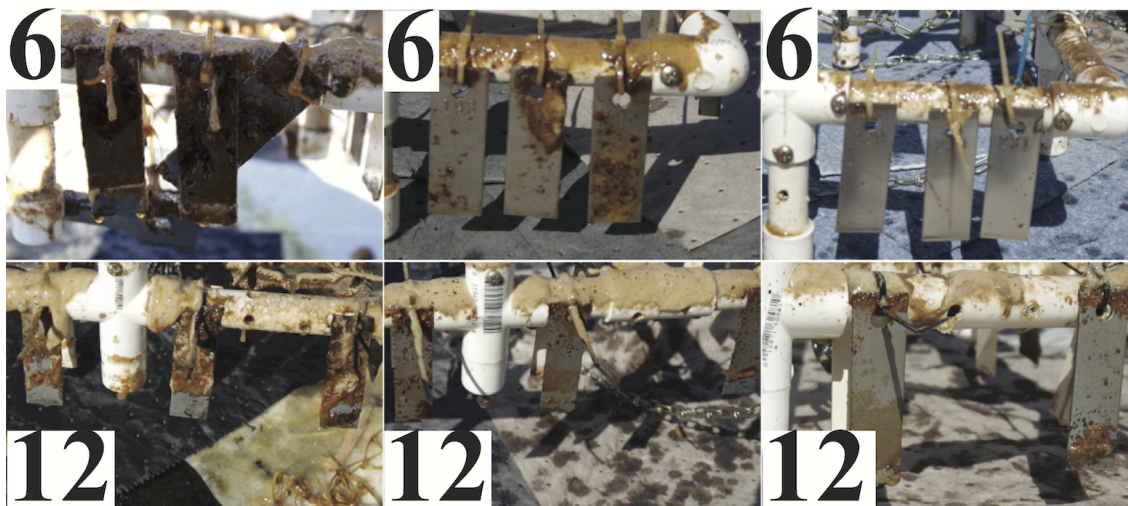


Figure 8. Images of uncoated steel witness coupons at each sampled time point at SE (top) and SW (bottom). Images are shown for SE 3 (left Top), SE 4 (middle top), and SE E (right top), SW 2 (bottom left), SW 3 (bottom middle), and SW 4 (bottom right) Twelve month samples at SE 4 and SE E are not shown

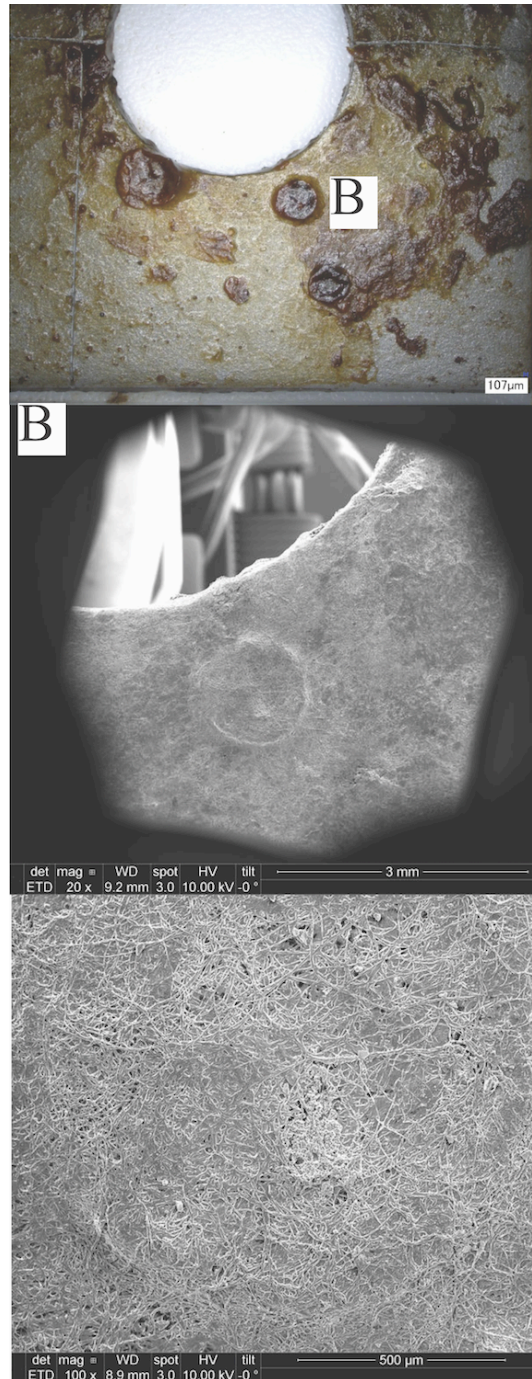


Figure 9. After 7 months exposure in SE 3 near the bottom of the tank a thick biofilm formed (top). The dark green biofilm (B) was composed primarily of filamentous fungi (middle, bottom).

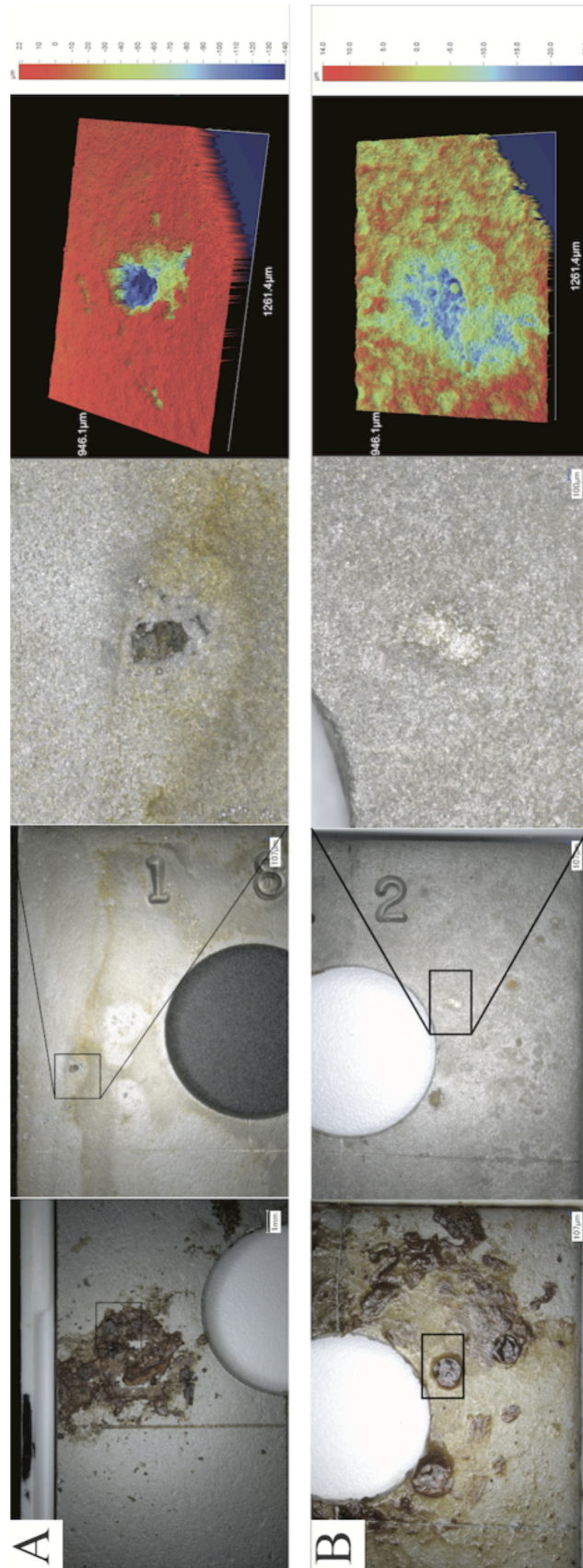


Figure 10. Biofilms at SE 3 were removed to identify pitting corrosion. After 3 months (A) and 7 months (B) exposure visible pits formed directly beneath biofilms.

Table 4. Acid index of select fuels from SE October of 2014, March and May of 2015. Values are expressed in mg KOH/g B20.

	Oct-14	Mar-15	May-15
SE 3	0.17	0.3	1.51
SE 4	0.08	0.16	0.28
SE E	0.22	0.09	0.24
Receipt^a			0.06

^aReceipt fuel taken only in May of 2015 due to availability

Corrosion rates (mm/yr) were significantly different ($p < 0.001$). Bottom coupons after 9 months at SE 3 were significantly different ($p < 0.05$) from controls with an average corrosion rate of 0.0014 mm/yr. Bottom coupons at SE E at 3, 7, and 9 months were also significantly different ($p < 0.05$) from controls (Fig. 11) averaging 0.0022, 0.0015, and 0.0014 mm/yr respectively. Coupons from the top position at SE 3 and 4 and controls from 3, 7, and 12 months were selected for additional analysis of pitting. Mean pit depth of control coupons was 11.40 μm . Pitting at SE 4 was not significantly different from controls at any sampled time point. Mean pit depth decreased from 11.49 μm to 10.99 μm over 12 months of exposure in SE 3 and SE 4. Pit depth was significantly different ($p < 0.001$) from controls in SE 3 for all sampled time points. Maximum median pit depth ranged from 14.73 μm to 16.87 μm (Fig. 12).

After 9 weeks, no significant difference in mass loss or corrosion rate was observed in laboratory-based consortia of fungi and bacteria isolated from SE and SW (Fig. 13). The rate of corrosion was initially high in all tested conditions including controls, but decreased over time under all tested conditions

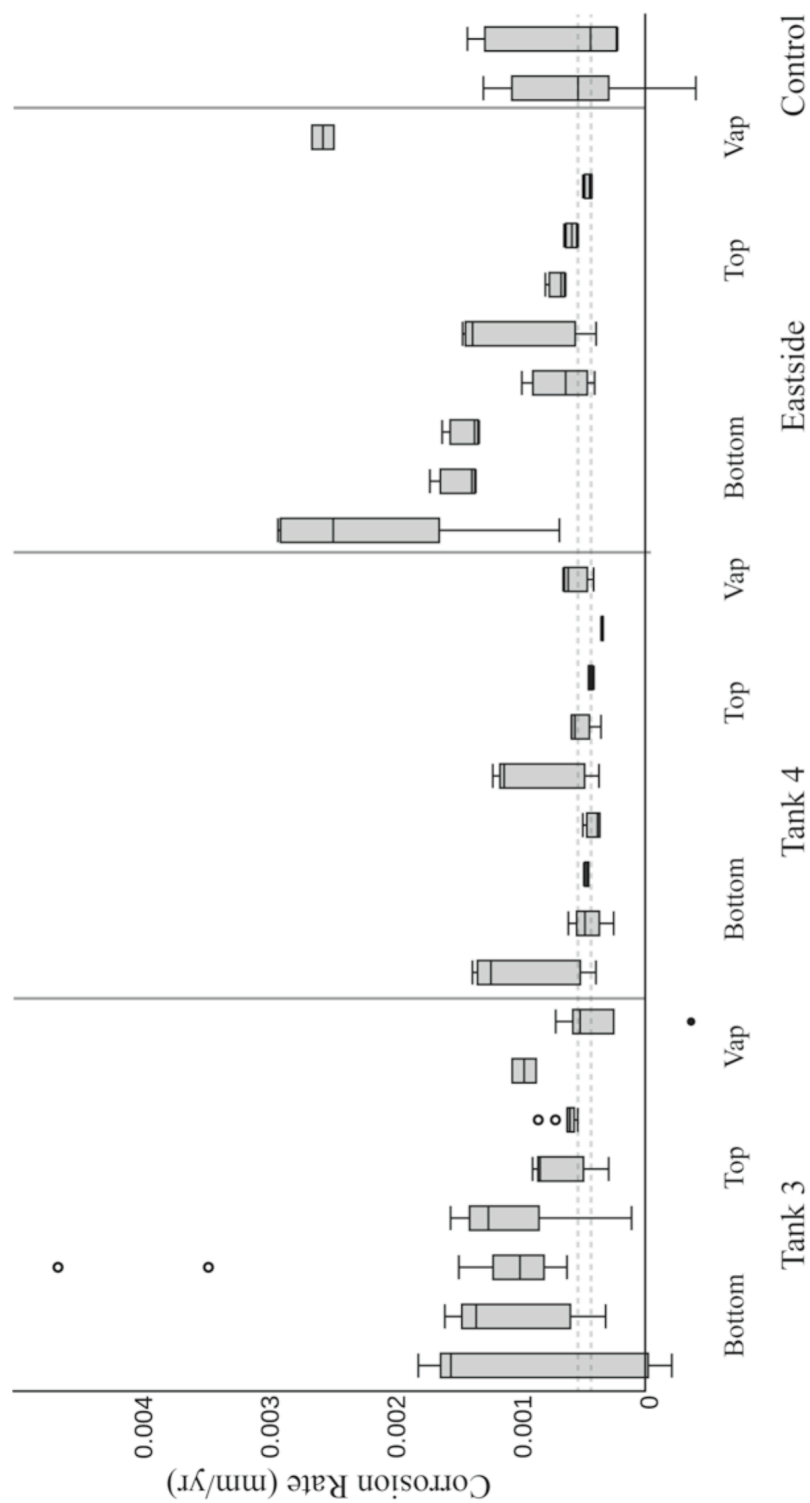


Figure 11. General corrosion rate (mm/yr) of uncoated steel witness coupons after 3, 7, 9, and 12 months exposure in all tanks at SE. Tank 3 was taken offline after 9 months. The dashed lines denote the median corrosion rate across fuel and vapor. Boxes indicate values within the first and third quartiles of data. Whiskers represent the 5th and 9th percentile of data while circles denote outlying points.

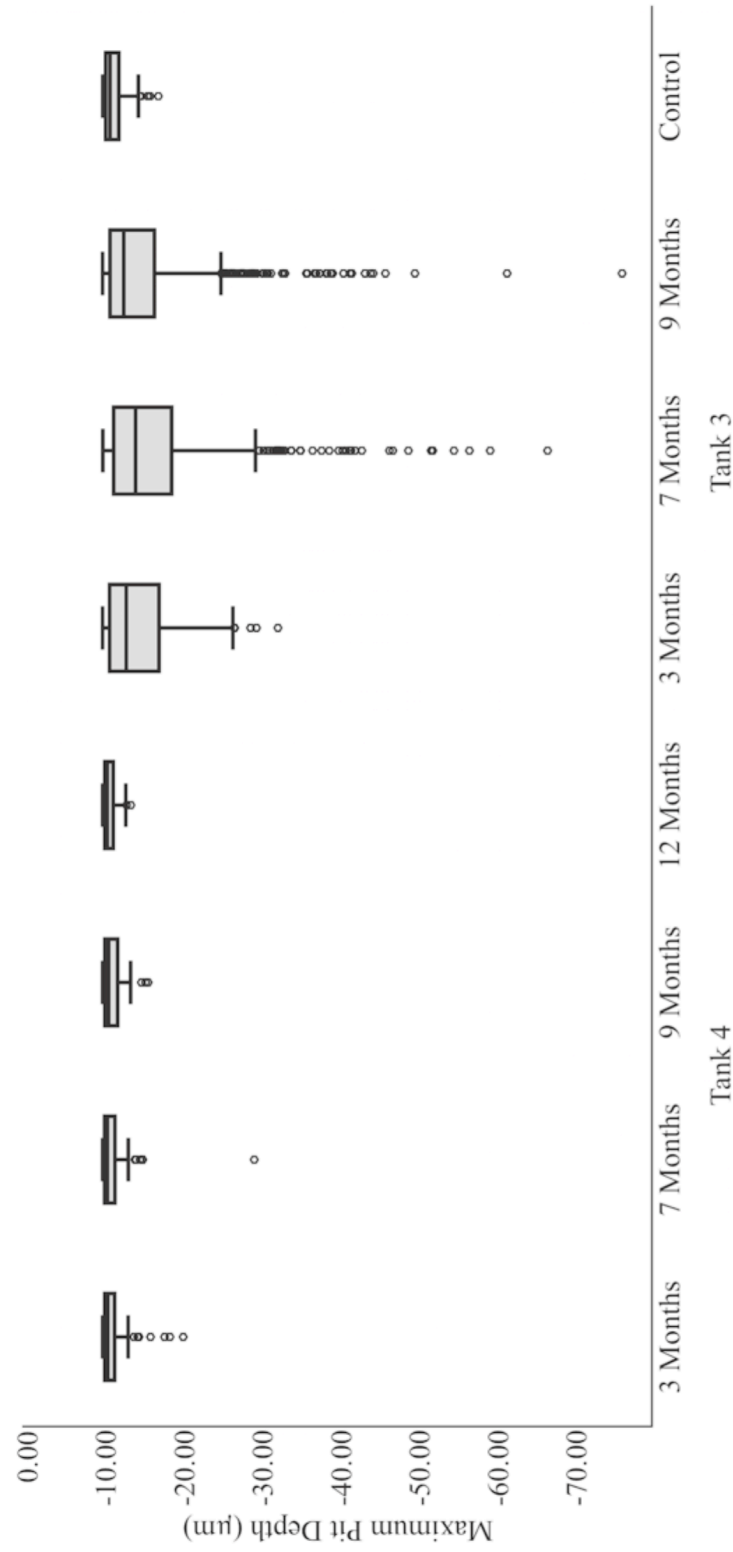


Figure 12. Maximum pit depth of uncoated steel witness coupons 60 cm above the tank bottom at SE 3 and SE 4. Boxes indicate values within the first and third quartiles of data. Whiskers represent the 5th and 9th percentile of data while circles denote outlying points.

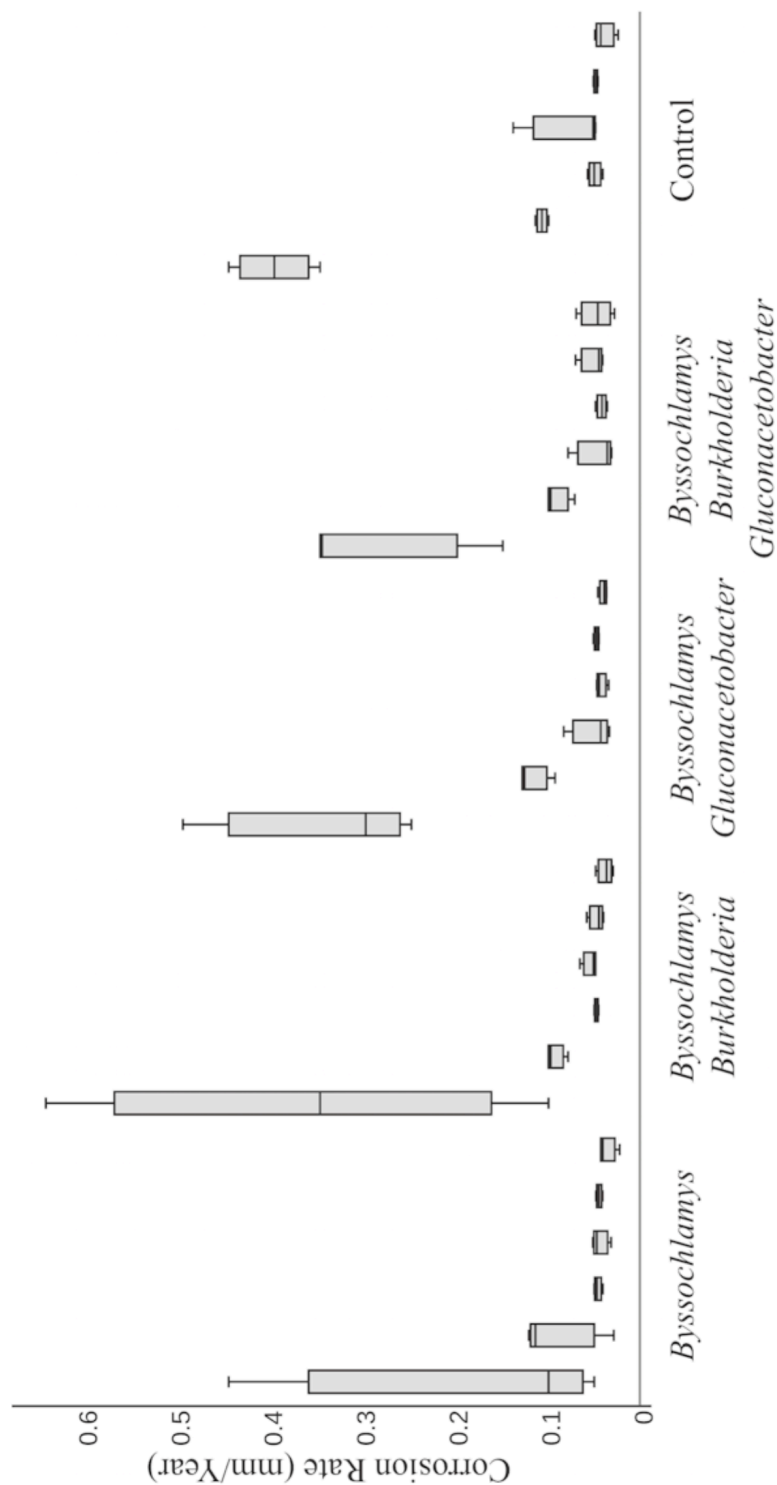


Figure 13. Corrosion rate of laboratory co-cultures incubated for 9 weeks. Samples were taken at 24 hours, 1, 3, 5, 7, and 9 weeks, represented from right to left in each condition. Boxes indicate values within the first and third quartiles of data. Whiskers represent the 5th and 9th percentile of data.

Discussion

Microbiology and its metabolism can increase the risk of corrosion to metal surfaces and affect other materials. In chapter 3, the microbial communities were shown to degrade FAME and produce organic acids, increasing the acidity of the fuel potentially posing a risk to tank materials. Biofilm associated microbial communities within B20 storage tanks at two sites were monitored over the course of one year. After three to six months, thick visible biofilms formed on uncoated steel witness coupons placed at the bottom of all tanks at SW and in SE 3 (Fig. 8). Imaging of coupon biofilms showed the material was primarily hyphal fungi with no visible bacterial cells (Fig. 9). When these biofilms formed on uncoated coupons, more pitting corrosion, with significantly deeper pits occurred, possibly due to the production of organic acids during the metabolism of FAME.

Community analyses of biofilms in tanks/on coupons showed that they were composed of the Trichocomaceae (Fig. 4 and 5), a family of filamentous fungi, and either aerobic or anaerobic acetogens (Fig. 2 and 3). The production of organic acids through microbial metabolism accelerates corrosion rates (De Leo et al., 2013). The Acetobacteraceae were abundant in the majority of biofilm samples taken at SW (Fig. 2) across all time points while the family was less abundant at SE (Fig. 3). The Acetobacteraceae are known for their ability to produce large quantities of acetic acid from the oxidative fermentation of ethanol (Sengun and Karabiyikli, 2011). The family is also assumed to be obligate aerobes (Schleppütz et al., 2013). Coated and uncoated steel coupons in SE 2 0.5 m from the bottom of the tank contained a greater relative

abundance of the Acetobacteraceae while materials placed near the bottom of the tank contained a greater abundance of the Clostridiaceae 1. It is possible that most of the available oxygen was consumed by biofilms and planktonic organisms above the tank bottom creating conditions suitable for the growth of acetogenic Clostridia 1. Anaerobic fermentative microorganisms may consume the byproducts of the oxidative metabolism of FAME. Transcripts recovered from a *Byssochlamys sp.* isolate grown on B20 suggest that the organism is capable of producing acetyl CoA during the metabolism of FAME (Chapter 3) that could lead to the production of ethanol. Alcohols could provide an important carbon source for community members at the bottom of each tank at SW.

The fuel in biodiesel tanks lack large quantities of fixed nitrogen that would be required for a biofilm community to grow. Rainfall could transport nitrogen and other required trace elements into a tank from surrounding soils, but unless there were significant structural failures in the tank closures, these events would only bring minimal amounts of water and nutrients into the tank. The Burkholderiaceae were found in greater abundance at SE, especially in SE tank 3, where the largest amount of fuel fouling, degradation, and biofilm formation occurred. Members of the Burkholderiaceae including the genus *Burkholderia* are capable of fixing nitrogen (Estrada-De Los Santos et al., 2001). While the single isolate recovered from the *Burkholderia* was not capable of fixing nitrogen (Oderay Andrade, unpublished data), nitrogen fixation genes were recovered from metagenomic sequence from a biofilm at SE 3 (Chapter 3). At SW, members of the Acetobacteraceae, which are also capable of fixing nitrogen (Luna and Boiardi, 2007), were more abundant and may fulfill this ecological role that we propose is held by *Burkholderia* in the tanks at SE.

Biofilms represent a physical barrier, where diffusion of nutrients, acids, and oxygen may be impeded. Anaerobic conditions likely to be present under or within biofilms could provide habitat that allows strictly anaerobic microorganisms to flourish. Families within the Clostridiales were abundant in biofilms found near the bottom of tanks at SE (Fig. 3) and SW (Fig. 2). Interestingly, different families within the Clostridiales were abundant at each sampled base. The Ruminococcaceae were more abundant at SE yet, the Clostridiaceae 1 were in greater relative abundance at SW. The Ruminococcaceae contain a number of acetogenic genera capable of growth at low pH and the production of high concentrations of acetic acid by the fermentation of both sugars and alcohols (Chen, 2004; ZELLNER et al., 1996). The Clostridiaceae 1 contain a number of acid producing organisms including the nitrogen fixing butyric acid producing *Clostridium pasteurianum* (Poehlein et al., 2015; Regestein et al., 2015). The presence of acetogenic bacterial taxa suggests that there could be higher concentrations of organic acids present within and underneath the biofilms on the surfaces within these storage tanks, likely responsible for the increased risk of pitting corrosion that was measured.

Acetogenesis, as a trait shared trait by many of the found within B20 biofilms, would suggest that this environment would be partially defined by considerable selective pressure for growth at low pH. Other microorganisms present within the biofilms at each location would then need to be able to survive at low pH, which seems to be the case. *Burkholderia*, which are found in abundance at SE tank 3, are capable of growth at a pH of 4.5 to 5.0 (Stopnisek et al., 2013) . Many members of the Acetobacteraceae, found across SW and in SE 4 and E, are able to grow at a pH (3.5-4.0) below the viable range known for *Burkholderia* (Castro et al., 2012). In E-10 gasoline storage tanks

acetic acid producing bacteria including *Gluconacetobacter* sp. can produce corrosive vapors which damage tank hardware (Williamson et al., 2015). Despite a unique community composition at each sampled location, most abundant bacterial families have the potential to produce potentially damaging quantities of acetic acid that may either accumulate locally in/under biofilms or in vapor spaces within tanks.

Fermentation of ethanol to acetic acid through either an anaerobic or aerobic mechanism is a trait shared among the Acetobacteraceae, Clostridiaceae 1, and Ruminococcaceae that are present in abundance at both SE and SW. While SEM imaging suggested that fungi compose the bulk of biomass in B20 biofilms, it is possible that bacteria present among the fungal hyphae. Even if the overall contribution to biomass is small, this bacterial community could contribute to localized decreases in pH due to acetic acid production, exacerbating the risk of microbial influenced corrosion.

Morphological analysis of images generated through electron microscopy suggested that the bulk of the observed biomass present on witness coupons was composed of fungal hyphae. In tanks with observable biomass (Fig. 8) the Trichocomaceae were consistently the most abundant fungal family. Until recently, fungal biofilm formation was poorly understood (Harding et al., 2009). Initial attachment to surfaces is similar to bacterial biofilm growth models, however during maturation the unique morphology of filamentous fungi includes the development of hyphae that can invade solid surfaces or produce hydrophobins that can penetrate into organic layers (Bayry et al., 2012).

Hyphae can extend far beyond the surface that the fungal mat is adhered to and allow greater access to carbon or oxygen, which may be in greater concentrations significant

distances away from the colonized surface. Thick biofilms created by filamentous fungi, like those observed at SE 3 (Fig. 9), can create a barrier and stratify physical spaces. Hyphal organisms are uniquely adapted to take advantage of multiple phases (Holden, 2001) including solid surfaces, water, and an organic fuel layer that can be present in biodiesel tanks.

Biofilms may also protect a microbial community from environmental or operational changes within a B20 storage tank. The SW AFB experiences a yearly monsoon season in which the area of storage tanks can be flooded. One of these monsoons corresponded to the 6-month sampling event where a large amount of water was present in the bottom of tank 2. Despite the change in tank environment, the relative abundance of the Trichocomaceae remained constant in bottom biofilms at SW (Fig. 4). This suggests that the community is resilient to changes in the surrounding environment such as flood events allowing infiltration of water into tank spaces, fuel deliveries, and removal of fuel due to normal operation of the tank system that occurred over the 18 months that the tanks were studied.

Even when generalized corrosion is low, localized production of acids can increase localized or pitting corrosion (Little et al., 1992). Pitting corrosion can potentially increase the risk of tank penetration and the release of fuel into the environment. In SE tank 3, where the biofilms composed largely of Trichocomaceae were the most pronounced, pit depth increased significantly compared to controls for analyzed coupons (Fig. 12). A direct connection between the microorganisms and pitting corrosion was observed under biofilms removed from a coupon at SE 3 after 3 months of exposure (Fig. 10). A dense mat of filamentous fungi was observed under SEM on

biofilms at SE 3 (Fig. 9) implicating filamentous fungi in the corrosion observed on coupons tested in SE 3. The greatest pit depths were also observed at SE 3. It is possible that fungi within coupon-associated biofilms are capable of producing significant concentrations of organic acids locally and producing a deep pit beneath. Filamentous fungi were previously shown to corrode metals in laboratory experiments (Juzeliūnas et al., 2007; Kip and van Veen, 2015; Little et al., 2001; Usher et al., 2014); however, this is the first study that has shown an abundance of fungi *in situ* within fiberglass and carbon steel B20 storage tanks. This, along with differential corrosion rates suggests that the microbial communities associated with fouling are responsible for pitting corrosion of carbon steel in B20 storage tanks.

The potential for corrosion is greatest at a biodiesel-water interface (Wang et al., 2012; 2011), where the microorganisms have access to an aquatic habitat and a large pool of oxidizable carbon and oxygen as a terminal electron acceptor. This could certainly explain the increased corrosion observed for coupons located on the bottom of the rack within each tank, as the fuel-water interface is usually no more than an inch or two from the bottom. At SE 3, maximum mean pit depth increased as the relative abundance of Trichocomaceae increased. This correlation between the presence of biomass and increased corrosion would implicate the Trichocomaceae in MIC. Despite the low corrosion rates observed *in situ*, localized pitting corrosion was significantly different from controls in SE 3 at all tested time points. Although fouling can occur within months, causing significant disruption to operations, the increased long-term risk of corrosion could be a much larger problem. Diesel storage tanks can be in operation for decades, and if a biofilm is allowed to grow on a steel surface for an extended time. Due

to the increased risk from MIC, these storage tanks and/or their associated infrastructure (piping, dispensers, and gauging) will need to be replaced more frequently. If these assets are not replaced frequently enough, these pits could eventually penetrate the tank wall resulting in a tank breach and release of fuel into the environment.

We have outlined the impact of microbial biofilm proliferation on corrosion of carbon steel in B20 diesel tanks, but the impact on storage tanks constructed of fiberglass has not been studied and remains largely unknown. While the rates of generalized steel corrosion were low and significantly different from controls only in SE tank 3, fiberglass tank surfaces may be at greater risk. Fungi are capable of delaminating fiberglass (Ezeonu et al., 1994) through the production of acids and the enzymatic degradation of binding resins. The relative abundance of acetic acid producing bacteria could also contribute to delamination risk. A more thorough laboratory experiment would be required to address fiberglass degradation, however representative fungal and bacterial isolates from both study sites could be used to establish a consortia similar to the one used to test carbon steel corrosion as a part of this chapter.

It is desirable to replicate corrosion observed *in situ* in the laboratory so that conditions may be more tightly controlled. Corrosion rates were greater in laboratory experiments than field incubations. Despite increased rates of corrosion, no significant differences were observed from sterile controls (Fig. 13). Significant rates of corrosion were observed *in situ* only after 3 months at SE E while laboratory consortia were only incubated for 9 weeks. It is likely the experiment was terminated before organisms could produce differential corrosion from controls. Without extended incubations under laboratory conditions it is unlikely we would see similar results as those observed *in*

situ. A layer of iron oxide was present on steel nails under all tested conditions unlike the uncoated steel surfaces observed in the field (Fig. 8). The laboratory corrosion experiments were designed to allow the microorganisms ample access to O₂ for maximal growth. It is certainly possible that this increased exposure to O₂ promoted abiotic corrosion (i.e. rust) that contributed more corrosion of the metal than MIC and/or caused passivation of the metal surfaces by iron oxides. These laboratory incubations also lacked the complexity of biofilms found in active biodiesel storage tanks. Anaerobic acetogenic clostridia were a major member of many biofilms across both bases (Fig. 2 and 3), and could play a role in enhanced production of organic acids within biofilms. These organisms could ferment the CO₂ produced by the degradation of FAME and H₂ to generate additional acetic acid (Mock et al., 2015).

Conclusions

The presence of biofilms composed of fungi and bacteria are a long-term risk to biodiesel storage infrastructure through pitting corrosion. The majority of both fungal and bacterial taxa observed in the biofilms studied had the ability or the potential to produce organic acids through aerobic or anaerobic fermentation of alcohols and carbohydrates. The Trichocomaceae were capable of degrading the FAME in B20 and generating organic acids that acidify the fuel (Chapter 3). Members of the fungal genus *Pichia* were also found in the B20 biodiesel tanks. These fungi are yeasts within the family Saccharomycetaceae also capable of growth on FAME by initially degrading the FAME to methanol and fatty acid, preferentially oxidizing methanol over the fatty acid (Kumari and Gupta, 2014). The Trichocomaceae likely follow a similar mechanism that

could significantly lower the pH near the tank surface due to the accumulation of fatty acids.

Most bacteria, including members of the Acetobacteraceae, Clostridiaceae 1, and the Ruminococaceae detected in the B20 biodiesel tanks are capable of both FAME degradation (Chapter 3) and the production of organic acids from the fermentation of residual glycerol (Almeida et al., 2012). Acid production within a biofilm can lower the pH relative to the bulk fluid (Liermann et al., 2000), which is likely the root cause of the pitting corrosion observed underneath biofilms and would explain the heterogeneous distribution of pits across the surface of the witness coupons. Biofilms were not evenly distributed across the surfaces of coupons and overall biomass was much lower in SE 4 and SE E (Fig. 8). The corrosion rates and effects were also more pronounced where biomass was in the greatest concentration, which is also why the bottom of B20 tanks are likely to experience the highest rates of corrosion. The research and data reported suggests that fungi are the primary contaminant within biodiesel storage tanks, and that fungal biofilm formation can be correlated to pit formation.

Mitigation of biofilms in B20 tanks is a critical concern. Tanks with less visible biomass (Fig. 8) also had lower overall corrosion rates (Fig. 11) and shallower pitting corrosion (Fig. 12). Physical removal of biofilms through pressure washing of tanks surfaces is effective at removing most of the biomass, but it proved ineffective in altering the tank community and ATP measurements (a proxy for microbial activity), as the microbial community in these tanks seemed to recover soon after cleaning events (Chapter 3). Whole tank sterilization is one approach to further mitigate biofouling and corrosion after initially pressure washing the tank. One potential mitigation method is

hot humid heat decontamination (Buhr et al., 2016), previously used in aircraft systems. To exclude most microorganisms from the tanks, aggressive water removal protocols should be implemented including the use of active dehumidification or chemical desiccants, and high-efficiency particulate air filters installed over existing venting hardware. Education on the risk of microbial contamination to service members within the DoD may also assist in ensuring proper handling of B20. Even without significant sterilization attempts or modification of tank venting, an attempt must be made to lower the microbial biomass in B20 storage tanks to prevent long-term pitting corrosion and the persistent, costly fouling of the fuel systems. Without longitudinal fuel (Chapter 3) and biofilm community analyses, it would have been impossible to understand the community dynamics at play within hydrocarbon storage systems. By combining molecular and cultivation-based microbial community analyses, surface and mass loss analyses of witness coupons, and repeated samplings, the risk of MIC in B20 biodiesel storage infrastructure was determined.

References

- Almeida, J. R. M., Fávaro, L. C. L., and Quirino, B. F. (2012). Biodiesel biorefinery: opportunities and challenges for microbial production of fuels and chemicals from glycerol waste. *Biotechnol. Biofuels* 5, 48. doi:10.1186/1754-6834-5-48.
- Anon: Detection, testing, and evaluation of microbiologically influenced corrosion on internal surfaces of pipelines, in NACE Standard TM0212-2012. 2012, NACE International: Houston, TX. p. 36.
- Bayry, J., Aïmanianda, V., Guijarro, J. I., Sunde, M., and Latgé, J.-P. (2012).

- Hydrophobins—Unique Fungal Proteins. *PLoS Pathogens* 8, e1002700.
doi:10.1371/journal.ppat.1002700.
- Beech, I. B., and Sunner, J. (2004). Biocorrosion: towards understanding interactions between biofilms and metals. *Curr. Opin. Biotechnol.* 15, 181–186.
doi:10.1016/j.copbio.2004.05.001.
- Benjamini, Y., and Yekutieli, D. (2001). The control of the false discovery rate in multiple testing under dependency. *Ann. stat.* doi:10.2307/2674075.
- Buhr, T. L., Young, A. A., Bensman, M., Minter, Z. A., Kennihan, N. L., Johnson, C. A., et al. (2016). Hot, humid air decontamination of a C-130 aircraft contaminated with spores of two acrySTALLIFEROUS *Bacillus thuringiensis* strains, surrogates for *Bacillus anthracis*. *J. Appl. Microbiol.*, n/a–n/a. doi:10.1111/jam.13055.
- Bücker, F., Santestevan, N. A., Roesch, L. F., Jacques, R. J. S., do Carmo Ruaro Peralba, M., de Oliveira Camargo, F. A., et al. (2011). Impact of biodiesel on biodeterioration of stored Brazilian diesel oil. *Int. Biodeter. Biodegr.* 65, 172–178.
doi:10.1016/j.ibiod.2010.09.008.
- Caporaso, J. G., Bittinger, K., Bushman, F. D., DeSantis, T. Z., Andersen, G. L., and Knight, R. (2010a). PyNAST: a flexible tool for aligning sequences to a template alignment. *Bioinformatics* 26, 266–267. doi:10.1093/bioinformatics/btp636.
- Caporaso, J. G., Kuczynski, J., Stombaugh, J., Bittinger, K., Bushman, F. D., Costello, E. K., et al. (2010b). QIIME allows analysis of high-throughput community sequencing data. *Nat. Meth.* 7, 335–336. doi:10.1038/nmeth.f.303.

- Castro, C., Zuluaga, R., Álvarez, C., Putaux, J.-L., Caro, G., Rojas, O. J., et al. (2012). Bacterial cellulose produced by a new acid-resistant strain of *Gluconacetobacter* genus. *Carbohydr. Polym.* 89, 1033–1037. doi:10.1016/j.carbpol.2012.03.045.
- Chen, S. (2004). *Acetanaerobacterium elongatum* gen. nov., sp. nov., from paper mill waste water. *Int. J. Syst. Evol. Microbiol.* 54, 2257–2262. doi:10.1099/ijms.0.63212-0.
- Clark, K. E., Siegel, S. M., and Siegel, B. Z. (1984). Bio-corrosion: A note on fungal solubilization of iron from stainless steels. *Water Air Soil Poll.* 21, 435–437. doi:10.1007/BF00163643.
- De Leo, F., Campanella, G., Proverbio, E., and Urzi, C. (2013). Laboratory tests of fungal biocorrosion of unbonded lubricated post-tensioned tendons. *Constr. Build. Mater.* 49, 821–827. doi:10.1016/j.conbuildmat.2013.08.071.
- Dixon, P. (2003). VEGAN, a package of R functions for community ecology. *J. Veg. Sci* 14, 927–930. doi:10.1111/j.1654-1103.2003.tb02228.x.
- Edgar, R. C. (2013). UPARSE: highly accurate OTU sequences from microbial amplicon reads. *Nat. Meth.* 10, 996–998. doi:10.1038/nmeth.2604.
- Enning, D., and Garrelfs, J. (2014). Corrosion of iron by sulfate-reducing bacteria: new views of an old problem. *Appl. Environ. Microbiol.* 80, 1226–1236. doi:10.1128/AEM.02848-13.
- Estrada-De Los Santos, P., Bustillos-Cristales, R., and Caballero-Mellado, J. (2001).

- Burkholderia, a genus rich in plant-associated nitrogen fixers with wide environmental and geographic distribution. *Appl. Environ. Microbiol.* 67, 2790–2798. doi:10.1128/AEM.67.6.2790-2798.2001.
- Ezeonu, I. M., Noble, J. A., Simmons, R. B., Price, D. L., Crow, S. A., and Ahearn, D. G. (1994). Effect of relative humidity on fungal colonization of fiberglass insulation. *Appl. Environ. Microbiol.* 60, 2149–2151.
- Gellings, C., and Gudger, K. (1998). The Emerging Open Market Customer. *Strategic Planning for Energy and the Environment* 17, 6–20.
doi:10.1080/10485236.1998.10530532.
- Gu, T. (2014). Theoretical Modeling of the Possibility of Acid Producing Bacteria Causing Fast Pitting Biocorrosion. *J. Microb. Biochem. Technol.* 06.
doi:10.4172/1948-5948.1000124.
- Harding, M. W., Marques, L. L. R., Howard, R. J., and Olson, M. E. (2009). Can filamentous fungi form biofilms? *Trends Microbiol.* 17, 475–480.
doi:10.1016/j.tim.2009.08.007.
- Herzberg, E. F., Morris, A., Kelly, A. R., Stroh, R. F., Rutledge, L., and OMeara, N. T. (2016). Estimated Impact of Corrosion on Cost and Availability of DoD Weapon Systems. LMI Government Consulting.
- Hestrin, S., and Schramm, M. (1954). Synthesis of cellulose by *Acetobacter xylinum*. II. Preparation of freeze-dried cells capable of polymerizing glucose to cellulose. *Biochem. J.* 58, 345–352.

- Holden, P. A. (2001). “[9] Biofilms in unsaturated environments,” in *Microbial Growth in Biofilms - Part B: Special Environments and Physicochemical Aspects* Methods in Enzymology. (Elsevier), 125–143. doi:10.1016/S0076-6879(01)37011-8.
- Juzeliūnas, E., Ramanauskas, R., Lugauskas, A., Leinartas, K., Samulevičienė, M., Sudavičius, A., et al. (2007). Microbially influenced corrosion of zinc and aluminium – Two-year subjection to influence of *Aspergillus niger*. *Corros. Sci.* 49, 4098–4112. doi:10.1016/j.corsci.2007.05.004.
- Kip, N., and van Veen, J. A. (2015). The dual role of microbes in corrosion. *ISME J.* 9, 542–551. doi:10.1038/ismej.2014.169.
- Koch, G. H., Brongers, M., Thompson, N. G., Virmani, Y. P., and Payer, J. H. (2002). Corrosion Cost and Preventative Strategies in The United States.
- Kumari, A., and Gupta, R. (2014). Novel strategy of using methyl esters as slow release methanol source during lipase expression by mut⁺ *Pichia pastoris* X33. *PLoS One* 9, e104272. doi:10.1371/journal.pone.0104272.
- Lee, W., Lewandowski, Z., Okabe, S., Characklis, W. G., and Avci, R. (2009). Corrosion of mild steel underneath aerobic biofilms containing sulfate-reducing bacteria part I: At low dissolved oxygen concentration. *Biofouling* 7, 197–216. doi:10.1080/08927019309386254.
- Liermann, L. J., Barnes, A. S., Kalinowski, B. E., Zhou, X., and Brantley, S. L. (2000). Microenvironments of pH in biofilms grown on dissolving silicate surfaces. *Chem. Geol.* 171, 1–16. doi:10.1016/S0009-2541(00)00202-3.

- Little, B., Staehle, R., and Davis, R. (2001). Fungal influenced corrosion of post-tensioned cables. *Int. Biodeter. Biodegr.* 47, 71–77. doi:10.1016/S0964-8305(01)00039-7.
- Little, B., Wagner, P., and Mansfeld, F. (1992). An overview of microbiologically influenced corrosion. *Electrochim. Acta* 37, 2185–2194. doi:10.1016/0013-4686(92)85110-7.
- Love, M. I., Huber, W., and Anders, S. (2014). Moderated estimation of fold change and dispersion for RNA-seq data with DESeq2. *Genome Biol.* 15, 1–21. doi:10.1186/s13059-014-0550-8.
- Lozupone, C., and Knight, R. (2005). UniFrac: a New Phylogenetic Method for Comparing Microbial Communities. *Appl. Environ. Microbiol.* 71, 8228–8235. doi:10.1128/AEM.71.12.8228-8235.2005.
- Luna, M. F., and Boiardi, J. L. (2007). Growth yields and glucose metabolism of N₂-fixing *Gluconacetobacter diazotrophicus* at different culture pH values. *World J Microbiol. Biotechnol.* 24, 587–590. doi:10.1007/s11274-007-9507-3.
- Mansfield, E., Sowards, J. W., and Crookes-Goodson, W. J. (2015). Findings and Recommendations from the NIST Workshop on Alternative Fuels and Materials: Biocorrosion. *J. Res. Natl. Inst. Stan.* 120, 28. doi:10.6028/jres.120.003.
- McNamara, C. J., Perry, T. D., IV, Leard, R., Bearce, K., Dante, J., and Mitchell, R. (2005). Corrosion of aluminum alloy 2024 by microorganisms isolated from aircraft fuel tanks. *Biofouling* 21, 257–265. doi:10.1080/08927010500389921.

- Mock, J., Zheng, Y., Mueller, A. P., Ly, S., Tran, L., Segovia, S., et al. (2015). Energy Conservation Associated with Ethanol Formation from H₂ and CO₂ in *Clostridium autoethanogenum* Involving Electron Bifurcation. *J. Bacteriol.* 197, 2965–2980. doi:10.1128/JB.00399-15.
- Parada, A., Needham, D. M., and Fuhrman, J. A. (2015). Every base matters: assessing small subunit rRNA primers for marine microbiomes with mock communities, time-series and global field samples. *Environ Microbiol.* doi:10.1111/1462-2920.13023.
- Poehlein, A., Grosse-Honebrink, A., Zhang, Y., Minton, N. P., and Daniel, R. (2015). Complete Genome Sequence of the Nitrogen-Fixing and Solvent-Producing *Clostridium pasteurianum* DSM 525. *Genome Announc.* 3, e01591–14. doi:10.1128/genomeA.01591-14.
- Pohlert, T., (2014). The Pairwise Multiple Comparison of Mean Ranks Package (PMCMR). R package. <http://CRAN.R-project.org/package=PMCMR>.
- Price, M. N., Dehal, P. S., and Arkin, A. P. (2010). FastTree 2 – Approximately Maximum-Likelihood Trees for Large Alignments. *PLoS One* 5, e9490. doi:10.1371/journal.pone.0009490.
- Pruesse, E., Quast, C., Knittel, K., Fuchs, B. M., Ludwig, W., Peplies, J., et al. (2007). SILVA: a comprehensive online resource for quality checked and aligned ribosomal RNA sequence data compatible with ARB. *Nucleic Acids Res.* 35, 7188–7196. doi:10.1093/nar/gkm864.

- Regestein, L., Doerr, E. W., Staaden, A., and Rehmann, L. (2015). Impact of butyric acid on butanol formation by *Clostridium pasteurianum*. *Bioresour. Technol.* 196, 153–159. doi:10.1016/j.biortech.2015.07.085.
- Salter, S., Cox, M. J., Turek, E. M., Calus, S. T., and Cookson, W. O. (2014). Reagent contamination can critically impact sequence-based microbiome analyses. *bioRxiv*.
- Schlepütz, T., Gerhards, J. P., and Büchs, J. (2013). Ensuring constant oxygen supply during inoculation is essential to obtain reproducible results with obligatory aerobic acetic acid bacteria in vinegar production. *Process Biochem.* 48, 398–405. doi:10.1016/j.procbio.2013.01.009.
- Schloss, P. D., Westcott, S. L., Ryabin, T., Hall, J. R., Hartmann, M., Hollister, E. B., et al. (2009). Introducing mothur: open-source, platform-independent, community-supported software for describing and comparing microbial communities. *Appl. Environ. Microbiol.* 75, 7537–7541. doi:10.1128/AEM.01541-09.
- Sengun, I. Y., and Karabiyikli, S. (2011). Importance of acetic acid bacteria in food industry. *Food Control* 22, 647–656. doi:10.1016/j.foodcont.2010.11.008.
- Shapiro, S. S., and Wilk, M. B. (1965). An Analysis of Variance Test for Normality (Complete Samples). *Biometrika* 52, 591. doi:10.2307/2333709.
- Stevenson, B. S., Drilling, H. S., Lawson, P. A., Duncan, K. E., Parisi, V. A., and Suflita, J. M. (2011). Microbial communities in bulk fluids and biofilms of an oil facility have similar composition but different structure. *Environ. Microbiol.* 13, 1078–1090. doi:10.1111/j.1462-2920.2010.02413.x.

- Stopnisek, N., Bodenhausen, N., Frey, B., Fierer, N., Eberl, L., and Weisskopf, L. (2013). Genus-wide acid tolerance accounts for the biogeographical distribution of soil Burkholderia populations. *Environ. Microbiol.* 16, 1503–1512. doi:10.1111/1462-2920.12211.
- Tran, T., Brown, B., Nesic, S., and Tribollet, B. (2013). Investigation of the mechanism for acetic acid corrosion of mild steel. *Corrosion/2013 paper*.
- Usher, K. M., Kaksonen, A. H., and MacLeod, I. D. (2014). Marine rust tubercles harbour iron corroding archaea and sulphate reducing bacteria. *Corros. Sci.* 83, 189–197. doi:10.1016/j.corsci.2014.02.014.
- Van Der Waerden, B. L. (1953). Order Tests for the Two-Sample Problem and their Power. *Indagationes Mathematicae (Proceedings)* 56, 80. doi:10.1016/S1385-7258(53)50012-5.
- Wang, Jenkins, Ren (2012). Electrochemical corrosion of carbon steel exposed to biodiesel/simulated seawater mixture. *Popul. Ecol.* 57, 5–5. doi:10.1016/j.corsci.2011.12.015.
- Wang, W., Jenkins, P. E., and Ren, Z. (2011). Heterogeneous corrosion behaviour of carbon steel in water contaminated biodiesel. *Corros. Sci.* 53, 845–849. doi:10.1016/j.corsci.2010.10.020.
- Williamson, C. H. D., Jain, L. A., Mishra, B., Olson, D. L., and Spear, J. R. (2015). Microbially influenced corrosion communities associated with fuel-grade ethanol environments. *Appl. Microbiol. Biotechnol.* 99, 6945–6957. doi:10.1007/s00253-

015-6729-4.

Zellner, G., Stackebrandt, E., Nagel, D., Messner, P., Weiss, N., and Winter, J. (1996).

Anaerofilum pentosovorans gen. nov., sp. nov., and *Anaerofilum agile* sp. nov.,

Two New, Strictly Anaerobic, Mesophilic, Acidogenic Bacteria from Anaerobic

Bioreactors. *Int. J. Syst. Bacteriol.* 46, 871–875. doi:10.1099/00207713-46-4-871.

Zhang, J., Kobert, K., Flouri, T., and Stamatakis, A. (2014). PEAR: a fast and accurate

Illumina Paired-End reAd mergeR. *Bioinformatics* 30, 614–620.

Chapter 5. Impact of Whole-Aircraft Sterilization on the Microbiome of a C-130 Hercules

Foreword

The samples discussed in this chapter were taken as part of the test of a full-scale whole-aircraft decontamination system. I participated significantly in the design, sampling, lab work, and analysis of all molecular biology samples. My advisor Dr. Bradley Stevenson conceived the experiment, assisted in sampling, data interpretation, and advised me on the creation and execution of laboratory experiments. Dr. Heather Nunn assisted in DNA extraction and PCR amplification. The work described here would not have been possible without our collaboration with Dr. Wendy J. Crookes-Goodson at the Air Force Research Laboratories (AFRL) and her personnel, who cultivated organisms from samples also taken for molecular analysis, and performed ATP testing on site. Carrie A. Drake, Audra L. Crouch, and Wendy J. Crookes-Goodson all contributed to the methods and results pertaining to cultivation and ATP testing. Without the help of these individuals, and those listed in the author list above, none of this work would have been possible.

Abstract

The United States Air Force (USAF) may need to decontaminate an aircraft quickly and effectively in order to return them to service following a biological attack or outbreak of disease. Decontamination of an entire aircraft would also affect microbial populations endogenous to the aircraft and; therefore, represent relatively facile means to mitigate

microbial influenced corrosion (MIC). An approach to whole-aircraft decontamination using hot, humid air was recently tested on a Lockheed Martin C-130 Hercules. The abundance and composition of microbial communities was assessed before and after decontamination through cultivation, ATP measurements, and high throughput sequencing of small subunit ribosomal RNA genes. After 72 hours of treatment, ATP readings were reduced by 87 percent, and the number of different cultivable microorganisms was reduced from 242 to 40. The abundant members of the bacterial community were significantly affected by the treatment, causing a loss in diversity and an increase in equitability. Fungal community composition was also significantly altered although the effect was less visible within the ordination. The use of hot, humid air decontamination appears to have been a viable means of rapidly decontaminating an entire aircraft as required in the event of a significant viral or bacterial outbreak, bioterror attack, or in response to widespread MIC.

Introduction

Microorganisms (fungi, bacteria and archaea) are ubiquitous in the biosphere, surviving and thriving in virtually all habitable locations. The exterior and interior surfaces of aircraft are no exception and can acquire microorganisms from the environment, crew, or passengers. Airline transportation is one of the most common means of transit worldwide, with almost 900 million passengers using US carriers and over 65 billion ton-miles of freight were carried globally in 2015 (<http://www.bls.gov/>). Therefore, aircraft play a significant role as a vector for rapid distribution of humans and their microbial passengers across vast distances.

While aircraft rapidly carry humans and cargo across the globe, they can also quickly spread infectious diseases. Once airborne, cargo and passenger aircraft are exposed to recirculated air, contributing to the transfer of microbial pathogens between passengers and remain aboard the aircraft for an extended amount of time (Clayton et al., 1976). A single individual carrying an infectious disease on a passenger or cargo aircraft could unknowingly infect other passengers or crewmembers, or contaminate the aircraft and its cargo. This potential risk is especially acute for aircraft operating in critical situations, such as the transport of infected individuals as a part of a humanitarian evacuation. Airline travel was determined to be a factor in a Coronavirus (SARS) outbreak, and aircraft have been previously found as a risk for transfer of *Mycobacterium tuberculosis* and *Neisseria meningitides* (Abubakar, 2010; Kenyon et al., 1996; Rachael et al., 2009). With these findings in consideration, the National Research Council has identified an attack on the air travel system with a bioterror agent represents a significant risk to national security (National Research Council, 2006). It is, therefore, essential to ensure proper quarantine and decontamination of affected aircraft.

The microorganisms found on aircraft are influenced by the microbiomes of its occupants (Dechow et al., 1997; La Duc et al., 2007; LaDuc et al., 2006; Wick and Irvine, 1995). A number of potential human pathogens were recovered through cultivation (LaDuc et al., 2006) and detected using microarray-based rRNA gene analyses (Korves et al., 2013) during studies aboard a commercial flights, highlighting the concern and need for a viable whole-aircraft decontamination approach. The microarray-based studies by Korves et al. (2013) determined that the microorganisms aboard the aircraft were enriched in *Pseudomonas* and *Comamonas*, and different from

those found in exterior air samples. The air filters sampled in the study did not focus on characterizing the fungi or protists that are likely also present within aircraft.

Additionally, biofilms distributed on surfaces throughout the aircraft were not studied, which could be important potential reservoirs of pathogenic microorganisms if the aircraft was not properly decontaminated.

Microorganisms aboard an aircraft not only pose a threat to its occupants, but they can also cause harm to the aircraft itself through microbially influenced corrosion (MIC). Organic acids produced by microbial biofilms on aircraft surfaces are capable of degrading the passivating oxide layer on aluminum, resulting in pitting corrosion (McNamara et al., 2005; Yang et al., 1996). Bacteria and fungi can also degrade polyurethane (PU) coatings that are common across aircraft, using the PU as a sole carbon substrate (Barratt et al., 2003; Cosgrove et al., 2007; Ocegüera-Cervantes et al., 2007; Ruiz et al., 1999; Stern and Howard, 2000). Decontamination of aircraft would also affect the microorganisms associated with the corrosion and degradation of aircraft surfaces, representing potentially effective means of mitigating MIC, extending the lifespan of the aircraft, and reducing the costs associated with corrosion maintenance.

Recently, new techniques to decontaminate whole aircraft were developed in which the entire aircraft is placed into an enclosure and exposed to an extended period of hot, humid heat (Buhr et al., 2016) instead of using formaldehyde vapor or vaporized hydrogen peroxide (Wagner et al., 2007). The effectiveness of this new technique, known as the Joint Biological Agent Decontamination System (JBADS), was measured against *Bacillus thuringiensis* Al Hakam (Bt) spores deposited on prepared slides and aerosolized throughout the aircraft (Buhr et al., 2012; 2015; 2016; Prokop et al., 2014).

Previous JBADS studies and the work of Clayton et al. (1976) are somewhat limited due to their focus on a single bacterium, and not the resident microbial community of the aircraft. In the study described here, we combined sequencing of small subunit rRNA gene libraries with ATP measurements and cultivation-based studies. We were able to monitor the effect of JBADS decontamination on the abundance and composition of the microorganisms found on a C-130 H aircraft.

Methods

Sampling

Sampling occurred during a test of the JBADS system on a Lockheed Martin C-130 aircraft at Orlando International Airport in November and December of 2014. Samples from an approximately 60-cm² area were collected using three sterile nylon flocked swabs (Therapak, Los Angeles, CA) across the interior of the aircraft for rRNA gene sequencing. At select sites, an additional swab was used simultaneously to collect material for cultivation. Two swabs were used in an adjacent location to collect samples for ATP testing. Sites were chosen to represent areas of the aircraft commonly touched by crewmembers, materials experiencing varying levels of corrosion, and non-corroded areas adjacent to corroded samples. Decontamination of the aircraft was carried out over the course of 72 hours at 90% relative humidity and a median temperature of 76°C. After treatment, samples were taken adjacent to the sampling locations used prior to decontamination. Personnel conducting the sampling wore nitrile gloves before decontamination and fresh Tyvek[®] suits and booties, face masks and nitrile gloves after decontamination to limit contamination of the aircraft. After a sample was collected from an area, the swab heads were cut off with alcohol-sterilized scissors and placed

into individual 2 ml screw cap tubes. For DNA preservation and eventual purification, these tubes also contained 0.7 ml (dry volume) of 0.5 mm ZR BashingBead™ lysis matrix (ZR BashingBead™ Lysis Tube, Zymo Research, Irvine, CA) and 0.75 ml Xpedition™ Lysis/Stabilization Solution (Zymo Research). For cultivation-based studies, the tubes contained 0.5 ml sterile phosphate buffered saline (PBS), pH 7.0 (Sambrook et al., 1989). Multiple controls including blank sterile swabs were also taken at both time points. In total, 372 samples were taken from 62 sites.

All samples for DNA extraction were preserved on site by the nature of homogenization for 30 sec in the presence of the Xpedition™ Lysis/Stabilization Solution (Zymo Research) in the field by attaching the ZR BashingBead™ Lysis Tubes (Zymo Research) to the blade of a reciprocating saw (One World Technologies, Inc., Anderson, SC) and frozen at -20°C until ready for extraction. Prior to extraction, samples were homogenized for an additional 30 seconds using a Mini-Beadbeater 8 (Biospec Products Inc., Bartlesville, OK) at the maximum setting. Total DNA was extracted from each sample following the Zymo Xpedition Soil/Fecal DNA extraction kit protocol (Zymo Research), including the addition of beta-mercaptoethanol (Sigma-Aldrich, St. Louis, MO).

SSU rRNA gene library preparation

All small subunit ribosomal RNA gene libraries were amplified with PCR using primers that evenly amplify bacteria, archaea, and eukaryotic SSU rRNA genes simultaneously (Parada et al., 2015). The forward primer 515F-Y (**GTA AAA CGA CGG CCA G** CCG TGY CAG CMG CCG CGG TAA-3') contains the M13 forward primer (in bold) fused to the ssuRNA gene specific forward primer (underlined) while the reverse primer

926R (5'-CCG YCA ATT YMT TTR AGT TT-3') was unmodified from Parada et. al 2015. Amplification reactions were conducted using 5 PRIME HOT master mix (5 PRIME Inc., Gaithersburg, MD), with the addition of 4 μ L of template DNA at a median concentration of 4.67 ng/ μ L prior to decontamination and 0.60 ng/ μ L after decontamination in a total reaction volume of 50 μ L. Initial amplification was conducted using the following protocol: initial denaturation at 94 °C for 2 m, followed by 30 cycles of denaturation at 94°C for 45 s, annealing at 50 °C for 45 s, and extension at 68 °C for 1.5 min, followed by a final extension at 68 °C for 5 min. Amplified SSU rRNA gene fragments were purified using Agencourt AMPure XP paramagnetic beads (Beckman Coulter Inc., Indianapolis, IN), and used in duplicate, subsequent PCRs containing M13 labeled barcodes as the forward primer, and the previously used reverse primer in order to add a unique 12 bp barcode to each sample. Thermal cycling conditions were otherwise identical to the initial amplification but only consisted of 6 cycles. Amplified SSU rRNA gene fragments containing unique barcodes were again purified and concentrated with Agencourt AMPure XP paramagnetic beads (Beckman Coulter Inc.), quantified using the QuBit HS dsDNA assay (Thermo Fisher Scientific, Inc., Waltham, MA) and pooled in equimolar amounts to a total of 2 μ g of DNA. This sample was then concentrated with a 0.5 mL Amicon 30 K centrifugal column (EMD Millipore, Billerica, MA) and the final amount of DNA was confirmed using the QuBit BR dsDNA assay (Thermo Fisher Scientific, Inc.). Amplicons were sequenced on an Illumina MiSeq using V2 PE250 chemistry.

SSU rRNA gene library analysis

Sequencing reads were overlapped using PEAR (Zhang et al., 2014) and demultiplexed using QIIME (Caporaso et al., 2010). Joined reads were retained for 16S SSU rRNA gene analysis and clustered into operational taxonomic units (OTUs) at a cutoff of 97 % sequence similarity using UPARSE (Edgar, 2013). Due to the length of the 18S rRNA gene fragment amplified (Parada et al., 2015) non-overlapping reads were used as input for eukaryotic SSU rRNA gene analysis. Any OTU not differentially abundant from extraction blanks or negative controls was discarded prior to analysis using DESeq2 (Love et al., 2014) within QIIME to reduce the potential impact of OTUs originating from contaminated PCR or DNA extraction reagents (Salter et al., 2014).

An even sampling depth of 1000 sequences for Bacteria and Archaea, and 500 sequences for Eukarya was chosen by first producing a multiple rarefaction of all samples within QIIME using the observed OTUs metric. The sampling depth was then chosen at a point in the multiple rarefaction analysis where few additional OTUs were gained for a corresponding increase in sequencing depth in an attempt to include the greatest number of samples while still accurately representing the microbial community. The richness of each sample was assessed using equitability, which is the inverse of the Shannon index H ($H = \sum_{i=1}^{Species} \frac{n_i}{N} \ln \frac{N}{n_i}$) (Shannon, 1948), the number of observed OTUs, and Faith's phylogenetic distance (Faith, 1992). Community structure was computed using the weighted UniFrac distance matrix (Lozupone and Knight, 2005).

Changes in the weighted UniFrac distance matrix were compared before and after decontamination and by location using a PERMANOVA. All statistical analyses were

performed within QIIME using the R package “vegan” (Dixon, 2003). The program DESeq2 (Love et al., 2014) was used within QIIME to determine what OTUs, if any were significantly different before and after JBADS treatment.

Viability of Microbial Communities by ATP Testing

Adenosine triphosphate (ATP) was used as a proxy for microbial metabolic activity across the aircraft before and after decontamination at 10 sites using the Hy-LiTE[®] assay system (Fuel Quality Services, Inc., Flowery Branch, GA) in duplicate. After decontamination, sites were re-swabbed in an area adjacent to the original sampled locations to ensure that a low ATP reading was not the result of removing biological material during the previous sampling. Swabs were first dipped into sterile phosphate buffered saline (PBS), used to swab a surface area, and then placed directly into the ATP pen lysis solution reservoir. The test was then carried out following the manufacturer’s protocol. Results are reported in relative light units (RLU), which is directly proportional to the amount of microbial contamination on a tested surface. Positive and negative controls were collected from the sampler’s face and arm, and sterile swabs respectively.

Cultivation of Microorganisms

After sampling, a single swab from selected sites was placed into a 2.0 mL vial with 500 µL of PBS and transported on ice. Samples were then serially diluted in 180 µL of sterile PBS following a 1:10 dilution series onto tryptic soy agar (TSA) and acid producing bacterium (APB) agar. Isolated colonies were then inoculated in a 3 mL broth tube and placed at 27 °C shaking to produce biomass for cryopreservation and DNA extraction. Isolates were tested for their ability to produce acid and degrade

Impranil[®], a common polyurethane aircraft coating (Covestro AG, Leverkusen, Germany).

Identification of Cultivated Microorganisms

Two methods were used to extract DNA from isolates. With all samples, 1 µl cells was mixed with 20 µl of GeneReleaser[®] according to the manufacturer's instructions (BioVentures, Inc., Murfreesboro, TN), followed by immediate PCR amplification of the SSU rRNA gene (described below). Any samples that failed to amplify with fungal or bacterial specific primers after using the GeneReleaser[®] protocol were re-extracted using the ZR Fungal/Bacterial DNA MicroPrep[™] Kit (Zymo Research) kit using approximately 50µL of cell culture.

A portion of the 16S rRNA gene was used to identify bacterial isolates using the universal primers 331F (5'-TCC TAC GGG AGG CAG CAG-3')(Nadkarni et al., 2002) and 1492R (5'-CGG TTA CCT TGT TAC GAC TT-3')(TURNER et al., 1999). A portion of the 18S rRNA gene was amplified using the universal fungal primers NS1 (5'-GTA GTC ATA TGC TTG TCT C-3') and NS4 (5'-CTT CCG TCA ATT CCT TTA AG- 3')(White et al., 1990). Final reaction volumes for both amplifications were 25 µl, containing 1x Green GoTaq[®] Flexi Buffer (Promega Corp., Madison, WI), 1x BSA, 2.5 mM MgCl₂ or 2.0 mM MgCl₂ for 16S or 18S rRNA gene amplifications respectively, 0.2 mM dNTPs, 0.2 µM of each primer, and 0.5 unit of GoTaq[®] Flexi DNA Polymerase (Promega Corp., Madison, WI), and 2 µL of template. Reaction conditions were as follows: Initial denaturation of 95 °C for 15 min, 30 cycles of 95 °C for 30 s, 55 °C (16S) or 46 °C (18S) for 30 s, and 60 °C (16S) or 72 °C (18S) for 90 s, and a final extension of 7 min (16S) and 10 min (18S) at 72 °C. Amplified gene

fragments were purified using the QIAquick PCR purification kit (Qiagen Inc., Germantown, MD) and sequenced using both forward and reverse primers by GeneWiz[®] (South Plainfield, NJ) on an ABI3730XL. Electropherograms were then concatenated using Sequencher[®] v5.2.4 and identified using BLAST (Altschul, 1990) against the NCBI refseq database (Tatusova et al., 2015).

Results

After sequencing and quality control, ≈ 1.5 million sequences were clustered into 1903 OTUs across 350 samples. After removing OTUs that were not significantly different from control samples, positive and negative controls were excluded from further analyses. Eukaryotic analyses produced 752 OTUs from ≈ 366 thousand sequences and 349 samples. As an indirect measure, significantly less quantifiable DNA was recovered after amplification in samples after exposure to JBADS at most sites ($p < 0.001$, Student's T-Test), with a median of 4.67 ng/ μ L prior to decontamination, and 0.60 ng/ μ L post decontamination (Fig. 1).

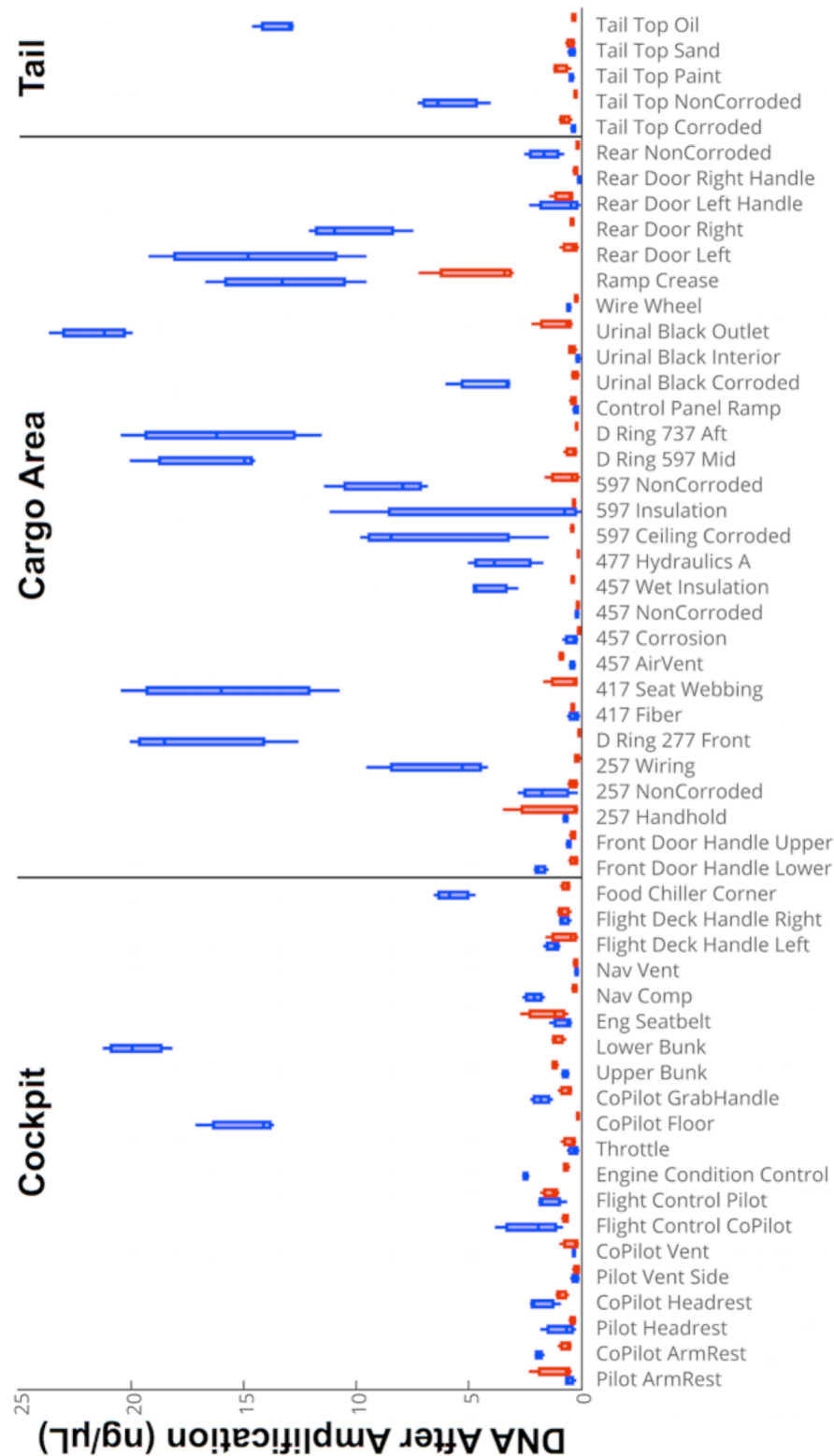


Figure 1. Amount of DNA after PCR amplification before (blue) and after (red) decontamination across all sampled sites.

There was a shift in the relative abundance of both the bacterial (Fig. 2) and eukaryotic (Fig. 3) communities after decontamination. The number of observed OTUs and phylogenetic diversity decreased significantly after decontamination ($p = 0.001$). The equitability (or evenness) of the bacterial and archaeal community was significantly greater after decontamination ($p = 0.001$), but not for the eukarya ($p = 0.076$).

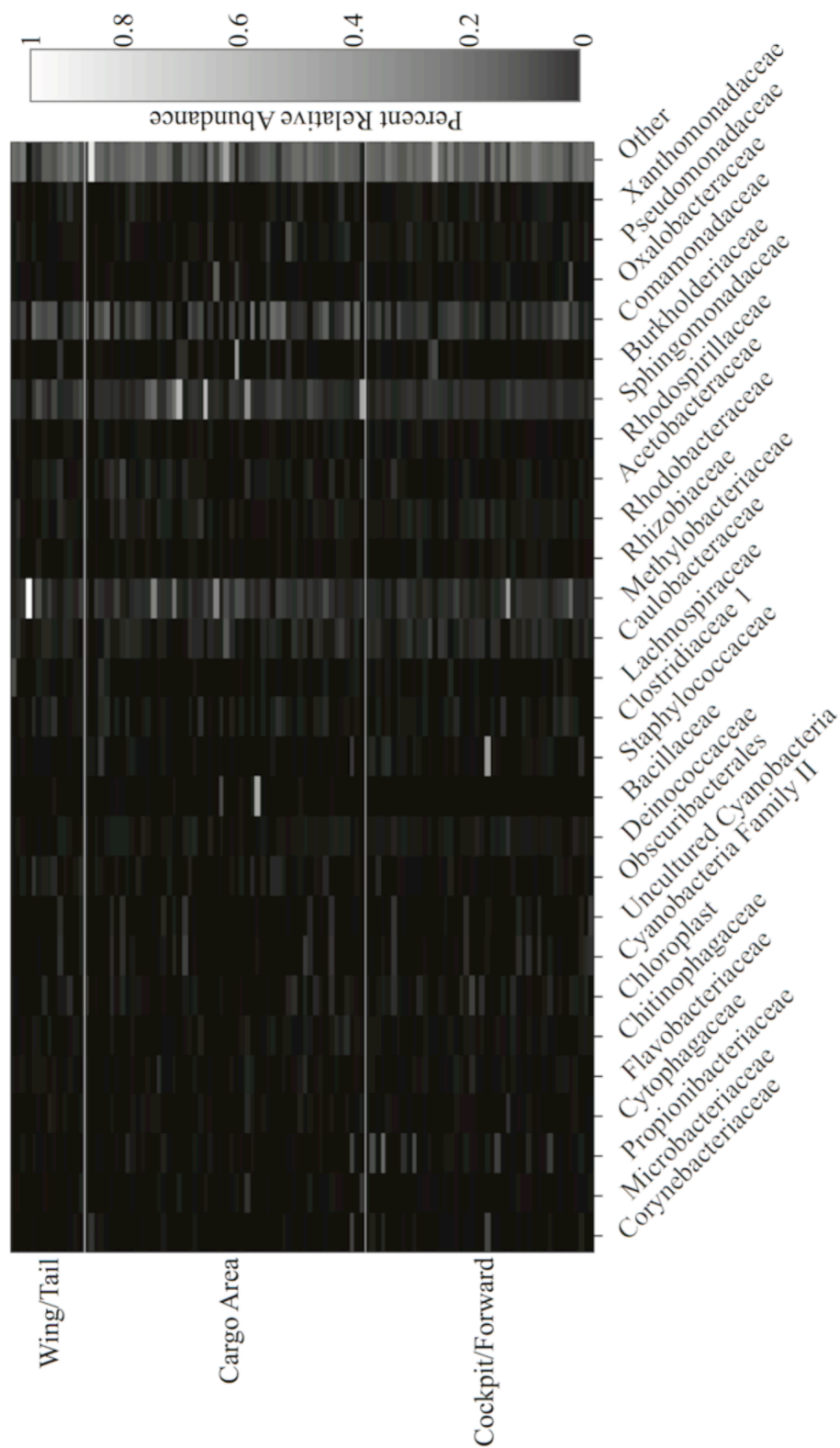


Figure 2. Bacterial families that comprise on average more than 1% relative abundance of any sample. Samples are arranged in alternating order of pre/post decontamination.

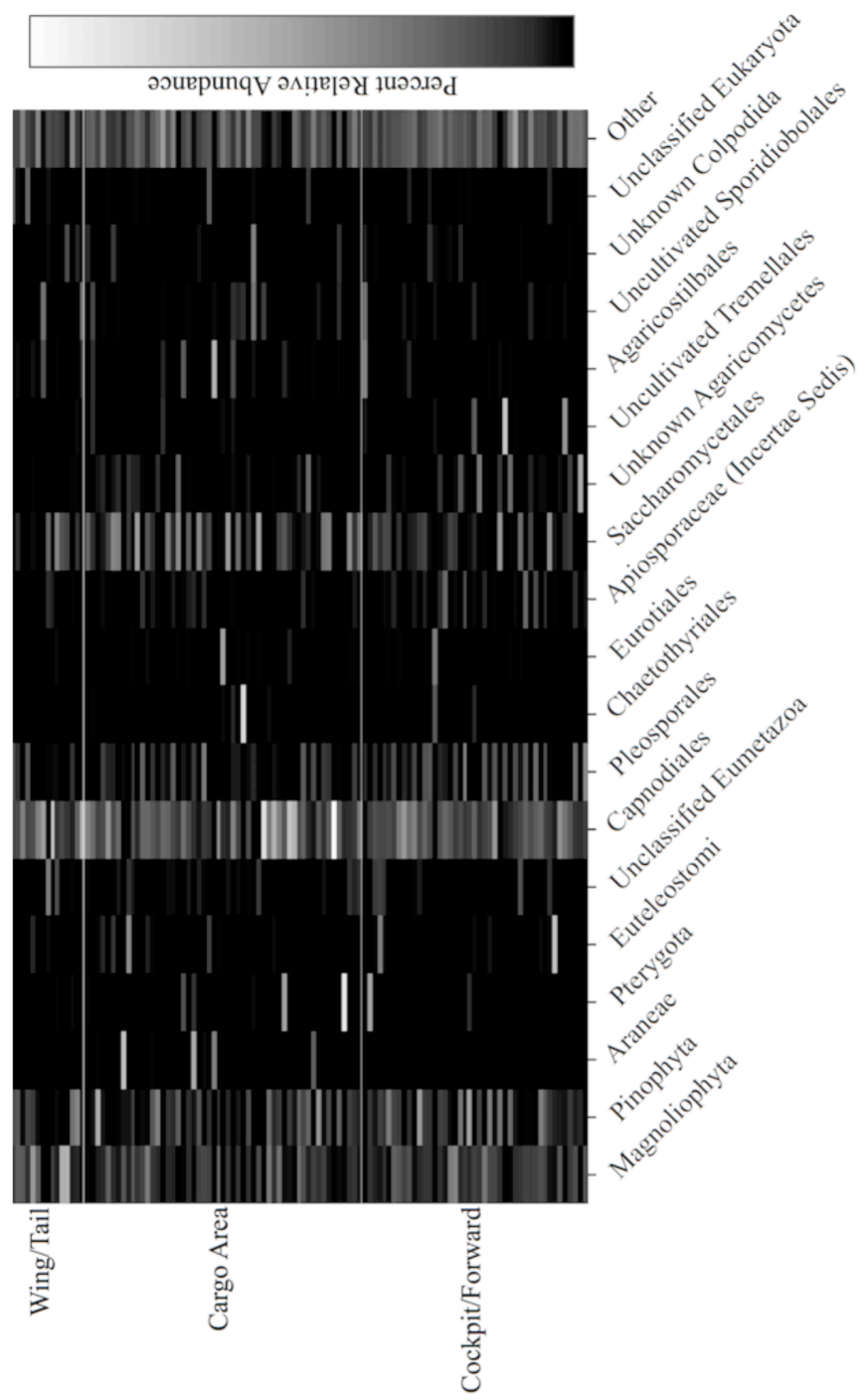


Figure 3. Fungal orders that comprise on average more than 1% relative abundance of any sample. Samples are arranged in alternating order of pre/post decontamination.

There was a significant difference in community structure ($p = 0.001$, $R^2 = 0.064$ for bacteria and archaea, and 0.087 for eukarya) prior to and post decontamination (Figs. 4 and 5). Microbial communities were more strongly defined by their location on the aircraft both prior to decontamination ($p < 0.001$, $R^2 = 0.272$ for bacteria and archaea, and 0.247 for eukarya) and after ($R^2 = 0.111$ for bacteria and archaea, and 0.225 for eukarya). Values for R^2 decreased after decontamination. The relative abundances of 163 Bacterial OTUs were significantly decreased ($p \leq 0.050$) after treatment (Table 3). Of these the largest single grouping was the Proteobacteria, with 33 OTUs that were significantly reduced in relative abundance post decontamination. The Methylobacteriaceae were distributed widely across the aircraft (Fig. 2). Members of the order were also cultivated from the cockpit to the rear of the aircraft and were identified as the genus *Methylobacterium* (Table 2). Several OTUs that were significantly reduced after decontamination were also cultivated from the aircraft both pre- and post-exposure (Table 2). Notably, there was a significant ($p < 0.001$) decrease in multiple OTUs most closely related to the genus *Cryptococcus* (Table 4, order Tremellales), which was isolated from multiple locations across the aircraft prior to decontamination (Table 2).

Table 1. ATP readings taken at select locations across the aircraft before and after decontamination.

Location	Pre Decontamination				Post Decontamination			
	Reading 1	Reading 2	Average		Reading 1	Reading 2	Average	
Top of Tail	250	460	355		17	17	17	
Tail Sandy	32	220	126		120	150	135	
Urinal	410	480	445		13	14	13.5	
Urinal Outlet	ADL ^a	ADL ^a	ADL ^a		15	12	13.5	
Tail, Under	450	510	480		5	6	5.5	
Insulation								
D-Ring 597	ADL ^a	63000	ADL ^a		3	320	161.5	
D-Ring 577	ADL ^a	ADL ^a	ADL ^a		45	35	40	

Cockpit, Crew	ADL ^a	ADL ^a	ADL ^a	41	23	32
Rest Bench						
Air Vent	350	470	410	23	9	16
Cockpit Floor	440	100	270	5	13	9
^a Above Detection Limit (ADL)						

Table 2. List of cultivated organisms before before (Pre) and after (Post) decontamination. The number of cultures producing acid or degrading Impranil® are summarized as positive (+), negative (-), or no reaction is denoted as “NR” or no reaction.

Number of Isolates	Acid Production (+/-/NR)	Impranil® Degradation (+/-/NR)	Genus
Before			
Decontamination			
1	(0/0/1)	(0/1/0)	<i>Willimsia</i>
2	(0/1/1)	(0/1/0)	<i>Tersicoccus</i>
1	(0/1/0)	(0/1/0)	<i>Streptomyces</i>
5	(4/1/0)	(2/3/0)	<i>Staphylococcus</i>
4	(3/1/0)	(3/0/1)	<i>Sporosarcina</i>
22	(4/11/7)	(0/22/0)	<i>Sphingomonas</i>
9	(2/2/5)	(1/7/1)	<i>Rhodotorula</i>
8	(5/0/3)	(1/7/0)	<i>Rhodospiridium</i>
5	(5/0/0)	(0/5/0)	<i>Rhodococcus</i>
3	(1/1/1)	(0/3/0)	<i>Rhizobium</i>
1	(1/0/0)	(1/0/0)	<i>Rasamsonia</i>
6	(6/0/0)	(6/0/0)	<i>Pseudomonas</i>
3	(0/3/0)	(0/3/0)	<i>Pigmentiphaga</i>
2	(1/1/0)	(1/1/0)	<i>Penicillium</i>
11	(0/2/9)	(0/11/0)	<i>Pantoea</i>
1	(0/1/0)	(0/1/0)	<i>Paenicaligenes</i>
3	(0/3/0)	(0/3/0)	<i>Ochrobacterum</i>

1	(0/0/1)	(0/1/0)	<i>Novosphingobium</i>
4	(1/3/0)	(0/4/0)	<i>Mycobacterium</i>
1	(0/0/1)	(0/1/0)	<i>Mucilaginibacter</i>
10	(4/6/0)	(0/10/0)	<i>Micrococcus</i>
18	(16/1/1)	(0/18/18)	<i>Microbacterium</i>
13	(0/5/8)	(0/10/3)	<i>Methylobacterium</i>
2	(0/2/0)	(0/2/0)	<i>Massilia</i>
2	(0/0/2)	(0/2/0)	<i>Luteibacter</i>
2	(1/0/1)	(0/2/0)	<i>Leifsonia</i>
3	(0/2/1)	(0/3/0)	<i>Jeotgalicoccus</i>
1	(0/0/1)	(0/1/0)	<i>Hyphozyma</i>
2	(1/0/1)	(0/2/0)	<i>Gordonia</i>
1	(1/0/0)	(1/0/0)	<i>Geobacillus</i>
3	(1/2/0)	(0/3/0)	<i>Fusarium</i>
1	(0/0/1)	(0/1/0)	<i>Flavobacterium</i>
14	(8/2/4)	(1/13/0)	<i>Enterobacter</i>
1	(0/0/1)	(0/0/1)	<i>Diatrypella</i>
17	(12/2/3)	(1/16/0)	<i>Curtobacterium</i>
2	(0/2/0)	(0/2/0)	<i>Cupriavidus</i>
10	(8/0/2)	(9/1/0)	<i>Cryptococcus</i>
1	(1/0/0)	(0/1/0)	<i>Cosmospora</i>
1	(0/0/1)	(0/1/0)	<i>Corynebacterium</i>
1	(0/0/1)	(0/1/0)	<i>Colacogloea</i>
5	(1/1/3)	(2/3/0)	<i>Cladosporium</i>

2	(2/0/0)	(0/2/0)	<i>Chryseobacterium</i>
1	(1/0/0)	(0/1/0)	<i>Cellulosmicrobium</i>
6	(1/1/4)	(0/6/0)	<i>Capronia</i>
1	(0/0/1)	(0/1/0)	<i>Burkholderia</i>
12	(10/2/0)	(2/10/0)	<i>Bacillus</i>
2	(0/2/0)	(2/0/0)	<i>Aureobasidium</i>
1	(0/1/0)	(0/1/0)	<i>Asterophora</i>
11	(3/8/0)	(5/6/0)	<i>Arthrobacter</i>
2	(0/2/0)	(0/2/0)	<i>Acinetobacter</i>
1	(1/0/0)	(0/1/0)	<i>Achromobacter</i>
242	(105/72/65)	(37/183/22)	Total
After			
Decontamination			
6	(4/0/2)	(0/2/0)	<i>Staphylococcus</i>
3	(0/2/1)	(0/0/0)	<i>Sphingomonas</i>
1	(0/0/1)	(0/0/0)	<i>Rhodotorula</i>
2	(0/0/1)	(0/0/0)	<i>Rhodococcus</i>
13	(0/10/3)	(0/0/0)	<i>Micrococcus</i>
2	(1/1/0)	(0/0/0)	<i>Microbacterium</i>
2	(0/0/2)	(0/0/0)	<i>Methylobacterium</i>
1	(0/0/1)	(0/0/0)	<i>Exophiala</i>
1	(0/0/1)	(0/0/0)	<i>Enterobacter</i>
2	(0/2/0)	(0/1/1)	<i>Enhydrobacter</i>

1	(1/0/0)	(0/0/0)	<i>Cladosporium</i>
2	(1/0/1)	(0/0/0)	<i>Burkholderia</i>
1	(0/1/0)	(0/0/0)	<i>Brevundimonas</i>
2	(1/0/1)	(1/1/0)	<i>Bacillus</i>
1	(1/0/0)	(0/0/0)	<i>Acinetobacter</i>
40	(9/18/13)	(1/38/1)	Total

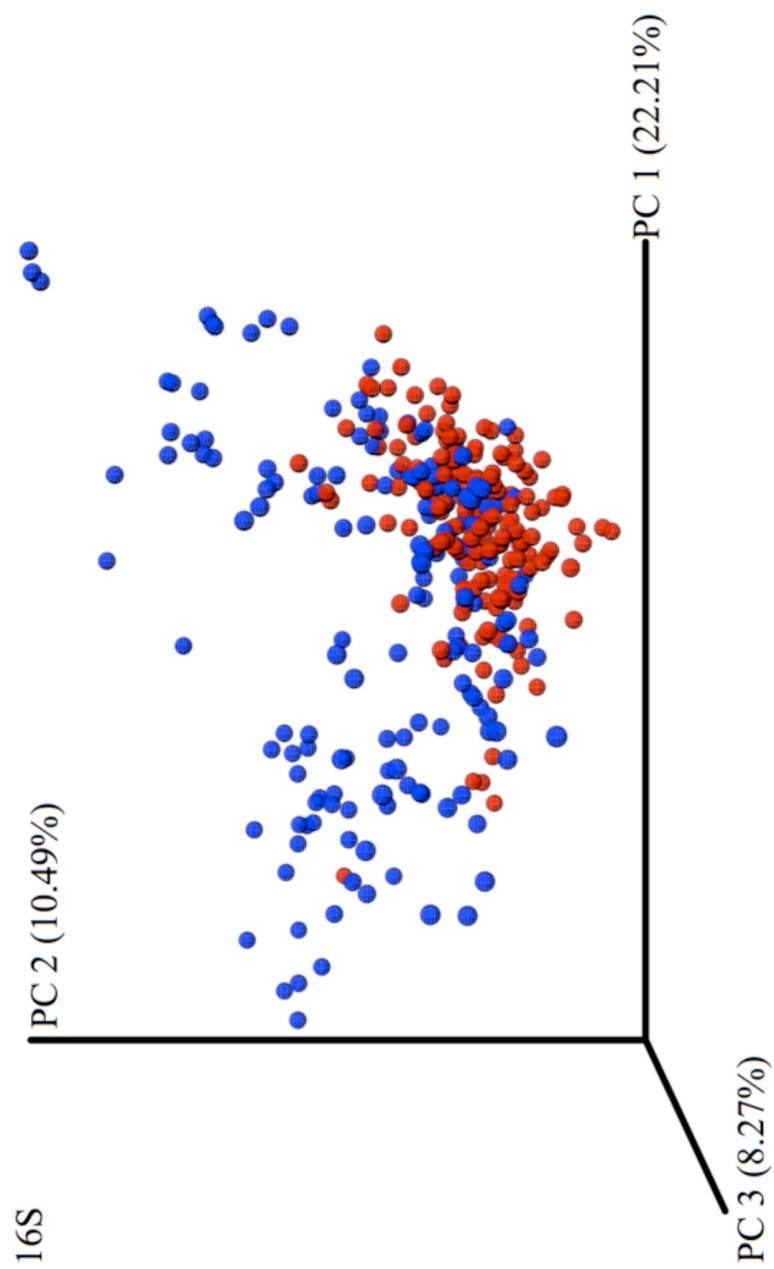


Figure 4. Principal Coordinates Analysis (PCoA) ordination of all bacterial and archaeal samples pre (blue) and post (red) decontamination.

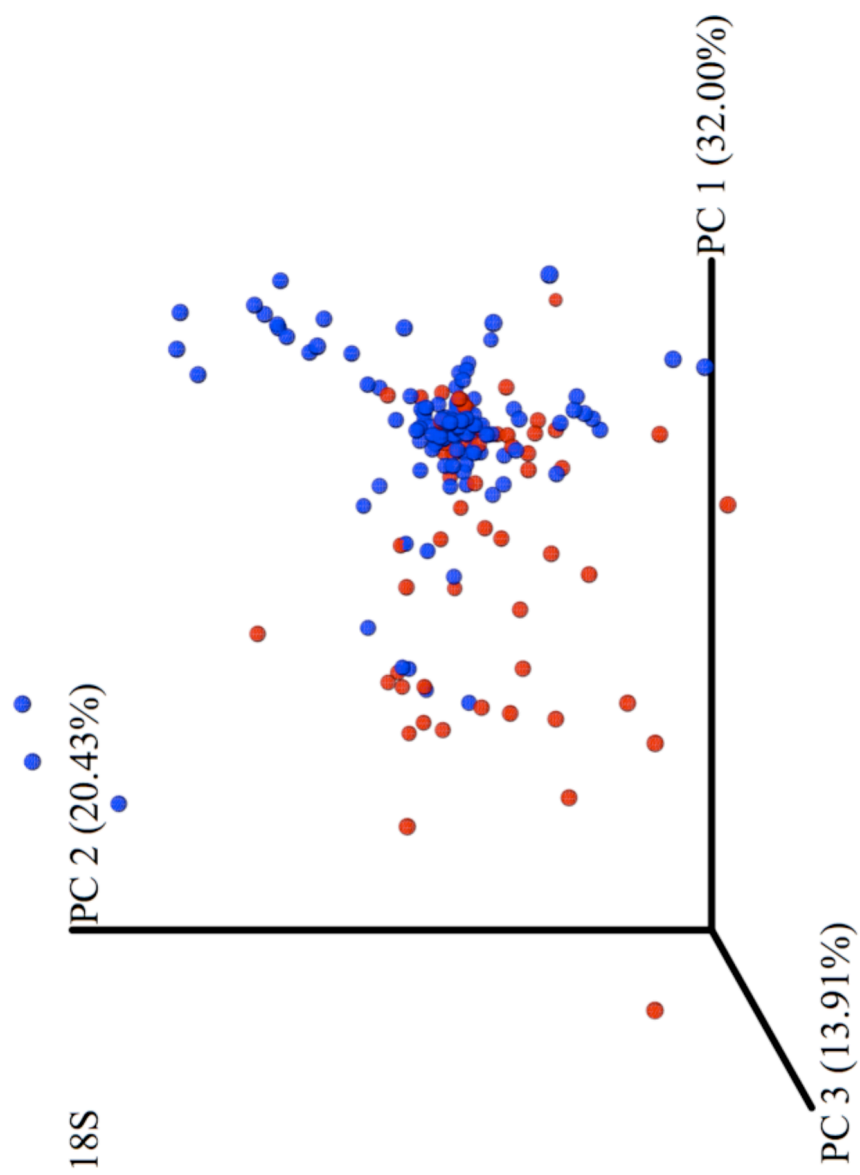


Figure 5. Principal Coordinates Analysis (PCoA) ordination of all eukaryotic samples pre (blue) and post (red) decontamination.

Cultivation produced 242 isolates from 93 unique fungal and bacterial species prior to JBADS exposure (Table 2), and 40 isolates from 22 species after exposure (Table 3). The crease near the bottom of the right side rear exit produced the greatest number of isolates (43). More generally, isolates were recovered at lower dilutions from the inner skin and pooled hydraulic fluid in the tail, left rear door crease, the exterior urinal vent tube, D-Rings at position 737 and 597, a corroded area beneath insulation at 597, and the lower crew rest bench area (Fig. 4).

ATP levels were highest at the urinal outlet, D-rings at position 597 and 577, and the crew rest bench area prior to decontamination (Table 1). ATP readings agreed with the highest quantified DNA after amplification (Fig. 1). In all cases, the areas with the highest measured microbial density correlated with the highest measured ATP levels (Fig. 6). A standard curve showed that ATP readings of greater than 500 indicated CFUs/mL of at least 1.9×10^6 , and lower than 100 indicated CFUs/mL of below 1.9×10^4 . The instrument was unable to accurately detect below 2.0×10^3 CFUs/mL, with an ATP reading of 20. After decontamination, 95 percent of all areas showed a decrease in the amount of detectable ATP, with the exception of the sandy area located in the tail (Table 1). D-rings with high ATP readings prior to decontamination were reduced to near the minimal level of detectable ATP after treatment.

Table 3. List of bacterial taxonomic lineages significantly decreased after JBADS treatment. Significance was assessed using a non-parametric Kruskal Wallace test after false discovery rate (FDR) correction. Number of detected OTUs that were significantly decrease in relative abundance is also listed.

Number of OTUs	Taxonomy
3	Acidobacteria, Acidobacteria, Subgroup 3
10	Acidobacteria, Acidobacteria, Subgroup 4
3	Acidobacteria, Acidobacteria, Subgroup 6
4	Actinobacteria, Actinobacteria, Corynebacteriales, Corynebacteriaceae
1	Actinobacteria, Actinobacteria, Corynebacteriales, Nocardiaceae
1	Actinobacteria, Actinobacteria, Kineosporiales, Kineosporiaceae
1	Actinobacteria, Actinobacteria, Micrococcales, Intraspangiaceae

1	Actinobacteria, Actinobacteria, Micrococcales, Microbacteriaceae
1	Actinobacteria, Actinobacteria, Micromonosporales, Micromonosporaceae
1	Actinobacteria, Actinobacteria, Propionibacteriales, Nocardioidaceae
2	Actinobacteria, Actinobacteria, Propionibacteriales, Propionibacteriaceae
1	Actinobacteria, Thermoleophilia, Solirubrobacterales
2	Actinobacteria, Thermoleophilia, Solirubrobacterales, Solirubrobacteraceae
1	Armatimonadetes, Armatimonadia, Armatimonadales, Armatimonadaceae
8	Uncultivated Armatimonadetes
1	Bacteroidetes, Bacteroidia, Bacteroidales, Porphyromonadaceae
12	Bacteroidetes, Cytophagia, Cytophagales, Cytophagaceae

1	Bacteroidetes, Cytophagia, Order II, Rhodothermaceae
1	Bacteroidetes, Flavobacteriia, Flavobacteriales, Flavobacteriaceae
8	Bacteroidetes, Sphingobacteriia, Sphingobacteriales, Chitinophagaceae
3	Bacteroidetes, Sphingobacteriia, Sphingobacteriales, Sphingobacteriaceae
1	Chloroflexi, Anaerolineae, Anaerolineales, Anaerolineaceae
1	Chloroflexi, Chloroflexia, Chloroflexales, Roseiflexaceae
1	Chloroflexi, Chloroflexia, Kallotenuales, AKIW781
1	Chloroflexi, Thermomicrobia, JG30-KF-CM45
1	Cyanobacteria, Chloroplast
1	Cyanobacteria, Cyanobacteria, SubsectionI, FamilyI

2	Cyanobacteria, Cyanobacteria, SubsectionII, FamilyII
5	Cyanobacteria, Cyanobacteria, SubsectionIII, FamilyI
3	Unclassified Cyanobacteria
16	Deinococcus-Thermus, Deinococci, Deinococcales, Deinococcaceae
1	Firmicutes, Bacilli, Lactobacillales, Streptococcaceae
1	Firmicutes, Clostridia, Clostridiales, Clostridiaceae 1
2	Firmicutes, Clostridia, Clostridiales, Family XI
1	Firmicutes, Clostridia, Clostridiales, Lachnospiraceae
1	Firmicutes, Erysipelotrichia, Erysipelotrichales, Erysipelotrichaceae
1	Firmicutes, Negativicutes, Selenomonadales, Veillonellaceae

4	Planctomycetes, Planctomycetacia, Planctomycetales, Planctomycetaceae
2	Proteobacteria, Alphaproteobacteria, Caulobacterales, Caulobacteraceae
1	Proteobacteria, Alphaproteobacteria, Rhizobiales, Aurantimonadaceae
1	Proteobacteria, Alphaproteobacteria, Rhizobiales, Beijerinckiaceae
1	Proteobacteria, Alphaproteobacteria, Rhizobiales, D05-2
1	Proteobacteria, Alphaproteobacteria, Rhizobiales, JG34-KF-361
7	Proteobacteria, Alphaproteobacteria, Rhizobiales, Methylobacteriaceae
1	Proteobacteria, Alphaproteobacteria, Rhizobiales, P-102
1	Proteobacteria, Alphaproteobacteria, Rhizobiales, Rhizobiaceae
1	Proteobacteria, Alphaproteobacteria, Unclassified Rhizobiales

2	Proteobacteria, Alphaproteobacteria, Rhodobacterales, Rhodobacteraceae
14	Proteobacteria, Alphaproteobacteria, Rhodospirillales, Acetobacteraceae
1	Proteobacteria, Alphaproteobacteria, Unclassified Rickettsiales
1	Proteobacteria, Alphaproteobacteria, Sphingomonadales, Ellin6055
1	Proteobacteria, Alphaproteobacteria, Sphingomonadales, Erythrobacteraceae
1	Proteobacteria, Alphaproteobacteria, Sphingomonadales, MN 122.2a
3	Proteobacteria, Alphaproteobacteria, Sphingomonadales, Sphingomonadaceae
1	Proteobacteria, Betaproteobacteria, Burkholderiales, Burkholderiaceae
2	Proteobacteria, Betaproteobacteria, Burkholderiales, Comamonadaceae
3	Proteobacteria, Betaproteobacteria, Neisseriales, Neisseriaceae

3	Proteobacteria, Deltaproteobacteria, Bdellovibrionales, Bdellovibrionaceae
2	Proteobacteria, Deltaproteobacteria, Myxococcales, Phaselicystidaceae
1	Proteobacteria, Deltaproteobacteria, Oligoflexales, Oligoflexaceae
1	Proteobacteria, Deltaproteobacteria, Uncultivated Oligoflexales
1	Proteobacteria, Gammaproteobacteria, Legionellales, Legionellaceae
1	Unclassified Proteobacteria
1	Unclassified Bacteria

Table 4. List of eukaryotic taxonomic lineages significantly decreased after JBADS treatment. Significance was assessed using a non-parametric Kruskal Wallace test after false discovery rate (FDR) correction. Number of detected OTUs that were significantly decrease in relative abundance is also listed.

Number of OTUs	Taxonomy
2	Amoebozoa, Myxogastria, Stemonitis
8	Archaeplastida, Chloroplastida, Charophyta, Phragmoplastophyta
3	Archaeplastida, Chloroplastida, Chlorophyta, Chlorophyceae
1	Archaeplastida, Chloroplastida, Chlorophyta, Trebouxiophyceae
1	Opisthokonta, Holozoa, Metazoa (Animalia), Eumetazoa, Bilateria, Arthropoda, Chelicerata
4	Opisthokonta, Holozoa, Metazoa (Animalia), Eumetazoa, Bilateria, Arthropoda, Hexapoda

1	Opisthokonta, Holozoa, Metazoa (Animalia), Eumetazoa, Unclassified Bilateria
1	Opisthokonta, Nucleotmycea, Fungi, Dikarya, Ascomycota, Pezizomycotina, Arthoniomycetes
1	Opisthokonta, Nucleotmycea, Fungi, Dikarya, Ascomycota, Pezizomycotina, Dothideomycetes, Botryosphaeriales
4	Opisthokonta, Nucleotmycea, Fungi, Dikarya, Ascomycota, Pezizomycotina, Dothideomycetes, Pleosporales
3	Opisthokonta, Nucleotmycea, Fungi, Dikarya, Ascomycota, Pezizomycotina, Unclassified Dothideomycetes
2	Opisthokonta, Nucleotmycea, Fungi, Dikarya, Ascomycota, Pezizomycotina, Eurotiomycetes, Chaetothyriales
2	Opisthokonta, Nucleotmycea, Fungi, Dikarya, Ascomycota, Pezizomycotina, Lichinomycetes, Lichinales
1	Opisthokonta, Nucleotmycea, Fungi, Dikarya, Ascomycota, Pezizomycotina, Sordariomycetes, Hypocreales
1	Opisthokonta, Nucleotmycea, Fungi, Dikarya, Ascomycota, Pezizomycotina, Sordariomycetes
2	Opisthokonta, Nucleotmycea, Fungi, Dikarya, Ascomycota, Pezizomycotina, Sordariomycetes, Xylariales

1	Opisthokonta, Nucletmycea, Fungi, Dikarya, Ascomycota, Pezizomycotina, Unclassified Sordariomycetes
1	Opisthokonta, Nucletmycea, Fungi, Dikarya, Ascomycota, Unclassified Pezizomycotina
6	Opisthokonta, Nucletmycea, Fungi, Dikarya, Basidiomycota, Agaricomycotina, Agaricomycetes, Agaricales
1	Opisthokonta, Nucletmycea, Fungi, Dikarya, Basidiomycota, Agaricomycotina, Agaricomycetes, Boletales
4	Opisthokonta, Nucletmycea, Fungi, Dikarya, Basidiomycota, Agaricomycotina, Unclassified Agaricomycetes
3	Opisthokonta, Nucletmycea, Fungi, Dikarya, Basidiomycota, Agaricomycotina, Tremellomycetes, Tremellales
1	Opisthokonta, Nucletmycea, Fungi, Dikarya, Basidiomycota, Basidiomycotina, Dacrymycetes, Dacrymycetales
3	Opisthokonta, Nucletmycea, Fungi, Dikarya, Basidiomycota, Pucciniomycotina, Pucciniomycetes, Pucciniales
2	Opisthokonta, Nucletmycea, Fungi, Dikarya, Basidiomycota, Ustilaginomycotina, Exobasidiomycetes, Malasseziales
2	Opisthokonta, Nucletmycea, Unclassified Fungi

1	SAR, Alveolata, Ciliophora, Intramacronucleata, Conthreep, Colpodea, Colpodida
1	SAR, Rhizaria, Uncassified Cercozoa
2	Unclassified Eukaryota

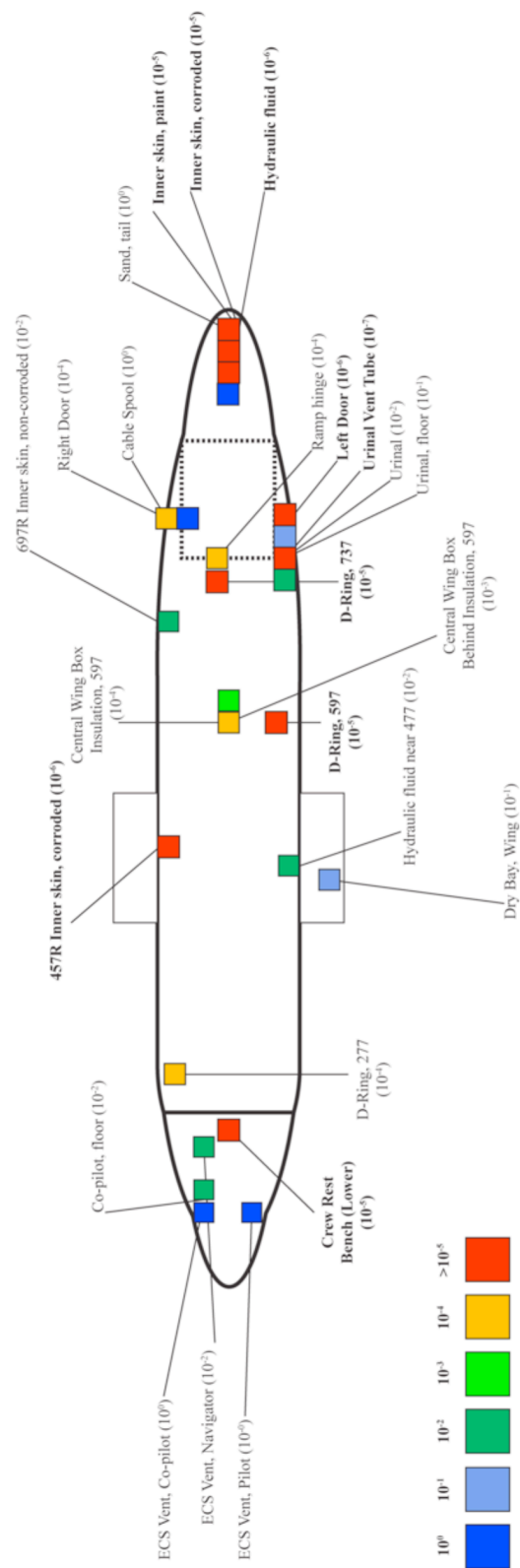


Figure 6. Overview of the number of cultivated microorganisms across the sampled C-130 prior to decontamination. Numbers in parentheses represent the lowest dilution in which an isolate was successfully recovered.

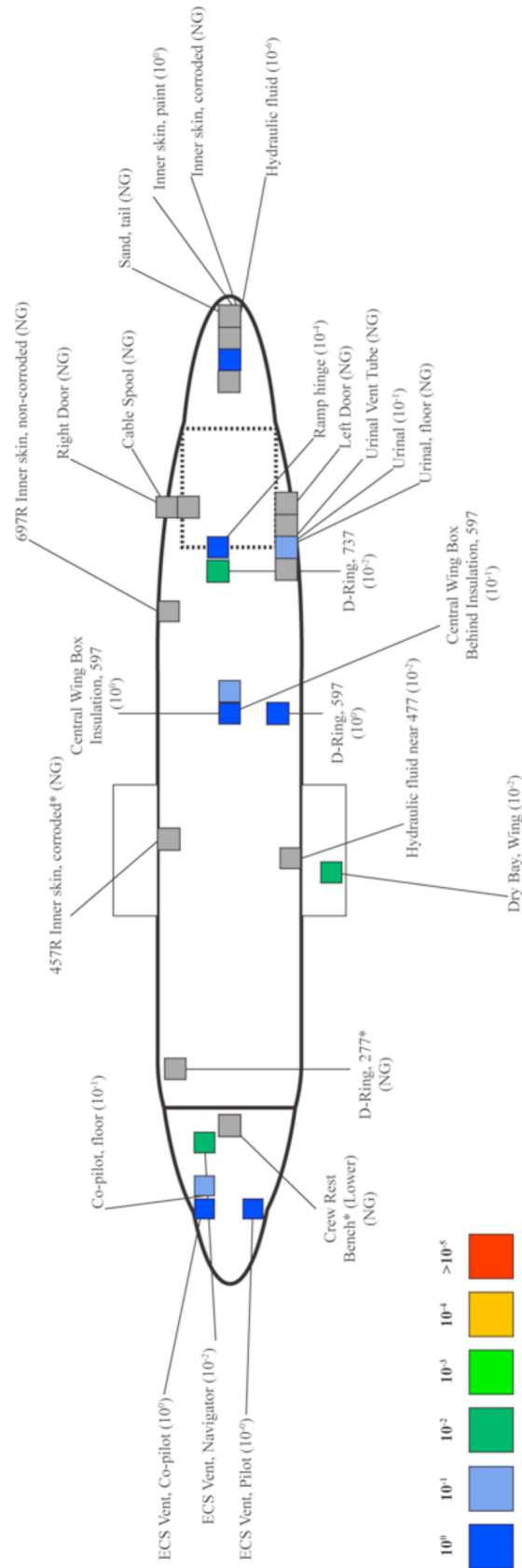


Figure 7. Overview of the number of cultivated microorganisms across the sampled C-130 after decontamination. Numbers in parentheses represent the lowest dilution in which an isolate was successfully recovered. Locations marked with an asterisk denote locations where the only microorganisms recovered are from potential laboratory contaminants.

Discussion

Ensuring the safety of aircraft, personnel, and cargo, as well limiting the spread of bioterror agents is of enormous concern (National Research Council, 2006). Traditional means of cleaning an aircraft can miss small or restricted spaces, allowing spores to remain dormant until disturbed by passengers or crew members (Clayton et al., 1976). Aircraft can also contain metabolically active populations of microorganisms across its surfaces that vary in ATP by more than an order of magnitude (Table 1). Aircraft surfaces are most commonly aluminum, and present little available carbon, phosphate, sulfur, or nitrogen for microorganisms to grow on. However any organism, including pathogens, that are capable of oxidizing carbonaceous compounds found in coatings, dust, dirt, or oils may can persist.

The microbial communities found on surfaces of the C-130 H aircraft in this study varied significantly across different locations. Specifically, floors, walls, and ceilings appeared to harbor distinct communities on the aircraft. Some bacterial families were broadly distributed both in the small subunit rRNA gene survey and cultivation efforts. The genus *Methylobacterium*, which is commonly in both soils and human associated microbiomes (Anesti et al., 2005; Cao et al., 2011), was broadly distributed across the aircraft. In one case the Methylobacteriaceae comprised over 95 percent of the relative abundance of the “dry bay” sample taken from the wing prior to decontamination. Despite being common contaminants of PCR (Salter et al., 2014), members of the Methylobacteriaceae were among a large number of recovered isolates from the aircraft. The Methylobacteriaceae were distributed broadly across the aircraft and were

relatively more abundant than many other detected taxa. None of the isolated Methylobacteriaceae were able to degrade polyurethane or produce acidic metabolic end products, and therefore were considered to represent a low risk of contributing to MIC.

Several OTUs most closely related to the genus *Pseudomonas* were also found across the aircraft. Members of this genus were previously described as part of the aircraft microbiome characterized by Korves et al. (Korves et al., 2013). *Pseudomonas* isolates were recovered from the rear of the aircraft in the gap surrounding the left rear exit door, and the urinal vent tube. All isolates produced acidic metabolic end products and were capable of degrading polyurethane, suggesting that the presence of *Pseudomonas* on any aircraft may be undesirable. After JBADS decontamination no *Pseudomonas* isolates were recovered (Table 2), showing that the method is effective in removing microorganisms that are undesirable under normal operating conditions.

The most dominant bacteria found in samples of the D-Rings in the cargo area were represented by 32 OTUs most closely related to the genus *Sphingomonas* (Fig. 2). Members of this genus have been found in soils contaminated with polycyclic aromatic hydrocarbons (Adkins, 1999; Cassidy et al., 1999; Leys et al., 2004) as well as hospitals and shower curtains (Holmes et al., 1977; Kelley et al., 2004). Cargo floor spaces may trap water and retain traces of jet fuel, hydraulic fluids, and other hydrocarbon bearing materials that may support a community of *Sphingomonas*.

At one location prior to decontamination near the front of the cargo area, the eukaryotic community was dominated by a single OTU most closely related to the order Capnodiales, which were the most abundant order of fungi across the aircraft. Multiple isolates were recovered from this order, most closely related to *Cladosporium*. Commonly referred to as the “kerosene fungus”, *Cladosporium* is associated with contamination of aviation fuels (Marsden, 1954). More worrisome to the maintenance of aircraft, isolates from this genus were capable of degrading Impranil® (Table 2) representing a risk to coatings across the aircraft. *Cladosporium* are also found in moisture damaged building materials suggesting that high humidity in the aircraft may allow for proliferation of this genus (HYVARINEN et al., 2002). After decontamination, the wiring harness had a large shift in the abundance of *Cladosporium* showing that it is possible to affect dominant fungal taxa found on the aircraft (Fig. 2). Other fungi included unclassified members of the Pleosporales, Saccharomycetales, and unclassified Agaricomycetes. Otherwise, many of the most dominant orders in the eukaryotic sequencing libraries came from pollen and metazoans.

Prior to decontamination, the microbial communities found on floors, ceilings, and walls were significantly distinct from one another. After heat treatment, the bacterial and archaeal communities became more even (e.g. homogenous), and while they were still significantly distinct, the coefficient of determination (R^2) was reduced from 0.272 to 0.111, suggesting that there was more similarity between locations. Eukaryotic communities were not significantly different from one another after decontamination (Fig. 3). Members of the Capnodiales and Eurotiales are highly heat resistant, with spores capable of surviving and germinating at 75°C (Seifert et al., 2004; Tournas,

1994). It is possible the many detected OTUs after decontamination were spores and although the extended period of heating may have rendered them unviable, their DNA was still detectable through PCR amplification. After decontamination, the cultivable fungal and bacterial diversity decreased (Table 2). Much of what remained was likely non-viable as suggested by very low ATP readings after decontamination (Table 1), a result that is contrasted by the non-significant differences in fungal diversity observed in DNA sequencing libraries. DNA sequencing results could be confounded by the presence of intact “relic” DNA from dead cells (Carini et al., 2016), although many of the sites tested shifted in community composition significantly. If this is true, it appears that fungal DNA is less susceptible to degradation than bacterial or archaeal DNA.

The apparent success of JBADS in decontaminating surfaces throughout an aircraft addresses the concerns of transporting patients with communicable bacterial or viral infections (Clayton et al., 1976) or if an aircraft was affected by a bioterror attack. Sterilization using chlorine dioxide (ClO_2) carries significant risk of metal and material corrosion (EPA, 2010) and vaporized hydrogen peroxide (VHP) has carries multiple materials restriction (Rutala and Weber, 2013) that JBADS does not (Buhr et al., 2016). Combined with the ability to transport the enclosure as needed suggests the technology is a promising method available in the event of disease outbreak, or bioterror attack.

While not specifically tested, viral particles would also likely be rendered inactive by the extended humidity and high temperature conditions of the JBADS approach (Chan et al., 2011; Mitchell and McCormick, 1984; Swayne and Beck, 2004). The spread of past outbreaks of SARS was exacerbated by infected airline passengers (Peiris et al., 2003). The JBADS approach could be used if an infected airline passenger were

identified prior to or after deplaning, and the aircraft could be placed back into service without the risk of further infection from surfaces of the plane. Additional testing of the JBADS technique using proxies for common viral pathogens could address this point, and further expand the potential role of hot, humid air decontamination.

Beyond the intended use of infectious disease decontamination, JBADS could serve as a useful method to decontaminate an aircraft if a large number of microorganisms capable of causing MIC were detected. Impranil degrading bacteria and fungi were eliminated from the aircraft after decontamination. Acid producing microorganisms were also not cultivable after decontamination. The elimination of microorganisms capable of corroding or otherwise damaging the aircraft after decontamination suggests that JBADS would be useful in the event of a significant fungal or bacterial contamination of an aircraft. The system could also serve beyond aircraft and decontaminate other human made structures such as above or below ground fuel storage tanks that experience varying levels of recurrent contamination (Chapter 3 and 4). Additional testing is required to confirm the use of JBADS beyond whole aircraft decontamination, but it appears it is a useful and rapid technique for decontamination of numerous structures.

Using a combination of DNA based community analysis, cultivation, and ATP measurements on site allowed for a definitive test of the ability of the JBADS process to decontaminate a whole aircraft. Each approach has potential drawbacks. DNA community analyses can be biased by relic DNA (Carini et al., 2016). Cultivation can miss a vast majority of microorganisms (Staley and Konopka, 1985), and ATP testing lacks the ability to discern what organisms are present. By combining each approach we

were able to interrogate the microbial community at a great depth, but also confirm the presence of numerous taxa and estimate the microbial load across the entire aircraft.

References

- Abubakar, I. (2010). Tuberculosis and air travel: a systematic review and analysis of policy. *Lancet Infect. Dis.* 10, 176–183. doi:10.1016/S1473-3099(10)70028-1.
- Adkins, A. (1999). Degradation of the phenoxy acid herbicide diclofop-methyl by *Sphingomonas paucimobilis* isolated from a Canadian prairie soil. *J. Ind. Microbiol. Biotechnol.* 23, 332–335. doi:10.1038/sj.jim.2900744.
- Altschul, S. (1990). Basic Local Alignment Search Tool. *J. Mol.* 215, 403–410. doi:10.1006/jmbi.1990.9999.
- Anesti, V., McDonald, I. R., Ramaswamy, M., Wade, W. G., Kelly, D. P., and Wood, A. P. (2005). Isolation and molecular detection of methylotrophic bacteria occurring in the human mouth. *Environ. Microbiol.* 7, 1227–1238. doi:10.1111/j.1462-2920.2005.00805.x.
- Barratt, S. R., Ennos, A. R., Greenhalgh, M., Robson, G. D., and Handley, P. S. (2003). Fungi are the predominant micro-organisms responsible for degradation of soil-buried polyester polyurethane over a range of soil water holding capacities. *J. Appl. Microbiol.* 95, 78–85.
- Buhr, T. L., Young, A. A., Barnette, H. K., Minter, Z. A., Kennihan, N. L., Johnson, C.

- A., et al. (2015). Test methods and response surface models for hot, humid air decontamination of materials contaminated with dirty spores of *Bacillus anthracis*ΔSterne and *Bacillus thuringiensis*Al Hakam. *J. Appl. Microbiol.* 119, 1263–1277. doi:10.1111/jam.12928.
- Buhr, T. L., Young, A. A., Bensman, M., Minter, Z. A., Kennihan, N. L., Johnson, C. A., et al. (2016). Hot, humid air decontamination of a C-130 aircraft contaminated with spores of two acrySTALLIFEROUS *Bacillus thuringiensis* strains, surrogates for *Bacillus anthracis*. *J. Appl. Microbiol.* doi:10.1111/jam.13055.
- Buhr, T. L., Young, A. A., Minter, Z. A., Wells, C. M., McPherson, D. C., Hooban, C. L., et al. (2012). Test method development to evaluate hot, humid air decontamination of materials contaminated with *Bacillus anthracis*ΔSterne and *B. thuringiensis*Al Hakam spores. *J. Appl. Microbiol.* 113, 1037–1051. doi:10.1111/j.1365-2672.2012.05423.x.
- Cao, Y.-R., Wang, Q., Jin, R.-X., Tang, S.-K., Jiang, Y., He, W.-X., et al. (2011). *Methylobacterium soli* sp. nov. a methanol-utilizing bacterium isolated from the forest soil. *Antonie Van Leeuwenhoek* 99, 629–634. doi:10.1007/s10482-010-9535-0.
- Caporaso, J. G., Kuczynski, J., Stombaugh, J., Bittinger, K., Bushman, F. D., Costello, E. K., et al. (2010). QIIME allows analysis of high-throughput community sequencing data. *Nat. Meth.* 7, 335–336. doi:10.1038/nmeth.f.303.
- Carini, P., Marsden, P. J., Leff, J. W., Morgan, E. E., Strickland, M. S., and Fierer, N.

- (2016). Relic DNA is abundant in soil and obscures estimates of soil microbial diversity. *bioRxiv*. doi:10.1101/043372.
- Cassidy, M. B., Lee, H., Trevors, J. T., and Zablotowicz, R. B. (1999). Chlorophenol and nitrophenol metabolism by *Sphingomonas* sp UG30. *J. Ind. Microbiol. Biotechnol.* 23, 232–241. doi:10.1038/sj.jim.2900749.
- Chan, K. H., Peiris, J. S. M., Lam, S. Y., Poon, L. L. M., Yuen, K. Y., and Seto, W. H. (2011). The Effects of Temperature and Relative Humidity on the Viability of the SARS Coronavirus. *Adv. Virol.* 2011, 1–7. doi:10.1155/2011/734690.
- Clayton, A. J., O'Connell, D. C., Gaunt, R. A., and Clarke, R. E. (1976). Study of the microbiological environment within long- and medium-range Canadian Forces aircraft. *Aviat. Space Environ. Med.* 47, 471–482.
- Cosgrove, L., McGeechan, P. L., Robson, G. D., and Handley, P. S. (2007). Fungal communities associated with degradation of polyester polyurethane in soil. *Appl. Env. Microbiol.* 73, 5817–5824. doi:10.1128/AEM.01083-07.
- Dechow, M., Sohn, H., and Steinhanses, J. (1997). Concentrations of selected contaminants in cabin air of airbus aircrafts. *Chemosphere* 35, 21–31. doi:10.1016/S0045-6535(97)00135-5.
- Dixon, P. (2003). VEGAN, a package of R functions for community ecology. *J. Veg. Sci.* 14, 927–930. doi:10.1111/j.1654-1103.2003.tb02228.x.
- Edgar, R. C. (2013). UPARSE: highly accurate OTU sequences from microbial

- amplicon reads. *Nat. Meth.* 10, 996–998. doi:10.1038/nmeth.2604.
- EPA, U. S. (2010). Compatibility of Material and Electronic Equipment With Hydrogen Peroxide and Chlorine Dioxide Fumigation. 1–106.
- Faith, D. P. (1992). Conservation evaluation and phylogenetic diversity. *Biol. Conserv.* 61, 1–10. doi:10.1016/0006-3207(92)91201-3.
- Holmes, B., Owen, R. J., Evans, A., Malnick, H., and Willcox, W. R. (1977). *Pseudomonas paucimobilis*, a New Species Isolated from Human Clinical Specimens, the Hospital Environment, and Other Sources. *Int. J. Syst. Bacteriol.* 27, 133–146. doi:10.1099/00207713-27-2-133.
- Hyvarinen, A., Meklin, T., Vepsäläinen, A., and Nevalainen, A. (2002). Fungi and actinobacteria in moisture-damaged building materials — concentrations and diversity. *Int. Biodeterior. Biodegradation* 49, 27–37. doi:10.1016/S0964-8305(01)00103-2.
- Kelley, S. T., Theisen, U., Angenent, L. T., St Amand, A., and Pace, N. R. (2004). Molecular analysis of shower curtain biofilm microbes. *Appl. Env. Microbiol.* 70, 4187–4192. doi:10.1128/AEM.70.7.4187-4192.2004.
- Kenyon, T. A., Valway, S. E., Ihle, W. W., Onorato, I. M., and Castro, K. G. (1996). Transmission of multidrug-resistant *Mycobacterium tuberculosis* during a long airplane flight. *N. Engl. J. Med.* 334, 933–938. doi:10.1056/NEJM199604113341501.

- Korves, T. M., Piceno, Y. M., Tom, L. M., DeSantis, T. Z., Jones, B. W., Andersen, G. L., et al. (2013). Bacterial communities in commercial aircraft high-efficiency particulate air (HEPA) filters assessed by PhyloChip analysis. *Indoor Air* 23, 50–61. doi:10.1111/j.1600-0668.2012.00787.x.
- La Duc, M. T., Stuecker, T., and Venkateswaran, K. (2007). Molecular bacterial diversity and bioburden of commercial airliner cabin air. *Can. J. Microbiol.* 53, 1259–1271. doi:10.1139/W07-093.
- LaDuc, M. T., Osman, S., Dekas, A., Stuecker, T., Newcombe, D., Piceno, Y., et al. (2006). *A Comprehensive Assessment of Biologicals Contained Within Commercial Airliner Cabin Air*.
- Leys, N. M. E. J., Ryngaert, A., Bastiaens, L., Verstraete, W., Top, E. M., and Springael, D. (2004). Occurrence and phylogenetic diversity of *Sphingomonas* strains in soils contaminated with polycyclic aromatic hydrocarbons. *Appl. Env. Microbiol.* 70, 1944–1955. doi:10.1128/AEM.70.4.1944-1955.2004.
- Love, M. I., Huber, W., and Anders, S. (2014). Moderated estimation of fold change and dispersion for RNA-seq data with DESeq2. *Genome Biol.* 15, 1–21. doi:10.1186/s13059-014-0550-8.
- Lozupone, C., and Knight, R. (2005). UniFrac: a New Phylogenetic Method for Comparing Microbial Communities. *Appl. Env. Microbiol.* 71, 8228–8235. doi:10.1128/AEM.71.12.8228-8235.2005.
- Marsden, D. H. (1954). Studies of the creosote fungus, *Hormodendrum resinae*.

Mycologia. doi:10.2307/4547809.

McNamara, C. J., Perry, T. D., IV, Leard, R., Bearce, K., Dante, J., and Mitchell, R.

(2005). Corrosion of aluminum alloy 2024 by microorganisms isolated from aircraft fuel tanks. *Biofouling* 21, 257–265. doi:10.1080/08927010500389921.

Mitchell, S. W., and McCormick, J. B. (1984). Physicochemical inactivation of Lassa,

Ebola, and Marburg viruses and effect on clinical laboratory analyses. *J. Clin. Microbiol.* 20, 486–489.

Nadkarni, M. A., Martin, F. E., Jacques, N. A., and Hunter, N. (2002). Determination of

bacterial load by real-time PCR using a broad-range (universal) probe and primers set. *Microbiology* 148, 257–266. doi:10.1099/00221287-148-1-257.

National Research Council (2006). *Defending the U.S. Air Transportation System*

Against Chemical and Biological Threats. Washington, D.C.: National Academies Press doi:10.17226/11556.

Oceguera-Cervantes, A., Carrillo-García, A., López, N., Bolaños-Nuñez, S., Cruz-

Gómez, M. J., Wachter, C., et al. (2007). Characterization of the polyurethanolytic activity of two Alicyclophilus sp. strains able to degrade polyurethane and N-methylpyrrolidone. *Appl. Env. Microbiol.* 73, 6214–6223.

doi:10.1128/AEM.01230-07.

Parada, A., Needham, D. M., and Fuhrman, J. A. (2015). Every base matters: assessing

small subunit rRNA primers for marine microbiomes with mock communities, time-series and global field samples. *Environ Microbiol.* doi:10.1111/1462-

2920.13023.

Peiris, J. S. M., Lai, S. T., Poon, L. L. M., Guan, Y., Yam, L. Y. C., Lim, W., et al. (2003). Coronavirus as a possible cause of severe acute respiratory syndrome. *Lancet* 361, 1319–1325.

Prokop, E. J., Crigler, J. R., Wells, C. M., Young, A. A., and Buhr, T. L. (2014). Response surface modeling for hot, humid air decontamination of materials contaminated with *Bacillus anthracis* ΔSterne and *Bacillus thuringiensis* Al Hakam spores. *AMB Express* 4, 565. doi:10.1186/s13568-014-0021-3.

Rachael, T., Schubert, K., Hellenbrand, W., Krause, G., and Stuart, J. M. (2009). Risk of transmitting meningococcal infection by transient contact on aircraft and other transport. *Epidemiol. Infect.* 137, 1057–1061. doi:10.1017/S0950268809002398.

Ruiz, C., Main, T., Hilliard, N. P., and Howard, G. T. (1999). Purification and characterization of two polyurethanase enzymes from *Pseudomonas chlororaphis*. *Int. Biodeterior. Biodegradation* 43, 43–47. doi:10.1016/S0964-8305(98)00067-5.

Rutala, W. A., and Weber, D. J. (2013). Disinfection and sterilization: An overview. *Am. J. Infect. Control.* 41, S2–S5. doi:10.1016/j.ajic.2012.11.005.

Salter, S., Cox, M. J., Turek, E. M., Calus, S. T., and Cookson, W. O. (2014). Reagent contamination can critically impact sequence-based microbiome analyses. *bioRxiv*.

Sambrook, J., Fritsch, E. F., and Maniatis, T. (1989). *Molecular cloning: A Laboratory Manual*. Cold Spring Harbor Press doi:10.1016/0167-7799(91)90068-S.

- Seifert, K. A., Nickerson, N. L., Corlett, M., Jackson, E. D., Louis-Seize, G., and Davies, R. J. (2004). *Devriesia*, a new hyphomycete genus to accommodate heat-resistant, cladosporium-like fungi. *Can. J. Bot.* 82, 914–926. doi:10.1139/b04-070.
- Shannon, C. E. (1948). A Mathematical Theory of Communication. *Bell Syst. Tech. J.* 27, 379–423.
- Staley, J. T., and Konopka, A. (1985). Measurement of in Situ Activities of Nonphotosynthetic Microorganisms in Aquatic and Terrestrial Habitats. *Annu. Rev. Microbiol.* 39, 321–346. doi:10.1146/annurev.mi.39.100185.001541.
- Stern, R. V., and Howard, G. T. (2000). The polyester polyurethanase gene (*pueA*) from *Pseudomonas chlororaphis* encodes a lipase. *FEMS Microbiol. Lett.* 185, 163–168.
- Swayne, D. E., and Beck, J. R. (2004). Heat inactivation of avian influenza and Newcastle disease viruses in egg products. *Avian Pathol.* 33, 512–518. doi:10.1080/03079450400003692.
- Tatusova, T., Ciufo, S., Fedorov, B., O'Neill, K., and Tolstoy, I. (2015). RefSeq microbial genomes database: new representation and annotation strategy. *Nucleic Acids Res.* 43, 3872–3872. doi:10.1093/nar/gkv278.
- Tournas, V. (1994). Heat-resistant fungi of importance to the food and beverage industry. *Crit. Rev. Microbiol.* 20, 243–263. doi:10.3109/10408419409113558.
- Turner, S., Pryer, K. M., Miao, V. P. W., and Palmer, J. D. (1999). Investigating Deep Phylogenetic Relationships among Cyanobacteria and Plastids by Small Subunit

- rRNA Sequence Analysis. *J. Euk. Microbiol.* 46, 327–338. doi:10.1111/j.1550-7408.1999.tb04612.x.
- Wagner, G. W., Sorrick, D. C., Procell, L. R., Brickhouse, M. D., Mcvey, I. F., and Schwartz, L. I. (2007). Decontamination of VX, GD, and HD on a surface using modified vaporized hydrogen peroxide. *Langmuir* 23, 1178–1186. doi:10.1021/la062708i.
- White, T. J., Bruns, T., Lee, S., and Taylor, J. (1990). PCR Protocols. Amplification and Direct Sequencing of Fungal Ribosomal RNA Genes for Phylogenetics. in *PCR Protocols* (Elsevier), 315–322. doi:10.1016/B978-0-12-372180-8.50042-1.
- Wick, R. L., and Irvine, L. A. (1995). The microbiological composition of airliner cabin air. *Aviat. Space Environ. Med.* 66, 220–224.
- Yang, S. S., Chen, C. Y., Wei, C. B., and Lin, Y. T. (1996). Microbial corrosion of aluminum alloy. *Zhonghua Min Guo Wei Sheng Wu Ji Mian Yi Xue Za Zhi* 29, 185–196.
- Zhang, J., Kobert, K., Flouri, T., and Stamatakis, A. (2014). PEAR: a fast and accurate Illumina Paired-End reAd mergeR. *Bioinformatics* 30, 614–620.

Chapter 6. Conclusions

In this dissertation, I investigated the diversity of microorganisms present in landfills across the United States, the extent of fouling within biodiesel storage systems in the United States Air Force (USAF), and the ability of hot, humid air to decontaminate and modify the microbiome of a C-130H aircraft. It is essential to understand not only what microorganisms are present within engineered ecosystems but how microbial community composition can change over time, either in response to a change in environmental conditions or after an anthropogenic attempt to control the presence of microorganisms. An ecological perspective on microbially impacted engineered systems aids in understanding why attempts to modify or remove microbial communities may succeed or fail.

Landfills Represent an Untapped Source of Microbial Diversity

The microbial diversity contained within leachates is immense. Geographic region and a limited set of chemical parameters significantly influenced the distribution of these diverse landfill leachate microbial communities (Stamps et al., 2016). Landfill leachates appeared to separate primarily into four clades although the specific set of environmental variables that produced this separation could not be determined. The microbiome of landfill leachates is also unique. The community structure of landfill leachates was significantly different from numerous microbial studies representing a broad cross section of both human associated and natural environments. Two of the four landfill clades contained abundant populations of candidate phyla (Chapter 2). Uncultivated candidate phyla have also been referred to as “microbial dark matter” and

represent a vast majority of microorganisms with unknown function (Hedlund et al., 2014).

A follow on study could use shotgun metagenomic sequencing of the same DNA used to produce the 16S rRNA gene libraries for a less biased study of the observed phylogeny in landfill leachate. Amplified 16S rRNA gene studies can miss or over-represent taxonomic lineages (Hong et al., 2009) including candidate phyla that metagenomic sequencing would discover (Sharpton, 2014), although the careful investigation of PCR primer biases to design the primer pair used in the study (Klindworth et al., 2013) likely resulted in a more even and representative amplification of the microbial taxa detected. More importantly metagenomic sequencing could interrogate the vast genomic potential of landfill leachate. Microarray hybridization-based studies of landfill leachates (Lu et al., 2012) might miss any gene with low similarity to those of known function that are part of the array of probes. Cultivation studies could then follow using information gained from the likely metabolic processes and limitations within leachate using directed cultivation (Bomar et al., 2011; Stevenson et al., 2004) or *in situ* isolation methods (Nichols et al., 2010) to isolate and identify microorganisms from abundant candidate phyla. The uncultivated majority within landfill leachates may also have the potential to unearth a broad swath of potentially industrially or medically useful enzymes (Rondon et al., 1999).

Landfill leachate contains numerous chemicals of emerging concern (CECs) (Masoner et al., 2014; 2015). Microorganisms with the enzymatic capability to degrade some CECs could be isolated or enriched to abate the risk of leachate release into the surrounding environment.

The diverse phylogeny of microorganisms within landfills may also harbor the ability to produce medically relevant secondary metabolites due to the presence of many CECs, including many antimicrobial compounds (Masoner et al., 2014; 2015). Drug resistance is an emerging concern (Boucher et al., 2009) and clinically relevant antimicrobial compounds are of vital interest. Metagenomic sequence can be assembled and screened for secondary metabolite synthesis pathways (Blin et al., 2013). After a pathway is found it could be synthesized and inserted into an appropriate host, and screened for activity (Brady et al., 2009).

More broadly, it is of interest to understand how landfill leachates are related at a more global scale. We were unable to identify any one variable that strongly correlated to the observed community structure across all tested landfill leachates. Geographic region could be moderately correlated to the observed community structure. It is possible we failed to sample an adequately large number of leachates to identify if geography plays a strong role in community structure and composition. By expanding the study to a greater number of landfill leachates across the globe, we may be able to better understand the observed community structure within each landfill clade. Efforts are underway to greatly expand the number of sampled microbiomes across the globe (Alivisatos et al., 2015). By expanding the number of sampled leachates as a part of the unified microbiome initiative we may be able to better understand the distribution of microorganisms present in landfill leachates and what role microorganisms they play in an active and diverse community.

Microbial Communities in Biodiesel Tanks are Geographically Distinct

The biodiesel study presented in Chapters 3 and 4 is the first to be conducted at a scale encompassing multiple sampling events across a one-year period. The tanks harbor an active community of both fungi and bacteria that was unknown prior to the sampling. Tanks reached unacceptable levels of contamination and fouling within six months to one year (Chapter 3). Fuel acidity rose in one tank (SE 3) above the allowable limit within seven months (ASTM D7467) representing a potential risk to infrastructure. Fuel acidification could have occurred through the microbial degradation of fatty acid methyl esters (FAME) that are the primary component of biodiesel. Many microorganisms isolated from biodiesel tanks at SE and SW were capable of growth on B20 (Oderay Andrade, unpublished data). Bacterial consortia have been shown to degrade FAME biodiesel under laboratory conditions previously (Aktas et al., 2010; Prince et al., 2008) and fungi are known to use FAME as a source of fatty acids and methanol (Kumari and Gupta, 2014). By combining sequence-based studies with genomic sequencing of isolates obtained from the field and the analysis of the transcriptome of a major member of the fungal community at two tested sites, we have shown that the FAME is likely activated by fungal and bacterial lipases before β -oxidation and fermentation (Chapter 3). The oxidation of FAME appears to be a ubiquitous process in genome sequence of bacterial and fungal isolates cultivated from B20 storage tanks (Chapter 3). The ability for FAME to be degraded by organisms isolated from USAF B20 tanks represents a significant risk to fuel stability and safety within the DoD.

The study described here also included an in-depth investigation of the ecology of fuel tank systems. Due to the vast diversity of microorganisms capable of degrading FAME, it is unlikely that carbon is a limiting nutrient in a tank. Instead, a major limitation within a biodiesel tank may be access to water or oxygen. Microorganisms require some amount of water to survive and while small populations may thrive in micro bubbles dissolved in organic liquids (Meckenstock et al., 2014), a greater population likely exists as a biofilm at or near the bottom of a tank. Any organism capable of preferentially excluding other microorganisms from the primary carbon source within an underground storage tank through a morphology that limits the access of other cells to the fuel-water interface or the production of antimicrobial secondary metabolites may have a competitive advantage. One fungal isolate most closely related to the genus *Byssoschlamys* produced thick, viscous hyphal mats and had the capability to produce a number of antibacterial and antifungal metabolites (Chapter 3). Thick filamentous biofilms were observed under scanning electron microscopy on biofilms on witness coupons from tanks in the southeastern United States (SE) under which pits were discovered. Microorganisms may produce high concentrations of acids under these biofilms that could enhance localized corrosion (Little et al., 1992). Based on the large number of acetogenic bacteria and fungi, and the lack of sulfate or nitrate reducing microorganisms, we concluded that the most likely corrosion mechanism was acetic acid production and localized dissolution of iron.

Accurate estimates of biomass are difficult to achieve in mixed fungal and bacterial environments. Filamentous fungi are difficult to quantify accurately (Pitt and Hocking, 2009). Bacteria and archaea can be accurately quantified using quantitative PCR

(qPCR). This is not a good estimate of biomass in fungi because rRNA gene copy number can vary significantly across phylogenetic lineages and life stages in fungi (Herrera et al., 2009). Fuels were quantified by qPCR at SE over a four month period however because of experimental design concerns it was decided that a greater number of samples should be taken for community analysis rather than focusing on qPCR estimations of biomass. In place of qPCR, ATP was used as a proxy for microbial activity. Visible flocculent material often correlated with high ATP measurements, or a high ATP measure preceded the visible detection of fouling. Therefore ATP is a useful method of detection of microbial activity and fouling although it cannot distinguish between fungal or bacterial activity.

Expanding the number of sites to a broader geographic region would provide a greater understanding of the microorganisms present in B20. While there was shared membership of many of the abundant fungal and bacterial community members, differences were present at each location. Determining if the differences were due to latitudinal diversity gradients (Fuhrman et al., 2008) or specific operating conditions at each site could be addressed by expanding the study to a number of locations spanning the continental United States and outlying areas where the USAF may use biodiesel. A careful multi-year study including storage tanks and fleet vehicles may also allow for an understanding of how contaminated fuel impacts the vehicles that use it. Only a small number of studies have attempted to track vehicles using biodiesel over time (Proc et al., 2006) and none have done so within the context of a microbial community study.

I was able to investigate a single fungal isolate using transcriptomics to understand what transcripts were present during the degradation of biodiesel. It would be desirable to attempt further transcriptomic sequencing in a number of environmental samples to further confirm the mechanism of FAME degradation in B20. Alkane degradation was not observed in the incubation period of my experiment. Isolated laboratory cultures fail to recreate the complexity of a biofilm *in situ* and determining which bacterial and fungal transcripts are expressed during the lifetime of an in-service biodiesel tank would be essential to know who is present in a biodiesel tank and how they are degrading the fuel. Biofilms could also be studied to confirm hypotheses related to the localized production of organic acids (Little et al., 1992). The mechanism of acetic acid biocorrosion is poorly understood and may increase due to the presence of elevated levels of CO₂ (Gu, 2014). By measuring the pH, CO₂ concentration, and redox potential using microelectrodes on witness coupons or other materials incubated *in situ*, predictions modeling the interaction of inorganic carbon chemistry and acetic acid within biofilms could be confirmed. Both anaerobic and obligately aerobic microorganisms were found in association within biofilms at SE and SW. The spatial distribution of both fungi and bacteria should also be investigated using fluorescent *in situ* hybridization probes to confirm the physical location that aerobic and anaerobic organisms occupy within tank biofilms, and to better correlate the presence of key fungal taxa to pit formation.

Translating our discoveries in the field and in the lab to educational materials and practical solutions for end users is an important outcome of this research. While it is an important finding that biodiesel can be degraded by a large number of fungi and

bacteria, a solution to the issue at hand is crucial. Tank operators should be aware of the high risk of fuel contamination and modify tank maintenance operations to include more regular cleaning cycles. An inspection of current tanks for any points of water infiltration to reduce the likelihood of microbial ingress during flooding events may also help in reducing the risk of fuel fouling. The contribution of bioaerosols (Brandl et al., 2008) to tank fouling is not known. Airborne microorganisms could potentially enter the tank through venting hardware. The risk could be abated by the use of high-efficiency particulate air filters to exclude particulate entry while still allowing for tank ventilation. As a final preventative measure biomass reduction or sterilization procedures should be implemented. By first removing large biofilms from tank surfaces and then using a secondary sterilization protocol such as vaporized hydrogen peroxide (VHP) (Brickhouse et al., 2007), chlorine dioxide (EPA, 2010), or hot, humid air (Buhr et al., 2016) it may be possible to reduce the overall biomass to an acceptable level over an extended period of time reducing the risk of fouling and corrosion.

Hot, humid air is a viable method of decontamination

Decontamination of surfaces is essential to human health; however not all materials and surfaces are easy to decontaminate. In the event of an outbreak or bioterror attack transport vehicles such as aircraft may require rapid and complete decontamination. The use of hot, humid air as a part of the Joint Biological Agent Decontamination System (JBADS) was proven to significantly reduce the number of viable *Bacillus* spores previously (Buhr et al., 2016) on the same aircraft investigated in Chapter 5. We expanded upon the previous study and showed that the decontamination process affects the entire microbial community of an aircraft and few viable organisms remain after 72

hours of heat exposure. Quantifiable ATP, the number of cultivable microorganisms, and the amount of quantifiable DNA after PCR amplification were all significantly reduced after JBADS treatment. The characterization of the microbial community across a C-130H was another significant contribution to our understanding of this engineered ecosystem. Aircraft HEPA filters have been investigated previously (Korves et al., 2013) however no previous study has assessed the microbial load and community structure of surfaces within an aircraft or at the scale we carried out. Microbial communities were distinct by physical location (cockpit, cargo area, and tail) as well as by the amount of human interaction. This mirrors other studies into engineered ecosystems (Lax and Gilbert, 2015; Wood et al., 2015) where microbial communities were greatly impacted by the level of human interaction. After decontamination, the communities were more homogenous. Interestingly all organisms capable of acid production or degradation of polyurethane coatings were eliminated after decontamination. This was a potentially positive but unintended effect of JBADS with implications into the elimination of biocorrosive organisms on aircraft. The use of hot, humid air decontamination could be a practical method of controlling corrosion and fouling on aircraft and in other built environments.

Extending the use of JBADS beyond aircraft to other engineered environments may be useful. Heavily fouled biodiesel storage tanks could benefit from integration of current cleaning techniques and JBADS along with the use of filtration devices on vents further reduce the risk of microbial contamination. There are potential unintended consequences to the total elimination of the microbiome of an engineered ecosystem. Opportunistic pathogens can colonize surfaces representing a continuing health risk

(Lax and Gilbert, 2015). Similarly, the heat resistant fungi (Tournas, 1994) in biodiesel storage tanks may survive decontamination and achieve total dominance within a tank. Prior to use *in situ*, biofilms should be assessed in the lab for their ability to withstand extended periods of heat decontamination. A large number of fungal and bacterial isolates obtained as a part of the biodiesel field study presented in chapters 3 and 4 could be tested in isolation and as a consortia. After confirmation that all organisms can be successfully eliminated through the use of JBADS a large-scale field study could be conducted monitoring the change in the microbial diversity of a tank system over the course of months or years to ensure the effectiveness of the approach.

Final Thoughts

By linking *in situ* microbial community data, laboratory-based degradation and corrosion experiments, and mitigation protocols, we can begin to understand how microorganisms can impact these engineered ecosystems. The microbial community that resides on surfaces both above and belowground can exert enormous control over the surfaces they inhabit. Degradation of coatings, delamination of fiberglass, and corrosion of steel surfaces are unintended consequences of microbial metabolism. By careful study of engineered ecosystems and selection of the proper control mechanisms we can mitigate the risk to human built and maintained systems.

References

- Aktas, D. F., Lee, J. S., Little, B. J., Ray, R. I., Davidova, I. A., Lyles, C. N., et al. (2010). Anaerobic Metabolism of Biodiesel and Its Impact on Metal Corrosion. *Energy Fuels* 24, 2924–2928. doi:10.1021/ef100084j.

- Alivisatos, A. P., Blaser, M. J., Brodie, E. L., Chun, M., Dangl, J. L., Donohue, T. J., et al. (2015). MICROBIOME. A unified initiative to harness Earth's microbiomes. *Science* 350, 507–508. doi:10.1126/science.aac8480.
- Blin, K., Medema, M. H., Kazempour, D., Fischbach, M. A., Breitling, R., Takano, E., et al. (2013). antiSMASH 2.0--a versatile platform for genome mining of secondary metabolite producers. *Nucleic Acids Res.* 41, W204–12. doi:10.1093/nar/gkt449.
- Bomar, L., Maltz, M., Colston, S., and Graf, J. (2011). Directed Culturing of Microorganisms Using Metatranscriptomics. *mBio* 2, e00012–11–e00012–11. doi:10.1128/mBio.00012-11.
- Boucher, H. W., Talbot, G. H., Bradley, J. S., Edwards, J. E., Gilbert, D., Rice, L. B., et al. (2009). Bad Bugs, No Drugs: No ESKAPE! An Update from the Infectious Diseases Society of America. *Clin. Infect. Dis.* 48, 1–12. doi:10.1086/595011.
- Brady, S. F., Simmons, L., Kim, J. H., and Schmidt, E. W. (2009). Metagenomic approaches to natural products from free-living and symbiotic organisms. *Nat. Prod. Rep.* 26, 1488–1503. doi:10.1039/B817078A.
- Brandl, H., Däniken, von, A., Hitz, C., and Krebs, W. (2008). Short-term dynamic patterns of bioaerosol generation and displacement in an indoor environment. *Aerobiologia* 24, 203–209. doi:10.1007/s10453-008-9099-x.
- Brickhouse, M. D., Turetsky, A., MacIver, B. K., Pfarr, J. W., Lalain Iain McVey, T. A., Alter, W., et al. (2007). Vaporous Hydrogen Peroxide (VHP) Decontamination of a C-141B Starlifter Aircraft: Validation of VHP and Modified VHP (mVHP)

Fumigation Decontamination Process via VHP-Sensor, Biological Indicator, and HD Simulant in a Large-Scale Environment. Report.

Buhr, T. L., Young, A. A., Bensman, M., Minter, Z. A., Kennihan, N. L., Johnson, C. A., et al. (2016). Hot, humid air decontamination of a C-130 aircraft contaminated with spores of two acrySTALLIFEROUS *Bacillus thuringiensis* strains, surrogates for *Bacillus anthracis*. *J Appl. Microbiol.*, n/a–n/a. doi:10.1111/jam.13055.

D02 Committee Specification for Diesel Fuel Oil, Biodiesel Blend (B6 to B20). West Conshohocken, PA: ASTM International doi:10.1520/D7467-15C.

EPA, U. S. (2010). Compatibility of Material and Electronic Equipment With Hydrogen Peroxide and Chlorine Dioxide Fumigation. 1–106.

Fuhrman, J. A., Steele, J. A., Hewson, I., Schwalbach, M. S., Brown, M. V., Green, J. L., et al. (2008). A latitudinal diversity gradient in planktonic marine bacteria. *Proc. Natl. Acad. Sci. U.S.A.* 105, 7774–7778. doi:10.1073/pnas.0803070105.

Gu, T. (2014). Theoretical Modeling of the Possibility of Acid Producing Bacteria Causing Fast Pitting Biocorrosion. *J Microb. Biochem. Technol.* 06. doi:10.4172/1948-5948.1000124.

Hedlund, B. P., Dodsworth, J. A., Murugapiran, S. K., Rinke, C., and Woyke, T. (2014). Impact of single-cell genomics and metagenomics on the emerging view of extremophile “microbial dark matter.” *Extremophiles* 18, 865–875. doi:10.1007/s00792-014-0664-7.

- Herrera, M. L., Vallor, A. C., Gelfond, J. A., Patterson, T. F., and Wickes, B. L. (2009). Strain-Dependent Variation in 18S Ribosomal DNA Copy Numbers in *Aspergillus fumigatus*. *J. Clin. Microbiol.* 47, 1325–1332. doi:10.1128/JCM.02073-08.
- Hong, S., Bunge, J., Leslin, C., Jeon, S., and Epstein, S. S. (2009). Polymerase chain reaction primers miss half of rRNA microbial diversity. *ISME J.* 3, 1365–1373. doi:10.1038/ismej.2009.89.
- Klindworth, A., Pruesse, E., Schweer, T., Peplies, J., Quast, C., Horn, M., et al. (2013). Evaluation of general 16S ribosomal RNA gene PCR primers for classical and next-generation sequencing-based diversity studies. *Nucleic Acids Res.* 41, e1. doi:10.1093/nar/gks808.
- Korves, T. M., Piceno, Y. M., Tom, L. M., DeSantis, T. Z., Jones, B. W., Andersen, G. L., et al. (2013). Bacterial communities in commercial aircraft high-efficiency particulate air (HEPA) filters assessed by PhyloChip analysis. *Indoor Air* 23, 50–61. doi:10.1111/j.1600-0668.2012.00787.x.
- Kumari, A., and Gupta, R. (2014). Novel strategy of using methyl esters as slow release methanol source during lipase expression by mut⁺ *Pichia pastoris* X33. *PLoS One* 9, e104272. doi:10.1371/journal.pone.0104272.
- Lax, S., and Gilbert, J. A. (2015). Hospital-associated microbiota and implications for nosocomial infections. *Trends Mol. Med.* 21, 427–432. doi:10.1016/j.molmed.2015.03.005.
- Little, B., Wagner, P., and Mansfeld, F. (1992). An overview of microbiologically

influenced corrosion. *Electrochim. Acta* 37, 2185–2194. doi:10.1016/0013-4686(92)85110-7.

Lu, Z., He, Z., Parisi, V. A., Kang, S., Deng, Y., Van Nostrand, J. D., et al. (2012). GeoChip-Based Analysis of Microbial Functional Gene Diversity in a Landfill Leachate-Contaminated Aquifer. *Environ. Sci. Technol.* 46, 5824–5833. doi:10.1021/es300478j.

Masoner, J. R., Kolpin, D. W., Furlong, E. T., Cozzarelli, I. M., and Gray, J. L. (2015). Landfill leachate as a mirror of today's disposable society: Pharmaceuticals and other contaminants of emerging concern in final leachate from landfills in the conterminous United States. *Environ. Toxicol. Chem.* 35, 906–918. doi:10.1002/etc.3219.

Masoner, J. R., Kolpin, D. W., Furlong, E. T., Cozzarelli, I. M., Gray, J. L., and Schwab, E. A. (2014). Contaminants of emerging concern in fresh leachate from landfills in the conterminous United States. *Environ. Sci. Process Impacts* 16, 2335–2354. doi:10.1039/c4em00124a.

Meckenstock, R. U., Netzer, von, F., Stumpp, C., Lueders, T., Himmelberg, A. M., Hertkorn, N., et al. (2014). Water droplets in oil are microhabitats for microbial life. *Science* 345, 673–676. doi:10.1126/science.1252215.

Nichols, D., Cahoon, N., Trakhtenberg, E. M., Pham, L., Mehta, A., Belanger, A., et al. (2010). Use of ichip for high-throughput in situ cultivation of “uncultivable” microbial species. *Appl. Environ. Microbiol.* 76, 2445–2450.

doi:10.1128/AEM.01754-09.

Pitt, J. I., and Hocking, A. D. (2009). *Fungi and Food Spoilage*. Boston, MA: Springer

US doi:10.1007/978-0-387-92207-2.

Prince, R. C., Haitmanek, C., and Lee, C. C. (2008). The primary aerobic

biodegradation of biodiesel B20. *Chemosphere* 71, 1446–1451.

doi:10.1016/j.chemosphere.2007.12.010.

Proc, K., Barnitt, R., Hayes, R. R., Ratcliff, M., McCormick, R. L., Ha, L., et al. (2006).

100,000-Mile Evaluation of Transit Buses Operated on Biodiesel Blends (B20). in

(400 Commonwealth Drive, Warrendale, PA, United States: SAE International),

2006–01–3253. doi:10.4271/2006-01-3253.

Rondon, M. R., Goodman, R. M., and Handelsman, J. (1999). The Earth's bounty:

assessing and accessing soil microbial diversity. *Trends Biotechnol.* 17, 403–409.

Sharpton, T. J. (2014). An introduction to the analysis of shotgun metagenomic data.

Front. Plant. Sci. 5, 209. doi:10.3389/fpls.2014.00209.

Stamps, B. W., Lyles, C. N., Suflita, J. M., Masoner, J. R., Cozzarelli, I. M., Kolpin, D.

W., et al. (2016). Municipal Solid Waste Landfills Harbor Distinct Microbiomes.

Front. Microbiol. 7, 507. doi:10.3389/fmicb.2016.00534.

Stevenson, B. S., Eichorst, S. A., Wertz, J. T., Schmidt, T. M., and Breznak, J. A.

(2004). New strategies for cultivation and detection of previously uncultured

microbes. *Appl. Environ. Microbiol.* 70, 4748–4755. doi:10.1128/AEM.70.8.4748-

4755.2004.

Tournas, V. (1994). Heat-resistant fungi of importance to the food and beverage industry. *Crit. Rev. Microbiol.* 20, 243–263. doi:10.3109/10408419409113558.

Wood, M., Gibbons, S. M., Lax, S., Eshoo-Anton, T. W., Owens, S. M., Kennedy, S., et al. (2015). Athletic equipment microbiota are shaped by interactions with human skin. *Microbiome* 3, 25. doi:10.1186/s40168-015-0088-3.